Advancing animal models of depression
A behavioural, cellular and molecular approach

Musaelyan, Ksenia

Awarding institution:
King's College London

Advancing animal models of depression: a behavioural, cellular and molecular approach

Ksenia Musaelyan

Thesis submitted for the degree of
Doctor of Philosophy in Neuroscience

Department of Basic and Clinical Neuroscience
Institute of Psychiatry, Psychology and Neuroscience
King's College London

2017

Abstract

Animal models of depression have provided invaluable insight into the disease neurobiology, yet when it comes to novel antidepressant targets, the research progress in this area struggled to keep up with the growing prevalence of the disease. Thus this thesis is dedicated to improvement and optimisation of two frequently used models in mice, the unpredictable chronic mild stress (UCMS) with its good construct and predictive validity, and lipopolysaccharide (LPS) exposure relevant for the inflammatory theory of depression.

The experiments described in this thesis show that following optimisation, UCMS can be a reliable model to induce some of the depression-like behaviours, as well as alterations in adult hippocampal neurogenesis (AHN) in mice. However, it appeared that the prefrontal cortex (PFC) but not the hippocampus responds to UCMS with profound gene expression changes and microglial activation. Importantly, UCMS was not associated with a strong profile of systemic inflammatory changes seen in depressed patients. Therefore, the need for an intervention specifically targeting the immune system became apparent.

For this, LPS exposure, which induces a depression-like phenotype by activating the immune system, was employed. Results suggested that repeated LPS injections rather than frequently used single LPS exposure might be a suitable model to induce chronic immune changes relevant for depression, as well as some alteration of AHN. However, measures such as dose increment and sufficient recovery time between injections should be taken to avoid development of tolerance towards LPS, although they were not successful in sustaining the long-term behavioural depressive-like phenotype.

In conclusion, this research showed that both UCMS and LPS-based interventions induce some endophenotypes relevant for depression, yet neither is sufficient to fully model behavioural changes and neurobiology of the disease in mice. It is suggested that future work combining the two treatments might be more suitable for uncovering and testing novel antidepressant targets.

Acknowledgements

I dedicate my PhD thesis to two previous generations of women scientists in my family, my mother Irina Musaelyan, a psychologist, and my grandmother Nelly Entin, a physicist, who due to gender discrimination and antisemitism imposed by the Soviet regime were not given a chance to undertake and defend their doctoral studies. It is therefore an exceptional honour and responsibility for me to defend this work on their behalf.

First and foremost, I would like to thank my supervisors for their support and guidance throughout the project. My supervisors' scientific expertise and generosity in sharing it, as well as empathy and never fading encouragement in the moments of difficulty were essential for me to be able to complete this work. Specifically, I would like to thank professor Carmine Pariante for giving me the chance to undertake this PhD and welcoming me into his research group; Dr Cathy Fernandes for teaching me the principles and practicalities of animal work and setting the highest standard of research; Dr Sandrine Thuret for the day-to-day guidance and inspiration, as well as her support through the highs and lows of this project. Importantly, I would like to thank Dr Declan Jones on behalf of Janssen Pharmaceutica who provided the funding for this project.

Next I would like to thank Dr Martin Egeland and Andrea Du Preez with whom we collaborated on the project, for the excellent team work we have done in and out of the animal facility. I would also like to thank the MSc Neuroscience students Katerina Christodoulou, Selin Yildizoglu, Steven Aldridge and James Bozeman for the contribution to the data collection. Their enthusiasm for this project, effort they put into collecting data and stimulating discussions we had about it made for a rewarding teaching experience and generally a highly enjoyable period of the project. In addition, I thank Dr Tytus Murphy for sharing his experience of microarray data analysis, Dr Aleksandra Maruszak for her generous advice on statistical issues and Dr Christoph Anacker for teaching me basic lab techniques and introducing me to the field of adult hippocampal neurogenesis. I would also like to thank the IOP animal facility staff for their care and help with animal husbandry.

I want to extend my thanks to all members of the Thuret and SPI lab groups, for their support in and out of the laboratory, daily companionship, great conference trips, multiple lunchtimes and pub evenings which became an integral part of my time as a PhD student. I want to specifically thank Drs Tytus Murphy and Mark Horowitz for the productive collaboration on a public engagement project we carried out; Drs Dominic Plant and Nilay Hepgul for the peer support and a wonderful friendship; Drs Aleksandra Maruszak and Chiara De Lucia for

companionship and support in the Maurice Wohl office; Dr Natalia Bakunina and Alice Russell for the peer support during writing up period.

Almost last but not at all least, I want to thank Antoine Nguyen for the unconditional love, support and respect for my PhD work. My very final thanks go to all my family members for their consistent support and encouragement of my academic interests and ambitions on our rocky immigration road.

Table of Contents

Table of Figures

Table of Tables

Statement of Contribution

This work has been funded by a Janssen Pharmaceutica grant to Dr Cathy Fernandes (CF), Dr Sandrine Thuret (ST) and Professor Carmine Pariante (CP) and Janssen Pharmaceutica studentship to Ksenia Musaelyan (KM).

The experimental design has been developed by KM, CF, ST and CP. The behavioural experiments were conducted by KM with the help and guidance of CF in collaboration with Dr Martin Egeland (ME) and Andrea Du Preez (ADP). Behavioural data analysis has been conducted by KM under the supervision of CF, ST and CP.

Tissue collection has been conducted by KM with the help and assistance of CF, ME and ADP. Immunohistochemistry, microscopy and data analysis has been conducted by KM with the help of MSc students Katerina Christodoulou, Selin Yildizoglu, Steven Aldridge and James Bozeman under the supervision of ST.

RNA extractions for the genome wide gene expression study have been done by KM with the help and guidance of CF. Microarray was run by Dr Lee Sang at the IoPPN Genomics & Biomarker Core Facility. Microarray data analysis has been conducted by KM with the help of Dr Tytus Murphy and guidance of CF and ST.

The thesis has been written by KM with helpful feedback and comments by ST and CF.

Chapter 1 Introduction

1 An introduction to depression and its neurobiology

1.1 Global burden of depression

Depression is one of the most prevalent psychiatric disorders. Together with dysthymia it has been identified as a leading cause of burden in the Global Burden of Disease (GBD) 2010 study, conducted by the World Health Organisation (Ferrari et al., 2013). This conclusion was drawn based on the calculation of the number of healthy life years lost to disability or premature mortality. The 2013 GBD study identified depression as the second leading cause of years lost to disability (Vos et al. 2015). The study also identified a 37.5% increase in the years lived with disability due to depression in the last 20 years. While this increase was attributed to the population growth and aging, these findings still highlight the enormous burden on and implications of depression for global health. Yet the development of efficacious pharmacological treatments of depression is struggling to keep pace with the growth of disease prevalence (Willner et al., 2013). To advance the development of new therapeutics, we first need to better understand the factors increasing susceptibility to depression and the neurobiological processes underlying and determining the course of this devastating disorder.

1.2 Clinical diagnosis and risk factors

Depression is a highly heterogeneous disorder, therefore its diagnosis is based on multiple criteria, but among others must include two key symptoms – depressed mood and/or loss of interest or pleasure in all or almost all activities, or in other words inability to experience pleasure (anhedonia). The Diagnostic and Statistical Manual (DSM) lists another 7 symptoms which represent a mixture of emotional cognitive and neurovegetative impairments, as diverse as weight change and sleep disruption, fatigue and psychomotor agitation or retardation, feelings of worthlessness and guilt, thoughts of death and suicidal ideation, and diminished ability to concentrate or indecisiveness (DSM-5, 2013). To meet the diagnostic criteria, the symptoms need to be severe enough to cause “clinically significant distress or impairment in social, occupational, or other important areas of functioning”. In the United Kingdom, the estimated prevalence of a single episode in a lifetime of major depression is 6.4%, 12.2% for recurrent moderate major depression, and 7.2% for recurrent severe depression (Smith et al., 2013). Therefore approximately 1 in 6 individuals will experience depression in their lifetime (Otte et al., 2016).

The approximate heritability of depression is estimated to be 35% (Geschwind and Flint, 2015), however genome-wide associated studies so far achieved limited success in identifying significant and replicable genetic polymorphisms associated with depression (Ripke et al., 2013). The failure of genomic studies has been attributed to highly polygenic nature of the disease with many genes displaying small effects, as well as high heterogeneity of the disorder requiring large sample sizes to achieve significance (Hyman, 2014). In addition, gene-environment interactions are likely to be required for some genetic polymorphisms to exert their effects (Caspi, 2003). Indeed, environmental factors play a major role in depression aetiology. Stressful life events, such as loss of income, severe medical problems, exposure to violence or bereavement, have been identified as major risk factors for the development of depression (Kendler et al., 1999). Chronic stress, such as low socioeconomic status and social isolation also present a significant risk for disease development (Fava and Kendler, 2000). A specific link has been recognised between depression and stressful life events experienced in childhood, such as childhood maltreatment or separation from parents, as well as exposure to maternal depression (Bernet and Stein, 1999; Pawlby et al., 2011).

1.3 Pharmacological treatment available

The first antidepressant medications imipramine and iproniazid were discovered by serendipity in the clinic in the 1950s (Lopez-Munoz and Alamo, 2009). Imipramine is a tricyclic compound with noradrenaline and serotonin reuptake inhibition properties, while iproniazid is an inhibitor of monoamine metabolising enzyme, monoamine oxidase (MAO). The observation that two drugs which increase monoamine availability within the synapse can improve depressive symptoms formed a foundation of the monoamine deficiency theory of depression neurobiology (Schildkraut, 1965). According to this theory, depression occurs due to the lack of monoamine signalling in the brain, thus compounds which increase monoamine availability exert antidepressant effects. Accumulating data on the particular importance of serotonin in depression prompted the industry to focus on the serotonin reuptake and to develop the first selective serotonin reuptake inhibitor (SSRI) fluoxetine (Lopez-Munoz and Alamo, 2009). The clinical success of fluoxetine asserted the role of serotonin signalling in depression. However, simple increases in serotonin levels within the synapse cannot explain some of the aspects of SSRI effect. For example, the rapid effect of fluoxetine on serotonin levels does not match the late onset of its antidepressant effect, which requires weeks of daily intake (Trivedi et al., 2006). Individual difference in therapeutic efficacy of various antidepressants also cannot be explained by such a straightforward mechanism of action. Therefore, mechanisms of antidepressant action became the focus of intense scientific scrutiny, and led to the rise of

alternative theories, based on the idea that an increase in monoamine signalling is just the first step in a cascade of events leading to antidepressant effect (Elhwuegi, 2004).

Currently all of the routinely prescribed antidepressants act on the monoamine neurotransmitter system. Yet monoaminergic drugs have a number of disadvantages, most importantly low response rates and late onset of clinical improvement, which frequently requires up to 12 weeks of treatment (Uher et al., 2011). It has been shown that only a third of depressed patients receiving antidepressants achieve complete remission after the first course of antidepressant therapy (Trivedi et al., 2006). Another study showed that antidepressant treatment only shows clinical efficacy in patients with severe depression, while for mild or moderate symptoms, the effect of antidepressants is close to that of placebo (Fournier et al., 2010). Tham et al. (2016) showed that in elderly patients serotonin reuptake inhibitors (SSRIs), the most frequently prescribed group of antidepressants, are not more effective than placebo in achieving remission, although they were more effective in preventing relapse. Treatment-resistant depression has been estimated to occur in up to 60% of patients (Fava, 2003), and sometimes requires up to 4 switches of medication before remission is achieved (Warden et al., 2007). Many factors could play a role in antidepressant resistance. Pharmacokinetic issues, such as hepatic metabolism (Mrazek et al., 2011) and blood brain barrier penetrance (Uhr et al., 2008) have been suggested to be involved. Specific aspects of depression neurobiology are also likely to play a role. Factors such as genetic background affecting serotonin metabolism and neural plasticity (Kocabas et al., 2011; Le François et al., 2008), as well as comorbid conditions with inflammatory (Scherrer et al., 2012) or neurodegenerative component (Price et al., 2011) have been associated with increased incidence of treatment resistance. Therefore currently most depression researchers agree that to overcome the drawbacks of monoaminergic antidepressants, novel compounds need to be designed to target other aspects of depression neurobiology (Belzung and Billette de Villemeur, 2010; Willner et al., 2014).

2 Neurobiology of depression

2.1 The role of the hypothalamic-pituitary-adrenal (HPA) axis in depression

The hypothalamic-pituitary-adrenal (HPA) axis is the primary stress response system of the body, which regulates the systemic levels of corticosteroid hormones (cortisol in humans and corticosterone in rodents) (see Figure 1). Stressful stimuli reach the hypothalamus via the amygdala and the subgenual prefrontal cortex (PFC) and activate the release of corticotropin-

releasing hormone (CRH) (Gold, 2015). CRH is produced by the hypothalamic paraventricular nucleus (PVN) and released into the local hypothalamic-pituitary blood circulation system. Via this system CRH reaches the anterior pituitary, where it stimulates the production of adrenocorticotropic hormone (ACTH), which is subsequently released into the systemic bloodstream. Once in the circulation, ACTH stimulates the release of glucocorticoids (cortisol in humans and corticosterone in rodents) by the adrenal glands. Cortisol acts on mineralocorticoid (MR) and glucocorticoid receptors (GR) which are widely expressed in many tissues of the body (Holsboer, 2000). This allows cortisol to coordinate the stress response of different body systems. Its primary role is to mobilise energy metabolism and to prevent harmful consequences of the primary stress response triggered by catecholamines and immune system overactivation in case of injury (de Kloet et al., 2005). In the brain cortisol activates the amygdala to induce arousal, adaptive anxiety and fear response (Gold, 2015). The HPA axis has a negative feedback mechanism which prevents its overactivation. This mechanism functions via the GR receptors highly expressed in the PVN and the hippocampus, which activation by systemic cortisol is thought to trigger hippocampal suppression of the CRH release (Anacker et al. 2011).

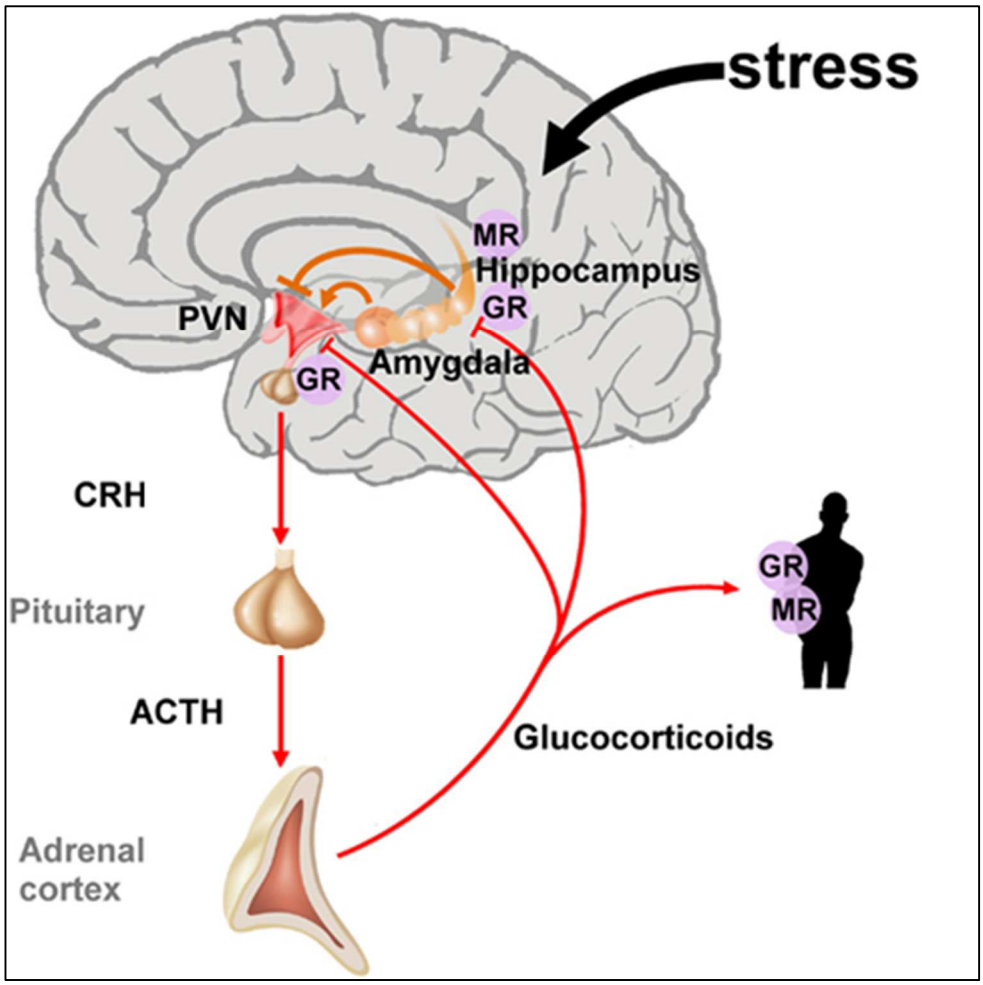

Figure 1 Stress response by the hypothalamic-pituitary-adrenal (HPA) axis
Stressful signals reach the hypothalamus from the activated amygdala and stimulate release of the corticotrophin-releasing hormone (CRH) from the paraventricular nucleus (PVN). CRH promotes the synthesis and secretion of adrenocorticotrophin (ACTH) by the pituitary. ACTH in turn stimulates the release of the glucocorticoid cortisol from the adrenal glands. Cortisol in the systemic circulation reaches many tissues throughout the whole body and the brain, where it activates intracellular nuclear mineralocorticoid and glucocorticoid receptors (MR and GR). GR is also widely expressed in the hippocampus, PVN, and anterior pituitary, where its activation by systemic cortisol terminates the stress response, thereby forming a negative feedback loop of HPA axis regulation. From Raabe, F. J. & Spengler, D. Epigenetic Risk Factors in PTSD and Depression. Front. Psychiatry 4, 80 (2013).

Multiple lines of clinical evidence suggest that in depression regulation of the HPA axis is disturbed. Depressed patients are consistently found to have increased blood and salivary levels of cortisol (Knorr et al., 2010). Increased levels of CRH have also been recorded in the cerebrospinal fluid (CSF) collected from depressed subjects (Nemeroff et al., 1984). To directly test the state of the negative feedback inhibition mechanism, researchers use the dexamethasone suppression test, wherein HPA axis activation is mimicked by the administration of the GR agonist dexamethasone. In healthy subjects dexamethasone administration should lead to a decrease in cortisol levels via the negative feedback loop mechanism. However in depressed patients cortisol levels are not decreased, indicating dysfunctional negative feedback regulation of the HPA axis, a condition called glucocorticoid

resistance (Pariante and Miller, 2001; Sher et al., 2013). Glucocorticoid resistance has also been observed in lymphocytes collected from depressed patients, in which proliferation and cytokine release was not suppressed by dexamethasone (Nikkheslat et al., 2015; Wodarz et al., 1991). Depression has also been associated with altered diurnal rhythm of cortisol release. In particular, depressed subjects display higher cortisol awakening response, the physiological elevation of cortisol shortly after awakening (Hardeveld et al., 2014). Such response is also associated with some of the key risk factors for depression, such as childhood trauma (Lu et al. 2016) and coronary heart disease (Nikkheslat et al., 2015). Importantly, antidepressants have been shown to reduce cortisol levels in the course of the treatment, which further confirms the importance of cortisol release in disease progression (McKay and Zakzanis, 2010).

Chronically elevated cortisol levels can negatively affect many processes related to depression neurobiology. Rodents chronically treated with corticosterone display depressive-like behaviour and reduction of adult hippocampal neurogenesis (David et al. 2009). Some of the metabolic abnormalities that are frequently associated with depression, such as obesity and insulin resistance, have been partly attributed to chronic cortisol elevation (Krishnan and Nestler, 2008). It is important to note however, that the relashionship between HPA axis regulation and obesity has not been completely understood. While many human studies report an association between hyperactive HPA axis and obesity, reports of hypoactive HPA axis in overweight subjects also exist (Incollingo Rodriguez et al., 2015). Interestingly, such dissociation is mirrored by rodent studies. Mice exposed to chronic stress, which is known to induce elevated levels of corticosterone, typically show lower weight gain than their undisturbed counterparts (Ducottet et al., 2003). Smilarly, exposure to chronic social defeat leads to slower weight gain in rats (Becker et al., 2008). However, chronic administration of corticosterone leads to increased weight in mice (Darcet et al., 2016; David et al., 2009). It is noteworthy that both effects have been shown to be reversed by chronic antidepressant treatment in the studies cited above.

Dysregulation of the HPA axis has been linked to the impaired function of the GR (Holsboer, 2000). Low expression of the GR or dysfunction of its nuclear translocation or mediation of gene expression, which prevent its response to cortisol, could explain the malfunctioning negative feedback and consequently lead to persisting elevated cortisol levels, as seen in depressed individuals. Reduced expression of the GR has indeed been shown in clinical and preclinical studies of depression. For example, reduced expression of the main GR transcript in peripheral blood cells was shown in depressed patients (Matsubara et al., 2006). Epigenetic changes in the GR promoter which could prevent its expression have been found in the

hippocampus of suicide victims with a history of childhood abuse, one of the main predisposing factors of depression (McGowan et al., 2009). Animal studies confirmed that deletion of the GR in the hippocampus and the pituitary is sufficient to induce HPA axis hyperactivity and depressive-like behaviour (Boyle et al., 2005; Schmidt et al., 2009). Moreover, it has been shown that antidepressant treatment increases GR expression in the hippocampus (Yau et al., 2007) and in fibroblast and neuronal cell cultures in vitro (Pariante et al., 2003). Therefore GR has been also implicated in antidepressants' mechanism of action (Anacker et al. 2011).

2.2 Structural and functional abnormalities in the depressed brain

Chronic elevation of glucocorticoid levels has also been implicated in some of the structural brain changes seen in depression. Due to high levels of GR expression in the hippocampus, this area is predicted to be one of the most sensitive areas to elevated cortisol levels. In line with this, reduction in hippocampal volume is consistently described in the structural brain imaging studies of depressed patients (Campbell et al., 2004). While this finding has been confirmed to be the most robust in a recent meta-analysis of neuroimaging studies which included 1728 depressed patients and 7199 controls, it also showed that the observed reduction is of low magnitude (less than 2% difference), which raises the question of its functional significance (Schmaal et al., 2016). Yet hippocampal volume was also found to significantly negatively correlate with the duration of the disease (Colla et al., 2007). Chronic exposure to elevated glucocorticoids can negatively affect many other brain regions involved in mood regulation. For example, a number of post-mortem and neuroimaging studies have reported decreased volume and activity in the PFC (Drevets et al., 1997; van Tol et al., 2014).

The hippocampus and the PFC belong to the limbic circuit, which has been implicated in emotional regulation and mood disorders. The limbic system can be divided into two functional domains: an emotional domain primarily comprised of ventral structures such as the amygdala, the ventral hippocampus, the ventral striatum, the insular cortex, the ventral part of the PFC including the subgenual anterior cingulate cortex (ACC) in humans and orbital PFC; and a cognitive or memory domain, involving the dorsal hippocampus and the dorsal (pregenual) parts of the PFC such as pregenual ACC and the dorsolateral PFC (Willner et al., 2013) (see Figure 2). All limbic regions within the two domains communicate via reciprocal connections, with the hippocampus and the PFC suggested to be key regulators of emotional control (Maier and Watkins, 2010; Willner et al., 2013). PFC, nucleus accumbens and the amygdala also receive dopaminergic inputs from the ventral tegmental area (VTA) implicated in reward and

anhedonia. The VTA is in turn highly receptive to the hypothalamic inputs including those regulated by gut metabolic hormones ghrelin and leptin (van Zessen et al., 2012).

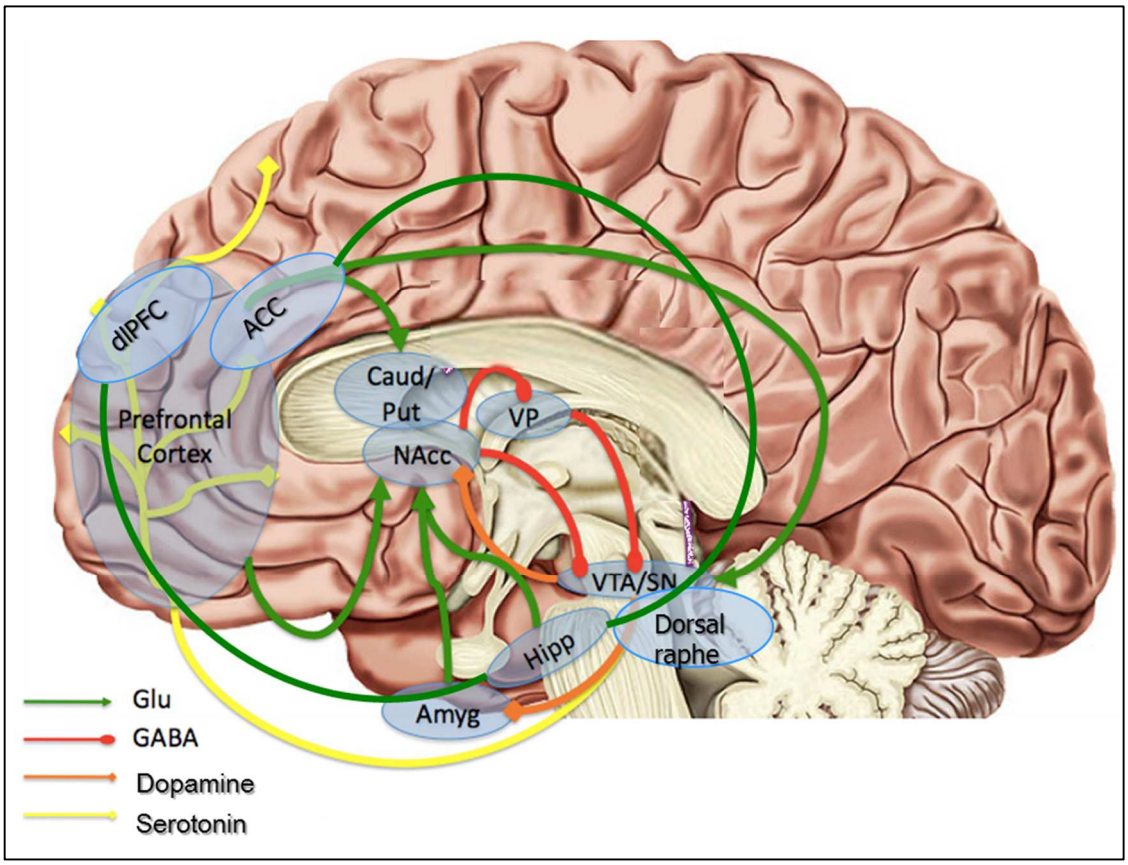

Figure 2 Corticolimbic circuit implicated in depression

A schematic representation of the main structures implicated in depression. Anterior cingulate cortex (ACC), amygdala (Amyg) and the anterior hippocampus (Hipp) form the emotional domain, while dorsolateral prefrontal cortex (dlPFC) and posterior hippocampus form the basis of the cognitive domain. Ventral tegmental area (VTA) and substatia nigra (SN) connected with nucleus accumbens (NAcc) form the reward/anhedonia complex. Caud – caudum, Put –Putamen, VP – ventral pallidum, Glu - glutamate. Adapted from Treadway and Pizzagalli (2014) Imaging the pathophysiology of major depressive disorder - from localist models to circuit-based analysis. Biology of Mood & Anxiety Disorders 4(1):5.

Functional imaging studies in depression generally show decreased activity of the cognitive domain, potentially underlying cognitive deficits, and overactivation of the emotional domain (Willner et al., 2013). In fact, increased connectivity and amplified activation of the amygdala is one of the most consistent functional neuroimaging findings in depression, while hyperactivity of the ACC and anterior insula have also been reported (Hamilton et al., 2012). At the same time, the dorsal PFC displays signs of hypoconnectivity, which can underlie an attention deficit seen in depressed patients (Kaiser et al., 2015). The nucleus accumbens has been shown to display reduced response to reward in depressed subjects, which could underlie anhedonia in depression (Pizzagalli et al., 2009).

The anatomy of the limbic circuit is well-preserved among mammalian species due to its ancient evolutionary origins allowing direct parallels between human and rodent studies of limbic regions. However such approach does not necessary apply when it comes to the structures of the neocortex such as the PFC, as it has undergone significant expansion in the course of the evolution of human primates (Rakic, 2009). Nonetheless, the neuroimaging findings in depression have been supported by animal studies which have found that chronic stress exposure leads to dendritic atrophy in the PFC, sparing the neurons that connect to the amygdala (Shansky et al., 2009). In the amygdala, chronic stress increases dendritic arborisation and growth (Vyas et al., 2002). These effects were attributed to the combined influence of catecholamines and glucocorticoids (Arnsten, 2015; Cerqueira, 2005).

Despite the findings highlighting the role of many brain regions in depression, hippocampus remains the focus of many depression-related studies due to one particular process taking place in the region of the dentate gyrus (DG), the adult hippocampal neurogenesis (AHN).

2.3 Adult hippocampal neurogenesis

AHN takes place in the subgranular zone (SGZ) of the DG and signifies a process of continuous birth of new neurons from neural stem cells throughout adult life. SGZ is the most well-described neurogenic region, however new methodological advances in tracing adult-born neurons continue to fuel the debate regarding the confinement of neurogenesis to certain brain areas in mammals in general and in humans in particular (Ernst and Frisen, 2015). Subventricular zone (SVZ) is another well-established neurogenic niche, which in rodents gives rise to the olfactory bulb neural progenitors, thus contributing to the olfaction-dependant behaviours (Lim and Alvarez-Buylla, 2016). However a recently developed technique to determine the age of cells in post-mortem tissue based on carbon dating did not confirm the presence of olfactory bulb neurogenesis in humans (Bergmann et al., 2012), which might reflect the limited role olfaction plays in human behaviour. Instead it has been suggested that the SVZ - derived neural progenitors in humans migrate to the striatum and give rise to striatal interneurons which delpletion is implicated in Hungtington's disease (Ernst et al., 2014), however more post-mortem studies are needed to confirm this hypothesis. Importantly, carbon dating studies of human tissue confirmed the presence of a relatively high (700 cells/day) rate of neurogenesis in adult humans (Spalding et al., 2013).

SGZ is a thin layer on the border of the DG and the hilus, which provides a neurogenic microenvironment permissive of the proliferation of neural stem cells and their differentiation into granule neurons throughout adult life. Apart from radial glial-like neural progenitors and

immature neurons at different stages of differentiation, SGZ contains glial progenitors, mature astrocytes and microglia, which are thought to define neural stem cells fate by releasing regulatory factors, including interleukins (Kempermann 2010). In addition, SGZ is a highly vascularised region, which provides an anatomical ground for the notion of plasma components influencing neural progenitors (Palmer et al., 2000) and allows factors such as vascular endothelial growth factor (VEGF) to regulate neurogenesis (Fournier and Duman, 2012). This specific microenvironment is often referred to as the neurogenic niche.

2.3.1 Stages of AHN

Neural stem cells go through several stages of development on their way of becoming mature granule neurons. Detection of stage-specific marker expression, as well as characterisation of the morphological and functional properties, allowed a classification of the main stages of neuronal differentiation in the SGZ (see Figure 3).

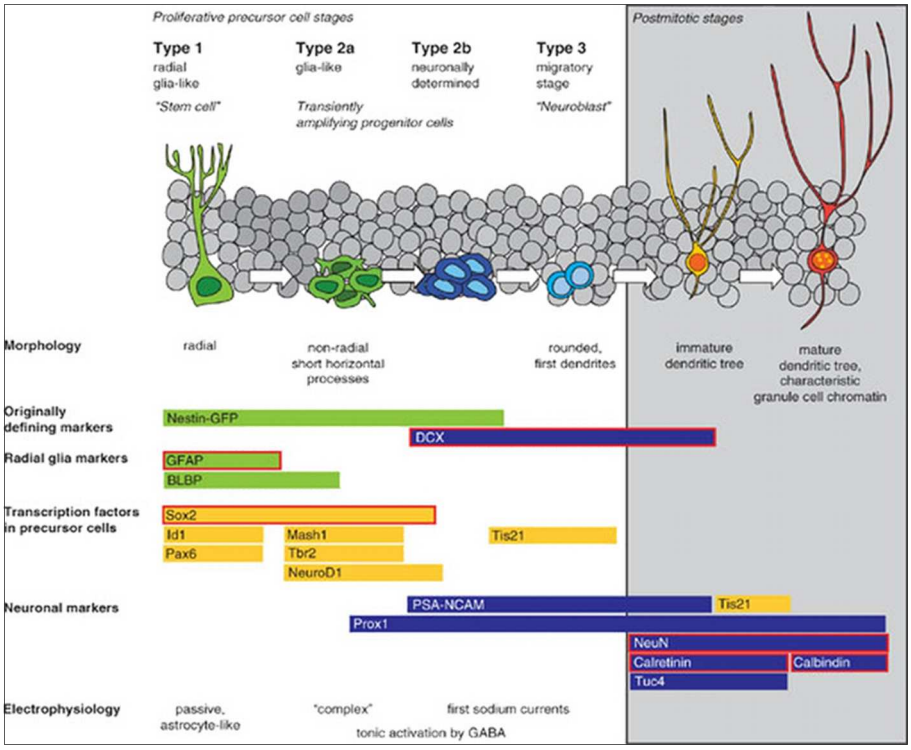

Figure 3 Developmental stages in AHN

Neuronal development in the DG can be separated into 3 major stages, which can be identified by expression of stage-specific markers. Type 1 are radial glia-like cells, which proliferate rarely and asymmetrically; type 2 is amplifying progenitors, among which type 2a actively proliferate and retain some of the glia-like properties, while 2b slightly less proliferative and express first markers of commitment to neuronal lineage. Type 3 neuroblast which undergo radial migration and begin dendritic tree development. From Kempermann, G. in Adult Neurogenesis ***2,*** *1–85 (Oxford University Press, 2010).*

Radial glia-like cells which express GFAP and possess many astrocytic properties are called type 1 progenitors. These cells are capable of asymmetric division and selectively express neural stem cell markers, such as Nestin and Sox2. The daughter cells of type 1 radial glial cells

comprise the most active proliferating population on the adult SGZ and have been named Type 2 cells (Fukuda et al., 2003). Morphologically they lack radial appearance of type 1 and instead possess short processes oriented along the SGZ. During the type 2 stage a final determination of neuronal lineage occurs in proliferating cells. This prompted Kronenberg et al. (2003) to suggest a distinction between early type 2 cells or type 2a, which already lost radial morphology but still express stem cell markers such as Nestin, and late type 2 or type 2b, which continue to proliferate but already show commitment to neuronal lineage by expressing neuroblast marker doublecortin (DCX). DCX is a microtubule binding protein which is highly expressed in the developing brain where it is required for neuronal migration (Bai et al., 2003), while in the adult brain its expression is almost exclusively confined to the immature neurons of the neurogenic regions (Ming and Song, 2005). Therefore the initiation of the DCX expression in type 2 progenitors is associated with the commencement of neuronal differentiation and tangential migration (Sun et al., 2015).

Late type 2b are not easily distinguishable from the next stage, type 3. These neuroblasts continue to express DCX but do not express any glial or precursor markers such as Sox2. Most importantly, they terminally exit the cell cycle. This phase is associated with significant morphological changes and with short-distance radial migration into the GZ. In healthy individuals, most neuroblasts remain in the SGZ and the inner third of the GZ and only few reach the outer layers of the GZ (Kempermann, 2003). Morphologically type 3 cells first develop apical dendrites. First apical dendrites reaching the molecular layer (ML) of the DG could be detected as early as 1 week after cell cycle exit. Branching of the dendritic tree is associated with a transition from a potentially proliferative state to the post-mitotic immature neurons, which eventually stop expressing DCX (Plümpe et al., 2006). In addition, more mature dendritic morphology suggests electrophysiological input, which indeed has been detected in the DCX-positive (DCX+) neuroblasts. First inputs detected in the dendrites within the GZ are GABAergic, while upon reaching the ML dendrites receive first glutamatergic inputs at about 3 weeks after cell cycle exit (Ambrogini et al., 2004). Dendritic spines are first detected in the neuroblast's dendrite at 2 weeks of post-mitotic development, and their density rapidly increases towards the end of the first month, before reaching a plateau by the end of the 2nd month (Aimone et al., 2014). During these 2 months immature neurons go through a period of high synaptic plasticity with spines being highly dynamic and particularly sensitive to neural activity.

Upon maturation dendrites of the adult-born granule cells form synaptic connections with the fibers from the enthorhinal cortex, thereby reinforcing the first synapse of the core trisynaptic

hippocampal circuit (Kempermann, 2010). Alongside dendrite development, axon mossy fibres of the immature neurons undergo growth through the hilus until they reach the CA3 region. These axons join the mossy fiber tract that reaches the pyramidal neurons in CA3, where they terminate in a synapse with the pyramidal CA3 neurons. This synapse is a 2nd synapse in the trisynaptic core circuit of the hippocampus. The third synapse completes the circuit by connecting the pyramidal CA3 neurons with the CA1, however AHN does not contribute to its formation.

In mice, the early post-mitotic stage of neuronal development is also characterized by the transient expression of a calcium-binding protein calretinin, which overlaps with DCX expression. Three to four weeks after cell cycle exit, calretinin gives way to expression of calbindin, a calcium-binding protein of mature granule cells (Brandt et al., 2003).

Therefore, it takes about 2 months from the exit of the mitotic cycle for neuroblasts to reach morphological and functional maturity of granule neurons, and DCX expression accompanies most crucial stages of the new neuron development (Jessberger and Kempermann, 2003). During these stages neural precursors go through several windows of susceptibility, when intrinsic and extrinsic factors can significantly affect their fate.

2.3.2 Regulation of AHN

2.3.2.1 Intrinsic factors affecting AHN

Activity of the surrounding circuitry can influence AHN at different stages. For example, activity of the DG reflected in the GABA levels can affect proliferation of the radial glial cells. Overactivation of the DG and an increase in tonic levels of GABA has been shown to suppress proliferation of type 1 cells, rather than promoting their quiescence (Song et al., 2012). On the type 2 stage when progenitors receive first GABAergic inputs, these inputs induce excitation and calcium influx via voltage-gated calcium channels, which stimulate expression of neuronal differentiation promoting factors, such as NeuroD1 (Deisseroth et al., 2004).

Glutamate plays an important role when immature neurons develop dendritic spines and start receiving glutamatergic inputs from the ML, which occurs approximately in the 3rd week of postmitotic development. During this critical period of neuronal survival, when many newborn cells which are not recruited into function undergo apoptosis, stimulation of the NMDA receptors is necessary for their survival (Tashiro et al., 2006).

The role of another neurotransmitter, serotonin, was established by studies looking at the effect of SSRI on AHN. SSRIs have been shown to promote all three components of the AHN,

namely proliferation, differentiation and neuronal survival (Banasr et al., 2006; Malberg et al., 2000). Effects of SSRIs were consistent with a direct effect of serotonin on proliferation that likely arises through the 5-HT_{1A} receptor, with possible contributions through the 5-HT_{1B} and 5-HT_{2A} receptors (Banasr et al., 2004; Samuels et al., 2015). Dorsal raphe nucleus is thought to be the main source of serotonin in the DG. However SSRI effect on neurogenesis has also been attributed to its effect on the GR signalling (Anacker et al. 2011). Dopamine has also been shown to play a role in neurogenesis, with dopamine D3 receptor blockade increasing cell proliferation in DG (Egeland et al., 2012).

Glial cells play a major role in the regulation of neurogenesis. Astrocytes are largely responsible for the formation of the neurogenic niche. Not only do they share many similarities with the radial glial cells, they also envelop neural stem cells and endothelial cells, ensuring a specific neurogenic microenvironment (Plümpe et al., 2006; Seri et al., 2001). Astrocytes release many factors which play a key role in the regulation of neurogenesis. One of them is Wnt3a, which modulates AHN by upregulating the expression of NeuroD1, an essential transcription factor in the generation of glial cells and neuronal differentiation (Kuwabara et al., 2009). Astrocytes also release many neurogenesis-stimulating growth factors, such as brain-derived neurotrophic factor (BDNF), insulin growth factor 1 (IGF1) and VEGF (Fournier and Duman, 2012; Mu et al., 2010; Waterhouse et al., 2012).

Microglia are another indispensable glial component of the neurogenic niche. Historically microglia's role in AHN regulation has been studied in the context of inflammatory or other pathological conditions, wherein activated microglia contribute to the antineurogenic effects. However, recent studies provided insight into the role of unchallenged microglial cells in normal AHN regulation (see Figure 4). Sierra et al. (2010) showed that ramified surveillant microglia phagocytose type 2b progenitors during the critical period of transition into the type 3 neuroblast stage, therefore being responsible for the regulation of survival in the AHN. Moreover, microglia have been shown to actively engulf synaptic components and therefore contribute to synaptic pruning during postnatal hippocampal development, suggesting that similar mechanism might be taking place during synaptogenesis in the adult DG (Paolicelli et al., 2011).

However activated microglia attract more frequent attention of the AHN research, as it has been implicated in the antineurogenic effects of many extrinsic factors, including infection, stress, neurodegeneration and aging (Sierra et al., 2014). These extrinsic factors share one important aspect of their mechanism of action – they induce neuroinflammation, wherein

activated microglia play a major role. Neuroinflammation is associated with a deramified activated state of microglial cells, in which they release proinflammatory cytokines with potent antineurogenic properties. Much of the insight into the effect of neuroinflammation on neurogenesis has been gained from the studies employing lipopolysaccharide (LPS) treatment. LPS is the main component of the outer membrane of Gram-negative bacteria and as such, it triggers a strong immune response without a resulting infection. Ekdahl et al. (2003) was one of the first to demonstrate that direct intracortical administration of LPS dramatically reduced the survival of newly generated neurons in the adult hippocampus. The detrimental effect of systemic LPS on neurogenesis via microglial activation has been demonstrated by Monje et al. (2003). Other studies supported the role of individual cytokines in this process, demonstrating that overexpression of interleukin 6 (IL-6) and interleukin 1 beta (IL-1β) in the brain, as well as systemic administration of tumor necrosis factor alpha (TNF-α) can reduce cell proliferation and neuronal differentiation in the adult hippocampus, stimulating more progenitor cells to differentiate into astrocytes (Seguin et al., 2009; Vallières et al., 2002; Wu et al., 2012). An *in vitro* study which employed human hippocampal stem cell line confirmed that this effect also occurs in human hippocampal cells (Zunszain et al., 2012). Moreover, recruitment of new neurons into hippocampal networks has also been shown to be reduced by chronic exposure to LPS (Belarbi et al., 2012). This effect was accompanied by longer distance of radial migration of neuroblasts into the GZ.

Currently, microglial activation and cytokine release are also suggested to be underlying mechanisms of neurogenic decline in non-infectious conditions such as Alzheimer's disease and normal aging (Kohman and Rhodes, 2013). On the other hand, ramified microglia have been implicated in proneurogenic effect of running and enriched environment (Sierra et al., 2014).

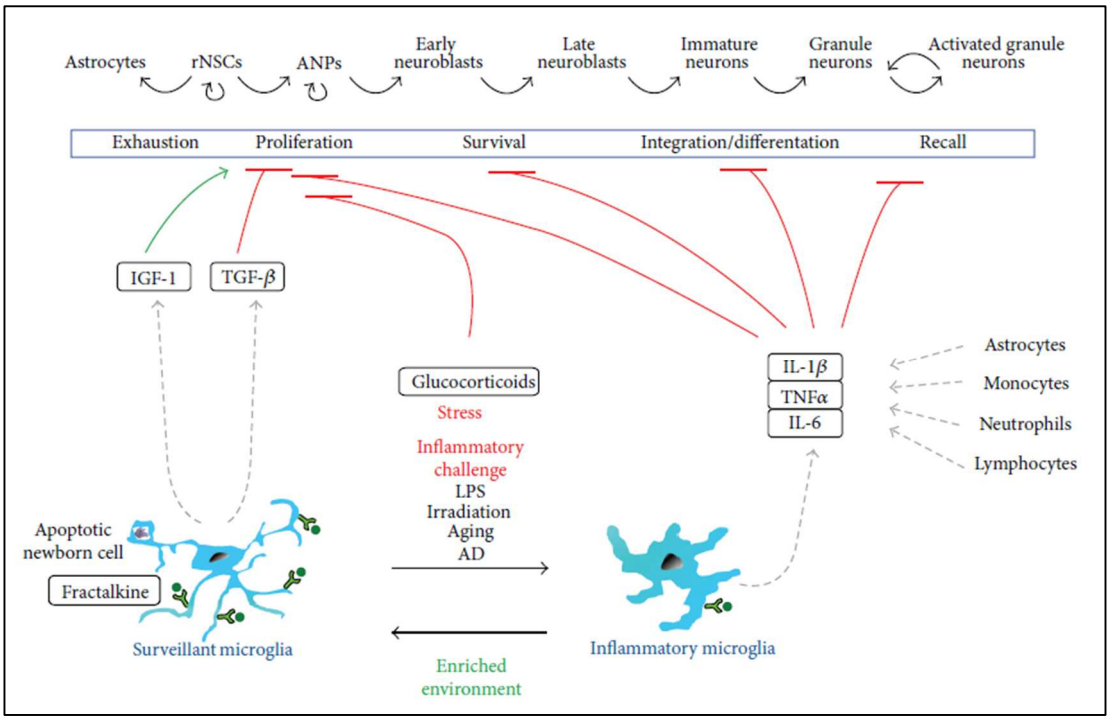

Figure 4 The effects of ramified (surveillant) and activated (inflammatory) microglia at different AHN stages. In physiological conditions, ramified microglia phagocytose apoptotic newborn cells and aid pruning of developing neuroblasts. Microglia can release factors which can promote (green arrow) (insulin-like growth factor 1, IGF1) and supress (red line) (transforming growth factor β, TGF β) proliferation of neural stem cells (NSCs) and amplifying neural progenitors (ANPs). Stress, inflammation (including lipopolysaccharide (LPS) exposure) and other aversive conditions including Alzheimer's disease (AD) on the contrary stimulate microglial activation, which leads to a release of proinflammatory cytokines interleukin 1β (IL-1β), tumor necrosis factor α (TNFα) and IL-6 and subsequent reduction of proliferation, survival, integration, and differentiation of the adult-born neurons. From Sierra et al. Neural Plast. 2014, 610343 (2014).

2.3.2.2 *Extrinsic factors affecting AHN*

Environmental enrichment (EE) is an enrichment of the housing conditions of laboratory animals, which provides them with social partners for interaction, novel objects and shelters to explore, as well as stairs and running wheels to stimulate locomotor activity. Enrichment significantly improves cell survival and neuronal differentiation in the DG, whereas wheel running profoundly increases cell proliferation (van Praag et al., 1999). Moreover, wheel running and EE are capable of rescuing neurogenesis impaired by genetic manipulation or exposure to detrimental extrinsic factors, such as chronic stress (Farioli-Vecchioli et al., 2014; Vega-Rivera et al., 2016). It is thought that the mechanism of these proneurogenic effects is related to the increased blood-brain barrier permeability, intensified cerebral blood flow, and accelerated glucose metabolism observed after exercise (Yancey and Overton, 1993). These changes might increase availability of the neurogenesis-promoting hormones and growth factors, such as VEGF and BDNF (Aimone et al., 2014). In addition, exercise has been shown to promote ramified state and IGF-1 secretion in microglial cells via chemokine fractalkine CX3CR1 receptor dependent mechanism (Vukovic et al., 2012).

Stress is another extrinsic factor potently regulating AHN. However the effect of stress was originally discovered through the antineurogenic effect of an intrinsic factor, the steroid hormone of the HPA axis corticosterone (CORT), which supressed cell proliferation in the dentate gyrus of rats (Gould et al., 1992). The same researchers first showed that acute stress following exposure to an unfamiliar intruder, reduced cell proliferation in rodents and primates (Gould et al., 1997, 1998). Subsequently, another type of acute stress (inescapable foot shock) also has been shown to reduce cell proliferation in rats (Malberg and Duman, 2003). Multiple studies demonstrated that proliferation, differentiation and survival of adult-born neurons were reduced by chronic stress exposure in mice (R Alonso et al., 2004; Mineur et al., 2007; Santarelli, 2003b). This effect has also been attributed to an increase in CORT signalling and activation of the GR in the hippocampus, as chronic CORT administration exerted similar effect on AHN (David et al. 2009; Lussier et al. 2013). However, neuroinflammation induced by chronic stress has also been proposed to play a role in its antineurogenic effects. Indeed chronic stress induces microglial activation and proinflammatory cytokine production in the hippocampus (Hinwood et al., 2012; Wang et al., 2015), therefore it is possible that these neuroinflammatory changes are partly responsible for AHN decline upon stress.

2.3.3 Functions of AHN

As AHN takes place in the DG, its functional effect is closely related to DG functions. The DG has been implicated in cognitive processes such as spatial and contextual learning and memory, specifically in the pattern separation of contextual information. Pattern separation is the process whereby similar experiences received from the cortical inputs are stored and recalled as distinct memories, thereby minimizing interference among similar memory cues (Colgin et al., 2008).

The role of adult-born granule neurons in pattern separation has been predicted by computational modelling (Rolls and Kesner, 2006) and was subsequently confirmed by behavioural studies showing a correlation between the level of AHN and performance in a spatial pattern discrimination task (Clelland et al., 2009; Sahay et al., 2011). It is thought that increased synaptic plasticity and excitability of young neurons during first few weeks of differentiation makes them particularly suited to encode novel information and mediate pattern integration and temporal encoding (Kempermann, 2010).

Interestingly, insufficient pattern separation has been suggested to play a role in overgeneralisation of fear thought to underlie post-traumatic stress disorder (Besnard and

Sahay, 2016). Pattern separation deficiency has been demonstrated in depressed patients (Déry et al., 2013; Shelton and Kirwan, 2013) and could explain some of the cognitive deficits seen in depression.

An alternative functional theory suggests that AHN on the contrary aids forgetting (Frankland et al., 2013). Authors suggest that continuous integration of new granule cells modifies established hippocampal circuits which recorded the activity pattern at the time of memory acquisition, thereby aiding memory fading. Indeed, it has been recently shown that increasing AHN by providing mice with access to running wheels facilitates fading of existing memories, but only those in conflict with the new memories, which encoding is enhanced by increased AHN (Epp et al., 2016). Therefore, this function of AHN is still beneficial for memory abilities. In fact, the authors argue that this effect has an adaptive benefit of cognitive flexibility. In this case, neurogenic deficit could prevent the decay of traumatic memories, which in turn could predispose individuals to mood disorders.

AHN has been also implicated in emotional regulation. Studies showing that AHN is reduced by stress initially suggested that it is also involved in stress effects on mood and behaviour, however this theory was not confirmed, as neurogenesis ablation did not cause stress-related behavioural changes (Santarelli, 2003a). Nonetheless, AHN has now been recognised to be required for some of the effects of antidepressant therapy (Surget et al. 2008; David et al. 2009). In addition, Snyder et al. (2011) suggested that AHN promotes resilience towards repeated stress exposure, as mice with deficient neurogenesis showed slower rates of recovery from the effects of stress. The emotional function of AHN has been mostly attributed to the ventral subregion of the DG, as a number of observations suggested its specific role in anxiety and stress-related responses. For example, studies investigating the effects of a specific ablation of AHN in ventral DG in rodents showed its specific involvement in anxiety-related tasks (Bannerman et al., 2002; Blanchard et al., 2005; Trivedi and Coover, 2004). In addition, some studies show that exposure to chronic stress preferentially affects the ventral subregion with minimal/no effect in the dorsal DG (Brummelte and Galea, 2010; Jayatissa et al., 2006; Oomen et al., 2010). Indeed anatomically, the ventral hippocampus is the area more closely connected to the mood-related brain areas, as it has reciprocal connections with the amygdala (Pitkänen et al., 2006) and the medial PFC (Thierry et al., 2000).

2.3.4 Neurogenic hypothesis of depression

The accumulating knowledge about the extrinsic and intrinsic regulation of AHN, together with clinical evidence highlighting the changes in the hippocampal volume in depressed patients

(Kendler et al., 1999) led to the formulation of the neurogenesis hypothesis of depression (Jacobs et al., 2000). The hypothesis stated that stress-induced decline of neurogenesis plays a causal role in the development of depression, and antidepressants achieve a therapeutic effect at least partly due to their proneurogenic properties. The hypothesis was supported by studies showing that in chronic stress models antidepressant therapy was effective in rescuing AHN levels (Malberg and Duman, 2003). However, ablation of AHN did not lead to depressive-like behaviour (Santarelli, 2003a; Surget, Saxe, et al., 2008), while AHN was only required for antidepressant effects in selected tasks (David et al. 2009). Nonetheless, in most of the available post-mortem clinical studies AHN has been shown to be decreased in depressed patients and to increase after antidepressant therapy (Boldrini et al., 2009, 2012; Lucassen et al., 2010). To determine neurogenesis levels in post mortem samples these studies used immuhistochemistry for markers of neural stem cells (nestin) and cell proliferation markers such as Ki67 and the minichromosome maintenance protein 2 (MCM2), thus their assement was limited to the stem cell pool and the rate of cell proliferation, but does not reflect neuronal differentiation and survival of newborn neurons. A certain controversy exists in the clinical literature, as a number of studies also report no change in hippocampal cell proliferation as detected by the number of Ki67-positive cells (Reif et al., 2006) or an increase in a specific patient group of young women (Epp et al., 2013). The latter study was the only one which used the neuroblast marker doublecortin, however the average age of patients in this study was significantly lower than in the previous reports. The study by Reif et al. (2006) did not account for age, sex and duration of illness, which could have affected the outcome. Interestingly, depressed individuals also exhibit a defect in hippocampal recruitment during processing of a spatial navigation task (Gould et al. 2007; Cornwell et al. 2010), confirming the presence of impaired hippocampal function. In addition, pattern separation deficits have been shown to correlate with depression scores (Déry et al., 2013; Shelton and Kirwan, 2013). Another indirect clinical evidence for the involvement of AHN in clinical depression comes from oncological studies, showing that depression and anxiety are frequent in cancer patients treated with drugs arresting cell proliferation, which are likely to impact AHN (Dias, Hollywood, et al., 2014). Therefore, while the primary causal role of AHN impairment in depression has not been sufficiently supported, numerous animal studies and indirect clinical evidence so far provided ample proof of the AHN involvement in depression pathogenesis and in the mechanism of antidepressant action (Miller and Hen, 2015). Future studies directly assessing AHN during the course of clinical depression and antidepressant treatment will allow more definitive conclusions to be made on the role of AHN in depression.

2.4 The inflammatory theory of depression

The immune system is another stress-response system of the body, which has been implicated in the neurobiology of mood disorders. The inflammatory theory of depression suggests that susceptibility factors such as chronic stress exposure, childhood trauma or comorbid conditions trigger immune system activation (Miller et al., 2009). Inflammatory processes subsequently contribute to, or potentially partly cause, deficiency in key systems regulating mood, such as neurotransmitter metabolism and the HPA axis (Raison and Miller, 2013). This hypothesis rests on ample clinical evidence of the presence of ongoing inflammatory processes in depressed patients, and experimental data showing that inflammation can trigger depression-like phenotypes and impact other systems involved in depression neurobiology.

2.4.1 Clinical evidence of inflammation in depression

Multiple studies have reported increased peripheral blood levels of proinflammatory cytokines and their soluble receptors in depressed patients compared to healthy controls (Liu, Ho, and Mak 2012). In particular, elevation of tumour necrosis factor-α (TNFα), interleukin-6 (IL-6) and C-reactive protein (CRP) are among the most reliable findings among cytokines in depression studies (Dowlati et al., 2010). However many other cytokines, such as IL-1β, IL-2, IL-4 and IL-10 have been reported to be elevated in depressed patients in individual studies (Maes et al., 1995; Simon et al., 2008). Moreover, some studies have found significant associations between inflammatory biomarkers and the severity of depressive symptoms, such as insomnia, fatigue and cognitive impairment (Bower et al, 2002; Meyers et al, 2005; Motivala et al, 2005). Reduction in cytokine levels have been shown to accompany improvement of symptoms following successful antidepressant treatment. (Dahl et al., 2014; Lanquillon et al., 2000). However increased cytokine levels persist in patients not responding to the therapeutic interventions (O'Brien et al., 2007). Furthermore, a predictive role of inflammatory biomarkers' levels was proposed in treatment resistance, as patients with increased inflammatory markers at baseline were found to display poorer response to treatment, suggesting a relationship between inflammation and treatment resistance (Cattaneo et al., 2016; Lanquillon et al., 2000).

Cytokines and chemoattractant cytokines known as chemokines are soluble signalling proteins produced by many cells comprising the immune system, such as neutrophils, monocytes, macrophages, B-cells, and T-cells. Their production is stimulated by an encounter of the immune cell with a pathogen. Endotoxin lipopolysaccharide, a component of the gram-negative bacterial wall, is one of the potent inducers of cytokine release (Biesmans et al.,

2016). The signalling pathway leading to cytokine production involves stimulation of transcription factor nuclear factor kappa B (NF-κB) and is discussed in more detail in Chapter 5 LPS-based model). Cytokines act as regulators of inflammation, immune cell function and cell-to-cell signalling. They affect multiple targets with various physiological consequences, and form a complex interactive network of regulators, which effect could be synergistic or antagonistic. As such, cytokines such as IL-1β, IL-6, IL-12 and TNFα are known to accelerate inflammatory response, while IL-10 prevents excessive immune activation by supressing macrophage function (Hiscott and Ware, 2011). IL-1β, IL-6 and TNFα are potent endogenous pyrogens, that is innate fever-inducing factors. IL-1β and TNFα activate vascular endothelium and increase vascular permeability, which allows entry of lymphocytes, complement and antibodies into the damaged tissues (Murphy et al., 2011). IL-1β, IL-6 and TNFα stimulate production of the acute phase proteins (APPs) such as CRP by the liver. Acute phase response is a complex and rapid innate body response to inflammation or tissue damage involving an increase in the production of APPs, which bind pathogens such as LPS and stimulate complement cascade (Schrodl et al., 2016). Other cytokines have their specific roles in immune response. IL-2 stimulates proliferation and differentiation of T-cells, while IL-12 activates natural killer cells and also contributes to the differentiation of T helper cells (Murphy et al., 2011).

In blood or other biological material collected from healthy subjects, cytokines either are not detectable or present at extremely low (picomolar) concentrations. Therefore elevated concentrations of cytokines are a useful indicator of ongoing inflammation (Dinarello, 2000) and their measurements are widely used in the clinic as biomarkers of inflammation, its detection and monitoring (Bienvenu et al., 2000). CRP is another common biomarker of inflammation routinely used in the clinic.

Thus elevation of cytokines and CRP in depressed patients and their correlation with symptom severity emphasises the importance of immune system activation in disease progression, however it does not address the question of causality of inflammation in the development of depression. The evidence which can support this theory comes from another body of data, based on the effect of therapeutic chronic inflammatory cytokine administration on the mood of treated patients. Inflammatory cytokine interferon alpha (IFN-α) administration is routinely used in Hepatitis C treatment (Feld and Hoofnagle, 2005). It has been observed that within 3 months, up to 50% of patients undergoing this treatment acquire depression symptoms which meet diagnostic criteria for major depression (Musselman et al., 2001; Raison et al., 2005). The IFN-α induced depression appears to be clinically similar to its natural counterpart (Capuron et

al., 2009). Moreover, pretreatment with antidepressants have been shown to prevent the IFN-α induced depression (Musselman et al., 2001; Raison et al., 2007). Importantly, IFN-α administration has been shown to stimulate the production of the innate immune cytokines involved in depression, such as IL-6 and TNFα (Prather et al., 2009; Raison et al., 2010). These data suggest that an increase in the levels of inflammatory factors might play a causal role in the induction of depression. Furthermore, with the advancement of neuroimaging techniques, clinical studies are starting to detect increased microglial activation marker translocator protein (TSPO) in the brain parenchyma depressed patients, and the first clinical trials for microglial activation supressing drug minocycline show promising results (Husain et al., 2015; Setiawan et al., 2015).

Further support for the inflammatory theory comes from studies showing that many risk factors for depression are associated with increased inflammation. In particular, chronic stress as well as stressful life events experienced in early childhood has been strongly linked to the onset of depression. Both chronic stress during adulthood, such as caring for cancer patients, as well as history of childhood abuse or early life trauma have been shown to be associated with increased levels of IL-6 and CRP (Carpenter et al., 2010; Danese et al., 2008; Rohleder et al., 2009). This evidence provides a very important link between stress, depression and immune system activation.

2.4.2 Experimental evidence for the mechanism of inflammatory involvement in depression

Another body of data which supports the inflammatory theory of depression comes from experimental studies looking at the mechanisms by which elevated cytokines and other inflammatory factors might influence the development of depressive symptoms. It has been demonstrated mostly by animal studies that cytokines interact with almost every system and process involved in depression, among them hypothalamic-pituitary-adrenal (HPA) axis regulation, monoamine metabolism and adult hippocampal neurogenesis (Raison and Miller, 2011), the evidence for which will be reviewed in more detail below.

2.4.2.1 Systemic inflammation induces depression-like behaviour

Infection-induced behavioural changes in humans have features common with the symptoms of depression, such as fatigue, cognitive impairment, change of appetite and sleep. In addition, inflammatory response induced by LPS or typhoid vaccine in human experimental medicine studies confirmed its ability to alter mood in a depression and anxiety-like manner (Harrison et al., 2009; Reichenberg et al., 2001). Similarly, acute inflammation in animals is accompanied by

a behavioural syndrome called sickness behaviour, which includes some behavioural changes resembling human depression symptoms, such as hypolocomotion and loss of appetite and weight. Importantly, it has been observed that immune challenge also induces anhedonia towards social, sexual and food rewards, as well as behavioural despair in specific antidepressant-receptive tests, such as Porsolt swim and tail suspension tests (Biesmans et al., 2013; O'Connor et al., 2009; Yirmiya, 1996). These depression-like behaviours have been shown to last beyond the duration of physical sickness, thereby representing a distinct depression-like behavioural phenotype (Frenois et al., 2007; Moreau et al., 2008; Painsipp et al., 2011). Therefore, stimulating the inflammatory response in animals allows us to study the neurobiology underlying these behavioural changes and the influence of inflammation on the other systems involved in depression.

Several methods are utilised in preclinical depression research to induce an inflammatory response. Systemic or intracerebral LPS administration is one of the most common ways to model inflammation, as it provides an advantage of triggering a fast and transient immune response in an absence of a specific living pathogen. However, other methods such as administration of the viral mimetic polyinosinic:polycytidylic acid (polyI:C), suspension of living E.coli or vaccines such as bacillus Calmette-Guerin (BCG) are also employed in some studies (Bilbo et al., 2005; Cunningham et al., 2007). All of these interventions lead to increase of blood levels of proinflammatory cytokines, which effect on other relevant systems can subsequently be studied in experimental animals.

2.4.2.2 Systemic inflammation acts beyond the blood-brain barrier

Bloodstream cytokines which release is stimulated by proinflammatory stimuli such as LPS, as well as macrophages activated by LPS have been shown to act within the brain tissue (see Figure 5). Although cytokines are relatively large molecules and do not easily cross the blood-brain barrier (BBB), their transport is possible through the saturable transport molecules or BBB regions of higher permeability, such as in the vasculature of the lateral ventricles (Banks, 2007). Moreover, systemic inflammation increases the permeability of the BBB, allowing more molecules to pass through (D'Mello et al., 2009). Similarly, leaky BBB eases transport of blood macrophages, which recruitment into the brain parenchyma has been shown to be increased in chronic stress models (Reader et al., 2015). However, transmission of inflammatory signal does not necessary require transfer across the BBB – macrophages and cytokines can affect cells of the endothelial wall and perivascular macrophages, which upon stimulation release proinflammatory factors into the brain parenchyma. Furthermore, astrocytes can also be affected via this route, as astrocytic processes take part in the BBB assembly (Hodes et al.,

2015). Indeed, systemic inflammation and stress exposure have been shown to affect astrocytic morphology and induce their release of chemokines, cytokines and growth factors (Biesmans et al., 2015; Camara et al., 2015; Norden et al., 2016).

Once in the brain parenchyma, cytokines can activate resident microglia and act directly on neurons. Increase in peripheral cytokines is consistently associated with increase in microglial numbers and its morphological changes typical for activated phagocytic phenotype (Buttini et al., 1996; Clark et al., 2015; Qin et al., 2007). These include enlargement of cell body, widening of primary processes and subtraction of distal processes, typically accompanied by increased production and release of proinflammatory cytokines (Colton, 2009). In addition to the effects of activated microglia on AHN described above, activated microglial cells can phagocytose axon terminals and destabilise dendritic spines of cortical neurons, thereby leading to dendritic atrophy (Kondo et al., 2011; Milior et al., 2016). However, it is thought that the main effect of microglial activation originates from the effect of cytokines released by activated microglial cells.

Cytokines can act directly on neurons via neuronal cytokine receptors. For example, in glutamatergic neurons IL-6 and TNFα have been shown to increase synaptic excitation via GABA (Garcia-Oscos et al., 2012) and AMPA receptors (Beattie, 2002). In serotonergic neurons cytokine effect is mainly exerted via changes in kynurenine metabolism.

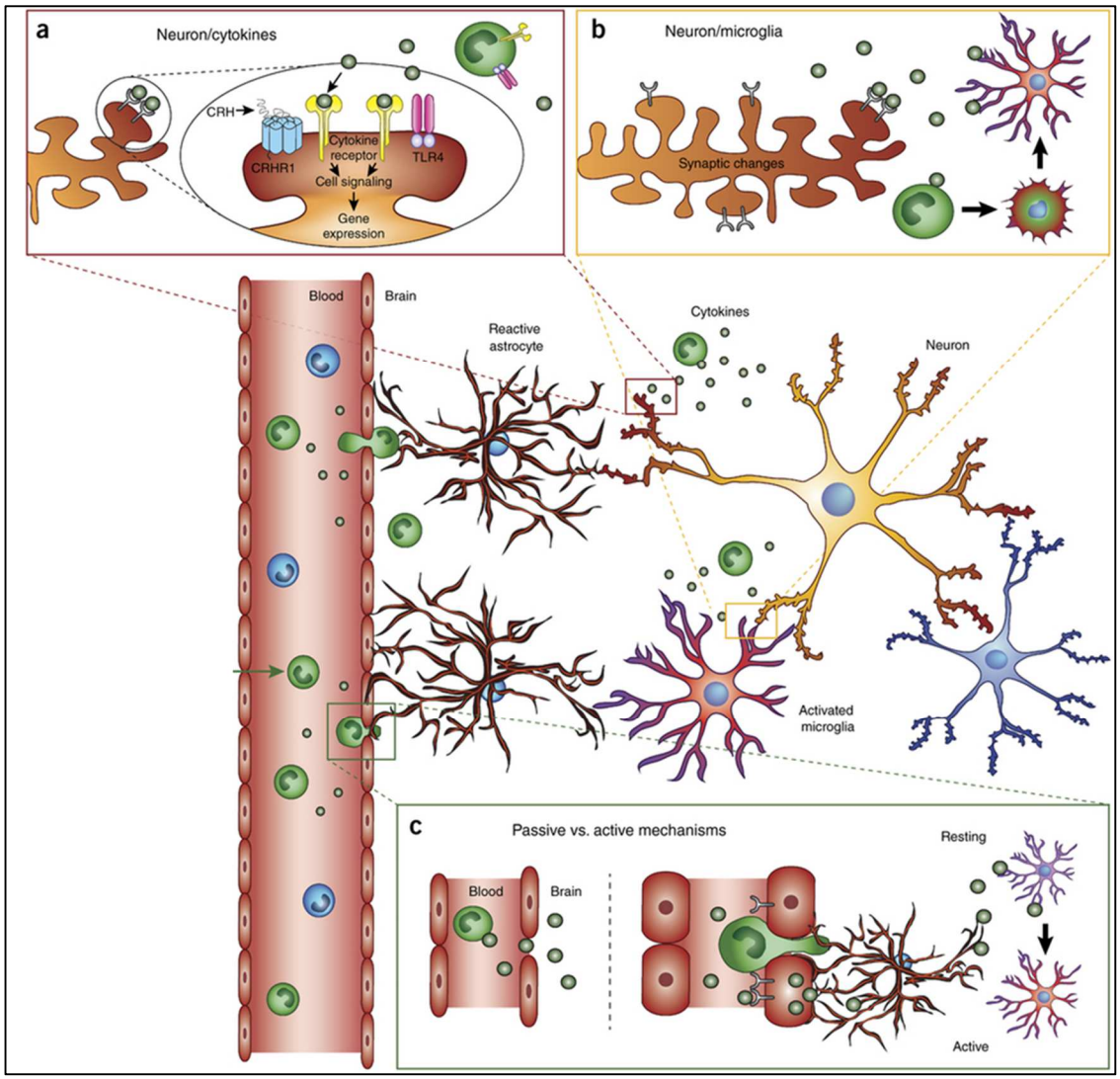

Figure 5 Systemic inflammation reaches the brain: mechanisms and consequences
(a) *Cytokines in the brain can affect neurons directly through activation of neuronal cytokine or Toll-like receptors 4 (TLR4) and corticotropin releasing hormone (CRH) receptors. (b) Macrophages recruited into the brain (in green) release proinflammatory cytokines and can adopt microglia-like properties. (c) Increase in blood brain barrier (BBB) permeability allows cytokines to passively diffuse between endothelial cells, while macrophages actively tunnel through the BBB. Inflammatory signal can also be transferred via activation to cytokine receptors on endothelial cells, which subsequently release inflammatory factors into the brain. Bloodstream factors can also trigger release of cytokines by astrocytes, which processes come in contact with the blood vessels. Once in the brain parenchyma, cytokines cause microglial activation which can trigger further inflammatory escalation, synaptic atrophy and decline in AHN. From Hodes et al., Neuroimmune mechanisms of depression. Nat. Neurosci. 18, 1386–1393 (2015).*

2.4.2.3 Effects of the cytokines on serotonin metabolism

The initial suggestion that there is an interaction between cytokines and monoamines, especially serotonin, came from the clinical evidence showing that selective serotonin reuptake inhibitors (SSRIs) can counteract and even prevent IFN-α induced depression. Cytokines affect serotonergic neurons via their ability to alter metabolism of serotonin precursor, tryptophan. A number of proinflammatory cytokines induce enzyme indoleamine 2,3-dioxygenase (IDO), which converts tryptophan into kynurenine instead of serotonin, thereby decreasing production of the neurotransmitter (Wirleitner et al., 2003; Zunszain et al.,

2012). Moreover, kynurenine metabolites have been associated with detrimental effects in the brain. As such, quinolinic acid have been associated with excitotoxicity and oxidative stress (Schwarcz, 2002), while kynurenic acid was implicated in glutamate and dopamine release (Felger et al. 2007; Kitagami et al. 2003). Importantly, IDO has been shown to mediate depressive-like effects of LPS exposure in mice (O'Connor et al., 2009). Clinical evidence also supports the role of kynurenine pathway in inflammation-induced depression. Indeed, it has been shown that tryptophan metabolism through the kynurenine pathway is increased in patients treated with IFNα, and kynurenine metabolites levels in the periphery as well as in the brain correlate with the development and severity of treatment-induced depressive symptoms (Capuron et al., 2003; Raison et al., 2010).

2.4.2.4 Effects of the cytokines on the HPA axis

Acute administration of proinflammatory cytokines including IFN-α treatment stimulates the production and release of the stress hormones of the HPA axis, such as ACTH and cortisol (Pace et al., 2007). While glucocorticoids are known in the clinic for their anti-inflammatory qualities in peripheral tissues, it has been suggested that in depression anti-inflammatory effect of cortisol is disrupted and in fact can even be replaced by pro-inflammatory action (Horowitz et al., 2013). This could be due to the impairment of glucocorticoid signalling known as glucocorticoid resistance, which has been attributed to the GR-mediated mechanism. Indeed, it has been shown that administration of proinflammatory cytokines can alter the transcription inducing function of the GR, a key player in the negative feedback mechanism of HPA axis regulation. For example, cytokines such as IL-1α and β have been shown to inhibit GR translocation to the nucleus (Engler et al., 2008), while IFNα has been shown to disrupt GR-DNA binding (Hu et al., 2009). In addition, chronic administration of cytokines has been shown to reduce GR expression (Pace et al., 2007). Via these mechanisms cytokines can contribute to the glucocorticoid resistance thought to play a major role in HPA axis dysregulation seen in depression. On the other hand, it has been hypothethised that the pro-inflammatory effect of glucocorticoids is specific for the brain in adverse pro-inflammatory conditions, such as stress, injury and potentially depression (Sorrells et al., 2009).

Experimental evidence described so far indicated many ways in which systemic inflammation can exert its effect on processes involved in the neurobiology of depression, thus supporting the causal role of inflammation in depression pathology. Additional support for the inflammatory theory comes from studies showing that other factors predisposing individuals to depression, such as chronic stress and increased corticosteroid levels, induce systemic and neuroinflammation.

2.4.2.5 Stress induces inflammation

Many animal studies of depression use chronic stress exposure to induce depressive-like behaviour and mimic HPA hyperactivation seen in depressed patients. It appeared that these manipulations also induce an increase in proinflammatory cytokines such as IL-1β, TNFα and IL-6 in the blood and in mood-related brain areas, including the PFC, hippocampus and amygdala (J Lu et al., 2016; Xue et al., 2015; You et al., 2011). Moreover, chronic stress exposure induces microglial activation and proliferation in the prefrontal cortex and the hippocampus (Couch et al., 2013; Hinwood et al., 2013). Pharmacological blockade of cytokine action or microglial activation has been shown to prevent development of depressive-like behaviour upon chronic stress exposure, asserting the causal role of neuroinflammation in chronic stress (Hinwood et al., 2012; Koo and Duman, 2008; Sahin et al., 2015). Moreover, it has been suggested that neuroinflammation could be an underlying mechanism through which chronic stress and ensuing glucocorticoid release exert their effect on AHN (Kreisel et al., 2014; Zunszain et al., 2011). It is thought that the immune system senses the stress via sympathetic and parasympathetic nervous systems, as immune cells express both adrenergic and glucocorticoid receptors and therefore can respond directly to sympathetic nerve signals and corticosteroid release (Marino and Cosentino, 2013; Tracey, 2015).

To summarise, clinical evidence collected so far strongly suggests the presence of systemic and neuroinflammation in depressed patients and hints at its causal role in studies of proinflammatory treatment. Experimental evidence confirms the association between inflammation and depressive-like behaviour, and suggests mechanisms behind this reciprocal relationship. However, the exact time of disease development at which immune processes come into play remains elusive. It is possible that immune activation precedes other neurobiological changes and potentially increases susceptibility of individuals to environmental factors such as stressful life events. On the other hand, inflammation could be triggered by stress exposure and HPA axis activation in susceptible individuals, predisposing them to the development of symptoms and treatment resistance. Future studies testing either scenarios will show if one of them is more prevalent than the other. In either case, it is clear that targeting systemic and neuroinflammation has a therapeutic potential for the patients suffering from inflammation-associated depression, as has been confirmed in recent clinical trials of microglia and cytokine inhibitors (Miyaoka et al., 2012; Raison et al., 2013).

3 Animal models in depression research

To further test the neurobiological theories of depression and to develop novel targets for drug discovery, valid animal models are required. The question of validity criteria of a successful model was raised very early on in the literature, with McKinney & Bunney (1969) setting out minimum requirements for an animal model of depression. The authors postulated that a suitable depression model should induce behavioural changes "reasonably analogous" to the human depression symptoms, which could be objectively quantified and reversed by the same treatment interventions used in clinical depression. Importantly, the requirement of reproducibility among research groups was also included in this assessment. Willner (1984) reformulated these requirements into two groups of validity types: face validity, or the similarity between the behavioural changes in the model and the symptoms of human disease, and predictive validity, which refers to the ability of a model to predict or replicate the efficacy of therapeutic interventions. Experimenting with stress exposure, Willner (1984) also added a third type, construct validity, which signifies the resemblance between the disease aetiology and interventions used to trigger behavioural changes in the model.

Achieving these criteria in animal depression research proved to be a challenging task for a number of reasons. The difficulty in achieving the face validity stems primarily from the obvious interspecies differences between mice and men, as key depression symptoms, such as depressed mood and suicidal thoughts are uniquely human. What complicates the task even further is the heterogeneity of depression symptoms. Indeed a large variability of symptoms means that the clinical picture of the disease might vary significantly from patient to patient, and therefore it is not immediately clear which behavioural pattern needs to be reproduced in a model (Nestler and Hyman, 2010). To partly overcome this difficulty, genetic studies suggested endophenotype approach – the use of separate entities of behavioural and neurobiological traits, supposedly predetermined by a small number of genes (Gottesman and Gould, 2003). As the genetics of such traits is expected to be less complex than of behavioural domains corresponding to psychiatric symptoms, modelling and pharmacologically targeting separate endophenotypes instead of human disease traits is expected to be a more feasible task (Kas et al., 2007).

The difficulty in achieving the construct validity is based on the fact that neurobiological aetiology of depression is not yet entirely understood and hence cannot be fully replicated. Therefore, an alternative approach has been suggested, to expose animals to a known environmental risk factor of the disease. As stress has been identified as a primary risk factor

for depression (Kendler et al., 1999), this strategy became widely utilised in animal depression studies using different types of stress exposure to induce depression-like behaviour.

3.1 Using stress to model depression

To date many different types of stress have been found to induce various depression-like behaviours in rodents. One of the first forms of stress-based models was application of electric foot shock which resulted in behavioural response named learned helplessness (Seligman and Maier, 1967). This behavioural phenomenon signifies acquisition of a passive approach to coping with stress, which occurs after several exposures in unescapable conditions and manifests itself as a failure to flee the shock when a means of escape is provided. While construct validity of this model has been disputed (Willner, 1984), it identified uncontrollability of stressor as a necessary factor to trigger the helpless behaviour (Drugan et al., 1997).

Passive coping has become a focus of attention in another model, Porsolt's swim test (Porsolt et al., 1977), commonly referred to as a forced swim test (FST). Porsolt found that rats placed in an unescapable cylinder with water first display active attempts to escape and vigorously swim around the cylinder, however in a few minutes become less active and finally resort to passive floating, with minimal movement just enough to keep the head above the water. During the second immersion, the majority of rats spend most of their time in the cylinder immobile. This response has been dubbed "behavioural despair", as it appears to reflect animals "giving up" on their chance to escape the water. Behavioural despair can also be triggered in a tail suspension test (TST), in which mice hung by the tail switch from initial struggling and climbing attempts to passive immobility (Steru et al., 1985).

The validity claims of the three models rest mainly on their sensitivity to the antidepressant treatment. Indeed antidepressants from most classes administered acutely and chronically have been shown to delay the onset of learned helplessness and behavioural despair in FST and TST (Cryan et al., 2005; Petit-Demouliere et al., 2005). However, the construct and face validity of these models have been heavily criticised. In addition, in mice genetic background of different strains has been shown to significantly affect their response (Powell et al., 2012). Some authors recommend to view behavioural despair tests solely as screening tests of antidepressant activity rather than stand-alone models (Nestler and Hyman, 2010). Currently FST and TST are widely utilised as tests of depression-like behaviour, to establish if more aetiologically relevant chronic stress exposure facilitates display of behavioural despair.

3.2 Chronic stress based models of depression

Introducing the chronicity of exposure into the model significantly improves its construct validity, as depression is a chronic disorder which is unlikely to be triggered by a single or few days long event. Also the intensity of chronic stressors need not be very high, which again brings them closer to daily life stressors predisposing individuals to depression. An extra advantage is the time frame the length of the chronic stress exposure provides to apply chronic antidepressant treatment. There are many types of chronic stress used in animal depression studies. Chronic stress can be applied in early life, such as in the maternal separation model, if childhood origins of the disease are being studied (Korosi et al., 2012). In adulthood repeated or variable stressors can be used. Repeated stress can be social, such as social isolation or chronic social defeat, or physical, such as chronic restraint stress (Nestler and Hyman, 2010). While repeated stress models have been shown to induce depressive-like behaviour, their construct validity is limited by the use of a single type of stress, while human experience is not limited to a single stressor. Moreover, repeated exposure to stressors removes the unpredictability factor and is likely to induce habituation, which can diminish behavioural outcome (Girotti et al., 2006).

Chronic unpredictable stress refers to protocols where a variety of stressors are applied. The stressors typically include alterations of housing conditions (removal of environmental enrichment and bedding, use of wet, novel or soiled bedding, tilt of cages), physical stressors such as shaking, immersion in cold water, restraint, tail suspension and lengthy periods of food and water deprivation. Other types of stressors could include alterations of the light/dark cycle, social isolation or exposure to intruder, exposure to predator cues (Willner, 2005). The severity of stressors can vary rather significantly between studies. Therefore, in this thesis I will distinguish between chronic unpredictable stress (CUS), which will be identified based on inclusion of more than one type of physical stressors, and unpredictable chronic mild stress (UCMS) mostly based on socioenvironmental stressors, which can include addition of a small amount of room temperature (RT) water at the bottom of the cage, restraint and food and water deprivation up to 24 hours (Willner et al., 1992). The UCMS model therefore has a construct validity advantage over other models, as it employs mild, variable and unpredictable stressors, more aetiologically relevant for risk factors of depression (Willner, 2005).

The strength of the face validity of UCMS model lies in the wide range of depression-related behavioural and neurobiological changes it induces. Indeed, apart from the uniquely human symptoms such as depressed mood, feeling of guilt or suicidal ideations, UCMS replicated changes in every behavioural domain affected by depression. Behavioural changes induced by

UCMS, together with methods of their assessment and corresponding clinical symptoms are summarised in Table 1, and will be discussed in more detail in Chapter 2 UCMS model. UCMS also replicates the main neurobiological phenotypes seen in depression. These include reduction of hippocampal volume, HPA axis activation, suppression of adult hippocampal neurogenesis and proinflammatory cytokine profile described above (Luo et al., 2014; Santarelli, 2003a; You et al., 2011).

Table 1 Symptoms of depression, corresponding behavioural changes induced by UCMS in rodents and behavioural tests used for their assessment
(Adopted from Czéh, B., Fuchs, E., Wiborg, O. & Simon, M. Animal models of major depression and their clinical implications. Prog. Neuro-Psychopharmacology Biol. Psychiatry (2015))

CLINICAL SYMPTOMS	**CHANGES INDUCED BY UCMS**	**ASSESSMENT IN RODENTS**
DSM-5 criteria symptoms		
Depressed mood	n/a	n/a
Markedly diminished interest or pleasure in activities	Anhedonia towards palatable or sexual rewards	Sucrose preference/consumption, novelty suppressed feeding, intracranial self-stimulation, cookie test, measures of sexual drive, female urine sniffing
Significant weight loss or weight gain, change of appetite	Weight loss, changes in food intake	Weight and food intake measurements
Insomnia or hypersomnia	Altered diurnal rhythm	Activity measures during light and dark phases, sleep EEG measures
Fatigue or loss of energy	Hypoactivity, grooming deficit, behavioural despair	Locomotor activity measures, coat state assessment; FST, TST
Feelings of worthlessness or excessive or inappropriate guilt	n/a	n/a
Diminished ability to think or concentrate, or indecisiveness	Cognitive deficit	Morris water maze, Y-maze, attentional set-shifting, novel object recognition
Recurrent thoughts of death, recurrent suicidal ideation	n/a	n/a
Psychomotor agitation or retardation	Hypoactivity or hyperactivity, grooming behaviour	Locomotor activity measures, coat state assessment, splash test
Additional symptoms and comorbidities		
Anxiety	Anxiety-like behaviour	Open field test, light-dark box test, novelty suppressed feeding, elevated plus maze
Anger and irritability in social interactions	Aggressiveness, social avoidance	Social interaction test

The predictive validity of UCMS is another strength of the model. Importantly, only chronic antidepressant treatment is effective in reversing behavioural and neurobiological deficits,

with most classes of antidepressants shown to exert therapeutic effect (Surget and Belzung, 2009).

However the replicability of the model has been called into question, as different laboratories reported conflicting outcomes and some struggled to replicate the model altogether (Nestler et al., 2002; Willner, 2005). Adaptation of the UCMS to mice and introduction of some of the new behavioural parameters such as coat state deterioration improved replicability in some laboratories (Griebel et al. 2002). Yet it has been shown that large difference in response to UCMS exists among different strains, with C57BL6 being one of the least responsive strains and BALB/c one of the most sensitive strain (Surget and Belzung, 2009). Moreover, within the same strain individual differences also exist in UCMS response, including inbred strains where the genetic background is identical within all test mice (Ducottet et al., 2004; Pothion et al., 2004). This difference is likely to be caused by slight variations in environment (e.g. parental behaviour, litter size and composition, experimental handling etc) between animals which could influence predisposing factors, such as state of the HPA axis or immune system of each individual animal. Thus while the UCMS model has significant advantages over many other models, it requires careful setup and validation in each laboratory.

The issue of replicability goes hand in hand with the issue of phenotype assessment. Indeed valid and reliable ways to measure depression-like phenotypes of interest are required to allow the comparison of different animal models. Most studies use a battery of behavioural tests to assess a variety of behavioural phenotypes corresponding to main symptoms of depression. A lot of effort has been put into attempts to measure anhedonia, one of the core depression symptoms. For this, animal's drive for hedonic stimuli, such as palatable solutions or sexual cues is measured. Such tests have good face validity, and their predictive validity have been shown with major antidepressant classes (Surget and Belzung, 2009). On the other hand, tests of so-called behavioural despair, such as forced swim or tail suspention test, lack the advantage of face validity and mainly used for their sensitivity to serotonergic antidepressants (Nestler and Hyman, 2010). Another large group of tests frequently used in depression studies are tests of anxiety-like behaviour. Indeed anxiety shows high comorbidity with depression, and antidepressant medications are now often used to treat anxiety disorders (Otte et al., 2016). Most tests of anxiety-like behaviour are based on the approach-avoidance task principle – exposure of a mouse to a novel yet open or well-lit arena to create a motivational conflict between two natural behaviours – an exploratory instinct and an aversion to areas of higher threat of exposure to predators. The examples of such tests are open field, elevated plus-maze and light-dark box. Measures of fearful threat-avoiding behaviours have

high face validity for anxiety, which is often characterised by avoidance of fearful objects (Cryan and Holmes, 2005). Importantly, these tests were developed based on their predictive validity for the first anxiolitycs benzodiazepines (Crawley and Goodwin, 1980), which further strenghethens their relevance. However not all tests used in depression research have been so well validated, which complicates interpretation of their results. Other tests used in UCMS research will be discussed in more detail in Chapter 2.

4 Thesis outline

To summarise, the design of a valid animal model of depression remains a challenging task to this day. Yet the success of novel drug target development hugely depends on their validity, therefore reliable models incorporating neurobiological aspects described in non-monoaminergic theories of depression are urgently required. In an effort to contribute to their development, in a series of experiments presented in the following chapters I revisit two animal models most frequently used in neurogenesis and the inflammatory depression research to pursue the following hypotheses.

1) BALB/c mice are a suitable strain to be used for developing mouse models of depression.

2) UCMS and its behavioural effects can be reproduced in a laboratory with no previous experience of UCMS research.

3) UCMS can induce numerous aspects of depression-like neurobiology including a reduction in adult hippocampal neurogenesis and neuroinflammation, as well as to provide insight into other neurobiological mechanisms of chronic stress relevant for depression.

4) LPS administration can be used to model chronic inflammatory state seen in depression and potentially induce some of the behavioural depression-like phenotypes.

Thus the experiments described in the following chapters were designed to pursue specific aims derived from the hypotheses listed above. Chapters 2, 3 and 4 are dedicated to the detailed assessment of the UCMS model, including its optimal setup to induce antineurogenic and inflammatory endophenotypes. In Chapter 2 I describe the set-up of the UCMS model in BALB/c mice and assess the replicability of different behavioural phenotypes described in the UCMS studies. In addition, I assess if change in inflammatory biomarkers is among the endophenotypes induced by UCMS, thereby contributing to the notion of an associative role of inflammation in depression. Chapter 3 is dedicated to the changes in AHN triggered by UCMS and possible inflammatory and endocrinal factors affected by UCMS, which could have

contributed to AHN modulation. In Chapter 4, a hypothesis-free approach of the genome-wide gene expression assay is used to investigate some of the molecular changes in relevant brain areas underlying behavioural and neurobiological phenotypes described in previous chapters. Finally, Chapter 5 explores the potential of proinflammatory agent LPS to model depression-like chronic changes in the immune system, neurogenesis and behaviour, thereby also testing the hypothesis supporting the causal role of inflammation in depression.

Chapter 2 UCMS model

1 Introduction

The unpredictable chronic mild stress (UCMS) model of depression became the focus of the first chapter of this PhD thesis due to a number of important advantages it has over other available animal models, and to controversies surrounding the replicability of its behavioural and neurobiological readouts (Willner, 2005). Indeed etiologically it is one of the most realistic models of clinical depression (Wiborg, 2013). In this model depressive-like phenotype is induced by repeated employment of mild mostly socio-environmental stressors, over which order and longevity the animal has no control. The variable, episodic and chronic nature of stress employed ensures good construct validity, as it resembles chronic psychosocial stress predisposing individuals to developing depression (Kendler et al., 1999). UCMS induces a plethora of behavioural changes, including but not limited to anhedonia, anxiety, behavioural despair, sleep disturbance, weight loss and locomotor retardation. Such variety of behavioural phenotypes corresponds to heterogeneic symptoms of depression, thus providing face validity of the model (Willner, 1997). Behavioural symptoms are also accompanied by neurobiological changes relevant for depression neurobiology, such as imbalance of neurotransmitter metabolism, hypothalamic-pituitary-adrenal (HPA) axis deregulation, reduction of adult hippocampal neurogenesis and modification of the immune response (Hill et al., 2012). Finally, the effectiveness of chronic treatment with virtually all classes of antidepressants on UCMS confirms its predictive validity (Surget & Belzung 2009).

Yet UCMS is surrounded by controversy, as many variations in the protocol exist, and many specific aspects of the protocol and outcome measurements, as well as laboratory conditions, have been shown to affect the results. Indeed, it seems that for every finding delivered by UCMS, there is at least one report showing opposing results (Willner, 2005). Such variation in UCMS findings among research groups brought about the need to adapt and validate the effectiveness of UCMS protocol for each laboratory wishing to utilise the model. Therefore, this study aimed to establish and optimise the UCMS protocol and its behavioural readouts for a mouse BALB/cAnNCrl strain and to conduct in depth study of behavioural phenotypes induced by UCMS and neurobiological changes underlying them. In terms of neurobiology the main focus of the study was on outcomes related to the two mechanisms currently appearing

most promising for future drug discovery, that is the activation of the immune system as indexed by cytokine levels, and on the level of adult hippocampal neurogenesis, which will be described in more detail in Chapter 3. The choice of the BALB/c strain was based on extensive literature suggesting specific sensitivity of this strain to stress and to antidepressant treatment. As such, it has been shown that this strain responds to stress exposure with hypersecretion of corticosterone (Zaharia et al., 1996), an effect which was attributed to low quality of maternal care in this strain (Anisman et al., 1998). BALB/c mice have been shown to display high anxiety levels in many approach/avoidance tests, such as open field, light-dark box and free exploration tests (Griebel et al., 2000; Kim et al., 2002; Kopp et al., 1999) In the comparison of UCMS response in 8 mouse strains conducted by Surget & Belzung (2009) BALB/c was one of the only 3 strains showing behavioural phenotype. BALB/c mice have also been shown to be highly responsive to antidepressant treatment. Dulawa et al. (2004) showed that BALB/c mice was the only strain out of four others which responded to chronic fluoxetine treatment with reduction of immobility in the forced swim test. Moreover, in the study by Ibarguen-Vargas et al. (2008) BALB/c was the only strain out of 8 compared in which antidepressant imipramine was effective in reversing UCMS-induced coat state alteration, anxiety in the novelty suppressed feeding test and increased levels of corticosterone. In addition, this strain has been reported to display increased immune system reactivity (Potter, 1985). Therefore, BALB/cAnNCrl substrain available from a UK supplier was selected for the experiments described in this thesis.

1.1 Behavioural parameters of UCMS

UCMS was developed by Willner (Willner et al., 1992) based on a study of the effect of severe repeated stress affecting locomotor activity and sucrose intake in rats (Katz, 1982). Willner modified intensive stress protocol used by Katz by removing the most severe physical stressors, such as footshock, cold water immersion and 48 hour food deprivation from the protocol, and by focusing attention on the behavioural readout measuring anhedonia, that is, a reduction of sucrose preference or consumption (Willner et al., 1987). The protocol which successfully reduced sucrose preference in rats during 5 to 9 weeks of exposure included 20-hour food and water deprivation, overnight illumination, 45° cage tilt, housing in cages soiled with 100ml of water and intermittent pair housing. Subsequent experiments showed that combination of only three stressors was sufficient to induce anhedonia in rats, namely cage tilt, wet bedding and pair housing (Willner, 1997). However, in a mouse version of the protocol developed over the next 10 years, intermittent pair housing had to be removed to avoid induction of aggression and fighting between temporarily paired mice. Instead exposure to

another mouse's cage in its absence was introduced, together with movement restriction and more ethologically relevant stressors such as predator odours and sounds (Surget and Belzung, 2009).

During the first decade of UCMS experiments the model caused some controversy as many laboratories struggled to replicate it (Nestler et al., 2002). However, since it was adapted to mice, numerous research laboratories successfully utilised it. Shortly after the first study by Kopp et al. (1999) describing 3 week UCMS protocol in mice, Griebel et al. (2002) suggested a new measure of the UCMS outcome: the physical state of the fur evaluated on a subjective rating scale. Griebel and coworkers (2002) showed that fur or coat state deteriorated during 7 weeks of UCMS in mice, while chronic treatment with fluoxetine (10 mg/kg) significantly improved it. The authors drew a parallel between reduction of daily grooming in animals which leads to coat state deterioration and the struggle depressed individuals face trying to accomplish even the smallest daily tasks, including maintenance of personal hygiene. Many laboratories adopted this measure, sometimes using it as a main behavioural readout (Ducottet et al., 2004; Mutlu et al., 2012). Belzung's group suggested and validated a more precise scoring system than that originally suggested by Griebel et al (2002), where 7 body parts of a mouse are given a separate score of 0 for clean shiny fur, or 0.5 or 1 for spiky dirty fur depending on the level of deterioration, and a total sum of scores is used as a final readout (Nollet et al., 2013). One of the big advantages of this measure is that unlike most behavioural tests including sucrose preference, which are affected by multiple exposure of animals to sucrose (Strekalova et al., 2011), it can be safely conducted repeatedly in the same animal. Hence it allows a more sensitive within subject monitoring of depressive-like behaviour during the weeks of stress exposure and antidepressant treatment.

Another measure which could be monitored during the stress is body weight. Most of the studies with UCMS in rats and mice report decreased body weight or reduced body weight gain, which is rescued by chronic antidepressant treatments (Bekris et al., 2005; Liu et al., 2014). However a number of mouse studies do not detect any change in body weight (Strekalova et al., 2011). It is important to remember that many chronic stress protocols, especially at the beginning of CMS research in mice (Griebel et al., 2002), utilised food and water deprivation as one of the stressors, which could lead to weight change unrelated to psychological effects of stress (Lu et al., 2016). However the protocol used by Belzung and colleagues does not include any food deprivation, and their studies frequently report decreased weight gain in different mouse strains (Nollet et al., 2013), albeit not in every experiment (Ducottet and Belzung, 2005; Santarelli, 2003a). Surget & Belzung (2009)

speculated that such variability in effect could be due to the fact that like depressed patients, mice might be responding either with weight gain or loss, however when individual parameters are averaged for group statistical analysis, such effects can no longer be detected. A difference in body weight response has also been attributed to mouse inter-strain variations (Schweizer et al., 2009).

Interestingly, variation in body weight response slightly resembles variation seen in another measure related to feeding, sucrose preference. While sucrose preference was at the centre of CMS research from the very first publication (Willner et al., 1987), not all studies report similar findings. In 2005 review Willner listed 38 different groups reporting decreases in sucrose intake (volume of sucrose consumed) or preference (percentage of sucrose consumed over total liquid volume consumed in two-bottle test) in rats or mice, along with 4 studies which showed the opposite effect, albeit mostly reported in conference proceedings (Willner, 2005). This review also mentioned several unpublished communications regarding no effect of CMS on sucrose preference. Publication bias could explain why such paradoxical or negative findings are less represented in the literature, however the existence of variation in anhedonic behaviour is now widely accepted. It appeared that result of the sucrose preference test is highly strain- and concentration-dependent. For instance, Pothion et al. (2004) demonstrated differences in sucrose intake and preference among 11 mouse strains subjected to 7 weeks of UCMS and concentrations of sucrose which varied between 1 and 50% percent. Authors went on to compare effect of UCMS on sucrose consumption in 3 out of 11 inbred strains (CBA/H, C57BL/6 and DBA/2) chosen for stable and high level of sucrose consumption, and showed that only 2 strains (CBA/H and C57BL/6) responded to UCMS with a reduction in sucrose consumption. Lewis et al. (2005) compared intake of sucrose solutions ranged from 0.0001% to 20% sucrose in 12 inbred mouse strains and showed strong interstrain differences, with C57BL/6 being one of the greatest sucrose consumers and BALB/c classified as intermediate consumers. Surget reported that 11 tested strains of mice only showed preference for sucrose concentrations of 4% and above (Surget and Belzung, 2009). This group also tested sucrose preference in 8 different mouse strains following the 6 week UCMS protocol, including BALB/cByJ, C57BL/6J, and DBA/2, and showed that stress had a supressing effect in only one of 8 strains, in-house laboratory-reared inbred strain BA from the Institut de Transgenose, Orleans (Ducottet and Belzung, 2005). Inter-strain comparisons and genetic studies of the sucrose taste receptor showed the importance of genetic background in the ability to demonstrate a sucrose preference (Powell et al., 2012). In addition, in the protocol developed by Willner, rats are subjected to 24-hour food and water deprivation before the test, therefore

appetite and metabolism can affect caloric sucrose consumption in food-deprived animals. To remove such confounding factor, Ducottet et al. (2004) performed the test in mice without food and water deprivation, and this protocol change could explain the results contradicting many studies showing decreased sucrose preference in mouse strains. Since then Belzung's group avoided the use of sucrose preference as an anhedonic measure in mice, which did not prevent this laboratory from publishing breakthrough studies using UCMS model (Santarelli, 2003a). Strekalova et al. (2011a) conducted a thorough investigation into the methodology of the sucrose preference measure during chronic stress in C57/BL6N mice, and pointed out many factors that could have influenced the outcome. These include individual variability of response in naïve animals, preventable by habituating animals to sucrose before the beginning of measurements; variation in liquid consumption during the time of day, which is highest in the active phase; habituation of animals to repeated exposures, counteracted by a change in concentration during chronic stress. Yet even when all these considerations are taken into account, the authors observed a large individual variation in the sucrose preference during chronic stress, which allowed them to divide stress-exposed animals into either susceptible or resistant to chronic stress effects (Strekalova et al., 2006). Importantly, this group utilises a chronic stress protocol which cannot be classified as mild as it consists of intense stressors such as tail suspension, social defeat and restraint. Intensification of stress could explain why the sucrose preference test is modulated by stress exposure in their studies.

As anhedonia is a core diagnostic feature of depression, it plays a central role in modelling depression, and other tests are being used to detect it in UCMS studies. The study by Santarelli et al (2003) used novelty-suppressed feeding as a readout of anhedonia to assess the effect of 4 different antidepressants in a 5 week UCMS protocol in mice and dependence of SSRI antidepressant activity on adult hippocampal neurogenesis, while a later study by the same group introduced a novel cookie test, which also measures motivation for a familiar, palatable and rewarding stimulus (chocolate cookie) in a novel arena (Surget et al., 2011).

However, behaviours affected by UCMS are not limited to the anhedonic phenotype. In parallel with depression and anxiety comorbidity observed in clinical depression, some studies report increased anxiety in chronic stress-exposed animals. As such, increases in anxiety-like behaviour in mice were observed in the light-dark box (Mineur et al., 2006), elevated plus maze (Papp et al., 2013), and open field test (Franceschelli et al., 2015). However, opposite results also have been documented by the very same groups. As such, Ducottet et al. (2003) described an anxiolytic effect of 9 weeks of UCMS exposure in the light-dark box, while D'Aquila et al. (1994) described anxiolytic profile of chronically stressed rats in elevated plus

maze. Increased locomotor activity has been proposed as a cause of such paradoxical effects (Strekalova et al., 2005). Indeed a number of studies report hyperlocomotion induced by chronic stress exposure, which usually accompanies “anomalous anxiolysis” (Schweizer et al., 2009). This effect also highlights inter-species differences, as it appears to be specific for mice and is opposed to the reduction of locomotor activity usually described in rats in response to chronic stress exposure. Change in locomotor activity has been attributed to the disturbance of circadian rhythms in mice. Indeed UCMS includes alteration of light/dark cycle, and many studies describe the change in circadian clock genes expression in the suprachiasmatic nucleus of the hypothalamus, the centre of circadian rhythm regulation (Jiang et al., 2011; Kinoshita et al., 2012). Logan et al. (2015) showed that chronic stress altered circadian fluctuation of activity in a way that stressed mice displayed hypoactivity in the dark phase and hyperactivity in the light phase. This together with existing evidence that light/dark phase of open field testing can significantly affect the activity outcome (Valentinuzzi et al., 2000) could explain existing controversies on locomotion and anxiety among UCMS studies.

Hyperactivity has also been shown to affect the outcome of tests assessing depressive-like behaviour or so called behavioural despair. While in both forced swim and tail suspension tests chronic (6 weeks) stress exposure has been shown to increase depressive-like behaviour in rats and mice (Bessa et al., 2013; Khemissi et al., 2014), these results were not always replicated (Mineur et al., 2006). Moreover, behaviour in FST is known to be highly strain-dependant (Petit-Demouliere et al. 2005, Powell et al. 2012). Yet due to the high predictive validity of these tests for detecting antidepressant effect of serotonergic compounds, most studies include it in the behavioural testing batteries following chronic stress exposure.

Behavioural changes described above do not complete a list of behavioural effects of chronic mild stress. Other behaviours previously reported in this paradigm include but are not limited to sleep disturbance, aggression, memory impairments and reduced sexual drive (D’Aquila et al., 1994; Erburu et al., 2015; Griebel et al., 2002). However, our experiments focused on behaviours most consistently reported in UCMS studies and most important for modelling depression and assessing the effectiveness of antidepressant treatment.

1.2 Effect of UCMS on systemic neurobiological parameters

Chronic stress has been shown to have many neurobiological effects highly relevant for depression research, including changes in neurotransmitter signalling, neural plasticity, HPA axis regulation, adult hippocampal neurogenesis and the immune system. However, in this chapter we will only focus on the systemic effects of UCMS which can be assessed in

peripheral blood, as separate chapters are dedicated to the molecular changes in the brain (see Chapter 3 for adult hippocampal neurogenesis and Chapter 4 for gene expression profiling of UCMS).

The HPA axis has been implicated in the neurobiology of depression by numerous clinical studies, therefore it is a key neurobiological process that should to be altered in a relevant/valid animal model of depression. Indeed, an early study by Ayensu et al. (1995) described elevation of serum corticosterone following 4 weeks of chronic stress exposure in rats. Interestingly in this study changes in corticosterone were accompanied by a reduction in serum complement activity, providing the first evidence of the effect of chronic stress on the immune system. Many subsequent studies replicated this finding in rats (Garcia et al., 2009; Liu et al., 2014), and complimented it with gene expression data showing increased CRH gene expression in the hypothalamus (Ge et al., 2013). Such a profile of HPA axis response suggests HPA axis hyperactivation arising from the malfunction of the negative feedback inhibition loop, which in health protects the body from excessive corticosteroid release. The negative feedback loop is thought to depend upon the hippocampal glucocorticoid receptor (GR). Decreases in GR expression or loss of function, named glucocorticoid resistance, has been implicated in the malfunction of the negative feedback mechanism of the HPA axis (de Kloet et al., 2005; Silverman and Sternberg, 2012). Indeed many studies show decreased GR expression upon UCMS exposure in the hippocampus and hypothalamus in rats and mice (Pan et al., 2010; Zhuang et al., 2016). Interestingly in the latter study by Zhuang et al (2016), a decrease in GR expression seen in mice after 8 weeks of UCMS exposure has been accompanied by an increase in proinflammatory cytokines TNFα and IL-6 expression in the same brain areas and in the peripheral blood.

Yet as with the behavioural parameters, strain and study variations exist in corticosterone data. When 8 mouse strains were compared, only 2 strains including BALB/cByJ, showed significant elevation of faecal corticosterone, while another 2 strains showed a decrease, and no effect was observed in the remaining 4 strains. Interestingly, chronic imipramine treatment reversed the effect of UCMS on corticosterone levels in only 2 strains, BALB/cByJ and C57BL/6J (Ibarguen-Vargas et al., 2008). Moreover, inter-individual variability in HPA axis response to UCMS has also been documented. Khemissi and colleagues used the dexamethasone suppression test, a test of negative feedback inhibition, to divide stress-exposed animals into those with high- or low-reactive HPA axis (Khemissi et al., 2014). These authors went on to show that a group with impaired low-reactive HPA axis regulation failed to respond to fluoxetine treatment in some behavioural outcomes (NSF), thereby modelling antidepressant

resistance seen in depressed patients. Such a profile of HPA axis response also resembles the reduced HPA axis activity seen in atypical depression (Gold, 2015).

The HPA axis is closely linked with the immune system function, as its activation has been shown to induce immune activation and vice versa (Bellavance and Rivest, 2014; Silverman et al., 2005). As has been already mentioned above, plasma inflammatory markers have been shown to be affected by chronic stress alongside corticosterone and other HPA axis parameters. Kubera and coworkers showed that 3 weeks of UCMS in mice decreased thymus weight, a key organ in the immune response, and induced IL-1 release by unstimulated splenocytes (Kubera et al., 1998). In a study by You et al. (2011) elevation of pro-inflammatory cytokines (IL-1β, TNFα and IL-6) and decrease in anti-inflammatory cytokines (IL-10 and TGFβ) in the spleen were accompanied by corresponding changes in the hippocampus, cortex, and the hypothalamus of rats after 4 weeks of UCMS exposure. Elevation of proinflammatory cytokine levels has also been shown in the peripheral blood after 4 weeks of UCMS, again accompanied by increased IL-1β, TNFα and IL-6 expression and protein levels in the rat hippocampus and prefrontal cortex (Lu et al., 2016). Similarly, Xue et al. (2015) showed increased IL-1β, TNFα, IL-6 and the NLRP3 inflammasome in the mouse hippocampus after 6 weeks of UCMS. Moreover, in these studies chronic treatment with 10mg/kg fluoxetine reduced proinflammatory cytokines to control levels. The increase in proinflammatory cytokines is not merely correlational. For example, IL-1β has been shown to be essential for chronic stress to induce anhedonia in mice (Koo and Duman, 2008). Treatment of UCMS-exposed rats with the TNFα inhibitor infliximab prevented cognitive decline induced by stress (Sahin et al., 2015). It is thought that the main source of the increased proinflammatory cytokines in the brain during stress is activated microglial cells. Indeed various types of chronic stress have been shown to increase the number and activation markers of microglial cells in the prefrontal cortex and the hippocampus (Lu et al., 2014; Tynan et al., 2010; Wohleb et al., 2011). It has been suggested that one of the ways through which microglia can sense stressful stimuli is via corticosterone activating its GR receptors (Carrillo-de Sauvage et al., 2013). In turn, microglial activation is thought to play a role in the behavioural outcome through its effect on adult hippocampal neurogenesis and synaptic plasticity (Kreisel et al., 2014; Wohleb and Delpech, 2016). The evidence supporting this notion will be reviewed in more detail in chapters 3 and 4.

2 Study aims

The aims of the UCMS experiments described in this chapter were to set up the UCMS protocol in our laboratory and explore its behavioural readouts, as previous literature highlighted above shows a large variation in the protocols used and the behavioural and neurobiological outcomes detected. An aetiologically relevant protocol without physical stressors, such as food/water deprivation, restraint or footshock, most closely resembling the protocol by Nollet et al. (2013) was utilised and optimised in the presented experiments. The outcome of behavioural tests relevant for depression, such as grooming, anxiety, anhedonia and behavioural despair was assessed. The systemic neurobiological effects of UCMS on the HPA axis and the immune system were measured in blood to evaluate the suitability of the UCMS model to study aspects of depression neurobiology with the aim of potentially identifying novel treatment targets.

3 Methods

3.1 Animal housing

Male inbred BALB/cAnNCrl mice aged 7 weeks were purchased from Charles River (Margate, UK). All animals were housed in the Biological Services Unit (BSU) at the Institute of Psychiatry, Psychology & Neuroscience in standard conditions (19-22°C, humidity 55%, 12h:12h light:dark cycle with lights on at 8.30am, food [Rat and Mouse No. 1 Diet; Special Diet Services, Essex, UK] and water ad libitum). Animals were allowed to acclimatise to the animal facility for at least 7 days before the beginning of the experimental procedures. Standard mouse Techniplast cages (32cmx16cm x14cm) with sawdust as a bedding material (Litaspen premium, Datesand Ltd, Manchester, UK) or larger rat cages (59.5x38x20cm) were used for housing depending on the design of individual experiments. Unless otherwise stated minor cage enrichment, consisting of sizzlenest (Datesand Ltd, Manchester, UK) and a cardboard shelter (LBS Biotech, Horley, UK) was provided. The number of animals per cage varied among experiments, therefore is specified below in the experimental design sections for each experiment. Cages were never cleaned the day before, or on the testing day to minimize the potential effects of cage disturbance on the behaviour of the mice. All housing and experimental procedures were performed in compliance with the local ethical review panel of King's College London under a U.K. Home Office project licence held in accordance with the Animals (Scientific Procedures) Act 1986 and the European Directive 2010/63/EU. All efforts were made to minimize animal suffering and to reduce the number of animals used.

3.2 UCMS protocol

The UCMS protocols used were based on the methodology described by Nollet et al. (2013) and modified to accommodate the conditions of the animal facility and to improve the ethological relevance of the stress by decreasing its severity. As such, restraint in a tube limiting the body movement of mice was removed or replaced with a confinement in a wire mesh cup which allowed free movement of the animal (see Figure 6) to reduce the severity of the procedures. The reversal of the light/dark cycle was not possible in the facility due to lighting conditions, therefore stressors were applied in the light phase. For predator odour commercially available fox urine was used instead of rat feces which were unavailable in the facility. The exact schedule of UCMS exposure used in each experiment is summarised in the respective experimental design sections. The length and the number of stressors per day varied depending on the experiment, but the following stressors were included in all protocols: tilting of the cage by 45° for a period varying between 30 min to 3 hours (see Figure 6), frequent change of bedding (new bedding), removal of sawdust and minor enrichment for up to 2 hours, exposure to wet sawdust produced by an addition of 150ml of room temperature water to the cage for up to 6 hours, exposure to a cage of another mouse in its absence (cage swap) for up to 6 hours, exposure to the odour of intruder mouse, when mice were returned to their home cages after cage swap (return to cage with intruder's odour up to 15 hours (overnight), exposure to predator's odour (Shake Away 2852228 Fox Urine Granules, 15ml per cage) up to 1 hour, exposure to predator's sounds (Birdsong CD (Birds of Prey and Crows), Music Digital 2009) for 30 minutes, replacement of sawdust with 1cm of water at room temperature for 30 minutes (water bath as shown in Figure 6), confinement in a restricted space for up to 1 hour (wire mesh cup 10cm height 8cm diameter alteration of light-dark cycle such as introduction of several intervals of daylight during the night (exact schedule is specified in individual experimental design sections). Control animals were always housed in a different room from UCMS-exposed groups as not to expose them to any of the stressors.

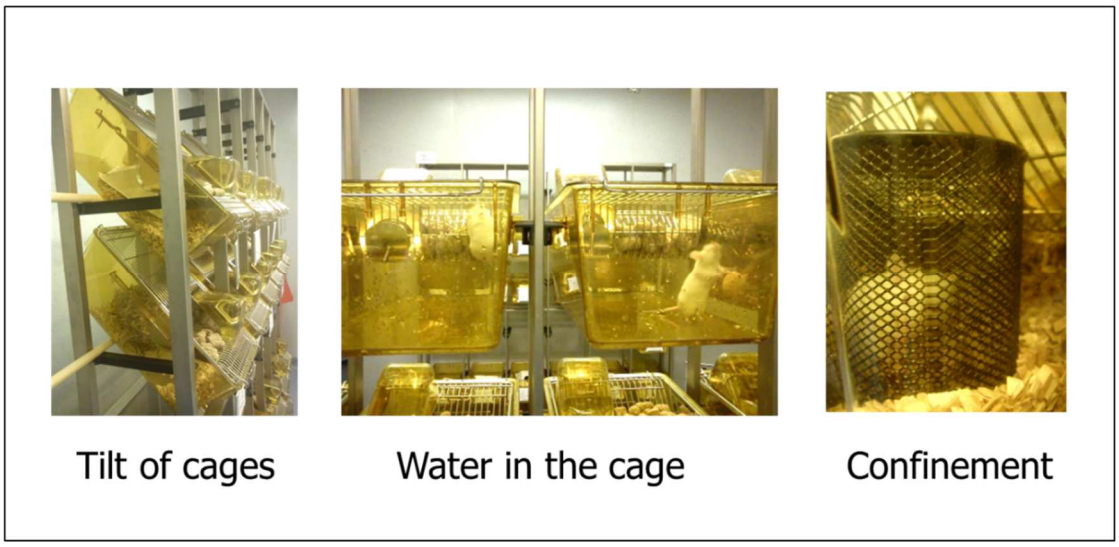

Figure 6 Photographs representing some of the stressors included in the UCMS protocol

Table 2 summarises the number of animals included in each UCMS experiment, including the numbers used for behavioural assessments, in the analysis of the blood and brain tissue and the number of animals which died during the UCMS exposure.

Table 2 Number of mice used in UCMS experiments 1-4

Experiment	Total number of mice used	Behavioural testing	Tissue analysis (blood and/or brain)	Number of mice died during UCMS
UCMS Experiment 1	60, 12 per group	60	48	0
UCMS Experiment 2	48, 12 per group	39	39	9
UCMS Experiment 3	20, 10 per group	20	20	0
UCMS Experiment 4	16, 8 per group	16	16	0

3.3 Behavioural assessments

3.3.1 Coat state assessment (Nollet et al., 2013)

Animals' weight and coat state were assessed during UCMS on a weekly basis. Coat state reflects an animal's grooming behaviour, which could be interpreted as an analogue of human self-caring behaviours, including upkeep of personal hygiene and appearance, which could be affected in severe depression (DSM-5, 2013). Control animals were brought into the UCMS housing room for coat state assessment to ensure blindness of assessment. Coat score was determined on a scale of 0 to 7 according to Nollet et al (2013) by a researcher blinded to experimental conditions. The total coat state score was the sum of the scores given to each of

the individual body areas (head, neck, back, abdomen, tail, forepaws and hindpaws). A score of 0 was given if fur on a body area was smooth and shiny without spikes or patches, a score of 0.5 was assigned to slightly spiky fur, and score of 1 was given to a body area covered with spiky and stained fur. Such coat state assessment has already been validated in UCMS studies and was shown to be responsive to antidepressant treatment (Khemissi et al., 2014).

3.3.2 Sucrose preference (Ducottet and Belzung, 2005)

Sucrose preference is a test measuring the presence of anhedonic behaviour. In this test mice are given a choice of drinking water or a sucrose solution, which due to its sweetness possesses rewarding properties. The preference for sucrose solution over water is considered as hedonic behaviour. Sucrose solution in drinking water at room temperature was prepared from sucrose crystals (Sigma, UK) fresh before the test. The percentage of sucrose used varied between experiments and therefore will be specified in each experimental design sections. Identical bottles with both solutions were placed on either side of a cage lid instead of the regular water bottles with food surrounding the bottles on both sides (see Figure 7C). To account for volume spilled from the bottles, 3 sets of bottles with water and sucrose were set up on empty cages, and volume spilled from these bottles during testing time was calculated. To avoid side preference, the location of the bottles on housing cages was switched during the test. Bottles were weighted before and after the test to measure liquid consumption. After subtraction of average volume spilled in empty cages, sucrose preference was calculated using the formula below:

$$Sucrose\ Preference\ (\%) = \frac{Vol_{\text{sucrose}}}{Vol_{\text{sucrose}} + Vol_{\text{water}}} * 100$$

Equation 1 Sucrose preference calculation,
where $Vol_{sucrose}$ is consumed volume of sucrose solution and Vol_{water} is consumed volume of water

3.3.3 Locomotor activity in a home cage (Lad et al., 2010)

To assess locomotor activity of animals in a familiar environment during the active dark phase, their behaviour in a home cage was recorded (Lad et al., 2010). Mice were transferred to the test room in their own home cage 2 hrs before the beginning of the dark phase. Enrichment materials were removed from the cages and clear, acrylic lids were placed on top of the cage to allow video recording and subsequent activity tracking. Six wetted food pellets were added to the cages to provide food and water throughout the test. The lighting for video recording was provided by red LED cluster lights (LED cluster red light No. 310-6757; RS Components Northants, UK) of approximate wavelength 705 nm which provided minimal red light to allow

video recording of the test. The wavelength of the LED cluster lamps is barely visible to mice due to their limited photonic vision (Jeon et al., 1998). Activity was recorded at the beginning of the dark phase (8.30-11pm), in the middle hour of the dark phase (1-4 am), and at the end of the night (6-8:30 am) using an overhead camera. The distance travelled in the home cage was subsequently tracked using Ethovision software (version 3.1; Noldus IT, the Netherlands).

3.3.4 Open field test (Gould, 2009)

The open field test is a common measure of general activity and anxiety-like behaviour in a novel environment. The anxiety aspect of this test is based on the conflict between exploratory drive and avoidance of a potentially threatening, novel and open space (Gould, 2009). A circular (40cm diameter) open field arena was used (see Figure 7A). During the test the arena was evenly lit with low light (~20 Lux). Each mouse was taken from its cage and placed in the outer part of the arena, facing the outer wall. Behaviours were video recorded for 10 minutes. For the analysis, the automated tracking software EthoVision (Noldus IT, The Netherlands) was used. The time spent in the centre zone (inner 30cm diameter circle) as a measure of anxiety was calculated using EthoVision. In addition, the total distance travelled in the least anxiogenic zone of the area (the remaining outer zone) also was calculated using Ethovision to acquire a measure of locomotor activity which is least confounded by anxiety triggered in the central zone of the arena (Lad et al., 2010).

3.3.5 Novelty-suppressed feeding (Dulawa and Hen, 2005)

Novelty-suppressed feeding (NSF) is a well-described test of anxiety and anhedonic behaviour (Dulawa and Hen, 2005). It is based on a choice faced by a food-deprived mouse forced into a novel environment between engaging in feeding or avoidance of a novel, potential threatening environment (neophobic behaviour). In our experiments mice were food-deprived for 24 hours prior to the test. A large (59.5x38x20cm) novel cage with a thin layer of fresh sawdust was used as a test arena. The food pellet was placed in the middle of the cage on a piece of white cardboard (see Figure 7B). Mouse behaviour in the test arena was video recorded for 5 min. The latency to feed was measured until the time the mouse started eating the pellet. If the mouse did not touch the pellet during the 5 min, its latency was recorded as 300 sec (less than 3 animals per group). After the end of the test mouse was returned into the home cage with the pellet for another 10 min. The weight of the pellet before and after the test, as well as after 10 min in the home cage was recorded to measure food intake in a novel and familiar environment.

3.3.6 Splash test (Surget and Belzung, 2009)

The splash test is quantitative measure of grooming behaviour. It has been developed by Catherine Belzung's group to be used in the UCMS model (Surget and Belzung, 2009). The test was performed once at the end of the UCMS paradigm according to Nollet et al. (2013). The animals were sprayed with approximately 0.5ml of 10% sucrose solution on the back and transferred to a novel cage devoid of any enrichment. Their latency to start, and time spent, grooming were recorded over 5 min.

3.3.7 Light-dark box (Crawley and Goodwin, 1980)

The light-dark box is another test to measure exploratory behaviour in the anxiogenic environment of a brightly lit arena. Unlike the open field, animals have a choice whether to stay in a "safe" dark chamber or venture into the brightly lit (100 Lux) light chamber, with latency to enter, and time spent in, the light area used as measures reflecting the anxiety-like behaviour of the experimental animal (Crawley and Goodwin, 1980). For this test, a white acrylic box 44×21×21 cm was used. The box was separated by a white acrylic sheet, 21×50 cm, into a smaller dark chamber (15×21×21 cm) with low lighting (10–15 Lux) and a bigger brightly lit light chamber' (100Lux) (see Figure 7D). The chambers were connected by a small entry within the partition (5×7 cm). At the beginning of the test, the mouse was taken from its home cage and placed into the dark chamber facing the wall opposite the partition. Activity in the light–dark box was video-recorded for 5 min. Latency to enter, the time spent and activity in, the light chamber were scored using the Ethovision software and manually scored. A mouse was considered to enter the chamber when all four paws crossed the partition.

3.3.8 Forced swim test (Lucki et al., 2001)

The forced swim test originally developed in rats by Porsolt et al. (1977) is interpreted to reflect behavioural despair in an inescapable stress situation, with antidepressant drugs robustly reducing immobility in this test (Powell et al., 2012). Mice were placed in a clear acrylic cylinder filled with 40 cm of water at room temperature for 6 minutes (see Figure 7E). For each type of behaviour, the latency of first appearance and its duration throughout the test period were manually scored from the recordings using the Ethovision software. Swimming was defined as movement of the limbs and body in a horizontal posture, paddling as movement of 2 or more paws in a horizontal posture without directed body movement (Belozertseva et al., 2007). An animal was considered to be immobile if passive floating was observed with only movements necessary to keep the head above water. Finally, struggling also known as climbing (Cryan and Mombereau, 2004) was defined as vertical posture with limb movement. To measure the HPA axis response to the swimming stress, tail vein blood

was collected 24 hours before (baseline measure) and 30 min after the forced swim test for subsequent corticosterone analysis.

3.3.9 Social interaction (Winslow, 2003)

To investigate social behaviours, test mice were exposed to an unfamiliar, sex-matched juvenile conspecific. Study mice were placed into a clean cage with fresh sawdust where conspecifics were subsequently introduced. Behaviours were video recorded for 5 min. Subsequently various types of social and non-social behaviours were manually scored using Ethovision. Social behaviours included investigative (sniffing and following), affiliative (grooming) and play soliciting (pushing over or under the conspecific). Non-social behaviours were considered to be self-grooming, cage exploration and digging. Biting and tail rattling were scored as aggressive behaviours (Winslow, 2003).

3.3.10 Buried cookie test (Yang and Crawley, 2010):

Olfactory information is essential for a wide range of mouse behaviours, including social interaction and food reward behaviours. It is therefore important to assess ansomia (absence of sense of smell) to rule this out as a confounder. Small chocolate cookies (Nestle Cookie Crisp®, Welwyn Garden City, U.K.) were used as the palatable food as previously described (Grayton et al., 2013). A cookie was placed in the home cage of each mouse for three consecutive days to habituate them to the taste. On the day of the test, each mouse was placed into a clean cage containing 5cm of fresh sawdust (Litaspen premium, Datesand Ltd, Manchester) and left to habituate in the test room for 5 minutes. (The light level in the test room was 10 Lux). The mice were then removed from the cage while a cookie was hidden 2 cm below the surface of the sawdust at the top of the cage. The mouse was returned to the cage and placed facing the wall on the side of the cage furthest from the cookie. The latency for the mouse to find and start eating the cookie was recorded.

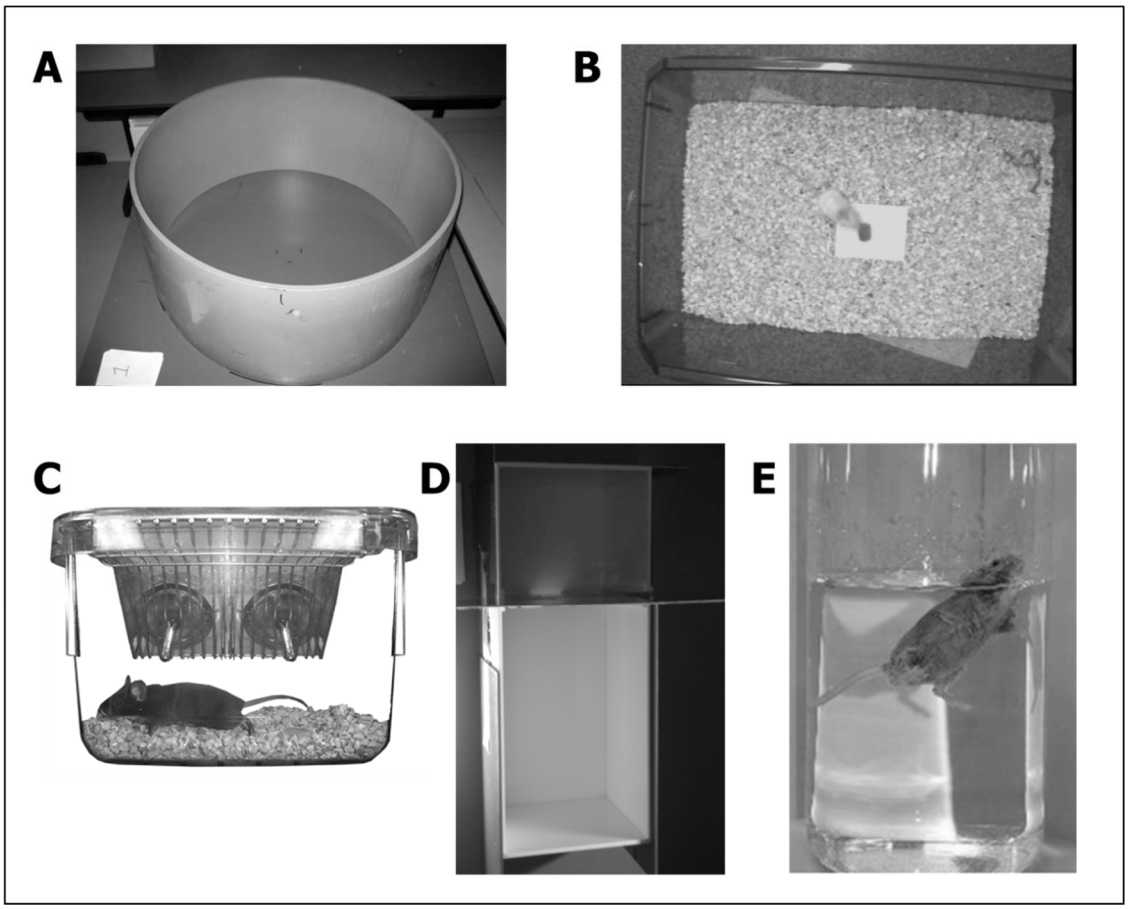

Figure 7 Examples of some behavioural tests used in UCMS experiments.
(A) A 40cm diameter arena used in the open field test (B) Mouse approaching the pellet in the middle of a novel large cage used in novelty-suppressed feeding test (C)Mouse exposed to a choice between sucrose solution and water in bottles set up for the sucrose preference test (D) A box separated into a smaller dark chamber (10–15 Lux) and a bigger brightly lit light chamber (100Lux) with a small entry in between the compartments used in the light-dark box test. (E) A mouse swimming in the inescapable cylinder filled with water in the Porsolt forced swim test

3.4 Blood collection

For cytokine and corticosterone analysis blood was collected by incision method from the lateral tail vein (Sadler and Bailey, 2013). The timing of blood collection was dependant on the experimental design and is specified in individual experimental sections. Whole blood (30-50 µL) was collected into EDTA microvette CB 300 tubes (Sarstedt, Leicester, UK) and separated by centrifugation for 10min at 3000 rpm (4°C), after which plasma was manually transferred into a new sterile tube (1.5ml 'Crystal clear' microcentrifuge tube sterile, Starlab UK Ltd) and stored at -80°C. Blood was also collected by the cardiac puncture after the terminal general anaesthesia has been induced by the injection of 100 µL of Euthatal i.p. (Merial Animal Health Ltd, Harlow, UK) containing 20 mg of pentobarbital sodium. 100-200 µL of whole blood was collected using syringe injected into the cardiac cavity and subsequently processed as described above.

3.5 Corticosterone measurement

Plasma corticosterone levels were measured using commercially available corticosterone enzyme-linked immunosorbant assay kit (ELISA, Enzo Life Sciences, Lausen, Switzerland) according to the manufacturer's instructions for small sample volume. Briefly, 10µL of plasma was diluted 1:40 with steroid displacement reagent and ELISA buffer. To generate standard curve serial dilutions of 200ng/µL corticosterone were used. Technical duplicates of 40 samples and 5 serial standard dilutions were added to the plate wells precoated with donkey anti-sheep IgG. Anti-corticosterone ELISA antibody raised in sheep was added to each well together with ELISA conjugate for 2-hour incubation on a shaker. After incubation wells were thoroughly washed with assay buffer and enzyme substrate was added to the wells. Reaction was stopped after 1 hour with trisodium phosphate solution. The optical density was read on a microplate reader at 450nm wavelength. Obtained data was analysed using five parameter logistic curve analysis using the My Assays online data tool, MyAssays Ltd., http://www.myassays.com/five-parameter-logistic-curve.assay. Specifically, the standard dilution data points (known concentration of standard dilution vs. obtained absorbance measurement) are plotted on semi-log axes and a 5 parameter standard curve is fitted through the points using logistical regression. The concentrations of the samples are then determined from the fit of the curve based on their obtained absorbance values. Background correction was applied by subtracting absorbance level obtained from blank wells in which no corticosterone was present. An example of the corticosterone standard curve is shown in Figure 8.

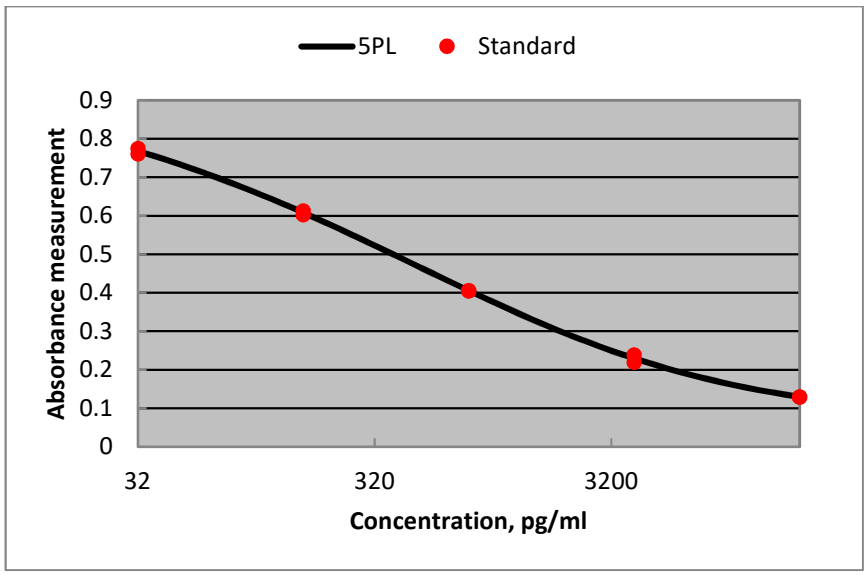

Figure 8 Example corticosterone ELISA standard curve fitted through the standard dilution datapoints. The datapoints were subsequently used to calculate unknown concentration of corticosterone in blood samples collected during the experiments based on their absorbance measurements in the assay. Datapoints for each standard dilution (20000, 4000, 800, 160 and 32 pg/ml) in technical duplicates are shown in red.

Average intrassay coefficient of variability (%CV) for duplicates is estimated at %CV=11. Average interassay variability for ELISA plates is estimated at %CV=4.6. %CV was calculated according to Equation 2:

$$\%CV = \frac{SD}{mean} * 100$$

Equation 2 %CV calculation for sample duplicates or control duplicates from different plates, where SD is standard deviation and mean calculated for the two sample duplicates included on a plate or controls on different plates.

3.6 Luminex

The level of cytokines in the plasma was determined using the multiplex screening assay based on magnetic Luminex® xMAP® technology as described in Hye et al. (2014). For this assay custom-made pre-mixed multianalyte kit was purchased from RnD systems, Minneapolis, USA (catalogue N LXSAMSM). This kit contained multi-coloured magnetic microparticles pre-coated with antibodies to 10 selected analytes (granulocyte-monocyte colony stimulating factor (GM-CSF), interleukins IL-1β, IL-2, IL-4, IL-5, IL-6, IL-10, tumour necrosis factor alpha (TNFα) and interferon gamma (IFNγ). C-reactive protein (CRP) and leptin were added to the panel in the UCMS Experiment 3. Sensitivity of the assay to each cytokine is presented in Table 3. To measure the fluorescent signal Luminex® 100/200™ system was used. Plasma samples were diluted 1:2 in calibration buffer, and all assay steps were conducted according to the manufacturer instructions. Due to small sample sizes technical replicates for plasma samples were not included. Intra-assay variability based on duplicates of the standard dilutions is estimated at 2.15 %CV. Inter-assay variability has not been calculated as all samples from one

experiment were analysed on a single plate. Obtained data was analysed using five parameter logistic curve analysis using the My Assays online data tool, MyAssays Ltd., http://www.myassays.com/five-parameter-logistic-curve.assay.

Table 3 Minimal detectable dose (MDD) of each analyte in the Luminex assay used in UCMS experiments for cytokine analysis as stated by the manufacturer

Analyte	MDD, pg/ml
GM-CSF	1.64
IL-1 beta	41.8
IFN-gamma	1.85
IL-2	0.481
IL-4	53.0
IL-5	0.237
IL-6	2.30
IL-10	8.20
IL-12	12.8
TNF-alpha	1.47
CRP	13.3
Leptin	12.6

3.7 Drug administration

All injections were administered intraperitoneally (i.p.). Fluoxetine powder was purchased from R&D Systems (Abingdon, UK), and dissolved in 0.9% saline (Aquapharm, Argyll, UK) saline to a 2.5 mg/ml solution. Fluoxetine solutions were kept at -20°C and freshly thawed on the day of injections. Fluoxetine was administered at a volume of 8 ml/kg in the UCMS Experiment 1 (20mg/kg) and 4 ml/kg in the UCMS Experiment 2 (10mg/kg) adjusted to individual mouse body weight. Both doses administered i.p. to BALB/c mice have been shown to effectively alleviate the depression-like behaviour and increase adult hippocampal neurogenesis (Santarelli et al. 2003; Surget et al. 2008). Vehicle-only treated groups received daily injections of saline at a volume of 8 ml/kg calculated for an average 25g mouse (200 µL in the UCMS Experiment 1 and 100µL in the UCMS Experiment 2).

3.8 Statistical analysis

In the UCMS Experiments 1 and 2 data was analysed using either a 2-way ANOVA or a 2-way repeated measures ANOVA, as appropriate. The between-factors were stress exposure and drug treatment, and within-factors time or test session. For post-hoc analysis of significant factors and/or interaction Bonferroni multiple comparisons method was used. In the UCMS Experiment 3 a Student's t-test or a Mann-Whitney test was used if assumption of normality was violated in a particular dataset. The only exception from these protocols was made for the

ordinal coat state data, which was analysed week by week using non-parametric Kruskal-Wallis test and Dunn's multiple comparisons corrections for post-hoc between-group comparisons.

Statistical tests were applied using IBM SPSS Statistics 22 (IBM SPSS Inc., USA) and GraphPad Prizm 6 (GraphPad Software Inc., USA) software. Data is presented as mean ± SEM, statistical significance was assumed at $p \leq 0.05$.

4 UCMS Experiment 1

4.1 Experimental design

The aim of this pilot UCMS experiment was to test out the UCMS protocol and behavioural tests which results have been shown to be affected by UCMS in the previous literature. Chronic treatment with 20mg/kg fluoxetine (FLX), a dose which has been shown to counteract the UCMS effect on behaviour and adult hippocampal neurogenesis (Surget et al., 2011; Tanti et al., 2013), was used. The following treatment groups were included in this experiment (N=12 per group): CNTRL – pair housed animals in standard mouse cages with standard enrichment, injected with 0.9% saline daily from the 3rd week of UCMS exposure; UCMS – single housed animals exposed to 2 stressors per day in random-like order according to the protocol in Table 4, injected with 0.9% saline daily from the 3rd week of UCMS exposure; CNTRL FLX – pair housed animals in standard mouse cages with standard enrichment, injected with fluoxetine (20 mg/kg) daily from the 3rd week of UCMS exposure; UCMS FLX – single housed animals exposed to 2 stressors per day according to the protocol in Table 4, injected with fluoxetine (20 mg/kg) daily from the 3rd week of UCMS exposure; CNTRL NO INJECT - pair housed animals in standard mouse cages with standard enrichment, not injected. Timeline of experimental procedures is represented in Figure 9.

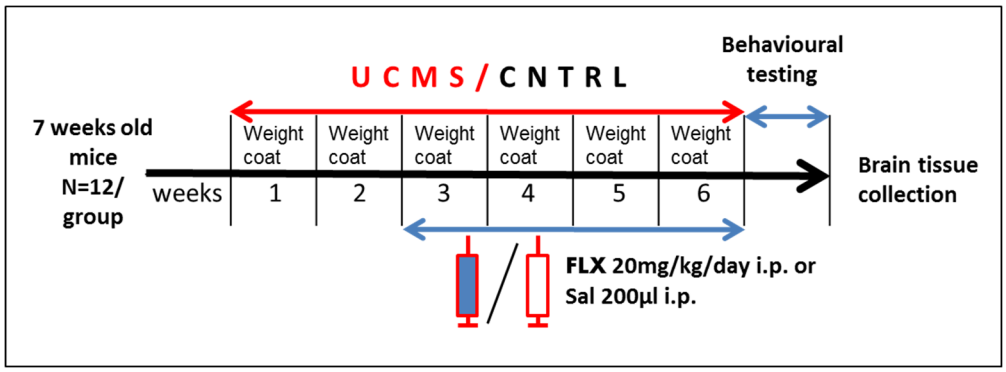

Figure 9 Timeline of experimental procedures in the UCMS Experiment 1.
Treatment groups (n=12) were exposed to UCMS or control conditions for 6 weeks; fluoxetine (20mg/kg/day) or saline injections commenced on the 2nd week of UCMS. All treatments ceased at the end of 6th week when behavioural testing began, followed by animal cull

Table 4 Schedule of stressors used in the UCMS Experiment 1.
The schedule was developed based on protocols by (Mutlu et al., 2012; Surget and Belzung, 2009) *with modifications. Control group animals were housed in a separate holding room to avoid exposure to stressors. All mice were weighed and their coat state was assessed each week on Monday morning (9am) before any stress exposure was applied. Fluoxetine and saline i.p. injections were administered each day on weeks 3-6 at 9am to CNTRL and UCMS groups.*

	Stressor 1	**Time**	**Stressor 2**	**Time**		**Stressor 1**	**Time**	**Stressor 2**	**Time**
Week 1					**Week 4 FLX/Saline injections – 9am each day before the stress exposure**				
day 1	**coat state, weighing**		cage tilt	15-18.00	day 1	**coat state, weighing**		cage tilt	15-17.30
day 2	cage swap	10.00-12.30	no bedding	15-16.30	day 2	water in the cage	10.00-10.30	no bedding	10.30-12.00
day 3	cage tilt	13-15.00	lights on	night time	day 3	cage tilt	11-14.00	white noise	16-17.00
day 4	water in the cage	14-14.30	white noise	16-18.00	day 4	air puff	10-12.30	lights on	night time
day 5	wet bedding	12-14.00	no bedding	14-15.00	day 5	cage swap	13-15.00	bedding after cage swap	o/n
day 6	white noise	11.-13.00	nothing		day 6	wet bedding	12-12.30	no bedding	12.30-15.00
day 7	air puff	14-16.00	lights on	night time	day 7	white noise	15.00-17.00	lights on	night time
Week 2					**Week 5 FLX/Saline injections – 9am each day before the stress exposure**				
day 1	**coat state, weighing**		water in the cage	11-11.30	day 1	**coat state, weighing**		cage tilt	16-19.00
day 2	cage tilt	11-15.00	white noise	16-17.00	day 2	cage swap	11-14.00	bedding after cage swap	o/n
day 3	cage swap	10-13.00	no bedding	13-15.00	day 3	wet bedding	11-12.00	no bedding	12-14.30
day 4	cage tilt	14-17.00	lights on	night time	day 4	cage tilt	12-15.00	lights on	night time
day 5	wet bedding	13-14.00	no bedding	14-15.30	day 5	no bedding	10-12.00	water in the cage	12-12.30
day 6	air puff	12-14.30	lights on	night time	day 6	white noise	12-14.00	nothing	
day 7	nothing		nothing		day 7	air puff	15-17.00	lights on	night time
Week 3 Start of FLX/Saline injections – 9am each day before the stress exposure					**Week 6 FLX/Saline injections – 9am each day before the stress exposure**				
day 1	**coat state, weighing**		no bedding	16-17.30	day 1	**coat state, weighing**		cage tilt	15-18.00
day 2	air puff	15-15.30	white noise	17-19.00	day 2	cage swap	12-15.00	bedding after cage swap	o/n
day 3	cage tilt	11-14.00	lights on	night time	day 3	wet bedding	11-13.30	no bedding	13.30-15.00
day 4	water in the cage	11-11.30	cage tilt	14-17.00	day 4	cage tilt	11-14.00	air puff	15-16.30
day 5	wet bedding	13-15.00	no bedding	15-17.30	day 5	water in the cage	10-10.30	no bedding	10.30-13.30
day 6	air puff	11-13.00	nothing		day 6	air puff	14-15.00	lights on	night time
day 7	white noise	16-18.30	lights on	night time	day 7	nothing		white noise	16-16.30

Behavioural were assessed during the UCMS (coat state score, locomotor activity in the home cage) and after its termination (all other behavioural tests). Coat state was assessed once a week as indicated in Table 4. For the locomotor activity assessment on the last week of the

UCMS exposure 10 animals were video recorded in their home cages each night for the 6 last nights of UCMS. Groups were counterbalanced across nights to minimise possible variations depending on the day of the UCMS. At the end of the UCMS exposure mice were not disturbed for 1 day (rest day) before their behavioural testing began. The order of behavioural tests and number of animals tested each day is indicated in Table 5. Groups were counterbalanced between 2 days for each test and throughout each day to minimise batch effect and effect of the time of day when testing was performed. All animals were tested between 9am and 4pm. Daily behavioural testing schedules were analogous to those shown in Table 7 and Table 9. For the sucrose preference test, 4% solution was freshly prepared on the day of the test. The concentration was selected based on a pilot test with 4 animals, which all showed strong preference for this concentration of sucrose over water.

Table 5 Schedule of behavioural tests in the UCMS Experiment 1.
Animals were left undisturbed for 1 day after the end of the UCMS protocol (Rest day), after which testing battery of anxiety and depression-related behavioural tests was applied. Numbers on grey background signify mouse identification numbers tested on particular day. FST – forced swim test

TESTING DAY	DAY1	DAY2	DAY3	DAY4	DAY5	DAY6	DAY7
Rest day	1-30	31-60					
Open field		1-30	31-60				
Novelty suppressed feeding			1-30	31-60			
Sucrose preference				1-30	31-60		
Pre-FST blood collection					1-30	31-60	
Forced swim test						1-30	31-60

4.2 Results

4.2.1 UCMS did not affect body weight of mice, but coat state of UCMS-exposed mice deteriorated from week 4

UCMS did not affect weekly rise of body weight in experimental groups as shown by 2-way ANOVA analysis (Effect of Time $F(7, 371) = 227.8$, $p < 0.0001$; Effect of Treatment group $F(3, 53) = 1.032$, $p = 0.3859$; Interaction $F(21, 371) = 2.870$, $p < 0.0001$). However, it was observed that in FLX groups, there was no weight gain over the first week of FLX injections (see Figure 10A). The coat state of UCMS-treated groups was significantly worse than in control groups

from week 4 of the protocol (see Figure 10A). More specifically, there was a significant effect of treatment group on coat state on week 4 (Kruskal-Wallis H(4)) = 10.8 p = 0.0129), week 5 (Kruskal-Wallis H(4)) = 10.01 p = 0.0185) and week 6 (Kruskal-Wallis H(4)) = 10.17 p = 0.0172). A slight increase in the coat deterioration score was also observed in control groups, potentially due to cage mate fighting. Interestingly, coat state was significantly different between CNTRL and CNTRL NO INJECT group on week 6 (Mann-Whitney U=39.5, p=0.029), suggesting an effect of i.p. injections. FLX did not affect coat state in control or UCMS exposed groups (see Figure 10B).

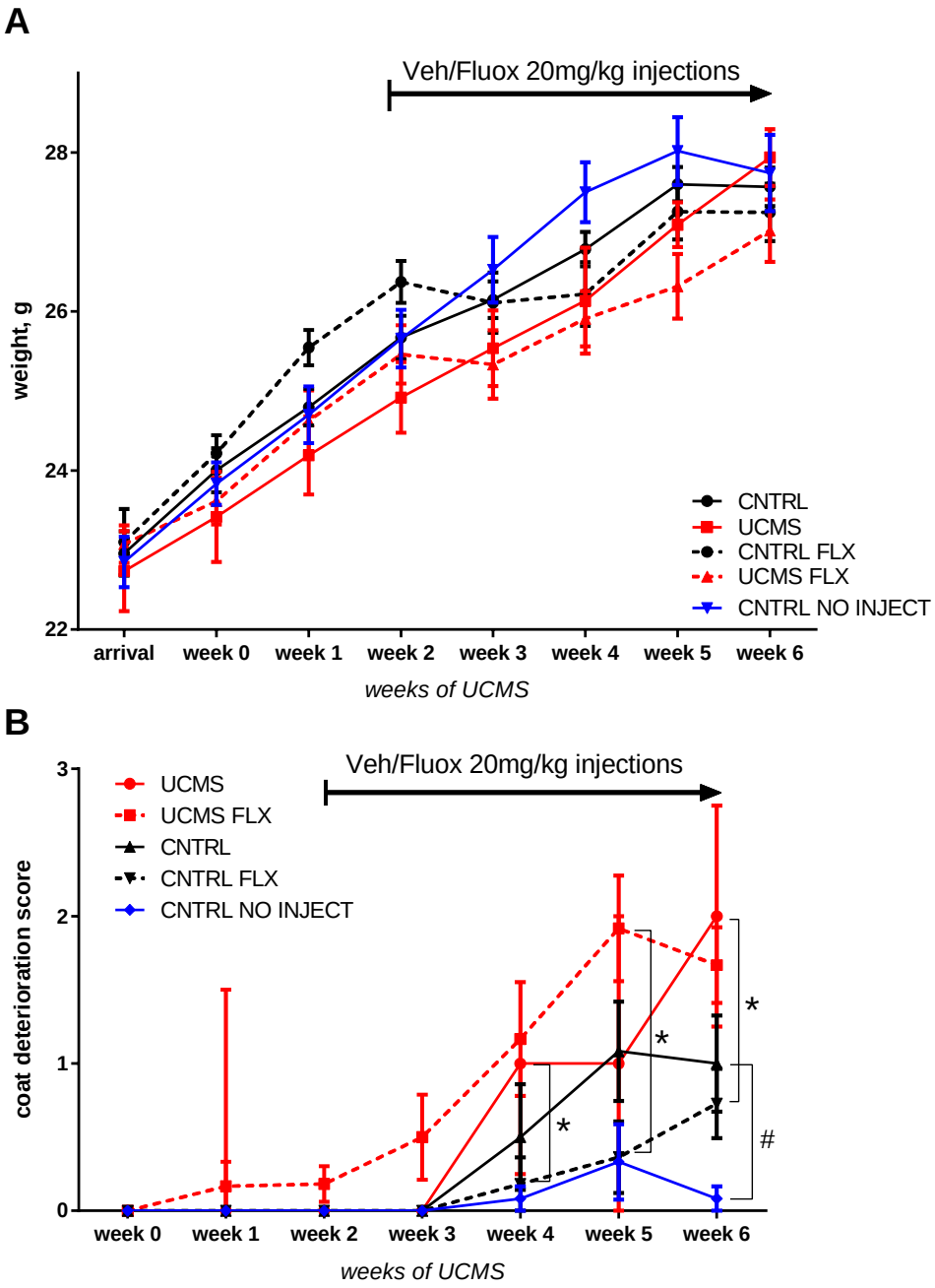

Figure 10 Weight and Coat state change in the UCMS Experiment 1

*Weight and Coat state change of 8 weeks old male BALB/c mice exposed to unpredictable chronic mild stress (UCMS) or control conditions (CNTRL) for 6 weeks and treated with fluoxetine 20mg/kg (FLX) or saline i.p. daily for 4 weeks, n=12/group **(A)** Body weight measured weekly during the UCMS (n=12/group, data represents mean±SEM) **(B)** Coat state scored weekly on the coat deterioration score (Nollet et al., 2013) (*p < 0.05 derived from post-hoc Dunn's multiple comparisons between groups joined by brackets on the figure; #p< 0.05 derived from Mann-Whitney test between CNTRL and CNTRL NO INJECT groups on week 6). Data presented as Median and interquartile range*

4.2.2 UCMS did not affect home cage locomotor activity during the dark phase

Locomotor activity data from early, mid and late (early morning) phases of the dark phase was analysed using 2-way ANOVA (Figure 11A, B and C). Neither UCMS nor FLX treatments affected locomotion in the early dark phase (UCMSxFLX F (1, 30) = 0.06885, p = 0.7948; FLX F (1, 30) = 0.1600, p = 0.6920; UCMS F (1, 30) = 0.3134, p = 0.5798), mid dark phase (UCMSxFLX F (1, 30) =

0.001231, p = 0.9722; FLX F (1, 30) = 1.266, p = 0.2694; UCMS F (1, 30) = 2.459, p = 0.1273) or late dark phase (UCMSxFLX F (1, 30) = 0.4507, p = 0.5071; FLX F (1, 30) = 0.04166, p = 0.8397; UCMS F (1, 30) = 0.3290, p = 0.5705).

Comparison between CNTRL and CNTRL NO INJECT groups conducted by means of unpaired t-test also showed no effect of injections in the early (F(18)=1.068, p=0.9444), mid- (F(18)=2.487, p=0.1783) or late dark phase (F(18)=1.402, p=0.6716).

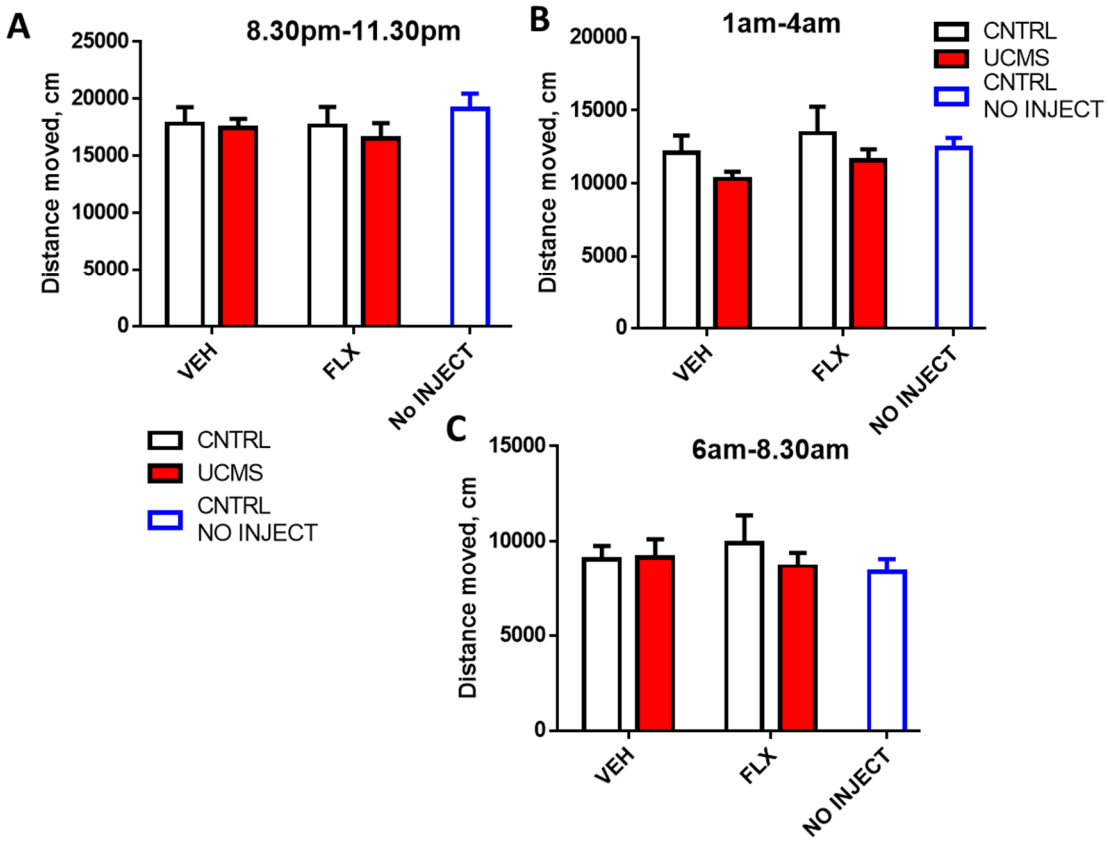

Figure 11 Locomotor activity during dark phase in the UCMS Experiment 1
*Locomotor activity during dark phase of adult male BALB/c mice exposed to unpredictable chronic mild stress (UCMS) or control conditions (CNTRL) for 6 weeks and treated with fluoxetine 20mg/kg (FLX) or saline (VEH) i.p. daily for 4 weeks, n=12/group **(A)** Distance moved in the home cage in the early dark phase **(B)** Distance moved in the home cage mid-dark phase **(C)** Distance moved in the home cage of mice late in the dark phase. Data represents mean±SEM*

4.2.3 UCMS did not induce anhedonia, but UCMS-exposed mice displayed reduced anxiety

Anxiety-like behaviour was measured in a novel anxiogenic open field test arena. Analysis of the locomotion in the novel environment data by 2-way ANOVA revealed main effect of interaction (UCMS x FLX F (1,40) = 8.1, p = 0.007), and of UCMS exposure (UCMS F (1,40) = 4.44, p = 0.04; FLX F (1, 40) = 0.031, p = 0.862) (see Figure 12A). 2-way ANOVA of the time spent in the centre zone, the measure of anxiety in the open field, showed significant effect of

UCMS (UCMS F (1,41) = 7.44, p = 0.009; FLX F (1, 41) = 0.112, p = 0.739; UCMSxFLX F (1, 41) = 1.472, p = 0.232) (Figure 12B). 2-way ANOVA of NSF and sucrose preference data showed that neither treatment exerted any effect on the anhedonia-like behaviours measured in these tests (see Figure 12C and D) (NSF UCMSxFLX F (1, 41) = 0.045, p = 0.833; FLX F (1, 41) = 0.126, p = 0.725; UCMS F (1, 41) = 0.002, p = 0.963; Sucrose preference UCMSxFLX F (1, 40) = 0.842, p = 0.364; FLX F (1, 40) = 0.008, p = 0.931; UCMS F (1, 40) = 1.429, p = 0.239). Comparison between CNTRL and CNTRL NO INJECT done by means of unpaired t-test did not reveal any significant difference (OF Distance t(21) = 1.814, p = 0.084; OF Centre time t(21) = 1.4, p = 0.17; Sucrose preference t(21) = 0.711, p = 0.485; NSF t(21) = 0.25, p = 0.807)

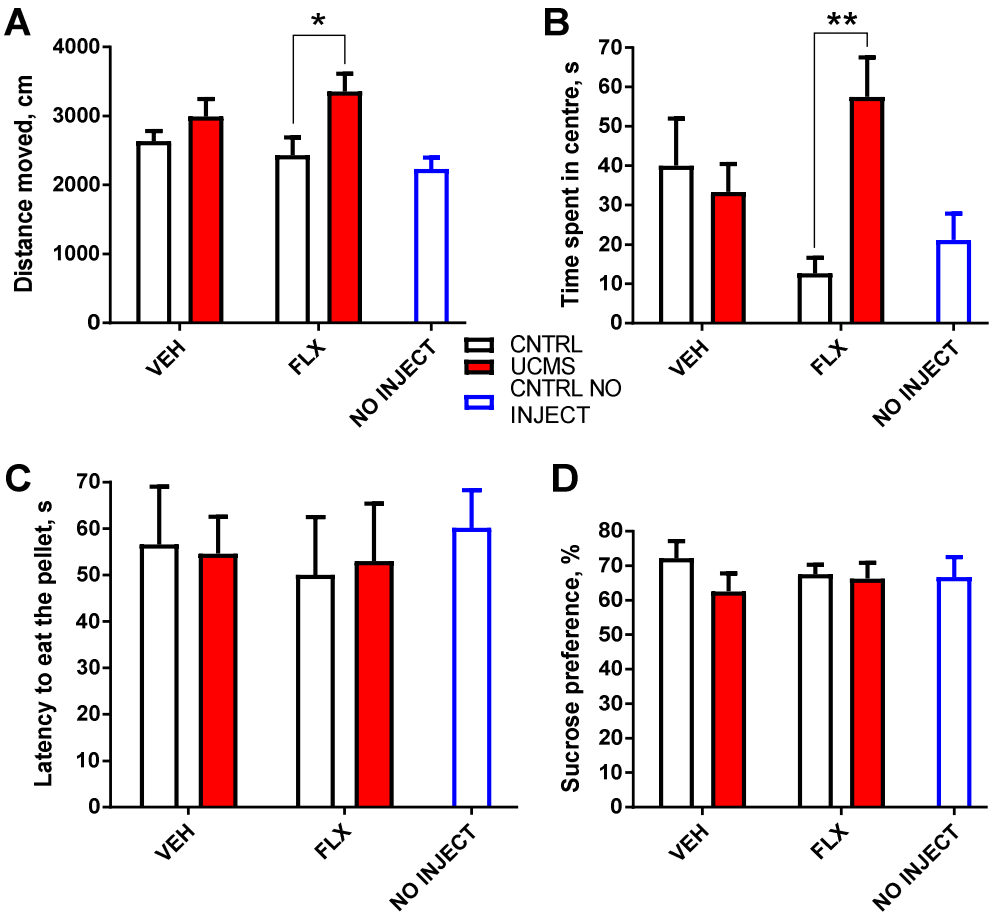

Figure 12 Anxiety and anhedonia-like behavioural measures in the UCMS Experiment 1

Anxiety and anhedonia-like behavioural measures of adult male BALB/c mice exposed to unpredictable chronic mild stress (UCMS) or control conditions (CNTRL) for 6 weeks and treated with fluoxetine 20mg/kg (FLX) or saline (VEH) i.p. daily for 4 weeks, n=12/group. ***(A)*** *Distance travelled in the open field arena as a measure of locomotor activity* ***(B)*** *Time spent in the centre zone of the open field arena used as a correlate of anxiety-like behaviour* ***(C)*** *Latency to begin eating the pellet in the novelty suppressed feeding trial* ***(D)*** *Preference for 4% sucrose over water measured over 48 hours as an indicator of the anhedonia – like behaviour. Data represents mean±SEM, *p > 0.05, **p>0.005 derived from post-hoc Bonferroni multiple comparisons between groups joined by brackets in the figures.*

4.2.4 UCMS did not induce behavioural despair parameters in the forced swim test

Latency of first immobility and time spent immobile during the FST where analysed as parameters of behavioural despair using 2-way ANOVA (see Figure 13A). Latency of immobility was not affected by any of the treatments (UCMSxFLX F (1, 40) = 0.738, p = 0.395; FLX F (1, 40) = 0.476, p = 0.494; UCMS F (1, 40) = 0.543, p = 0.465). However FLX was a significant factor in the time of immobility FLX F(1,40) = 12.61, p = 0.001; UCMSxFLX F (1, 40) = 3.119, p = 0.085; UCMS F (1, 40) = 0.017, p = 0.896). Interestingly, the time spent immobile was reduced in the CNTRL injected group compared to the non-injected control group (Unpaired t-test t(21) = 2.626, p = 0.017, suggesting a potential effect of repeated injections (see Figure 13B). This effect however was not apparent in the analysis of the latency of immobility data between the two groups (t(21)=0.425, p = 0.6756).

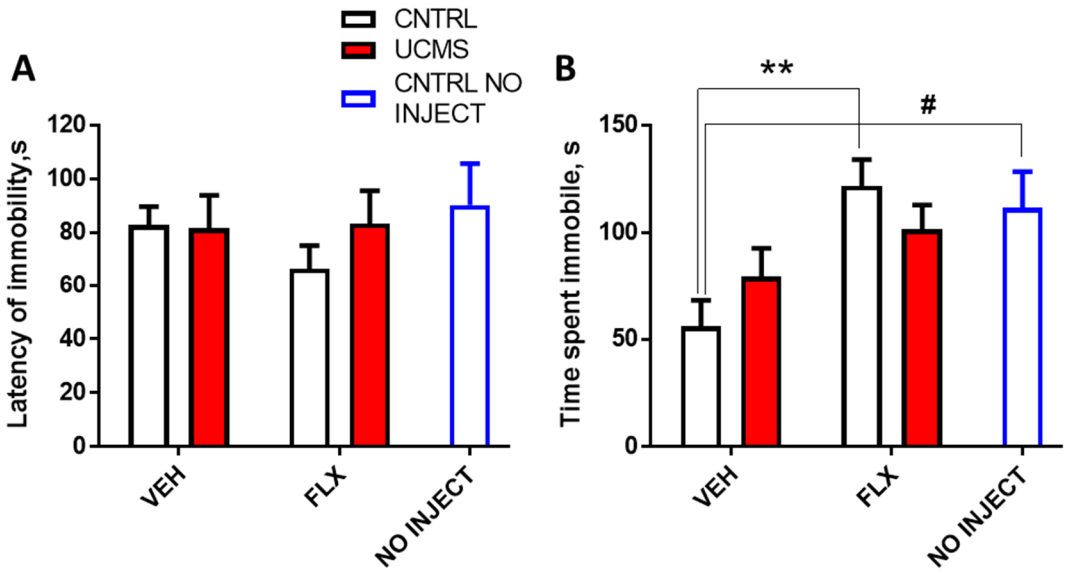

Figure 13 Forced swim test (FST) parameters measured in the UCMS Experiment 1
Forced swim test (FST) parameters measured in the adult male BALB/c mice exposed to unpredictable chronic mild stress (UCMS) or control conditions (CNTRL) for 6 weeks and treated with fluoxetine 20mg/kg (FLX) or saline (VEH) i.p. daily for 4 weeks, n=12/group. ***(A)*** *Latency of first immobility* ***(B)*** *Total time spent immobile during the FST trial time. Data represents mean±SEM, **p>0.005 derived from post-hoc Bonferroni multiple comparisons between groups joined by brackets on the figure; #p=0.017 derived from unpaired t-test between CNTRL and CNTRL NO INJECT groups*

4.3 Discussion

While multiple studies have shown that UCMS can reduce the rate of body weight gain in mice (Nollet et al., 2011; Surget, Wang, et al., 2008), no effect of body weight gain was observed in this study. This might be suggestive of an insufficient intensity of stressors. At the same time some studies show effective UCMS in the absence of weight change (Mutlu et al., 2012; Surget, Saxe, et al., 2008). A study by Schweizer et al (2009) showed that the effect of UCMS

on body weight can be substrain-dependant, as one substrain of C57BL6 mice showed a reduction of body weight gain upon UCMS while another substrain did not. It is therefore possible that the Balb/cAnNCrl substrain used in this study does not respond to chronic stress with a change in body weight gain, as it differs from the BALB/cByJ substrain frequently used in UCMS studies. While describing the UCMS protocol, Nollet and colleagues (2013) pointed out that due to a varied effect of UCMS on body weight its change should not be a primary measure of the success of the UCMS protocol. Moreover, Strekalova and coworkers (2011a) suggested that body weight differences between groups are not desirable, as they might trigger difference in liquid consumption and subsequently alter the results of sucrose preference test, which assesses anhedonic behaviour. Therefore, absence of body weight differences among groups might be a positive finding. However, during the first week of injections, body weight remained constant in FLX treated groups. The weight reducing effect of fluoxetine at similar doses has been described previously in rodents. For example, Kroeze et al. (2015) showed that treatment of adult Wistar rats with 12mg/kg FLX by gavage significantly reduced their body weight from day 4 of treatment. Aggarwal et al. (2016) showed that treatment of albino rats with 20mg/kg FLX for 2 weeks led to their weight reduction, while treatment with 40mg/kg led to animal death associated with gastrointestinal adverse effects. In mice appetite-suppressing effects of SSRI were attributed to their activation of 5HT2C and 5HT1B receptors in the hypothalamus (Nonogaki et al., 2007). While this effect did not lead to significant weight differences in FLX-treated groups, it suggested that the dose of fluoxetine used in the next experiment should be reduced.

Coat deterioration score monitoring across the weeks of UCMS showed that UCMS increased in coat state score albeit only from the 4^{th} week of treatment, while many studies report significant increase already after 2 weeks of stress exposure (Law et al., 2016; Mutlu et al., 2012). Additionally, the score reached by the UCMS groups was somewhat lower than those reported in previous studies, again suggesting there may have been an insufficient intensity of the stress protocol used. Importantly, on the last week of UCMS exposure coat score in the injected control group was also significantly higher than that of the non-injected controls, indicating a level of stress induced by i.p. injections. Additionally, some fighting and increased aggression were observed in some of the paired housed control mice, which could have provided an additional source of stress.

Results of the open field test showed that UCMS and FLX treatment affect anxiety-related behaviours in BALB/c mice. UCMS-exposed group treatment with the antidepressant displayed signs of hyperactivity in the open field arena, as demonstrated by increased distance travelled

and time spent in the anxiogenic centre zone. While UCMS has been shown previously to increase locomotion of exposed animals in the novel arena (Mineur et al., 2006), the role of FLX in these effects remains a concern. The absence of anxiety-like behaviour in UCMS-exposed groups could be attributed to the low lighting conditions of the testing room, which could have limited the anxiogenic effect of the testing conditions.

Similarly, the effect of FLX on the CNTRL group in the forced swim test suggests that chosen dose of FLX exerted effects in CNTRL mice. Such an effect of FLX in FST has been shown previously to be dose-dependent (Doosti et al., 2013), therefore it became apparent that a reduction of the FLX dose should be considered for the next experiment. At the same time comparison between injected and non-injected control groups showed that daily exposure to i.p. injections decreased immobility time in the FST trial. It is important to note that FLX-treated mice displayed level of immobility similar to that of the non-injected group, resembling rescuing effect of the FLX treatment albeit in an unexpected direction. Indeed, considering disagreements in the interpretation of the FST which exist in the current literature (Nestler and Hyman, 2010) the unexpected direction of this effect may not readily diminish the implication of these findings.

Finally, the lack of changes in the NSF and sucrose preference tests suggested that UCMS protocol utilised was not optimal and/or sufficiently intense to result in depression-like behaviours. At the same time, it is possible that lack of phenotype in these tests was due to the limitations of the behavioural methodology, such a single-day exposure to sucrose might have not allowed the animals to habituate to the taste of sucrose and display group differences in its preference.

5 UCMS Experiment 2

5.1 Experimental design

In the design of the UCMS Experiment 2 the findings of the UCMS experiment 1 were taken into account. As such, to avoid fighting in control group, control animals were singly housed in standard mouse cages. To intensify the effect of UCMS, a new stressor schedule included 4 stressors per day instead of 2 as was done previously (seeTable 6). To minimise the predictability of the stressors, the duration of each stress exposure was increased across the weeks of UCMS, but to avoid habituation during later weeks the stressors overlapped in time. Confinement in a wire mesh cup was added to the list of stressors used. Finally, the length of UCMS exposure was extended to 8 weeks. However due to increased mortality in the UCMS

group during 7th week UCMS exposure was terminated at the end of that week (see Figure 14). Unexpected adverse effects were discussed with the named veterinary surgeon and communicated to the Home Office by the project licence holder. After the commencement of increase in mortality in experimental groups additional monitoring of mice was introduced. This included daily checks for any adverse signs of ill-health or discomfort such as reduced mobility, piloerection, laboured breathing, hunched posture, excessive vocalisation, lack of normal movement in the cage or signs of infection. However, the onset of health deterioration was rapid as mice found dead in the morning did not show any signs of health deterioration the previous evening, therefore it was not possible to apply intervention procedures or humane endpoints to relieve animal suffering. The UCMS exposure was terminated immediately after the 3rd death (25%) occurred in the UCMS group, however 3 more mice died during the next week. The carcasses were subjected to post-mortem examination for gross anatomical abnormalities, however none were found. Behavioural testing was delayed for 3 days to allow animals to recover from UCMS exposure.

To avoid the side effects of fluoxetine in CNTRL mice, its dose was reduced from 20 to 10 mg/kg, as this lower dose has also been shown to be effective in reversing the behavioural and neurobiological effects of UCMS (Santarelli, 2003a; Tanti et al., 2012). In addition, FLX treatment continued during behavioural testing to avoid possible withdrawal effects. Experimental groups were the same as in the UCMS Experiment 1 (CNTRL, CNTRL FLX, UCMS, UCMS FLX, N=12 per group) with the exclusion of NO INJECT group, as the data on the effect of injections was already collected in the UCMS Experiment 1. In addition to behavioural measures, in this experiment blood samples were collected to assess the response of the HPA axis and the immune system to UCMS.

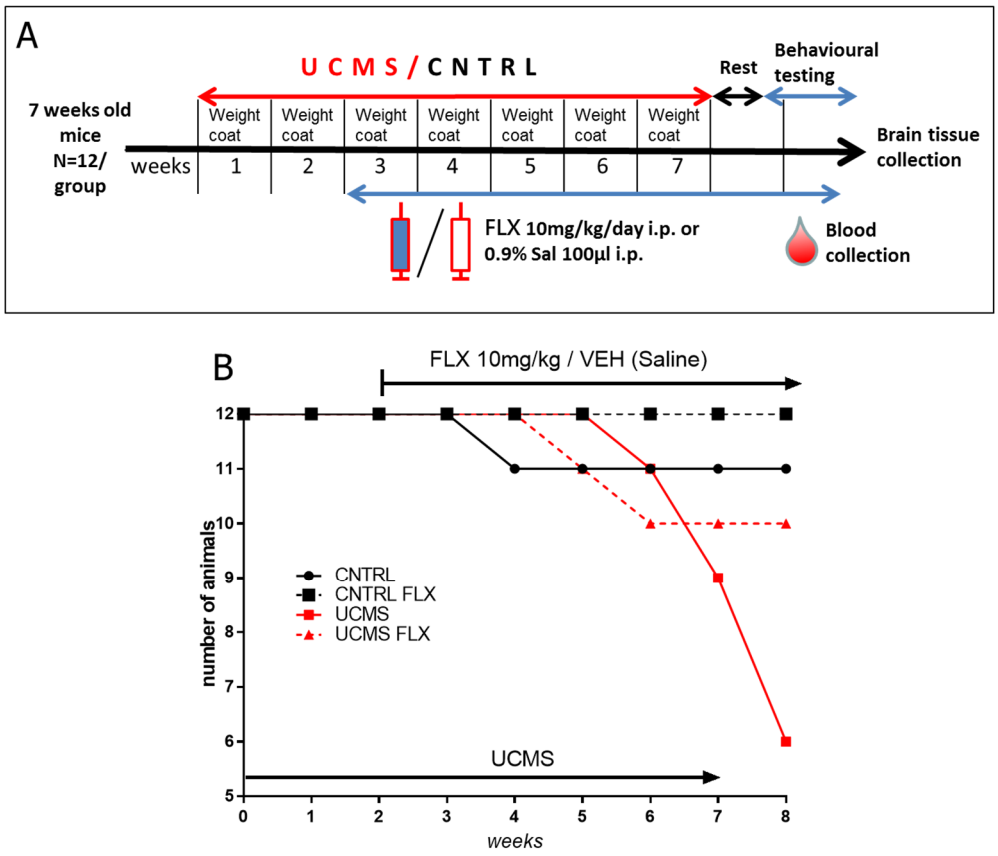

Figure 14 Timeline of experimental procedures in the UCMS Experiment 2.

(A) Male BALB/cAnNCrl mice (n=12/group) aged 7 weeks at the beginning of the experiment were subjected to UCMS or CNTRL conditions for 7 weeks; fluoxetine (FLX) or saline injections commenced on the 3rd week of UCMS and continued during behavioural testing until mice were culled for brain tissue collection (B) Animal death occurred more frequently in UCMS group (50% by the end of the UCMS exposure), while death rate was lower in UCMS FLX-treated group (16.7%)

Table 6 Schedule of stressors used for UCMS Experiment 2
Male BALB/cAnNCrl mice (n=12/group) aged 7 weeks at the beginning of the experiment were subjected to UCMS or CNTRL conditions for 7 weeks; fluoxetine (FLX) or saline injections commenced on the 3rd week of UCMS and continued during behavioural testing until mice were culled for brain tissue collection. In this experiment number of stressors per day was increased to 4 and their longevity was incrementally increased across weeks to avoid habituation as recommended by Nollet et al. (2013). In addition, a confinement stressor was added to the protocol to increase its intensity, however its severity was lower than that described by Nollet et al. (2013) as it allowed free movement of mice inside the confinement space to avoid physical impact; "+" sign next to the time of the stressor indicates that this stressor continued after the commencement of the next one

Week	Stressor 1	Time	Stressor 2	Time	Stressor 3	Time	Stressor 4	Time
Week 1								
1	cage swap	30min	new bedding		light off	30h	predator sounds	15min
2	**weight, coat state**		confinement	15min	cage swap	1.5h	light on/off	2h
3	cage tilt	30min	wet bedding	30min	no bedding	30 min	new bedding	
4	predator odor	15 min	light on/off	1h	light on/off	1h	light on/off	1h
5	bath	15 min	no bedding	1h	predator sounds	30 min	cage tilt	2h
6	light on/off	3h	light on/off	3h	light on/off	3h	light on/off	3h
7	light on/off	3h	light on/off	3h	light on/off	3h	light on/off	3h
Week 2								
1	cage swap	30min+	cage tilt	1h	lights off	30min+	predator odor	30 min
2	**weight, coat state**		no bedding in new cage	1h	confinement	15min+	bath	15min
3	wet bedding	30min+	cage tilt	2h	no bedding	2h	new bedding	
4	light off	2h	light on	2h	lights off	2h+	confinement	30min
5	cage swap	1h+	wet bedding	2h+	no bedding	1h+	tilt+ new bedding	1h
6	light on/off	3h	light on/off	3h	light on/off	3h	light on/off	3h
7	light on/off	3h	light on/off	3h	light on/off	3h	light on/off	3h
Week 3 Start of FLX 10 mg/kg or saline injections - 9am, daily								
1	wet bedding	1h+	cage swap	1h+	cage tilt	3h	return to empty cage, new bedding	3h
2	**weight, coat state**		no bedding in new cage	2h	bath	15min+	confinement	15min
3	light off	3h	light on	2h	lights off	3h +	predator odor	30 min
4	cage swap	2h+	cage tilt	2h+	swap back		predator sounds	o/n
5	wet bedding	2h+	confinement	30min	no bedding	3h	new bedding	o/n
6	light on/off	3h	light on/off	3h	light on/off	3h	light on/off	5h
7	light on/off	3h	light on/off	3h	light off	3h+	light on/off	1h
Week 4 FLX 10 mg/kg or saline injections - 9am, daily								
1	cage swap	2h+	wet bedding	3h	no bedding	2h	new bedding	o/n
2	**weight, coat state**		no bed	1h+	tilt	3h	new bedding	o/n
3	light off	3h+	predator odor	1h+	confinement	30min	light on/off	3h
4	no bedding, new cage	1h+	bath 2cm	30min	no bed	2h+	predator sounds	30min
5	cage swap	2h	tilt	2h	return to flat cage	1h	tilt	2h
6	light on/off	3h	light on/off	3h	light on/off	3h	light on/off	5h
7	light on/off	3h	light on/off	3h	lights off	3h	light on/off	5h
Week 5 FLX 10 mg/kg or saline injections - 9am, daily								
1	cage swap	2h+	cage tilt	3h	predator odor	30 min	swap back	

Week	Stressor 1	Time	Stressor 2	Time	Stressor 3	Time	Stressor 4	Time
2	**weight, coat state**		no bedding in new cage	3h	confinement	30min+	bath	30min
3	wet bedding	3h+	cage tilt	3h	no bedding	3h	new bedding	
4	light off	3h	light on	3h	lights off	3h+	confinement	30min
5	cage swap	2h+	wet bedding	2h+	no bedding	2h+	tilt	2h
6	light on/off	3h	light on/off	3h	light on/off	30 min	light on/off	5h
7	light on/off	3h	light on/off	3h	light on/off	3h	light on/off	5h
Week 6 FLX 10 mg/kg or saline injections - 9am, daily								
1	wet bedding	2h+	cage swap	3h+	cage tilt	3h	return to empty cage	3h
2	**weight, coat state**		no bedding in new cage	2h	bath	30min+	confinement	30min
3	light off	3h	light on	2h	lights off	3h +	predator odor	30 min
4	cage swap	2h+	cage tilt	2h+	swap back		predator sounds	night
5	wet bedding	2h+	confinement	30min	no bedding	3h	new bedding	
6	light on/off	3h	light on/off	3h	light on/off	3h	light on/off	5h
7	light on/off	3h	light on/off	3h	light off	3h+	light on/off	1h
Week 7 FLX 10 mg/kg or saline injections - 9am, daily								
1	cage swap	2h+	wet bedding	4h	no bedding	3h	new bedding	o/n
2	**weight, coat state**		no bedding	2h+	tilt	4h	new bedding	0/n
3	light off	3h+	predator odor	1 h+	confinement	1hr	light on/off	3h
4	no bedding, new cage	3h+	bath 2cm	30min	no bed	3h+	predator sounds	30min
5	cage swap	3h	cage tilt	2h	return	1h	cage tilt	2h
6	light on/off	3h	light on/off	3h	light on/off	3h	light on/off	3h
7	light on/off	3h	light on/off	3h	lights off	3h	light on/off	3h

Coat state was assessed once a week as indicated in Table 6. At the end of the UCMS procedure mice were left undisturbed for 1 day (rest day) before their behavioural testing began. The order of behavioural tests and number of animals tested each day is indicated in Table 7. All animals were tested in the light phase between 9am and 5.12pm according to the schedule indicated in. Groups were counterbalanced throughout each day to minimise effect of the time of day when testing was performed as shown in Table 7.

Table 7 Schedule of behavioural testing in the UCMS Experiment 2.
Male BALB/cAnNCrl mice (n=12/group) aged 7 weeks at the beginning of the experiment were subjected to UCMS or CNTRL conditions for 7 weeks and subsequently subjected to a series of behavioural tests in the following order: open field, sucrose preference (continuous 3-day measurement), splash test, novelty-suppressed feeding (NSF), forced swim test (FST) which included baseline (PRE-FST) and POST-FST (30 min after the test) blood collections

	TESTING DAY	DAY 1	DAYS 2-4	DAY 5	DAY 6	DAY 7	DAY 8	
ID	GROUP	Open field	Sucrose preference	Splash test	NSF	PRE-FST blood collection	FST	POST-FST blood collection
1	CNTRL	09:00	ALL DAY MEASURE-MENT	09:40	09:40	10:38	10:08	10:38
2	UCMS	09:12		09:50	09:50	10:46	10:16	10:46
3	CNTRL FLX	09:24		10:00	10:00	10:54	10:24	10:54
4	UCMS FLX	09:36		10:10	10:10	11:02	10:32	11:02
5	CNTRL	09:48		10:20	10:20	11:10	10:40	11:10
6	UCMS	10:00		10:30	10:30	11:18	10:48	11:18
7	CNTRL FLX	10:12		10:40	10:40	11:26	10:56	11:26
8	UCMS FLX	10:24		10:50	10:50	11:34	11:04	11:34
9	CNTRL	10:36		11:00	11:00	11:42	11:12	11:42
10	UCMS	10:48		11:10	11:10	11:50	11:20	11:50
11	CNTRL FLX	11:00		11:20	11:20	11:58	11:28	11:58
12	UCMS FLX	11:12		11:30	11:30	12:06	11:36	12:06
13	CNTRL	11:24		11:40	11:40	12:14	11:44	12:14
14	UCMS	11:36		11:50	11:50	12:22	11:52	12:22
15	CNTRL FLX	11:48		12:00	12:00	12:30	12:00	12:30
16	UCMS FLX	12:00		12:10	12:10	12:38	12:08	12:38
17	CNTRL	12:12		12:20	12:20	12:46	12:16	12:46
18	UCMS	12:24		12:30	12:30	12:54	12:24	12:54
19	CNTRL FLX	12:36		12:40	12:40	13:02	12:32	13:02
20	UCMS FLX	12:48		12:50	12:50	13:10	12:40	13:10
21	CNTRL	13:00		13:00	13:00	13:18	12:48	13:18
22	UCMS	13:50		13:50	13:50	14:20	13:50	14:20
23	CNTRL FLX	14:00		14:00	14:00	14:28	13:58	14:28
24	UCMS FLX	14:12		14:10	14:10	14:36	14:06	14:36
25	CNTRL	14:24		14:20	14:20	14:44	14:14	14:44
26	CNTRL FLX	14:36		14:30	14:30	14:52	14:22	14:52
27	UCMS FLX	14:48		14:40	14:40	15:00	14:30	15:00
28	CNTRL	15:00		14:50	14:50	15:08	14:38	15:08
29	CNTRL FLX	15:12		15:00	15:00	15:16	14:46	15:16
30	UCMS FLX	15:24		15:10	15:10	15:24	14:54	15:24
32	CNTRL	15:36		15:20	15:20	15:32	15:02	15:32
33	CNTRL FLX	15:48		15:30	15:30	15:40	15:10	15:40
34	UCMS FLX	16:00		15:40	15:40	15:48	15:18	15:48
35	CNTRL	16:12		15:50	15:50	15:56	15:26	15:56
36	CNTRL FLX	16:24		16:00	16:00	16:04	15:34	16:04
37	CNTRL	16:36		16:10	16:10	16:12	15:42	16:12
38	CNTRL FLX	16:48		16:20	16:20	16:20	15:50	16:20
39	CNTRL	17:00		16:30	16:30	16:28	15:58	16:28

5.2 Results

5.2.1 Coat state of UCMS-exposed mice deteriorated from week 2, with no effect of FLX treatment

UCMS significantly affected coat state of the exposed mice from week 2 of the protocol; however FLX treatment did not reverse this effect (Kruskal-Wallis H(4))= 30.66 (week 2), 25.37

(week 3), 27.52 (week 4) 28.27 (week 5), 24.98 (week 6), 22.36 (week 7), p<0.0001 for each week) (see Figure 15C). 2-way repeated measures ANOVA showed that body weight of animals was not affected by UCMS exposure or FLX treatment (Effect of Interaction F (21, 340) = 0.184, p>0.999; Time F (7, 340) = 27.24, p<0.0001; Treatment F (3, 340) = 0.054, p = 0.984) (Figure 15A).

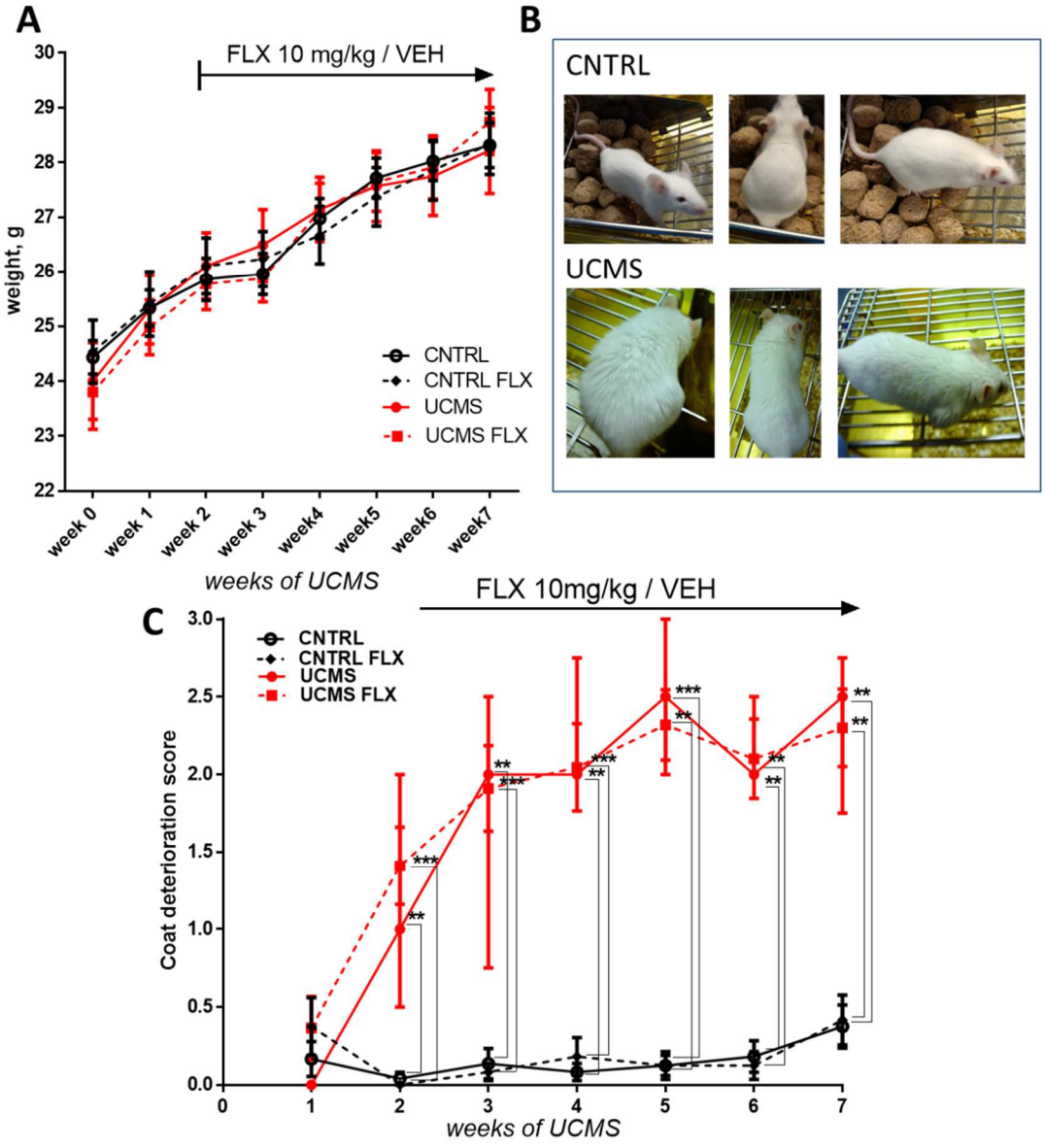

Figure 15 Body weight change and coat state in UCMS Experiment 2
*Male BALB/cAnNCrl mice (n=12/group) aged 7 weeks at the beginning of the experiment were subjected to UCMS or CNTRL conditions for 7 weeks; fluoxetine (FLX) or saline (VEH) injections commenced on the 3rd week of UCMS and continued during behavioural testing until mice were culled for brain tissue collection (A) Weekly body weight measurements of experimental groups, data represents mean±SEM (B) representative photographs of coat state of CNTRL (top panel) and UCMS (bottom panel) mice (C) Coat deterioration score was measured every week throughout the UCMS exposure, **p<0.01,***p<0.001 derived from post-hoc Dunn's multiple comparisons within CNTRL vs UCMS and CNTRL FLX vs UCMS FLX group pairs) Data presented as Median and interquartile range*

5.2.2 UCMS induced hyperactivity in the open field test, while FLX affected grooming of CNTRL

In addition to the coat state measure, grooming behaviour was assessed in the splash test according to the protocol by Nollet et al. (2013). 2-way ANOVA showed that neither UCMS nor FXL were significant factors (FLX $F(1, 36) = 2.285$, $p = 0.139$; UCMS $F(1, 36) = 0.398$, $p = 0.532$, however the interaction between these two factors on duration of grooming was close to reaching statistical significance (UCMSxFLX $F(1, 36) = 3.075$, $p = 0.088$). 2-way ANOVA analysis of another outcome measure of the splash test, latency to first grooming, showed that FLX significantly affected latency to groom (FLX $F(1, 35) = 5.856$, $p = 0.02$; UCMS $F(1, 35) = 2.664$, $p = 0.112$; UCMSxFLX $F(1, 35) = 1.474$, $p = 0.233$) (see Figure 16A and B).

2-way ANOVA analysis of the open field test showed that UCMS was a significant factor affecting locomotor activity in the novel environment (UCMS factor $F(1, 36) = 25.78$, $p<0.0001$; FLX $F(1, 36) = 0.077$, $p = 0.783$; UCMSxFLX $F(1, 36) = 2.515$, $p = 0.122$). Similarly, the time spent in the central zone was affected by UCMS (Effect of UCMS $F(1, 34) = 5.025$, $p=0.032$; FLX $F(1, 34) = 0.945$, $p = 0.338$, UCMSxFLX $F(1, 34) = 0.736$, $p = 0.397$). (Figure 16 C, D).

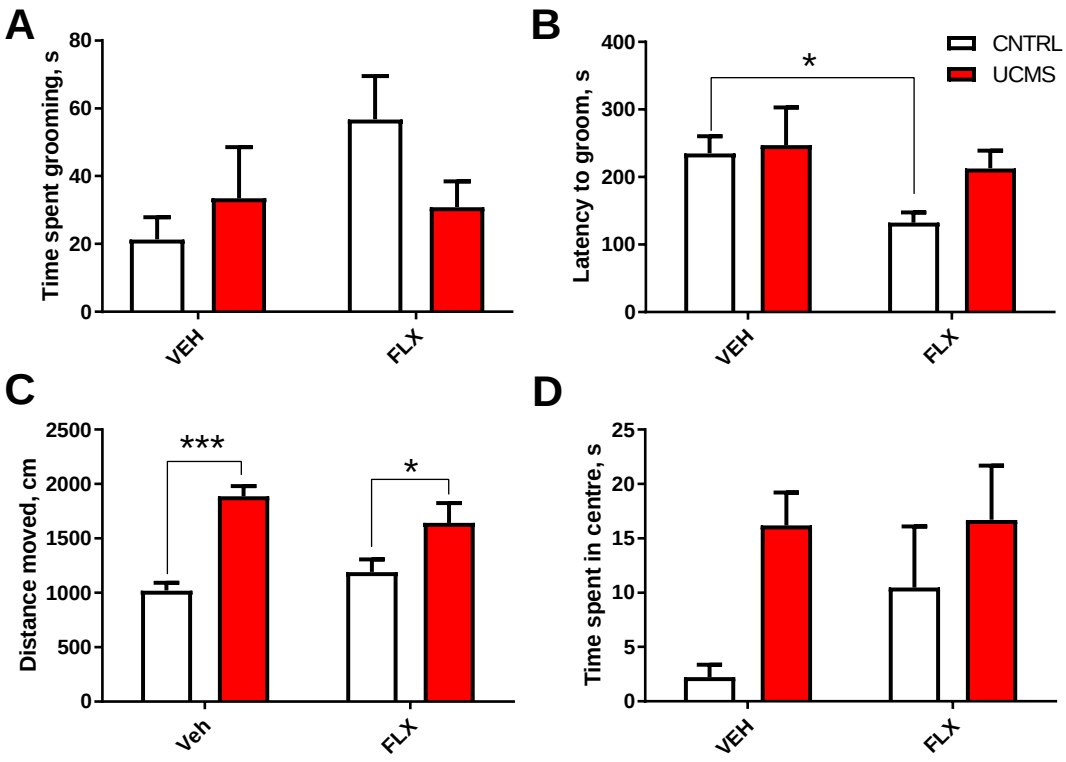

Figure 16 Grooming behaviour in the splash test and locomotion and anxiety measures in the open field test Male BALB/cAnNCrl mice (n=12/group) aged 7 weeks at the beginning of the experiment were subjected to UCMS or CNTRL conditions for 7 weeks; fluoxetine (FLX) or saline (VEH) injections commenced on the 3rd week of UCMS and continued during behavioural testing until mice were culled for brain tissue collection (A) *Time mice spent grooming during (B) Latency to begin grooming in the splash test trial (C) Distance moved around the arena in the open field test (D) Time mice spent in the anxiogenic centre zone of the open field arena. Data represents mean±SEM, *p<0.05 **p<0.005 derived from post-hoc Bonferroni multiple comparisons between groups joined by bracket lines*

5.2.3 UCMS did not induce anhedonia or behavioural despair

In NSF, 2-way ANOVA showed that UCMS exposure was a significant factor affecting the latency to start eating the pellet (UCMS factor F (1, 36) = 6.807, p = 0.013; FLX F (1, 36) = 3.237, p = 0.08; UCMSxFLX F (1, 36) = 1.505, p=0.228) (see Figure 17A). For sucrose preference test, mice were exposed to a choice of 4% sucrose solution or water continuosly for 3 consecutive days and measurements were taken every 24 hours. In all groups mice showed preference after 48 hours (2nd day) of exposure. While on day 3 more variability emerged among groups, repeated measures 2-way ANOVA showed no effect of treatment (Time F (2, 68) = 120.2, p < 0.0001; Treatment F (3, 34) = 0.952, p = 0.426; Interaction F (6, 68) = 0.72, p = 0.635) (see Figure 17B). In the FST 2-way ANOVA showed no effect of treatment factors on the time mice spent immobile (UCMSxFLX F (1, 36) = 0.003, p = 0.96; FLX F (1, 36) = 0.043, p = 0.837; UCMS F (1, 36) = 0.059, p = 0.81) or on latency to first immobility (UCMSxFLX F (1, 36) = 0.882, p = 0.354; FLX F (1, 36) = 0.5, p = 0.485; UCMS F (1, 36) = 0.039, p = 0.845). In addition, time spent

swimming was scored in this test, however no treatment effect was detected (UCMSxFLX F (1, 36) = 0.042, p = 0.84; FLX F (1, 36) = 0.041, p = 0.841; UCMS F (1, 36) = 1.303, p = 0.261) (see Figure 17 C, D and E).

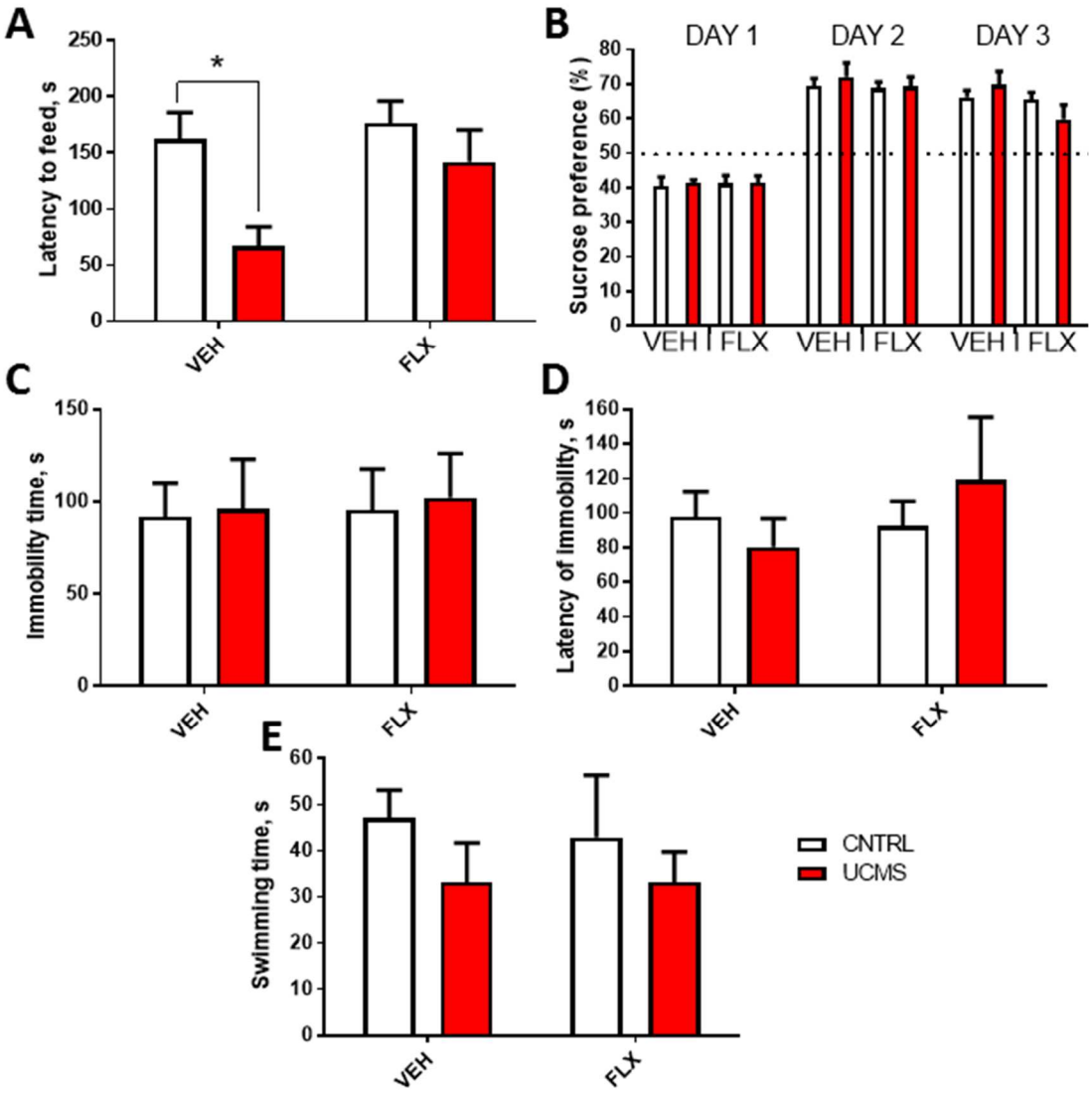

Figure 17 Anhedonia and behavioural despair in NSF, sucrose preference test and FST
Male BALB/cAnNCrl mice (n=12/group) aged 7 weeks at the beginning of the experiment were subjected to UCMS or CNTRL conditions for 7 weeks; fluoxetine (FLX) or saline (VEH) injections commenced on the 3rd week of UCMS and continued during behavioural testing until mice were culled for brain tissue collection (A) *Latency to approach and start eating the pellet in the novelty suppressed feeding (NSF) test; (B) Sucrose preference over 24 hours measured for 3 continuous days; (C) Time mice spent immobile in the forced swimming test (FST) (D) Latency to first immobility in the FST; (E) Time mice spent swimming during the FST trial. Data represents mean±SEM, *p<0.05 derived from post-hoc Bonferroni multiple comparisons*

5.2.4 UCMS suppressed corticosterone response to acute stress but did not affect cytokine levels

In this experiment plasma was collected by incision method from the lateral tail vein (Sadler and Bailey, 2013) to gain insight into neurobiological changes accompanying behavioural

effects of UCMS. To investigate the state of the HPA axis regulation, corticosterone (CORT) levels were measured 24 before the FST (PRE-FST) and 30 min after FST (POST-FST) to assess the HPA axis response to acute swim stress. Repeated measures 2-way ANOVA showed that both timepoint of collection (FST factor) and treatment group factor significantly affected CORT levels (Effect of Treatment X FST $F(3, 32) = 15.69$, Effect of FST $F(1, 32) = 87.23$, Effect of Treatment $F(3, 32) = 12.84$, $p<0.001$ for all effects) (see Figure 18A).

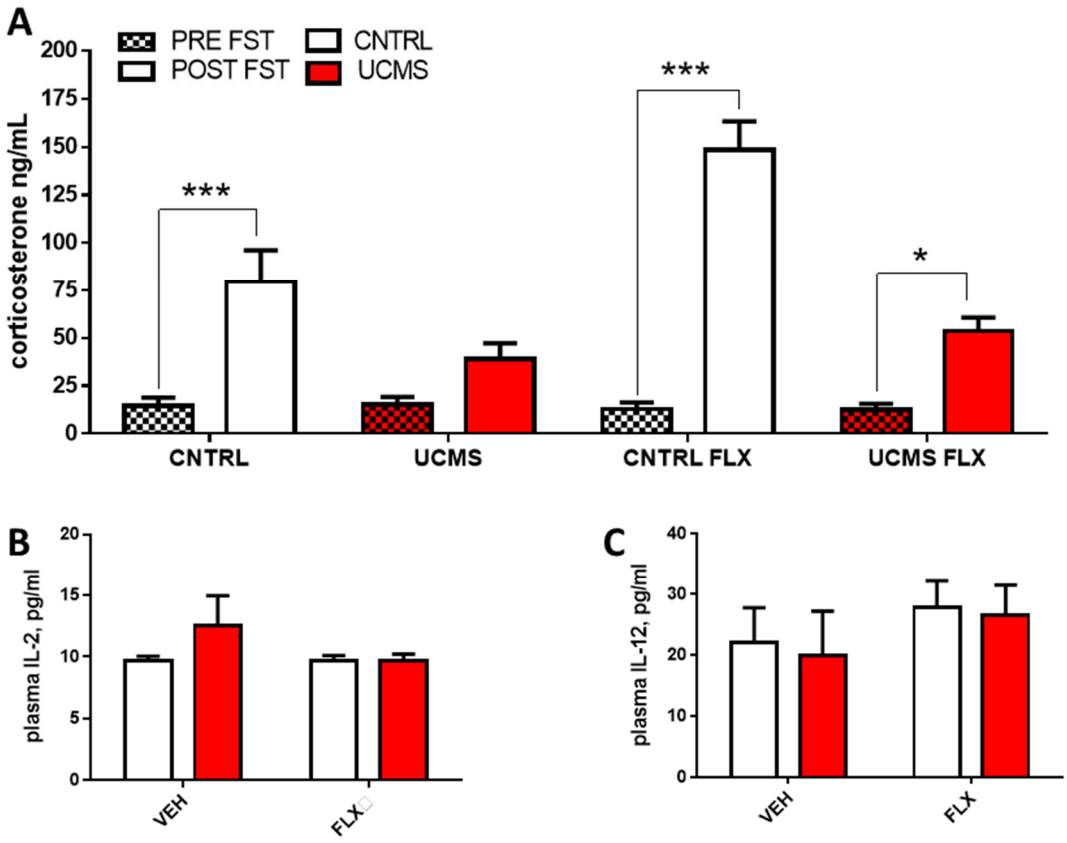

Figure 18 Plasma Corticosterone and cytokine levels in UCMS Experiment 2
*Male BALB/cAnNCrl mice (n=12/group) aged 7 weeks at the beginning of the experiment were subjected to UCMS or CNTRL conditions for 7 weeks; fluoxetine (FLX) or saline (VEH) injections commenced on the 3rd week of UCMS and continued during behavioural testing until mice were culled for brain tissue collection (A) PRE-FST plasma Corticosterone (CORT) levels were measured 24 hours before FST (PRE-FST) and 30 min after FST (POST-FST) to detect swimming stress-induced CORT (B and C) 10 cytokines were measured in the PRE-FST plasma to detect effect of treatment on the immune system. Among those only IL-2 and IL-12 shown were above detectable levels in 6 or more animals per group. Data represents mean±SEM, *p<0.05, **p<0.01, ***p<0.001 derived from post-hoc Bonferroni multiple comparisons between PRE-FST and POST-FST data points for each group*

To assess the effect of UCMS on the immune system, plasma levels of 10 cytokines were measured in peripheral blood in the PRE-FST samples collected 24 hours before the FST trial using the Luminex multiplex custom-designed assay (for details of the assay see section 3.6 of Methods on p67). Most cytokines (IL-6, TNFα, IL-1β, IL-4, IL-5, IL-10, GM-CSF, IFNγ) were not detectable, as most probably levels fell below the detection threshold of the assay (see Table

3). 2-way ANOVA of the levels of 2 cytokines (IL-2, IL-12), which were detectable in most samples (6 or more per group), showed that their levels were not affected by UCMS or FLX exposure (IL-2 UCMSxFLX $F(1, 32) = 2.272$, $p = 0.142$; FLX $F(1, 32) = 2.309$, $p = 0.139$; UCMS $F(1, 32) = 2.413$, $p = 0.13$; IL12 UCMSxFLX $F(1, 24) = 0.005$, $p = 0.942$; FLX $F(1, 24) = 1.233$, $p = 0.278$; UCMS $F(1, 24) = 0.099$, $p = 0.756$) (see Figure 18B and C).

5.3 Discussion

In this experiment, a modified version of UCMS Experiment 1 protocol, as well as modified conditions for control mice were used to optimise the model, increase the chance of detecting depression-like behaviours, and to look at the HPA axis and immune system response to UCMS. Single housing of control animals indeed ensured that coat deterioration score remained stable and low in control groups, while UCMS significantly increased coat state score from week 2 of stress exposure in line with previous studies (Surget et al. 2008). Yet FLX (10 mg/kg) treatment failed to improve coat state in UCMS-exposed animals, although this has been shown to be effective in this model previously (Santarelli, 2003a). However, when grooming behaviour was assessed in the splash test, fluoxetine appeared to have a positive effect on grooming in the CNTRL group by prolonging the time animals spend grooming in a novel cage. It is possible to argue that anxiety also plays a role in this test as animals are faced with a choice of reacting to a change in environment (novel cage, testing room and researcher exposure) or engaging in self-grooming behaviour. Indeed Spruijt et al. (1992) argued that self-grooming reflects the process of de-arousal due to termination of exposure, or habituation, to a stressful environment. The fact that FLX was improving grooming in controls might suggest that control animals experienced a level of anxiety or stress perhaps due to the social isolation as a result of single housing, and fluoxetine was able to reverse its detrimental effect. The ineffectiveness of FLX in the UCMS group could be explained by the fact that the level of stress experienced by UCMS group was beyond the therapeutic potential of the lower FLX dose used in this experiment. Indeed, loss of 50% of animals during last weeks of UCMS suggested that the UCMS protocol employed in this experiment was too severe. Interestingly FLX seemed to be protective of the fatal outcome (see Figure 15C).

UCMS-exposed groups displayed a significant hyperlocomotion in the open field arena. Hyperlocomotion following UCMS has been described previously in BALB/c strain. Dournes et al. (2013) showed that the same dose of FLX (10mg/kg) was not able to reverse this effect, even though FLX was effective in restoring coat state in these animals. In a study by Couch et al. (2013) of male C57BL/6J mice exposed to 10 days of chronic stress which involved intruder exposure, restraint and tail suspension, increased locomotion was described as a behavioural

response specific to stress-susceptible animals, as determined by their loss of sucrose preference after the stress. At the same time, both stress susceptible and stress resilient groups in this study displayed anxiety-like behaviour in the light-dark box test. In a more recent study by this group the same stress paradigm induced increased amount of time animals spent in the open arms of the O-maze (Couch et al., 2016). This behavioural change was interpreted as a sign of impulsivity corresponding to the depression-like phenotype, and was not accompanied by a change in the locomotion measured in a novel cage. In another study (Ito et al., 2010), chronic restraint stress induced hyperlocomotion, which was linked to enhanced short-term and long-term synaptic plasticity in the anterior cingulate cortex possibly caused by reduced GABAergic inhibition observed in this study. However, glutamate signalling has also been shown to be involved in hyperlocomotion. As such, novelty-induced hyperlocomotion was described in glutamate AMPA receptor Glu1A subunit knockout mice along with depressive-like behaviour (Procaccini et al., 2011). This subunit is mostly expressed in the hippocampus, and behavioural changes in this model were attributed to excessive neuronal activation in the hippocampus in response to novelty, as measured by c-Fos expression. Interestingly, treatment with SSRI escitalopram did not reverse these effects. Ineffectiveness of SSRI antidepressants confirms the fact that stress-induced hyperactivity is not related to changes in serotonergic signalling. Indeed, Logan et al. (2015) showed that following UCMS exposure, hyperactivity during the light cycle was accompanied by hypoactivity detected during the active dark phase. Therefore, it is possible that the hyperactivity observed during testing was not present during the night. The absence of night time activity measure is a limitation of the UCMS Experiment 2 study. Moreover, it has been shown that the UCMS-induced phenotype varies depending on the diurnal phase of its application, as has been demonstrated by Aslani et al. (2014). Many studies employing UCMS reverse light-dark cycle in the animal facility and hence apply the stressors during dark phase. For example, Mineur et al. (2006) showed an increase in locomotor activity in the open field test in C57BL/6J, BALB/cJ and DBA/2J mice exposed to UCMS in the dark phase, which was significant in female but not male mice. Yalcin et al. (2008) reported no change in locomotor activity in 8 mouse strains (including BALB/cByJ) exposed to UCMS during the dark phase. Thus it is possible that some of the behavioural effects which differed in this study from those commonly described in the literature derive from the fact that the stressors in these experiments were applied during the light phase. In fact, the absence of diurnal cycle reversal in our experiments might play a crucial role in occurrence of hyperactivity. Unfortunately, conditions in the animal facility where our experiments were conducted did not allow to effectively reverse the light/dark cycle due to technical issues with the lighting setup.

Similarly, UCMS reduced the latency to eat in NSF, a test of anhedonia influenced by changes in anxiety, indicating a state of a paradoxical reduced anxiety (or "anomalous anxiolysis") in the mice. While this effect could be confounded by hyperactivity in the novel brightly-lit arena of the test, importantly FLX blocked this effect by increasing the latency in UCMS FLX group to control levels. As open field data showed that FLX was not capable of reducing hyperactivity, it is possible to argue that this effect was not in fact due to hyperactivity, but some other behavioural phenomenon, such as increased impulsivity or indeed increased appetite or drive towards food reward in UCMS-exposed animals. Activity measure in the NSF could have helped to distinguish these effects. However, the sucrose preference test results oppose the food reward behaviour change hypothesis, as stressed animals displayed control levels of preference for sucrose. On the other hand, the high level of sucrose concentration used in this study (4%), utilised to avoid low BALB/c strain preference for sucrose (Ducottet and Belzung, 2005), might have produced a ceiling effect, so that all animals preferred it after initial 24 hours of habituation.

No change in the immobility time was observed in FST. Assuming FST also provided an exposure to novelty, it would be expected to see hyperactivity in this test as well, which would make mice less likely to appear immobile. While some studies report increased immobility after UCMS protocol in mice (Lu et al., 2014), Nollet et al. (2013) did not recommend it as a suitable behavioural outcome measure in a recent UCMS protocol review, and it does not appear in many recent UCMS studies. Therefore, current literature suggests that behavioural despair might not be a part of UCMS-induced behavioural phenotype.

CORT was measured pre and post FST as forced swimming as an acute stressor is known to induce plasma corticosterone release (Anisman et al., 2001). Previous studies have shown that chronic stress modifies HPA axis regulation by increasing the baseline level of plasma CORT in BALB/c mice (Vega-Rivera et al. 2016) and increasing the CORT response to acute stress, which reflects increased reactivity and potentially impairment of negative feedback inhibition of the CORT release. Yet this effect is not universal – Ibarguen-Vargas et al. (2008) demonstrated that among 7 mouse strains only two including BALB/cByJ responded to UCMS with CORT increase, while 3 strains showed no change in CORT levels and two showed a decrease (C57BL/6J, DBA/2J). In this experiment baseline levels of CORT were similar to those reported for BALB/c strain in previous studies (Kubera et al., 2013; Law et al., 2016) and were not affected by UCMS. However, exposure to acute swim stress revealed modulation of HPA reactivity by chronic stress and FLX. As such, UCMS blocked corticosterone elevation following FST, while FLX treatment restored this effect in UCMS-exposed mice, even though the magnitude of CORT

elevation was smaller than in FLX-treated CNTRL group. At the same time, it appeared that FLX stimulated CORT release in controls, as elevation of CORT post-FST in CNTRL FLX group was higher and more significant than in CNTRL group. If to allow a possibility that control animals also experienced some level of stress, such modulation of CORT levels by FLX could be seen as a therapeutic effect of FLX restoring HPA axis reactivity to normal levels. Response of controls is then contrasted by UCMS-treated animals' reduced level of HPA reactivity and a much smaller albeit significant response to FLX. In fact, published literature provides some evidence of a modification of FLX effect based on the state of HPA axis regulation. As such, a previous study by Khemissi et al. (2014b) divided mice into groups based on the level of HPA axis negative feedback measured by dexamethasone (DEX) suppression tests. The authors went on to show that animals with low negative feedback inhibition also had low levels of basal CORT during UCMS, and in contrast to high DEX suppressors, did not respond to FLX treatment during UCMS, especially in the NSF test. Such differences in response resembles the difference seen between the control and stressed groups in this study. It is interesting to speculate if UCMS exposure impaired the HPA axis regulatory mechanism so that the mice acquired features of low DEX suppressors, while limited amount of stress experienced by controls remained highly sensitive to antidepressant effect.

Previous studies have shown that UCMS affects immune system function. Studies on rats exposed to UCMS showed increased serum complement (Ayensu et al., 1995) and proinflammatory cytokine levels (Lu et al. 2016). The latter study also showed increased IL-6, TNFα and IL-1β expression and protein levels in the hippocampus and prefrontal cortex. Kubera et al. (1998) showed that splenocytes extracted from stressed C57/BL6 mice responded to *in vitro* LPS stimulation with a strong increase in IL-1 secretion and a significant decrease in IL-2 secretion. *In vivo* Xue et al. (2015) showed increased IL-6, IL-1β, TNFα and NLRP3 in the hippocampus of male ICR mice. Moreover, in these studies chronic treatment with fluoxetine (10 mg/kg) reduced proinflammatory cytokines to control levels. Therefore, we assessed the plasma level of 10 most commonly studied pro- and anti-inflammatory cytokines to see if UCMS induced immune system changes in this experiment. However, the assay utilised did not detect the majority of the cytokines, and the ones above detection levels were not modulated by UCMS or FLX. It is possible that the Luminex assay used was not sensitive enough to detect subtle changes induced by UCMS. Indeed, Lu and colleagues (2016), reported very small increases (15-20 pg/ml) in the proinflammatory cytokines. It is also important to note that plasma levels of cytokines might not be representative of cytokine levels in the brain,

therefore our findings do not exclude the possibility that UCMS affected immune parameters in relevant brain areas, such as the hippocampus or prefrontal cortex.

To summarise, the UCMS Experiment 2 showed that several experimental design factors need to be optimised to achieve a better outcome. First, single-housing of CNTRL group did avoid cage mate fighting and preserved coat state of mice, but also exposed them to social isolation, which can have detrimental effect on HPA axis and induce anxiety-like behaviour. Indeed, FLX improved behaviour of CNTRL mice in the splash and open field tests, which suggests that these mice were detrimentally affected during the experiment. Another possible source of stress could have been repeated injections. Next, the UCMS protocol might have been of excessive intensity, as fatality was higher in UCMS group, and FLX did not reverse any of the behavioural changes induced by UCMS. Third, hyperactivity potentially confounded the results of many behavioural tests, thus measures are needed to be taken to avoid its development or to access behaviours in activity-independent tests. Therefore, further optimisation of the control, UCMS and testing protocols was required.

6 UCMS Experiment 3

6.1.1 Experimental design

The UCMS Experiment 3 was designed to address issues which arose in the previous study. To improve CNTRL conditions, mice in the control group were pair-housed with their siblings in large cages (59.5x38x20cm) to avoid social isolation and minimise home cage aggression. As data from the UCMS Experiment 1 showed that daily i.p. injections induce coat state deterioration and affect mouse behaviour in the forced swim test, it was decided not to expose animals to daily injections in this experiment to avoid interference with UCMS-induced phenotype. Indeed, it has been shown previously that i.p. injections increase CORT levels in BALB/c mice and can interfere with psychological stress studies by affecting stress response of control groups (Drude et al., 2011). Therefore FLX treatment was not included in this experiment, which was solely focused on the effect of UCMS. The UCMS group was exposed to 4 daily stressors as indicated in the protocol in Figure 19. The stressors were introduced in a random-like order which was repeated every week; however, the longevity of stressors varied from 30 min on week 1 to 4 hours towards the end of the UCMS protocol to avoid habituation. Overlap of the stressors was not included to avoid mortality seen in UCMS Experiment 2. Removal of i.p. injections in UCMS-exposed groups was also aimed to reduce stress exposure in these mice.

Significant changes were made to the way sucrose preference measurement was done in this experiment. Unlike in previous experiments, it was measured repeatedly once every two weeks. Animals were constantly housed with 2 bottles of water and food on both sides to avoid development of any side preference. According to recommendations by Strekalova et al. (2011b), before the first test of sucrose preference, mice were exposed to a single bottle with 2.5% sucrose for 4 hours to habituate them to the taste of sucrose. For the actual test, 1% solution was used for weeks 0 and 2, and 2% for weeks 4 and 6. An increase of concentration was related to a loss of preference in the CNTRL group observed on week 2 and the data from the Strekalova et al. (2011b) study, which showed that mice habituate to the concentration of sucrose and in order to continue measuring sucrose preference, a change of concentration is required. Sucrose preference was measured across two consecutive nights but not during the days to capture the most active drinking phase, and sides of the sucrose and water bottles were switched between each night test. The average preference during the two nights was used for statistical analysis.

To test if the development of hyperlocomotion was related to the longevity of stress, an open field test was performed after first 3 weeks of stress. In the final behavioural battery light-dark box test was included, as behaviour in this test is less likely to be affected by hyperactivity as it is a small arena. To assess aggressive behaviours social interaction test was added to the behavioural battery. As sense of smell plays an important role in social interaction as well as in appetitive behaviours, buried cookie test also was added to assess olfaction. In addition, leptin was added to the list of analytes in the Luminex assay to gain further insight into the appetite control of UCMS exposed mice. Blood collected from cardiac puncture before cull was added to ensure sufficient plasma volume for all measurements. Timeline of experimental procedures for the UCMS Experiment 3 is shown in Figure 19.

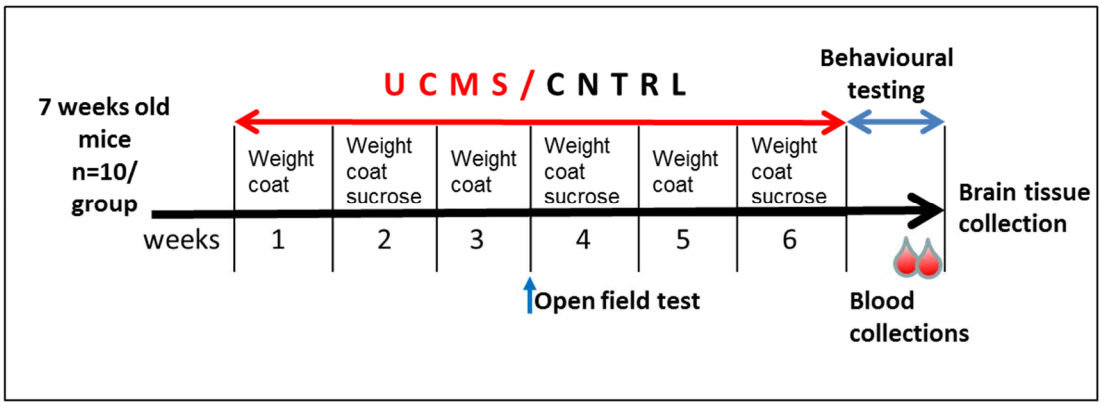

Figure 19 Timeline of experimental procedures in the UCMS Experiment 3.
Male BALB/cAnNCrl mice (n=10/group) aged 7 weeks at the beginning of the experiment were subjected to UCMS or CNTRL conditions for 6 weeks, during which weight, coat state and sucrose preference were monitored weekly. After 6 weeks of UCMS exposure mice were subjected to behavioural testing battery, at the end of which blood was collected and mice were culled for brain tissue collection.

Table 8 Schedule of stressors used in the UCMS Experiment 3
The schedule was repeated every week for 6 consecutive weeks. Male BALB/cAnNCrl mice (n=10/group) aged 7 weeks at the beginning of the experiment were subjected to UCMS or CNTRL conditions for 6 weeks, during which weight, coat state and sucrose preference were monitored weekly. After 6 weeks of UCMS exposure mice were subjected to behavioural testing battery, at the end of which blood was collected and mice were culled for brain tissue collection

Day	Stressor 1	Duration	Stressor 2	Duration	Stressor 3	Duration	Stressor 4	Duration
Mon	cage swap	2h	no bedding	2h	new bedding, no enrichment	2h+	new cardboard shelter (no sizzle nest)	over-night
Tue	cage tilt	2h	wet bedding	1,5h	new bedding	2h	predator sounds	30 min
Wed	water bath	30 min	No cardboard shelter	2h	confinement	2h	new house and sizzle nest	over-night
Thu	predator odour	30 min	cage swap	2h	return to cage with intruder's odour	2h	cage tilt	2h
Fri	ruin sizzle nest	n/a	**weight, coat assessment**	n/a	confinement	2 hr	no sizzle nest	1h
Sat	light on/off	4h	light on/off	4h	light on/off	4h	light on/off	4h
Sun	light on/off	4h	light on/off	4h	light on/off	4h	light on/off	4h

Coat state was assessed once a week as indicated in Table 8. At the end of the UCMS procedure mice were left undisturbed for 1 day (rest day) before their behavioural testing began. The schedule of behavioural testing is shown in Table 9.

Experiment 3 was conducted in parallel with Experiment 4 which followed an identical protocol, however was terminated after 4 weeks for fresh frozen brain tissue collection which was used to study effects of UCMS on gene expression, described in Chapter 4.

Table 9 Schedule of behavioural testing in the UCMS Experiment 3.
Male BALB/cAnNCrl mice (n=10/group) aged 7 weeks at the beginning of the experiment were subjected to UCMS or CNTRL conditions for 6 weeks, during which weight, coat state and sucrose preference were monitored weekly. After 6 weeks of UCMS exposure mice were subjected to behavioural testing battery which included open field test, splash test, novelty suppressed feeding (NSF), light-dark box (LD box), cookie test and forced swim test (FST) which included blood collection 24 hours before FST (Pre-FST) and 30 min after FST (Post-FST) for corticosterone response measurements.

	TESTING DAY	DAY1	DAY2	DAY2	DAY3	DAY4	DAY5	DAY5	DAY6	
N	GROUP	Rest day	Open field	Splash test	NSF	LD box	Cookie test	Pre-FST blood collection	FST	Post-FST blood collection
1	CNTRL		8:58	13:12	14:00	10:14	9:30	14:20	13:50	14:20
2	UCMS		9:10	13:24	14:07	10:21	9:45	14:28	13:58	14:28
3	CNTRL		9:22	13:46	14:14	10:28	10:00	14:36	14:06	14:36
4	UCMS		9:34	13:58	14:21	10:35	10:15	14:44	14:14	14:44
5	CNTRL		9:46	14:10	14:28	10:42	10:30	14:52	14:22	14:52
6	UCMS		9:58	14:22	14:35	10:49	10:45	15:00	14:30	15:00
7	CNTRL		10:10	14:34	14:42	10:56	11:00	15:08	14:38	15:08
8	UCMS		10:22	14:46	14:49	11:03	11:15	15:16	14:46	15:16
9	CNTRL		10:34	14:58	14:56	11:10	11:30	15:24	14:54	15:24
10	UCMS		10:46	15:10	15:10	11:17	11:45	15:32	15:02	15:32
11	CNTRL		10:58	15:22	15:17	11:24	12:00	15:40	15:10	15:40
12	UCMS		11:10	15:34	15:24	11:31	12:15	15:48	15:18	15:48
13	CNTRL		11:22	15:46	15:31	11:38	12:30	15:56	15:26	15:56
14	UCMS		11:34	15:58	15:38	11:45	12:45	16:04	15:34	16:04
15	CNTRL		11:46	16:10	15:45	11:52	13:00	16:12	15:42	16:12
16	UCMS		11:58	16:22	15:52	11:59	13:15	16:20	15:50	16:20
17	CNTRL		12:10	16:34	15:59	12:06	13:30	16:28	15:58	16:28
18	UCMS		12:22	16:46	16:06	12:13	13:45	16:36	16:06	16:36
19	CNTRL		12:34	16:58	16:13	12:20	14:00	16:44	16:14	16:44
20	UCMS		12:46	17:10	16:20	12:27	14:15	16:56	16:22	16:52

6.2 Results

6.2.1 UCMS impaired coat state and grooming behaviour in exposed mice

UCMS induced a strong change in the coat state of the mice with significant deterioration detectable from week 4 of stress exposure (Mann-Whitney for week 0 $U = 40$ $p = 0.65$, for week 1 $U = 26$ $p = 0.052$; for week 2 $U = 36$, $p = 0.342$, for week 3 $U = 38.5$ $p = 0.418$, for week 4 $U = 2$ $p < 0.0001$, for week 5 $U = 21$ $p = 0.023$, for week 6 $U = 9$ $p = 0.004$) (see Figure 20A). Repeated measures 2-way ANOVA showed that body weight of animals was significantly affected by week of exposure (Effect of Time $F (6, 108) = 127.2$ $p < 0.0001$) and UCMS X Time

interaction (F (6, 108) = 5.026 p = 0.0001; UCMS F (1, 18) = 2.397, p = 0.1389) (see Figure 20B). In the splash test, two-tailed unpaired t-test analysis of group means showed that UCMS mice had higher latency to start (t = 2.515 df = 18 p = 0.022), and shorter time spent in, grooming (t = 3.304, df = 18, p= 0.004) (see Figure 20C and D).

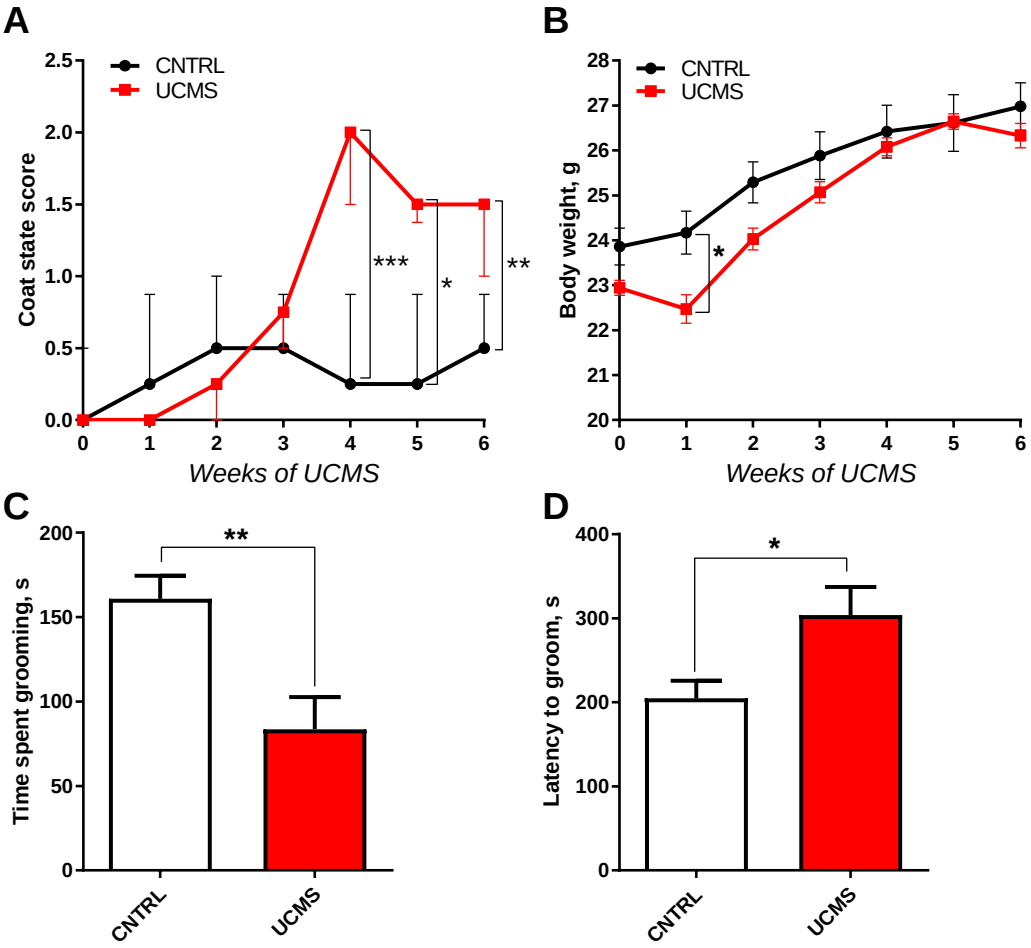

Figure 20 Coat state and grooming behaviour in the UCMS Experiment 3.
*Male BALB/cAnNCrl mice (n=10/group) aged 7 weeks at the beginning of the experiment were subjected to UCMS or CNTRL conditions for 6 weeks, during which weight, coat state and sucrose preference were monitored weekly. After 6 weeks of UCMS exposure mice were subjected to behavioural testing battery, at the end of which blood was collected and mice were culled for brain tissue collection (A) Weekly coat state deterioration score measurements from week 4, *p<0.05, **p<0.01 ***p>0.001 derived from Mann-Whitney U-test between CNTRL and UCMS, data represents median and interquartile range (B) Weekly weight monitoring, *p<0.05 derived from Bonferroni multiple comparison between CNTRL and UCMS group means at week 1 of UCMS (C) Grooming latency in the splash test and (D) time animals spent grooming during the splash test trial *p<0.05, **p<0.01 derived from two-tailed unpaired t-test, data represents mean±SEM*

6.2.2 UCMS - induced hyperlocomotion was present from week 3 in all anxiety-related tests

Statistical analysis of open field test data showed that UCMS induced hyperactivity in the open field test (see Figure 21A and C). The effect was already present after 3 weeks of UCMS

exposure (t = 9.868, p < 0.0001) and remained at 6 weeks (Mann-Whitney U = 16, p = 0.009). Hyperlocomotion was also accompanied by an anxiolytic-like increase in centre time in stressed animals, which was not significant at 3 weeks (Mann-Whitney U = 39, p = 0.425) but reached significance after 6 weeks of UCMS exposure (t = 4.491 p = 0.003) (see Figure 21B and D). Similarly, in a light-dark box test UCMS group displayed reduced latency (Mann-Whitney U = 14, p = 0.008), however the time spent in the light zone was not significantly different between groups (Mann-Whitney U = 25.5, p = 0.111) (see Figure 21E and F).

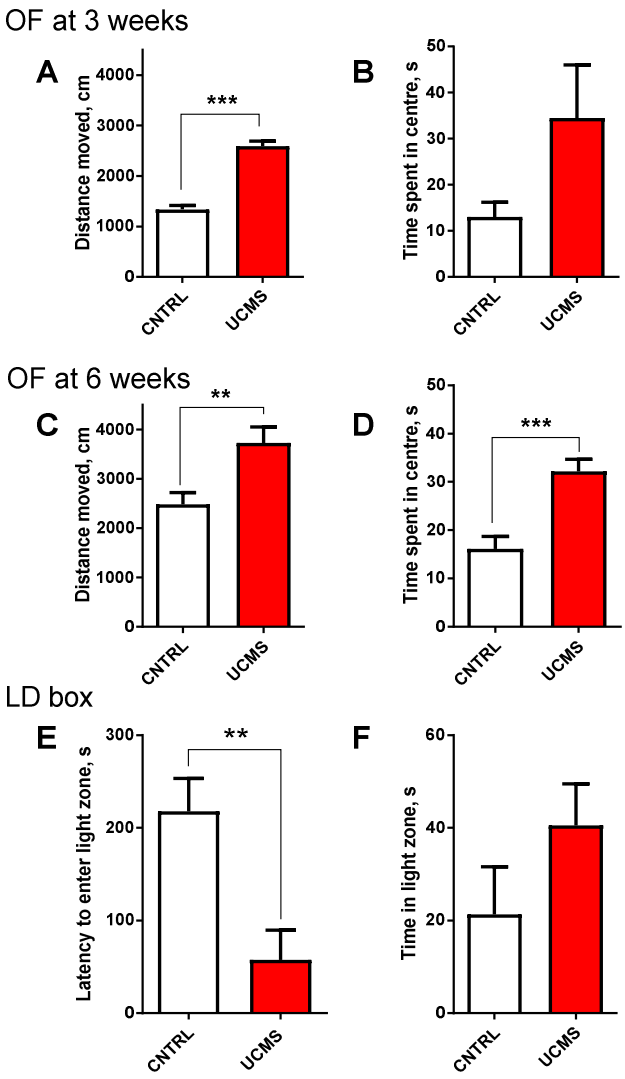

Figure 21 Hyperlocomotion in anxiety-related tests in the UCMS Experiment 3
*Male BALB/cAnNCrl mice (n=10/group) aged 7 weeks at the beginning of the experiment were subjected to UCMS or CNTRL conditions for 6 weeks, during which weight, coat state and sucrose preference were monitored weekly. After 6 weeks of UCMS exposure mice were subjected to behavioural testing battery, at the end of which blood was collected and mice were culled for brain tissue collection (A) Locomotor activity in the open field (OF) arena after 3 week of UCMS exposure (B) Time spent in the centre of the OF arena after 3 week of UCMS exposure (C) Locomotor activity in the open field (OF) arena after 6 week of UCMS exposure (D) Time spent in the centre of the OF arena after 6 week of UCMS exposure (E) Latency to enter the light zone of the light-dark box (LD box) (F) Time spent in the light zone during the light-dark box test trail **p<0.01 derived from Mann-Whitney test, ***p<0.001 derived from two-tailed unpaired t-test. Data represents mean±SEM*

6.2.3 UCMS induced anhedonia on week 4 in sucrose preference test, but not in the NSF

On weeks 0 and 2 of UCMS, 1% sucrose solution was used for the test. Control and UCMS-exposed groups showed only slight preference at first exposure (Figure 22A). On week 2, the percentage of sucrose consumption fell below 50%, while preference in UCMS group reached 62%. Because of the low preference in the control group, sucrose concentration on week 4 was increased to 2%. The control group responded to 2% sucrose with 79% preference, while the UCMS-exposed group did not prefer it over water (46%). Interestingly on week 6, preference in controls fell to 49% and rose in the UCMS group to 55%, so the inter-group difference was no longer significant in the post-hoc Bonferroni multiple comparison applied post repeated measures 2-way ANOVA (Effect of Time x Stress $F(3, 39) = 13.15$, $p < 0.0001$; Time $F(3, 39) = 2.289$, $p = 0.094$; UCMS $F(1, 13) = 1.732$, $p = 0.211$). In the NSF test UCMS-exposed group's latency to feed was reduced compared to control group (unpaired two-tailed t-test $t = 3.227$, $p = 0.005$), while latency to find the chocolate cookie in the buried cookie test was not significantly affected by UCMS (unpaired two-tailed t-test $t = 1.152$, $p = 0.264$) (see Figure 22B, C). Food pellet used in the NSF test was weighted out straight after to the test to measure amount of food consumed by a mouse during the trial, and after first 10 min the mouse spent in its home cage after the end of the NSF test. Repeated measures 2-way ANOVA showed no effect of UCMS exposure on pellet consumption either during the NSF or upon return to the home cage (Effect of UCMSxTime interaction $F(1, 15) = 0.952$, $p = 0.345$; Time $F(1, 15) = 2.69$, $p = 0.122$; UCMS $F(1, 15) = 0.302$, $p = 0.591$).

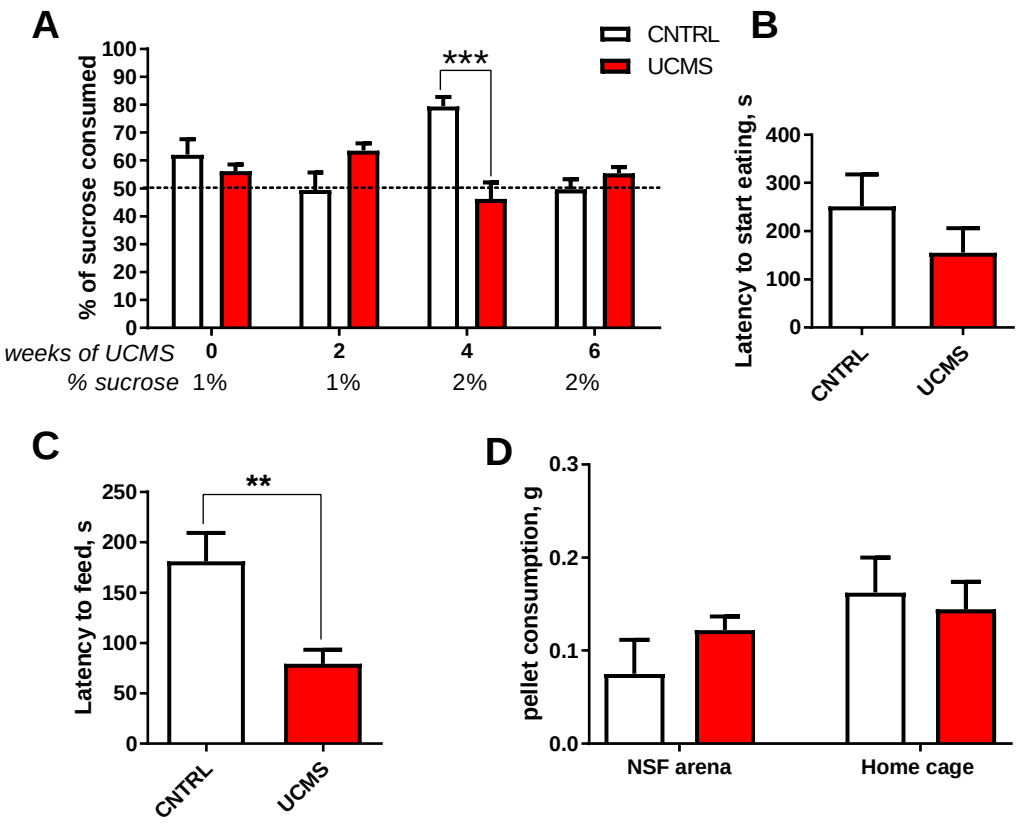

Figure 22 Anhedonia in food reward related tests in UCMS Experiment 3
*Male BALB/cAnNCrl mice (n=10/group) aged 7 weeks at the beginning of the experiment were subjected to UCMS or CNTRL conditions for 6 weeks, during which weight, coat state and sucrose preference were monitored weekly. After 6 weeks of UCMS exposure mice were subjected to behavioural testing battery, at the end of which blood was collected and mice were culled for brain tissue collection (A) Average sucrose preference measured over 2 consecutive nights once every 2 weeks. (B) Latency to find and start eating a cookie in the buried cookie test (C) Latency to start eating the pellet in the novelty suppressed feeding test (D) Food pellet consumption in the NSF arena during the trial and in the home cage during first 10 min after the trial, **p<0.01 derived from unpaired t-test; Data represents mean±SEM*

6.2.4 UCMS did not induce behavioural despair in FST, while isolated UCMS-exposed animals displayed more social behaviours than controls

In the FST, UCMS exposure did not affect duration of any of the four main types mouse behaviour, namely swimming, struggling, paddling also known as climbing, and immobility (see Figure 23A) (2-way ANOVA UCMS factor F (1, 60) = $-1.279*10^{14}$, p>0.999; Type of behaviour F (3, 60) = 387, p<0.0001; Interaction F (3, 60) = 1.178, p = 0.326). Social behaviours and aggression was evaluated during 5 min exposure to an unfamiliar conspecific juvenile mouse. 2-way ANOVA showed the main effect of interaction between UCMS and type of behaviour (Interaction F (7, 144) = 6.001, p< 0.0001; UCMS F (1, 144) = 0.001, p = 0.975; Behaviour type F (7, 144) = 97.87, p<0.0001). Post-hoc Bonferroni multiple comparisons showed that UCMS-exposed animals spend more time engaging in social behaviours targeted at an unfamiliar animal, such as sniffing and allogrooming, while CNTRL animals spent more time in non-social

behaviours, such as digging and rearing. UCMS did not significantly increase aggression in mice (see Figure 23B).

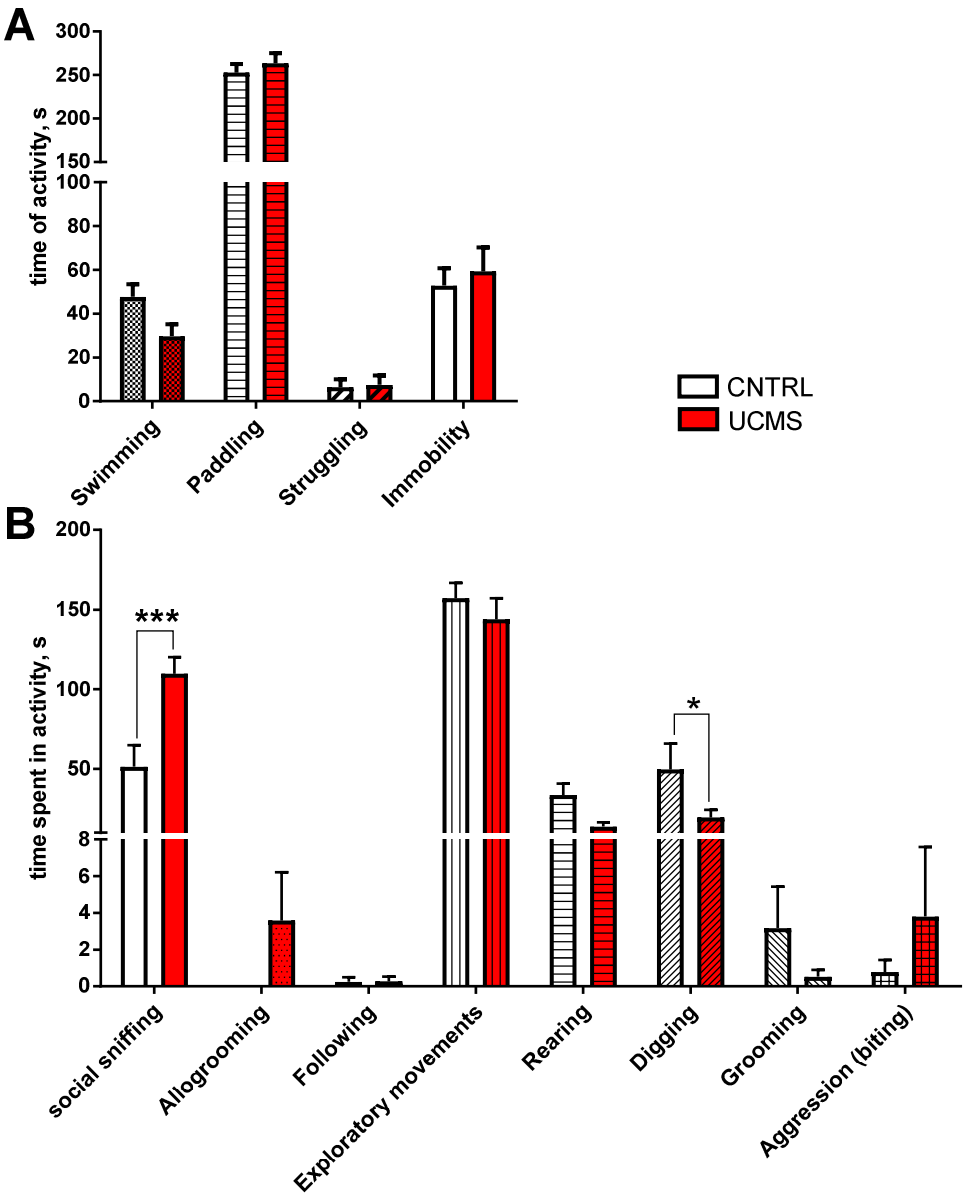

Figure 23 Behavioural despair and social behaviours in the UCMS Experiment 3

*Male BALB/cAnNCrl mice (n=10/group) aged 7 weeks at the beginning of the experiment were subjected to UCMS or CNTRL conditions for 6 weeks, during which weight, coat state and sucrose preference were monitored weekly. After 6 weeks of UCMS exposure mice were subjected to behavioural testing battery, at the end of which blood was collected and mice were culled for brain tissue collection (A) Duration of each type of mouse behaviour during the 6 min forced swim test trial (B) Social behaviours evaluated during 5 min exposure to an unfamiliar conspecific mouse. Data represents mean±SEM, *p<0.05, ***p<0.001 derived from post-hoc Bonferroni multiple comparisons CNTRL vs UCMS*

6.2.5 UCMS did not affect plasma corticosterone response to FST but increased plasma CRP and reduced plasma leptin levels

Results showed that UCMS did not affect the baseline level of CORT or response to swim stress (Effect of FST F (1, 16) = 108.6, p< 0.0001; UCMS F (1, 16) = 0.288, p = 0.599; FSTxUCMS F (1, 16) = 2.98, p = 0.103) (see Figure 24A).

A panel of 10 cytokines was also measured in the plasma derived from cardiac blood, however none of the analytes reached the detection level of the assay apart from C-reactive protein (CRP), which was significantly elevated in UCMS-exposed group (unpaired two-tailed t-test t= 2.508, p = 0.023) (see Figure 24B). Leptin levels were also measured in plasma to gain insight into hormonal regulation of appetite. Leptin levels were significantly decreased in UCMS group compared to controls (unpaired two-tailed t-test t = 2.477, p = 0.027) (see Figure 24C).

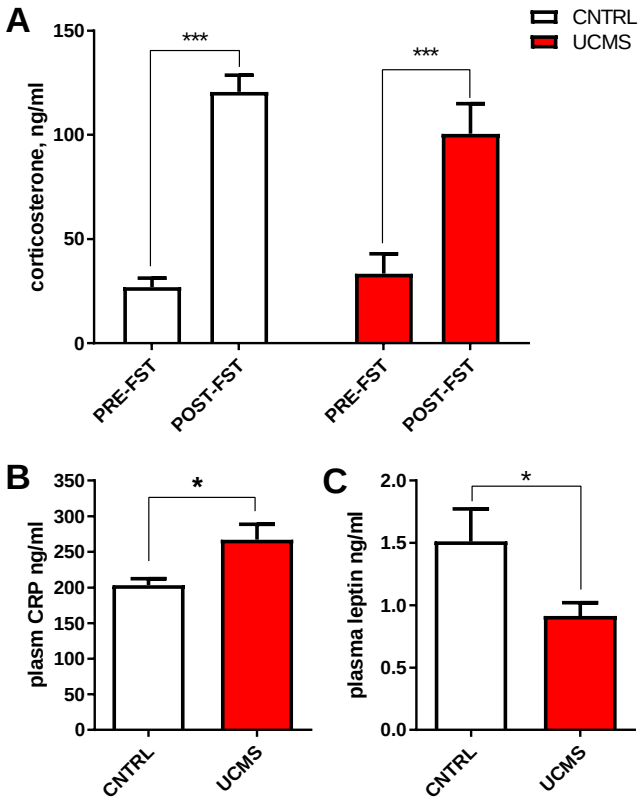

Figure 24 Plasma parameters measured in the UCMS Experiment 3
*Male BALB/cAnNCrl mice (n=10/group) aged 7 weeks at the beginning of the experiment were subjected to UCMS or CNTRL conditions for 6 weeks, during which weight, coat state and sucrose preference were monitored weekly. After 6 weeks of UCMS exposure mice were subjected to behavioural testing battery, at the end of which blood was collected and mice were culled for brain tissue collection (A) Plasma corticosterone (CORT) response to forced wim test (FST) measured 24 hours before (PRE-FST) and 30 min after (POST-FST) the test (B) Plasma levels of the C reactive proteie (CRP) in the blood collected by the cardiac puncture at the end of the behavioural testing battery (7 days after termination of the UCMS protocol) (C Plasma levels of leptin in the blood collected by the cardiac puncture at the end of the behavioural testing battery (7 days after termination of the UCMS protocol). Data represents mean±SEM, *p<0.05 derived from unpaired t-test, ***p<0.001 derived from Bonferroni multiple comparisons CNTRL vs UCMS*

6.3 Discussion

The results of the UCMS Experiment 3 showed that the protocol utilised in this study was sufficient to induce low grooming phenotype, however ensured mild severity of the protocol and 100% survival of animals. Indeed, grooming behaviour was strongly affected, however visible changes of coat state only appeared on week 4. The delay with a change in coat state was probably due to a decrease in the intensity of the protocol compared to UCMS Experiment 2, as the overlap of the stressors was not utilised to reduce its severity. In addition, daily injections and therefore drug administration was not included in this protocol with the same aim of reducing its severity. This was based on the comparison between saline injected and non-injected mice conducted earlier (see Figure 10) which showed that daily injection reduce grooming in BALB/c mice, supported by previous studies showing stress-like effect of daily injections (Drude et al., 2011; Meijer et al., 2006). Despite the late onset of low grooming phenotype, in this experiment UCMS group displayed significantly lower weight on week 1 confirming the effectiveness of the protocol used. The absence of this effect on later weeks could be related to habituation of mice to UCMS exposure.

In this experiment, we wanted to determine if novelty-induced hyperlocomotion appears already after 3 weeks of stress exposure. The results of open field test showed that hyperlocomotion was already strongly present at week 3. Moreover, it was accompanied by a significant increase in the centre time. This data suggests that hyperactivity is not related to the longevity of stress, but more likely to the frequent nature and unpredictability of stressors. As it has been shown previously that behaviour in a light-dark box test is less affected by hyperlocomotion (Ito et al., 2010), this test was added to the behavioural battery in this experiment. However, in the light-dark box, the UCMS group also displayed reduced anxiety ("anxiolysis-like behaviour"). This observation allows to suggest that the reduced anxiety induced by UCMS might not be fully dependent on hyperactivity. Interestingly, the very first paper to describe UCMS in mice also showed that mice spent more time in the light zone of the test, which was interpreted as a decreased sensitivity towards affective environmental stimuli (Kopp, Vogel, MC Rettori, et al., 1999). Other studies interpret reduced anxiety induced by UCMS as impulsivity reminiscent of impulsive behaviour in psychiatric patients (Couch et al., 2016).

Sucrose preference measurements during weeks of UCMS provided interesting data. On week 1, when animals were exposed to 1% solution, both groups showed a small preference, which could be explained by a low percentage of sucrose and low sensitivity of BALB/c. On week 2 CNTRL animals did not prefer sucrose, which could be a result of habituation. Interestingly the

UCMS group showed a small preference on this week, although the difference between the groups was not statistically significant. Finally on week 4, when sucrose concentration was raised to 2%, CNTRL showed preference while the UCMS group did not. This could be a consequence of the UCMS exposure, as on this week coat state of mice also significantly deteriorated. On week 6 the difference was no longer present, which again can be a result of habituation on a second exposure to the same dose. Therefore, anhedonia observed on week 4 in sucrose preference coincided with a significant increase in coat deterioration score on this week and could be reflecting a true effect of UCMS. Indeed suppressing effect of UCMS on the preference for 2% sucrose in BALB/c mice has been shown previously (Liu et al., 2010).

As in previous experiments, the UCMS group also showed a decreased latency to approach and start eating the pellet in the NSF. While this effect could be attributed to hyperlocomotion, a change in food reward behaviours could also play a role in this effect. Importantly, in Experiment 2 FLX reversed this effect in NSF but did not have any effect on hyperlocomotion, suggesting a distinct mechanism for the two behavioural phenotypes. This observation supports the notion of a potential change in non-locomotor activity related behaviour, such as the drive towards food rewards. To see if this notion could be supported by neurobiological evidence, plasma levels of the appetite-controlling hormone leptin was measured and found to be reduced in the UCMS group. Low levels of leptin could explain a higher drive for food rewards, as leptin is known to act as a negative feedback inhibitor released by adipose tissue to regulate food consumption through leptin receptors in the hypothalamus (Ahima and Osei, 2004). Such an effect of chronic stress on leptin levels has been previously documented in the literature. Ge et al. (2013) described a decrease in plasma leptin levels and a decrease in hypothalamic leptin receptor levels following UCMS in rats, while Liu et al. (2015) showed a suppressing effect of chronic mild stress on mRNA leptin levels in the rat prefrontal cortex. In this study the authors also connected leptin and ghrelin signalling to a stress-induced increase in inflammatory factors such as NLRP3 and GSK-3β, which might have particular relevance for this experiment in light of the increased inflammatory biomarker detected in the UCMS group. Moreover, another study reported an antidepressant effect of leptin on sucrose preference and FST immobility in unpredictable chronic mild stress and social defeat models (Lu et al., 2006). In this study stress exposure was also accompanied by a decrease in plasma leptin levels. Therefore, decrease in leptin levels plays an important role in UCMS-induced phenotype and could potentially underlie changes in food-reward related behaviours. The change in leptin might be reflecting a shift in circadian rhythm which affected the time of feeding drive and levels of hormones regulating it. Indeed it has been shown previously that mice with circadian

rhythm gene knockouts or exposed to disrupted light-dark cycles show changes in leptin levels throughout light and dark phases (Kettner et al., 2015).

One important limitation to the study of food reward related behaviour in this experiment is the lack of food consumption data during the UCMS exposure, which could have helped to distinguish between appetite-related and motivation-related changes in behaviours towards food reward such as those measured in NSF and sucrose preference tests. However, the measure of pellet consumption during the NSF test and upon return to the home cage did not show any difference between UCMS and CNTRL group, suggesting no difference in appetite both in stressful and familiar environment.

In the UCMS Experiment 3, as well as in previous UCMS experiments described in this chapter, no change in immobility or any other behaviours during the FST was observed. Similarly, FST induced a significant plasma CORT increase 30 min after the trial in both CNTRL and UCMS groups. Interestingly, the levels of stimulated POST-FST CORT in this experiment were higher than the corresponding levels in the UCMS Experiment 2, especially in the UCMS group. More robust CORT response in the last experiment could be explained by the absence of daily injection in this study. Indeed it has been shown previously that BALB/c mice exposed to daily injections and repeated psychosocial stress show lower levels of plasma CORT compared to non-injected repeatedly stressed mice (Drude et al., 2011).

In this experiment the social behaviour of animals was assessed, as some aggression during handling was observed in the UCMS Experiment 2. However, single-housed animals spent more time engaging in social behaviours and less time - in non-social activities compared to CNTRL group. While social isolation in juvenile mice is often described to induce social withdrawal and reduce social affiliation (Liu et al., 2016; Okada et al., 2015), some studies do show increase in social behaviours (Naert et al., 2011; Orikasa et al., 2015). It is therefore possible that aggression observed previously in UCMS-exposed group could be a result of daily exposure to injections, which were not present in the UCMS Experiment 3.

Lastly, this experiment provided evidence for the involvement of cytokines in the UCMS response. Plasma levels of CRP were elevated in the UCMS-exposed group. CRP is an acute phase protein widely used in the clinic as an inflammatory biomarker, and it has been found to be elevated in depressed patients (Cepeda et al., 2016). As has been mentioned above, chronic stress in rodents has already been shown to increase level of proinflammatory cytokines in the blood as well as in stress-responsive brain areas, such as the hippocampus, prefrontal cortex and the amygdala (Guan et al., 2015; Wang et al., 2015). However, changes in

CRP have not yet been reported. This could be partly explained by the fact that most of the proinflammatory markers in UCMS studies have been done in rats, in which unlike in mice, CRP has not been detected in the acute phase response (Schreiber et al., 1989). The fact that CRP was the only protein found to be elevated out of a panel of 9 proinflammatory cytokines, which included those previously found to be affected by chronic stress (IL-6, IL-1β and TNFα), could probably be explained by a low sensitivity of the Luminex assay utilised. Unlike cytokines, CRP is normally present in the blood in higher concentration, which could explain why the assay selectively detected its elevation. Therefore, elevation of CRP provides an evidence of modulation of the immune system state by chronic stress, which due to prevalence of clinical CRP data could be of potential translational value. Yet in the future studies a usage of high sensitivity assay could be recommended.

7 Discussion

UCMS experiments 1,2 and 3 showed that adult male BALB/cAnNCrl mice respond to UCMS with reduced grooming and novelty-induced hyperactivity. Manipulation of the control conditions throughout the UCMS experiment showed that sibling pair housing in large cages as used in Experiment 3 is the most optimal housing condition for control group to avoid social isolation stress and reduce risk of cage mate fighting. Daily intraperitoneal injections are not recommended as a drug delivery route as they appear to also add to the allostatic load of control and stress - exposed groups and appear to suppress HPA axis response to acute stress as reflected by a difference in post-FST CORT levels between Experiments 2 and 3.

Experimentation with a schedule of stressors during UCMS showed that 2 stressors per day is not sufficient to induce significant behavioural changes, while 4 stressors can successfully affect behavioural outcome. However, UCMS Experiment 2 showed that a combination of 4 overlapping daily stressors with daily i.p. injections exceeded the severity of the protocol and increased risk of fatality in the stress-exposed group to 50%. In this experiment animal welfare was prioritised as soon as fatality reached 25% and all measures were taken to reduce animal suffering, including preliminary end of the UCMS exposure, however more deaths occurred after UCMS termination potentially due to its long-term effects. Subsequently UCMS Experiment 3 was designed to reduce stress exposure and ensure welfare of animals.

The behavioural phenotypes induced by our protocol included an increase in coat deterioration score, indicative of reduced grooming, and a reduction in grooming time in the splash test as shown in Experiments 2 and 3. Also novelty-induced hyperactivity was a phenotype consistent across all 3 experiments and with previous literature (Strekalova et al.,

2005). It appeared that hyperlocomotion potentially skewed changes in behavioural tests of anxiety, such as the open field and light-dark box, as anxiety in these tests is evaluated based on the time animals spend moving around potentially threatening areas. Yet it is possible that this reduced anxiety ("anxiolysis-like behaviour") was not solely a result of hyperactivity, as the time spent in light box has been shown to be less affected by the hyperactivity of animals. If so, one could speculate that reduced anxiety behaviour in these animals stems from the lack of environmental awareness or an increase in impulsivity. Such hypothesis could be tested in tests assessing impulsive behaviours, such as five-choice serial reaction time task. A study of signalling pathways activated by UCMS in stress-responsive brain areas could shed light on molecular and neurotransmitter mechanisms underlying these behaviours.

Regarding anhedonia, assessed in the sucrose preference tests as a loss of preference to sweetened water, it was detected only when animals were first exposed to 2% sucrose solution in the UCMS Experiment 3. It is possible that 4% solution used in previous experiments triggered ceiling effect in all animals, therefore no effect of stress was observed in the UCMS Experiment 1 and 2. In addition, in these experiments sucrose preference was measured during the whole 24-hour cycle, while in the last experiment most of the measurement was done in the dark phase. The fact that the difference was more apparent in the dark phase suggests the possibility that circadian rhythm alteration might have shifted the dark phase and main period of activity of the UCMS-exposed animals. Sucrose measurements taken separately in light and dark phases would be able to confirm or oppose this notion. One important limitation to the sucrose preference data across all experiments is a lack dose-response type data comparing effect of UCMS or CNTRL conditions on BALb/c mice preference for sucrose solution with different concentrations of sucrose.

However, contrary to expectations, in NSF test animals consistently displayed an increased drive to food reward instead of anhedonia in Experiments 2 and 3. Importantly locomotion can also affect the outcome of the NSF test, as the latency to approach the food pellet in the centre of large arena is the outcome measure. At the same time as animals are food-deprived for 24 hours before the test, appetite and metabolism can also influence the result. Indeed, changes in the plasma level of leptin detected in stressed animals confirmed the possibility of increased appetite. However, a profound change in appetite would be expected to lead to a weight change, which was not observed in these experiments. Moreover, pellet consumption measurements conducted in the Experiment 3 during the NSF trial and upon return to the home cage did not show any difference between CNTRL and UCMS groups. Interestingly in the same experiment repeated sucrose preference measures showed an opposing dynamic of

habituation to sucrose in control and stressed animals, whereby the latter acquired preference to sweet solution with repeated exposures while the former displayed preference only during first exposure. A shift in circadian rhythms induced by UCMS also could have played a role in these effects. If daily disturbance of mice by stressors during the light phase shifted their resting time towards the night, it could explain why they appeared more active and driven to palatable stimuli during the day time testing compared to CNTRL animals. This could also explain why apparent increase in appetite was not accompanied by weight change, if the mice only shifted their feeding to day time, but did not increase overall food consumption. In this case reversal of light/dark cycle and application of stressors during the dark phase could have avoided development of such effects. However, to confirm this hypothesis sleep cycle monitoring and circadian rhythm measures, as well food consumption measurements during the light and dark phases would be required. The latter could also help to distinguish between appetite-driven and hedonic reward – driven motivation for food stimuli. Indeed motivation towards food rewards is regulated by both dopaminergic mesocorticolimbic circuit responsible for reward behaviours, as well as by the metabolic state of the body, encoded in the brain by insulin, ghrelin, leptin and orexin neuropeptide signalling, which influence appetite centres in hypothalamic and hindbrain areas (Fulton, 2010). As these pathways closely interact with each other and could both be affected by stress, their distinction requires careful consideration.

As for behavioural despair, no change in immobility was observed in FST in any of the experiments. It is possible that the absence of increased immobility was related to hyperlocomotion of mice. While interpreting the results of the FST, it is important to remember that this test has been developed as a screening tool for monoaminergic antidepressant activity (Porsolt et al., 1977) and its main strength lies in its predictive validity, as indeed it is sensitive to all classes of antidepressants and can distinguish antidepressants from other classes of psychopharmacological compounds (Gould, 2009). While Porsolt et al. (1978) claimed it to possess face validity, its interpretation as a model of behavioural despair has received significant criticism. West (1990) argued that immobility in the FST can be interpreted as an adaptive, energy conserving response to inescapable conditions, more indicative of the cognitive functions of the animal rather than of its mood state. Therefore, some authors urge to limit its use to screening antidepressant compounds (Nestler and Hyman, 2010; Petit-Demouliere et al., 2005). Indeed, in the UCMS Experiment 1 Fluoxetine but not UCMS was a significant factor affecting immobility time. In light of this, the absence of the UCMS effect in FST in the UCMS Experiment 3, where antidepressant treatment was not

included, does not necessary compromise the validity of the UCMS protocol used in this experiment.

Lastly, plasma corticosterone measures did not show an increase in HPA axis activity described as a consequence of UCMS in the literature. In fact, the opposite effect was observed in the UCMS Experiment 2 where UCMS prevented elevation of POST-FST CORT levels but FLX treatment restored CORT response to control levels. Interestingly, attenuation of the CORT response during chronic restraint stress exposure has already been described in BALB/cAnNCrl substrain (Sadler and Bailey, 2016), which could suggest a strain-specific response of the HPA axis to chronic stress. However, limitations of the single CORT measure taken during the light phase rather than in the active phase might have affected the outcome. Importantly it has been described that release of corticosterone follows a diurnal rhythm, therefore a single corticosterone measure does not capture the full profile and is not representative of the overall dynamics of the HPA axis. Indeed Aslani et al. (2014) showed that corticosterone is lowest during the light phase, when most of our blood collection was done, so it is possible that the data would differ had the blood been collected during the active period. CORT measured at various time points during the 24 hours would improve the understanding of the HPA axis regulation in this study.

Yet the corticosterone data taken together with the FLX treatment data allows speculation that UCMS in these experiments might have triggered an impairment of HPA axis regulation, which has been linked to antidepressant resistance (Khemissi et al., 2014; Surget et al., 2016). Dexamethasone suppression test would be able to show if indeed UCMS triggered alteration of the HPA axis negative feedback inhibition. As in the latter study this phenotype also included a modification of the effect of FLX on adult hippocampal neurogenesis, a histological study will investigate this hypothesis further. Finally, measures of plasma inflammatory biomarkers detected elevation of only one analyte, CRP. This analyte was only included in the assay in the last experiment, therefore it is not possible to assess if this finding was consistent across experiments. Given the insufficient sensitivity of the assay to the small changes typically induced by chronic stress, it was not possible to assess whether other key cytokines were altered in UCMS. While analysis of blood samples with hypersensitive assays in the future might provide more evidence for the involvement of the immune system, the presence of CRP elevation, frequently used in the clinic, is already suggestive of occurring immune system involvement. Investigation of protein or mRNA levels of proinflammatory factors in the stress-responsive brain areas could show if such systemic effect corresponds to the changes in the central nervous system.

8 Conclusions

To summarise, data collected from the experiments described in this chapter provide a basis for recommendations on the improvement of the UCMS protocol and behavioural testing for the future studies, particularly if using a stress-susceptible strain such as BALB/c. Control groups should be housed in large cages with their siblings to avoid social isolation and cage mate fighting. It is preferable that the light/dark cycle is reversed in the facility to allow to carry out UCMS protocol, behavioural testing and blood collection in the active phase and avoid a shift in the circadian rhythm in UCMS-exposed mice, which could have triggered hyperactivity in experiments described here. At the same time day time exposure to UCMS likely disrupts light phase rest in mice therefore might have an advantage of resembling disturbed sleep also seen in depressed patients (Motivala et al., 2005), which could be relevant for some studies. The schedule of stressors used in the UCMS Experiment 3 could be recommended for future studies. Furthermore, it would be recommended to carry out sucrose measurement during the last weeks of UCMS, with 2% solution being optimal for the BALB/cAnNCrl mice. Separate light and dark phase measurements might provide extra insight into anhedonic behaviour. While NSF and FST did not prove to be very informative in our experiments, prevention of hyperactivity could allow for better results in activity-dependant tests, such as open field, NSF and FST. In addition, food consumption measurements during light and dark phases could add extra insight into appetite changes and help distinguish appetite – related motivation from hedonic motivation toward food rewards.

As for neurobiological measures, specific assessment of HPA axis negative feedback regulation, such as dexamethasone suppression test, could be beneficial for a future study. While no elevation of plasma proinflammatory cytokines was detected in my experiments, a use of high sensitivity assay might be able to show if small changes could by triggered by UCMS. However, assessment of the brain tissue would provide a better insight into the effect of chronic stress inflammatory processes in the CNS, as will be partly done in the next chapter by looking at the effect of UCMS on hippocampal microglia. Next chapter will also complete the study of neurobiological effects of UCMS in the brain by exploring the effects exerted by UCMS exposure on adult hippocampal neurogenesis and relating these effects to the phenotypes described here.

Chapter 3 Adult hippocampal neurogenesis in the UCMS model

1 Introduction

Investigating adult hippocampal neurogenesis (AHN) has become an indispensable part of preclinical depression research ever since the neurogenic hypothesis of depression was postulated by Jacobs et al. (2000). Extensive research into the role of AHN in depression highlighted its involvement in disease development and in the mechanism of actions of antidepressant medications (Tanti and Belzung, 2013). AHN is seen as a promising target for novel drug discovery, therefore assessing its status and involvement in an animal model of depression is of particular importance.

1.1 Adult hippocampal neurogenesis in UCMS studies

Much of the research on the role of neurogenesis in depression has been conducted using the UCMS model. Specifically, the model remains instrumental in deciphering the role of AHN in the mechanism of antidepressant action. As such, Santarelli et al. (2003) used UCMS to show that when neurogenesis is ablated, fluoxetine (FLX) treatment is not effective in improving depression-like behaviours such as anhedonia in the NSF or reduction of grooming following UCMS. However, ablation of neurogenesis on its own does not promote development of these behaviours. These findings asserted the role of neurogenesis in antidepressants' mechanism of action, however questioned the causal role of neurogenesis decline in the development of depression. Yet later studies showed that UCMS is capable of reducing cell proliferation and neuronal differentiation (Alonso et al., 2004; Mineur et al., 2007). Mineur et al. (2007) also hypothesised that decline of neurogenesis would correlate with a decline in hippocampal-dependent contextual memory. However such a link was not found, again questioning the functional consequences of neurogenic deficit. To address the role of neurogenesis in UCMS-induced behavioural deficits Surget et al. (2008) ablated neurogenesis with focal irradiation in mice before UCMS exposure. The results showed that the absence of neurogenesis did not induce depressive-like behaviour and did not prevent UCMS effects. However, neurogenesis ablation prevented reversal of UCMS-induced behavioural deficits in grooming and anhedonia by FLX and imipramine. Interestingly, corticotrophin-releasing factor 1 (CRF1) receptor antagonist, SSR125543, was still effective in irradiated mice (Surget et al., 2011; Surget, Saxe, et al., 2008). As a compound directly affecting HPA axis did not require neurogenesis to

produce an antidepressant effect, the authors concluded that suppression of the HPA axis might be the mechanism through which neurogenesis promotes the therapeutic action of monoaminergic antidepressants. Moreover, the latter study also showed that neurogenesis is required for fluoxetine to repair UCMS-induced hypothalamo-pituitary-adrenal (HPA) axis dysregulation and hyperactivity, asserting the role of neurogenesis in antidepressant effect on the HPA axis function (Surget et al., 2011).

A study by Snyder et al. (2011) supported this notion by showing that genetic ablation of neurogenesis in mice is sufficient to cause impaired negative feedback inhibition, and some behavioural deficit in behavioural despair and anhedonia. Yet the biggest effect of neurogenesis ablation became apparent after animals' exposure to acute restraint stress – neurogenesis-depleted animals showed more profound deficits in anhedonia than their neurogenesis-intact counterparts. These results prompted the authors to conclude that the role of neurogenesis is to protect the mouse against the effects of acute stress by supporting the negative feedback inhibition of HPA axis, but repeated stress exposure and neurogenesis decline increase stress susceptibility. Such a hypothesis could explain why ablation of neurogenesis on its own does not cause any behavioural deficits in many studies which employed various neurogenesis ablation strategies in both rats and mice (Bessa et al., 2009; Jayatissa et al., 2009; Lagace et al., 2010).

Indeed, the interplay between the AHN and the HPA axis has been extensively studied. As has been mentioned above, increasing glucocorticoid levels has been shown to reduce AHN *in vivo* as well as *in vitro* (Anacker et al., 2011). The glucocorticoid receptor (GR) is thought to play a key role in this effect. Indeed, GR is highly expressed in the hippocampus and in neural progenitor cells (Egeland et al., 2015). Treatment with the GR antagonist mifepristone has been shown to block the antineurogenic effect of glucocorticoid administration as well as of CUS exposure (Mayer et al., 2006; Oomen et al., 2007). At the same time GR downregulation in the hippocampus has been linked to HPA axis hyperactivity and depression-like behaviours. Mice with a deletion of GR in the forebrain neurons, including the hippocampus, display impaired feedback inhibition, HPA axis hyperactivity and depression-like behaviour (Boyle et al., 2005). Taken together these studies suggest that GR dysfunction in the hippocampus leads to HPA axis hyperactivity and elevated level of systemic corticosterone (CORT). Moreover, it has been shown that antidepressants increase neurogenesis via a GR-dependent mechanism (Anacker et al., 2011).

The relationship between the HPA axis and AHN was further investigated in the study by David et al. (2009) where depressive-like behaviour was induced by chronic CORT injections. In this model, a behavioural deficit was accompanied by a decline in neurogenesis, and both were reversed by chronic fluoxetine treatment. Similar to the UCMS studies, ablation of neurogenesis did not prevent a depressive effect of CORT, but it blocked the therapeutic effect of fluoxetine (FLX) on anhedonia in the NSF test. Furthermore, in this study neurogenesis was not required for FLX-induced reversal of the anxiety and behavioural despair. Therefore, this study further confirmed that neurogenesis is dispensable for the induction of a depression-like phenotype by HPA axis hyperactivity, but it is required for reducing anhedonia by antidepressants. A distinction between neurogenesis-dependent and independent behaviours was further confirmed in a UCMS-based study, where animals were separated into hyperactive and hypoactive HPA axis groups based on the state of their HPA regulation (Khemissi et al., 2014). FLX elevated anxiety and behavioural despair in both groups, but exerted antidepressant effect on anhedonia in the NSF only in a group where it also increased neurogenesis levels, the hyperactive HPA axis group. This study further highlighted the complex relationship between HPA axis, AHN and the effect of antidepressant drugs.

Interestingly a recent study by Hill et al. (2015) showed that increasing AHN with an inducible transgenic model could reduce anxiety and depressive-like behaviours induced by chronic CORT, but did not improve HPA axis regulation. It is important to note however that in the CORT model, as opposed to the UCMS model, HPA axis shows hypoactive response to acute stress (David et al., 2009). Therefore, the absence of increased neurogenesis in this model does not exclude the possibility that increased neurogenesis could improve regulation of the hyperactive HPA axis.

1.2 Dendritic morphology of adult born and prenatally born neurons in chronic stress models

Bessa et al. (2009) suggested a different approach to the role of neuronal plasticity in the effects of chronic stress and antidepressants. Their study confirmed the division between neurogenesis dependent and independent effects of antidepressants outlined by Santarelli et al. (2003) and David et al. (2009). However, the authors went beyond neurogenesis by showing that chronic stress also caused deterioration in dendritic morphology and spine density in mature neurons of the dentate gyrus (DG), cornu ammonis (CA) 3 and the prefrontal cortex (PFC). These changes persisted and were elevated by antidepressants in the absence of

neurogenesis, suggesting that dendritic remodelling not only in the hippocampus, but also in the PFC, might underlie effect of stress and the mechanism of antidepressant action.

Indeed, several other studies support the neuroplasticity hypothesis. Sousa et al. (2000) described reduction of dendritic length and branching density in hippocampal granule and pyramidal neurons following chronic stress, and linked these effects to the elevation of CORT levels. Similarly Lussier et al. (2013) showed that chronic CORT treatment reduced the number of DCX+ cells with complex dendritic morphology. In this study classification of DCX+ cells based on the dendritic tree architecture, similar to that suggested by Plümpe et al. (2006), was utilised to detect dendritic changes. The authors showed that chronic CORT exposure selectively depleted the population of DCX+ cells with a more developed dendritic tree extending into the molecular layer but no effect on dendritic architecture of the mature neurons was found. These results were replicated in a UCMS study which also classified DCX cells based on their morphology and found that chronic stress led to a reduction in DCX+ cells with complex dendritic arborisation, which was attributed to a rise of CORT levels (Vega-Rivera et al., 2016). However, in this study dendritic remodelling of mature neurons was not investigated. Nonetheless, the ability of chronic stress to induce dendritic atrophy and reduction in spine density in mature neurons was documented multiple times in different areas of the hippocampus, as well as in the PFC, amygdala and nucleus accumbens (Hains et al., 2009; Liston et al., 2006; Qiao et al., 2016; Yuen et al., 2012).

The role of glucocorticoid signalling in neuroblast maturation was further elucidated in a study by Fitzsimons et al. (2012). The authors showed that GR knockdown in the neurogenic niche *in vivo* accelerates dendritic maturation and increases spine density and maturation in newborn neurons, as well as promoting radial migration of neuroblasts into the external layers of the GZ. These changes were accompanied by hippocampal-dependant contextual memory deficits. This data suggests that GR activation could be limiting the speed of dendritic maturation and migration of neuroblasts, which in normal conditions is necessary to support hippocampal function, but pathological overstimulation of the GR by excessive CORT levels might be reducing the rate of neuroblast maturation below the level necessary to buffer effects of stress.

1.3 The role of microglia in AHN changes upon UCMS

Another mechanism through which chronic stress might lead to a dendritic deficit is through the dendritic loss triggered by activated microglia. In healthy adult brains, microglia residing in the neurogenic niche play an important role in maintaining functional neurogenesis by

phagocytising apoptotic neural progenitors at an early stage of their transition into the postmitotic neuroblasts (Sierra et al., 2014). Interestingly, this phagocytosis has been shown to be carried out by unchallenged microglia with resting state-like morphology (Sierra et al., 2010). However when activated by an inflammatory stimulus, microglia have been shown to exert detrimental effect on neurogenesis directly or via release of proinflammatory cytokines capable of reducing the rate of cell proliferation and differentiation (Ekdahl, 2012). As such, Ekdahl et al. (2003) showed that treatment with the microglia-supressing drug minocycline prevents antineurogenic effects of systemic LPS injections. Microglia-derived cytokines such as IL-1β, IL-6 and TNFα have been shown to be instrumental in the effect of inflammation on AHN (Cacci et al., 2005; Koo and Duman, 2008; Monje, 2003).

Indeed chronic stress exposure has been shown to increase the number of microglial cells in various brain areas where dendritic atrophy was observed, including DG, CA1, CA3 and the PFC (Hinwood et al., 2012; Tynan et al., 2010; L Zhu et al., 2015). Moreover, some studies report increases in the number of microglial cells displaying activated phagocytic morphology or an increase in the expression of activation markers, such as CD11b or MHCII (Liu et al., 2015; Lu et al., 2014). The functional importance of microglial activation in the effect of chronic stress has been demonstrated in a chronic social defeat study where treatment with minocycline prevented development of depression-like behaviour (Chijiwa et al., 2015). However it is important to note that a complete consensus over the effect of chronic stress on microglial activation has not been reached in the literature. For example, Kopp et al. (2013) showed that 14 days of UCMS unlike homotypic chronic restraint stress did not induce microglial activation in the PFC in rats. These negative results could be explained by the time-dependent dynamics of microglial response to stress observed by Kreisel et al. (2013). This study reported that in C57BL6 mice microglial proliferation and activation induced by the first few days of CUS exposure is then followed by reduction of microglial numbers due to apoptosis and dystrophic changes in microglial morphology, such as shortened processes and small cell body size in the hippocampus after 5 weeks of continuous CUS exposure.

Nonetheless, a recent study demonstrated that housing rats in a stressful environment leads to an increase in phagocytic morphology and showed an increase in microglia phagocytosing of axon terminals and dendritic spines (Milior et al., 2016). In another study, microglia activated by systemic LPS exposure caused destabilisation of spines and reduction of spine density in the neocortex (Kondo et al., 2011). Microglia might be affecting dendritic remodelling not only via direct interaction, but also through the effect of proinflammatory factors released from microglia in the activated state. For example, the proinflammatory cytokine IFNγ has been

shown to induce dendritic retraction and reduction in the rate of synapse formation in hippocampal cultures *in vitro* (I-J Kim et al., 2002). Thus microglial activation could play a role in dendritic atrophy seen in chronic stress animal models of depression.

Overall chronic stress has been shown to reduce neurogenesis and dendritic maturation of immature neurons, as well as causing dendritic remodelling in the mature cells. Glucocorticoid signalling, microglial activation and proinflammatory cytokines were implicated in these effects.

2 Study aims

The aim of the analyses described in the Results section of this chapter was to assess AHN changes in UCMS-exposed mice, and to attempt identification of neurobiological parameters affected by UCMS which modulate these changes. AHN was assessed in two experiments: the UCMS Experiment 2, where single-housed mice were exposed to CNTRL or UCMS conditions for 7 weeks and treated with FLX 10mg/kg or saline for 6 weeks; and the UCMS Experiment 3, wherein sibling pair-housed CNTRL group was compared to UCMS group exposed to stressors for 6 weeks. AHN assessment was not conducted in the pilot UCMS experiment as UCMS did not induce a strong behavioural phenotype, and therefore was not expected to induce detectable neurobiological changes.

In both experiments, the density of DCX-positive cells in the dentate gyrus was used as an estimate of a level of AHN. DCX is a marker of migrating neuroblasts and is expressed from the stage of late type 2 progenitors (type 2b) as a sign of neuronal lineage determination (Kronenberg et al., 2003). In DCX-positive cells transition from proliferating progenitors into immature neurons occurs, as reflected by neuritogenesis, migration into the granular zone (GZ) and increasing electrophysiological input received by these cells (Steiner et al., 2006). Indeed, most of the dendritic tree develops during the period of DCX expression. Importantly, most of cell death also occurs in the DCX+ cells (Plümpe et al., 2006). DCX expression seizes on the last stage of neuronal maturation, when granule neurons transition from calretinin to calbindin expression, a marker of mature granule neurons (Brandt et al., 2003). Therefore, DCX+ cell population comprises a wide variety of progenitors at different stages of neuronal maturation. To gain insight into the DCX+ cell subtypes most affected by UCMS, classification of DCX+ cells based on dendritic morphology according to Plümpe et al. (2006) was used to distinguish between different levels of neuroblast maturation. This analysis together with migration distance estimates were conducted only in the tissue collected during the UCMS

Experiment 3, as in this experiment satisfactory CNTRL conditions were achieved and behavioural effects of the UCMS exposure were the most consistent.

For the above-mentioned reasons only AHN changes in the UCMS Experiment 3s were followed by the assessment of possible factors involved in the modulation of neurogenesis. This assessment included the determination of the changes in the density of hippocampal microglia, which could reflect microglial proliferation as a result of its activation. To assess the combined and individual contribution of plasma parameters reported in the previous chapter, multiple regression analysis approach was utilised. This approach has a number of advantages over other statistical approaches. Firstly, it is able to evaluate not just associative, but predictive relationship between independent and dependent variables. Secondly, it simultaneously assesses the contribution of a group of factors rather than a single factor to the modulation of the dependent variable, which is likely to be relevant for the complex effects occurring in the heterogeneous UCMS model. Finally, stepwise regression method utilised allows to compare predictive ability of different factors and to use exploratory approach to selecting the combination of measures best predicting the outcome variable (Miles and Shelvin, 2001). As the effect of a combination of immune, corticosteroid and metabolic factors on AHN in UCMS has not been evaluated before, such exploratory approach appeared to be most suitable to meet the aims of the analysis.

3 Methods

3.1 Brain tissue collection

To collect fixed tissue, animals were anaesthetised with Euthatal i.p. (Merial Animal Health Ltd, Harlow, UK) at a dose of 40 mg/kg pentobarbital sodium. Deep anaesthesia was confirmed by the loss of righting and pain reflexes and slowing of the rate of respiration. Animals were subsequently transcardially perfused with 30ml of saline and 50ml of 4% paraformaldehyde (Paraformaldehyde, prills, 95%, 441244, Sigma-Aldrich, Poole, UK) in phosphate-buffered saline (pH = 7.4 from PBS tablets, 18912-014, Gibco by Life Technologies, Paisley, UK) through the left cardiac ventricle. Brains were post-fixed overnight in 4% PFA at 4°C for 24 hours, and subsequently stored at 4°C in 30% sucrose (Sigma-Aldrich, Poole, UK) in PBS until sectioning (1-3 weeks).

3.2 Immunohistochemistry

Serial coronal sections of 40µM thickness were cut on a HM430 sliding freezing microtome (Thermo Scientific) and stored in tris-buffered saline (TBS, pH=7.4) with 30% v/v glycerol, 15%

w/v sucrose and 0.05% w/v sodium azide (all Sigma Aldrich, UK) to prevent bacterial growth and for cryoprotection at -20°C during subsequent freezer storage. For immunohistochemistry on free floating sections every sixth section was used. Free floating sections were treated with 1% hydrogen peroxide (Sigma-Aldrich, UK) for 30 minutes to block endogenous peroxidase activity within the tissue. After a triple wash in phosphate buffered saline (PBS pH=7.4, Gibco LifeTechnologies UK) sections were incubated in blocking solution containing 10% normal goat serum (Vector Laboratories, Peterborough, UK) and 0.01% Triton X (Sigma-Aldrich, UK) to prevent non-specific staining. After subsequent 3 washes in PBS sections were incubated in primary antibodies dilutions in blocking solution overnight at 4°C. For neuroblast detection anti-DCX antibody (Ab18723 raised in rabbit, Abcam, UK, 1:1000 dilution) was used; for microglia immunostaining antibody for Iba1 (019-19741, Wako, Japan, 1:500 dilution) was used. Separate sections were incubated in PBS without primary antibody to act as a negative control for immunostaining, see Figure 25 for representative images of immunohistochemical staining performed with and without primary antibodies. Next day sections were rinsed in PBS, incubated with an appropriate biotinylated secondary antibody (goat anti-rabbit or rat, 1:200, Vector Laboratories, Peterborough, UK) diluted in blocking solution for 2 hr, followed by signal amplification step with an avidin-biotin complex (Elite ABC kit, Vector Laboratories, Peterborough, UK). The staining was visualized with 0.05% diaminobenzidine (DAB) solution (Sigma-Aldrich, UK). When stained, sections were mounted on Superfrost Plus glass microscope slides (Thermo Scientific, UK) in anatomical order. Mounted sections were air dried for 24 hours and subsequently dehydrated in ethanol and cleared in xylene for 10 min. Slides were sealed with cover glass with distyrene plasticizer xylene (Sigma-Aldrich, UK).

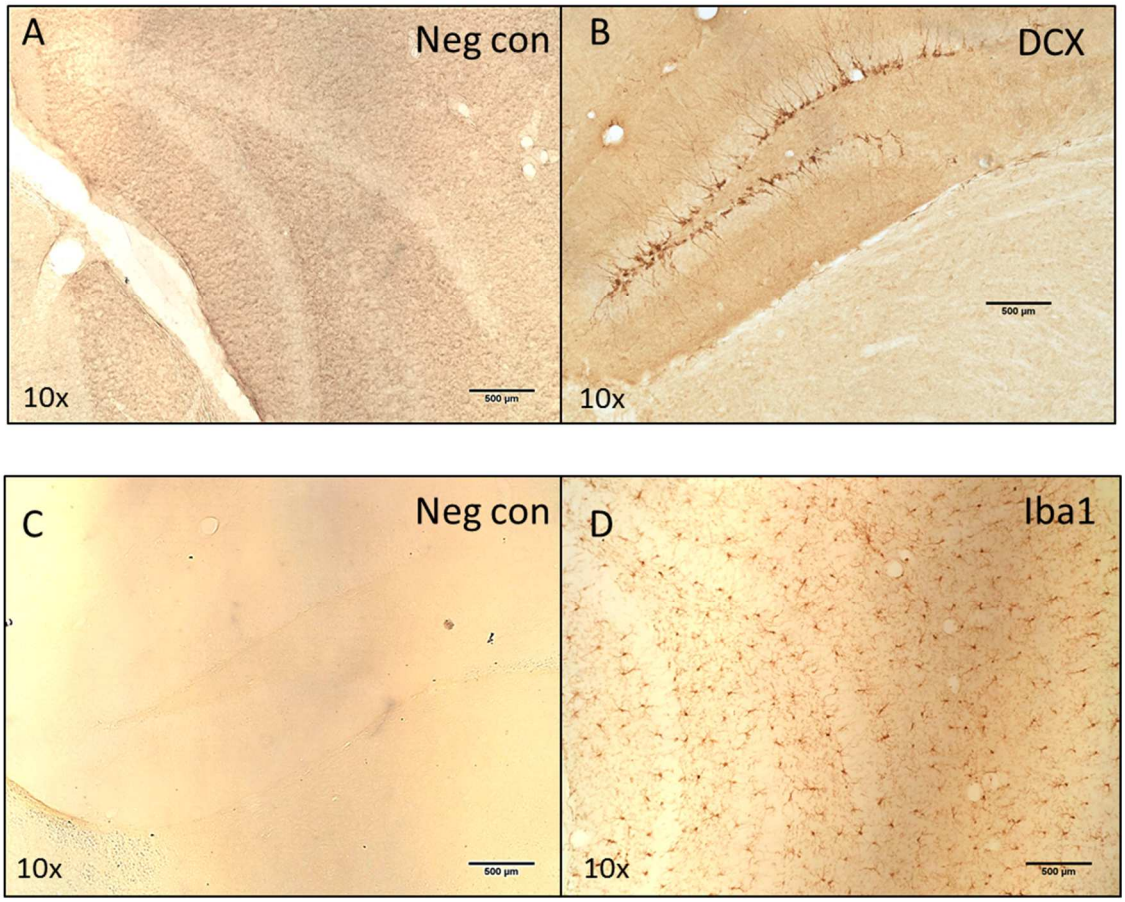

Figure 25 Examples of photomicrographs of immunostaining reactions performed with primary antibodies and in their absence for negative control (Neg con)
(A) Photomicrographs of tissue immunostained according to the protocol for doublecortin (DCX) omitting the primary antibody (B) Photomicrographs of tissue immunostained according to the protocol for DCX with the primary antibody (C) Photomicrographs of tissue immunostained according to the protocol for and ionized calcium-binding adapter molecule 1 (Iba1) omitting the primary antibody (D) Photomicrographs of tissue immunostained according to the protocol for Iba1 with the primary antibody; scale bar = 500 µm, 10x magnification

3.3 Stereological analysis of immunopositive cell density

For microscopy, the Axioskop 2 MOT Plus Miscroscope (Zeiss) with automated stage connected to Stereoinvestigator v.7 (MBF Bioscience, US) software was used. Immunopositive cell density was determined using the volume and cell population number estimated by semi-automated Optical Fractionator method applied by the stereological software. For this analysis an equal number of sections per brain were used. The region of interest (ROI) was delineated under 10x magnification and overlaid with a grid (X=94.6µm, Y=182.5µm) for systematic random sampling, a method of unbiased selection of virtual counting frames with equal distance in X and Y directions between them. The size of a counting frame was set at 50µmx50µm with 50 desired sampling sites per ROI, according to parameters previously validated for the study of hippocampal neurogenesis (Dias, Bevilaqua, et al., 2014). The number of immunopositive cells within each frame was manually counted from the camera image at 40x magnification based

on their morphological appearance and position in relation to acceptance and rejection lines of the counting frame (Gundersen, 1977). Subsequently the optical fractionator was applied in the Stereoinvestigator software, a method which estimates the total volume based on the known sections thickness (15µm) and intersection distance (240µm) and cell population by extrapolating the number of cells counted within the counting frames to the total estimated volume of ROI (Slomianka and West, 2005). Subsequently cell density was calculated by diving the estimated population number by the estimated total volume.

3.4 DCX cell classification based on dendrite morphology

The DCX positive cells were visually classified according to the categorization of Plumpe et al. (Plümpe et al., 2006). The AB group included cells with no, or short, plump processes, most closely resembling the morphology of late type 2b amplifying progenitors (see Figure 3), which are already committed to the neuronal lineage as reflected by their DCX expression, yet are still capable of proliferation (Kempermann, 2010); the CD group included cells with medium length processes without branching usually directed along SGZ and not extending beyond the granular zone, most likely representing the cells in transition from amplifying progenitors to the postmitotic stage of neuronal maturation with first neuritogenesis occurring; the EF group comprised cells with long branching dendrite(s) reaching the molecular layer (see Figure 26). These cells are likely to be the type-3 postmitotic progenitors which already receive electrophysiological input (Ambrogini et al., 2004). The density of each type of cells was determined using stereology as described in section 3.3.

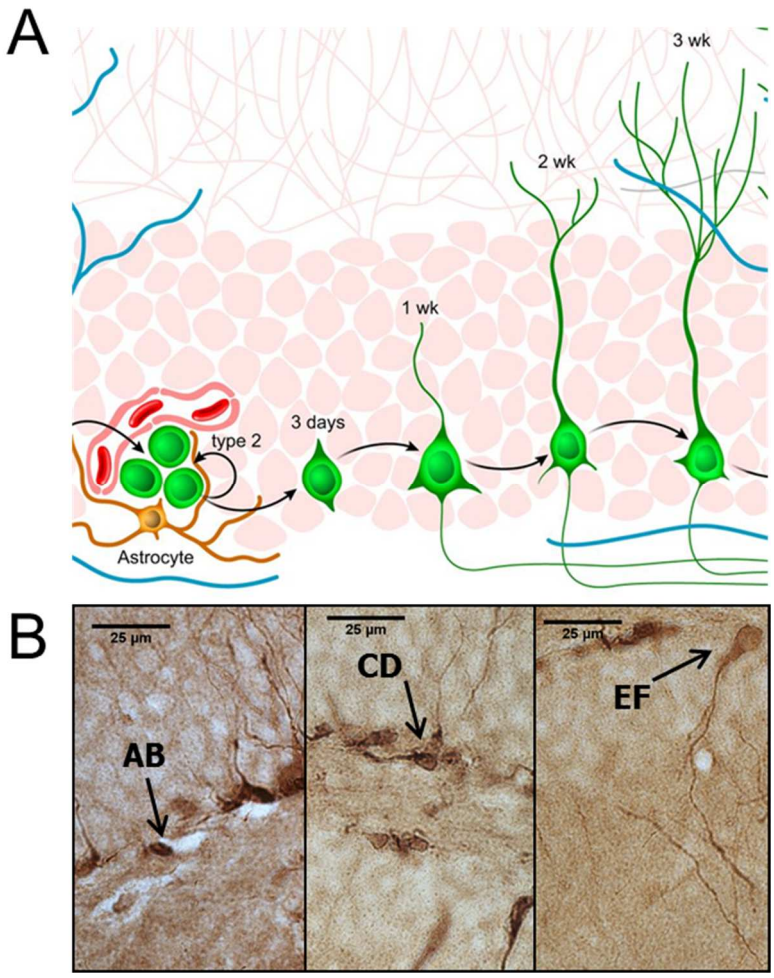

Figure 26 Morphological classification of DCX+ neuroblasts.
(A*) Timeline of neuronal development in the subgranular zone of the dentate gyrus showing type 2 amplifying progenitors and type 3 neuroblasts at different stages of dendritic tree maturation with corresponding timeline, from Aimone et al. Physiol Rev 2014;94:991-1026; (B) Photomicrographs show three types of DCX+ cells used in the dendritic morphology classification. Arrow on the left-hand panel shows type AB DCX+ cells, with no or very short processes; centre panel shows CD type cell with short plump processes often growing along the SGZ; right-hand panel arrow points at the EF-type DCX+ neuroblast with a long, branching dendritic tree reaching into the molecular layer of the DG*

3.5 Morphometric analysis of dendrites

EF-type neurons from each section were selected for morphometric analysis of dendrites. For this sections were imaged using a 40× objective, and micrographs were acquired using a Zeiss AxioCam MR Rev3 camera. Primary, secondary and tertiary dendrites were manually traced using the NeuronJ plugin for ImageJ developed by Meijering (Meijering et al., 2004) and measured using image pixel to mm calibration as has been done previously (Dias, Bevilaqua, et al., 2014; Srivastava et al., 2012).

3.6 Migration distance of DCX+ cells

To estimate relative distance of DCX+ cells migration through the granular zone, the height of the GZ has been divided into 10 bins, and a relative distance of migration was estimated by

assigning a score from 0 to 1 to each DCX+ cell based on the position of its cell body relative to the borders of the GZ (see Figure 27). For example, cells positioned in the subgranular zone were assigned 0 distance, cells in the middle of the GZ height were assigned 0.5, and those on the border between granular zone and molecular layer were given a score of 1, as has been done previously (Han et al., 2016). The average percentage of cells positioned within each distance bin for each brain was used in statistical analysis.

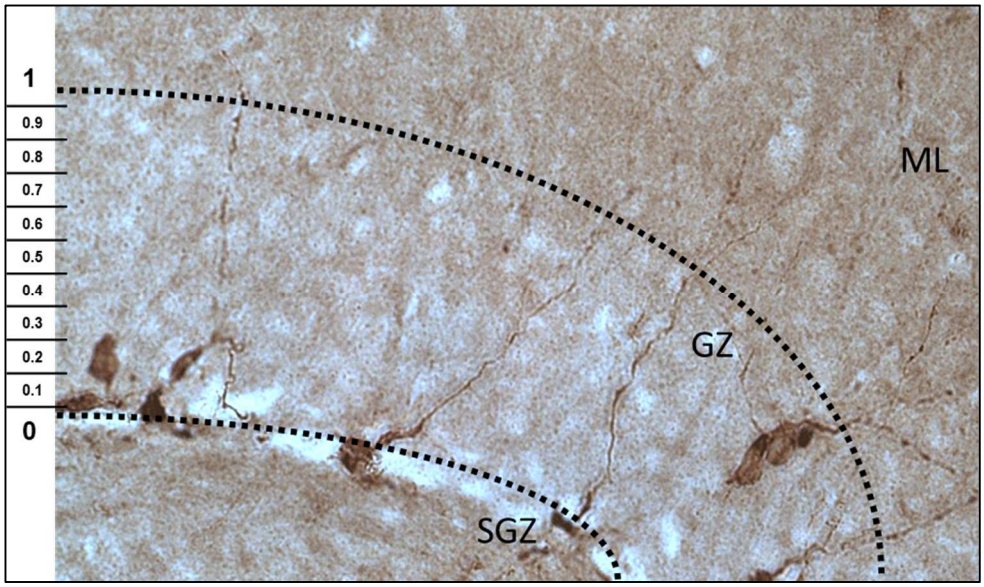

Figure 27 Relative neuroblast cell migration scale through the height of the Granular zone of the hippocampal dentate gyrus
ML – molecular layer, GZ – granular zone, SGZ - subgranular zone, immunostaining for doublecortin

3.7 Statistical analysis

For histological analysis presented in this chapter, tissue was collected from mice in Experiments 2 and 3 after completion of behavioural testing (12 days after termination of UCMS in Experiment 2 and 7 days after termination of UCMS in Experiment 3). In experiment 2 6 animals per group were included into the histological analysis due to animal loss described in Chapter 2 (section 5.1) Behavioural and serological parameters of these animals were reported in Chapter 2 sections 5.2.1-5.2.4. In Experiment 3 9 animals per group were included into the histological analysis. Behavioural and serological parameters of these animals were reported in Chapter 2 sections 6.2.1-6.2.5. 10 sections at 240µM interval which included dentate gyrus were included into the stereological analysis for each animal. For statistical analysis in the UCMS Experiment 2 two-way ANOVA was used and post-hoc Bonferroni multiple comparisons between individual groups were applied. For the UCMS Experiment 3, unpaired two-tailed t-test was used after normal distribution of the data was confirmed with the Kolmogorov-Smirnov test for single measures. For related measures, such as DCX+ cells, dendritic

morphology types and migration distance groups two-way ANOVA was used with post-hoc Bonferroni multiple comparisons within each type or distance group.

To determine collective and individual contributions of available neurobiological measures to the changes in DCX+ cell density, multiple linear regression approach was used. Multiple linear regression with the stepwise backward method of predictor entry was conducted using SPSS software (IBM SPSS Statistics version 22, USA). DCX+ cell density was entered as a dependant variable, and baseline and post-anaesthetic CORT measures, Iba+ microglial cell density, leptin and CRP levels as independent predictors. To meet the assumption of no multicollinearity, prior to regression absence of correlations among predictors was confirmed by Pearson's correlation analysis in all possible pairs of independent variables.

4 Results

4.1 UCMS and FLX modify hippocampal DCX+ cell density

The effect of 7 weeks of UCMS exposure and 5 weeks of chronic fluoxetine treatment with 10mg/kg was investigated in UCMS Experiment 2 (for experimental design see Chapter 2). In the UCMS Experiment 2 the level of adult hippocampal neurogenesis was estimated based on the density of DCX-positive neuroblasts. 2-way ANOVA showed that FLX was a significant factor affecting density of DCX+ cells in the hippocampal dentate gyrus (FLX factor $F(1, 17) = 11.17$, $p = 0.0039$; UCMS x FLX factor $F(1, 17) = 3.514$, $p = 0.0781$; UCMS factor $F(1, 17) = 3.410$, $p = 0.0823$) (see Figure 28). As the effect of UCMS was not significant, and the behavioural phenotype of UCMS-exposed mice was not sufficiently distinct from CNTRL mice, further analysis of the DCX+ cell population was not conducted.

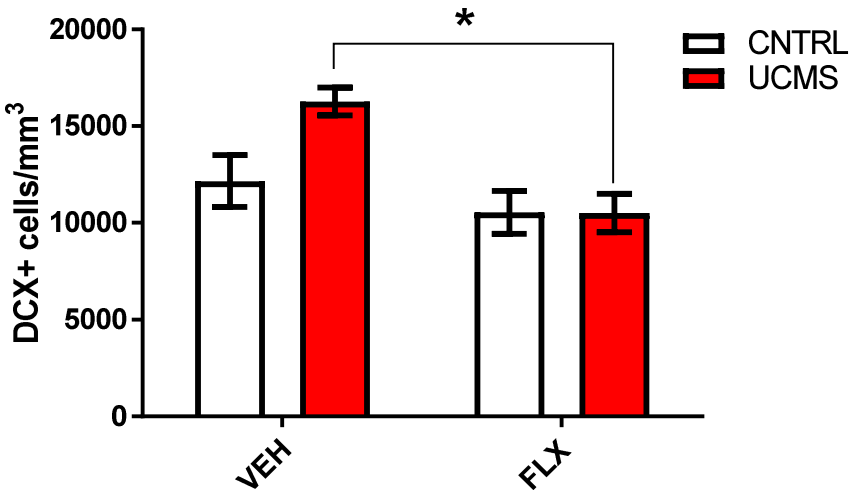

Figure 28 Density of doublecortin-positive (DCX+) cells in the UCMS Experiment 2
*Male BALB/cAnNCrl mice (n=6/group, 10 sections per animal) aged 7 weeks at the beginning of the experiment were subjected to UCMS or CNTRL conditions for 7 weeks; fluoxetine (FLX) 10mg/kg or saline (VEH) i.p. injections commenced on the 3rd week of UCMS and continued during behavioural testing until mice were culled for brain tissue collection; DCX+ cell density calculated using stereological analysis reflects the level of adult hippocampal neurogenesis in experimental mice. Data represented as mean±SEM, *p<0.05 derived from post-hoc Bonferroni multiple comparisons UCMS vs UCMS FLX.*

4.2 In Experiment 3 UCMS reduces the density of DCX+ neuroblasts and their dendritic morphology

Two-tailed unpaired t-test of DCX+ cell density in CNTRL and UCMS groups showed that in the UCMS Experiment 3 stress-exposed group displayed a reduced number of DCX+ neuroblasts in the hippocampal dentate gyrus (t=2.954, p=0.01) (see Figure 29 A and B for representative photomicrographs and C for data analysis). To investigate which stage of neuroblast maturation was particularly susceptible to UCMS effect, DCX+ cells were classified based on the level of maturity of their dendritic tree. 2-way ANOVA for UCMS and neuroblast type showed that bith factors significantly affected the density of each type in treatment groups (Effect of type $F(2,28)=17.3$, $p<0.001$; Effect of UCMS $F(1, 14) = 8.725$, $p = 0.01$) Post-hoc Bonferroni multiple comparisons between CNTRL and UCMS showed that the density reduction was specific to the populations of cells with "EF" type mature-like dendritic trees, with their branches reaching into the molecular layer of the DG (see Figure 29 A and B for representative photomicrographs and C for data analysis). However, when the dendritic trees of these cells were analysed, no difference in the number of processes (two-tailed unpaired t-test t=0.31, p=0.76) or their length was detected between groups (two-tailed unpaired t-test with total length values t=0.058, p=0.95) (see Figure 29 D and E).

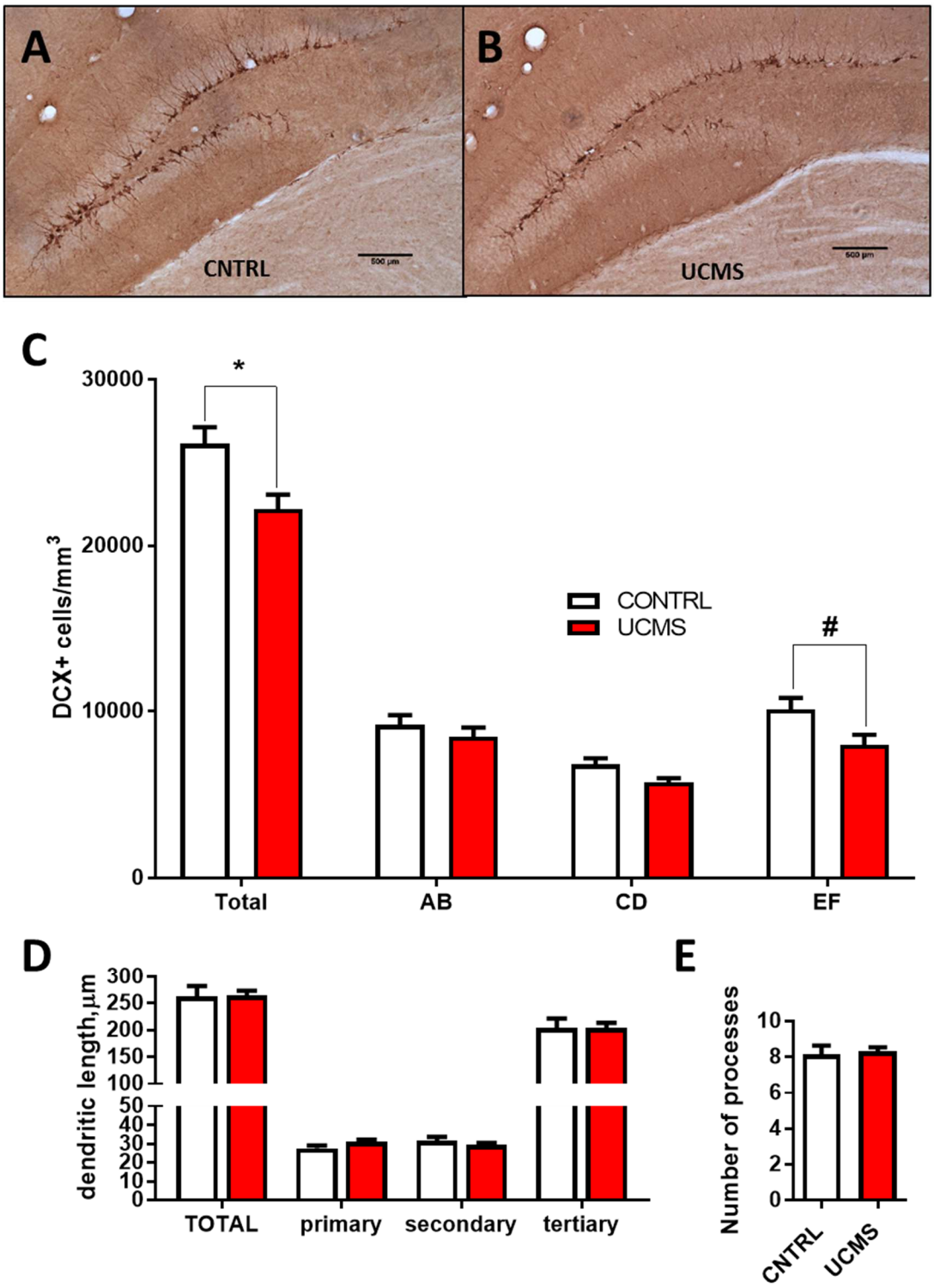

Figure 29 Effect of UCMS on the density and morphology of doublecortin-positive (DCX+) neuroblasts in the UCMS Experiment 3

*Male BALB/cAnNCrl mice (n=10/group) aged 7 weeks at the beginning of the experiment were subjected to UCMS or CNTRL conditions for 6 weeks. After UCMS exposure mice were subjected to behavioural testing battery, at the end of which blood was collected and mice were culled for brain tissue collection. 10 sections per brain were used in immunohistochemical staining for DCX as a marker of immature neuroblasts in the hippocampal dentate gyrus. Representative photomicrographs of the hippocampal GZ of mice exposed to CNTRL **(A)** or UCMS (**B**) conditions show DCX+ cells and their dendritic trees, scale bar = 500µm **(C)** The density of all DCX+ neuroblasts (TOTAL) and of the "AB", "CD" and "EF" types classified based on their dendritic tree morphology **(D)** Average length of DCX+ dendrites of all DCX+ cell types (TOTAL) and separately for each neuroblast type **(E)** the number of processes in "EF" type neuroblasts. Data presented as mean±SEM, *p<0.05 derived from unpaired t-test CNTRL vs UCMS; #p<0.05 derived from post-hoc Bonferroni multiple comparisons CNTRL vs UCMS*

4.3 UCMS reduces the percentage of DCX+ cells residing in the SGZ

As adverse environment has been previously shown to affect migration of the adult-born neuroblasts, the effect of the UCMS Experiment 3 on migration distance of the DCX+ cells was analysed. For this granular zone was divided into 10 equal migration distance bins, with cells bin 0 assigned to the subgranular zone and bin 10 to the layer of GZ bordering with the molecular layer of the dentate gyrus. Each DCX+ cell was assigned to the distance bins according to the position of its nucleus. 2-way ANOVA of average percentages of cells residing in each bin showed that interaction between bin distance and UCMS exposure significantly affected cell position (Effect of Interaction $F(10,170) = 1.99$, $p = 0.037$; Effect of UCMS $F(1,17) = 1.57$, $p = 0.227$; Effect of distance $F(10,170) = 622$, $p<0.0001$). Post-hoc Bonferroni multiple comparisons UCMS vs CNTRL within each bin showed that UCMS reduced the percentage of DCX+ cells residing in the SGZ ($p = 0.005$), and a trend towards increase in the percentage of cells residing within several relative distance units was found in the UCMS group (see Figure 30A). Photomicrographs in Figure 30B show examples of DCX+ cells in the DG of the UCMS-exposed mice which are residing further from the SGZ. However, the average relative distance cell bodies of DCX+ neuroblasts migrated from the SGZ was not significantly different between the two groups (two-tailed unpaired t-test $t = 1.57$, $p = 0.134$) (see Figure 30C).

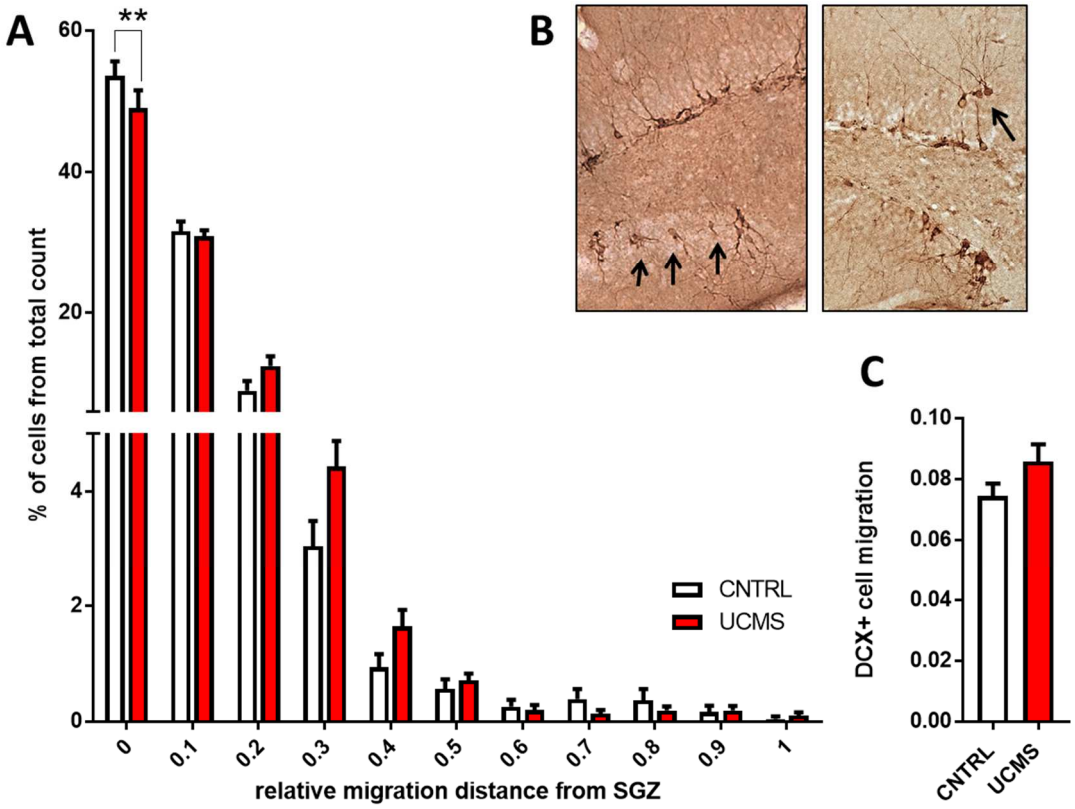

Figure 30 Migration parameters of the doublecortin-positive (DCX+) cells in the UCMS Experiment 3
Male BALB/cAnNCrl mice (n=10/group) aged 7 weeks at the beginning of the experiment were subjected to UCMS or CNTRL conditions for 6 weeks. After UCMS exposure mice were subjected to behavioural testing battery, at the end of which blood was collected and mice were culled for brain tissue collection. 10 sections per brain were used in immunohistochemical staining for DCX as a marker of immature neuroblasts in the hippocampal dentate gyrus. ***(A)*** *the number of neuroblasts residing in the SGZ (0) and in 10 different layers of the granular zone (0.1-1) (GZ)* ***(B)*** *photomicrographs of the DCX+ cells in the hippocampal GZ of the UCMS-exposed mice. Arrows point at cells with a high relative migration distance* ***(C)*** *Average relative migration distance of DCX+ cell bodies). Data presented as mean±SEM, *p<0.05 derived from unpaired t-test; #p<0.05, ##p<0.01 derived from post-hoc Bonferroni multiple comparisons CNTRL vs UCMS*

4.4 UCMS does not affect the number of Iba1+ microglia in the hippocampal GZ, but increases its density in the mPFC

To detect signs of microglial activation accompanying decline of AHN, analysis of the number of Iba1+ hippocampal microglia in the GZ was conducted. Unpaired two-tailed t-test of microglial density showed that no significant effect of UCMS on the number of microglial cells was found ($t = 1.384$, $p = 0.187$) (see Figure 31A). However, unpaired two-tailed t-test showed that density of Iba1+ microglia was increased in the mPFC of the UCMS-exposed group compared to control ($t = 3.139$, $p = 0.006$) (see Figure 31B). For this analysis, region of interest was defined as a 5000µmX5000µm area between stereotactic coordinates +1.70 and +1.90 relative to Bregma which includes some prelimbic, infralimbic and cingulate cortex (Franklin and Paxinos, 2012)

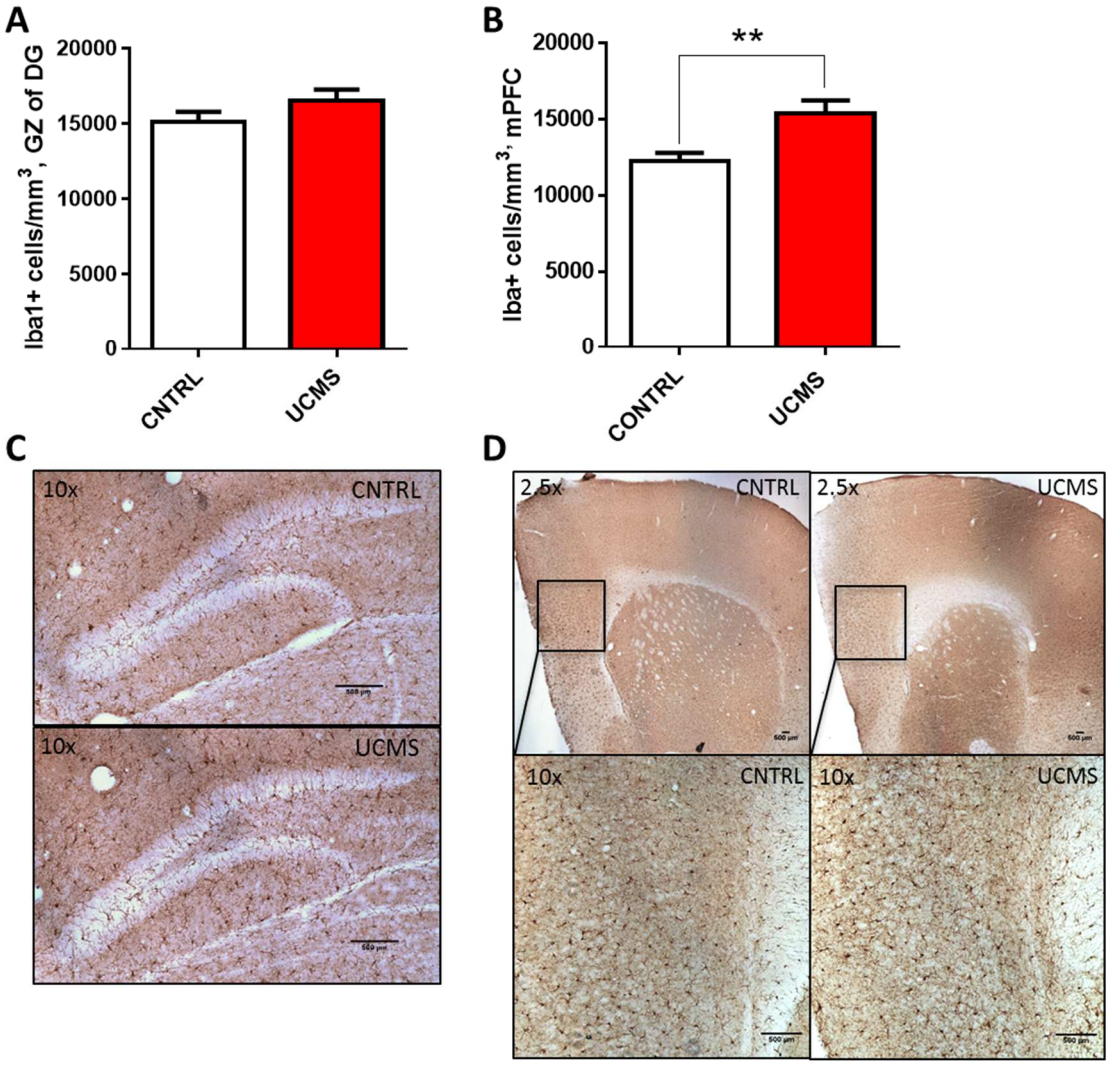

Figure 31 Iba1-positive microglia in the hippocampal GZ and mPFC in the UCMS Experiment 3
Male BALB/cAnNCrl mice (n=10/group) aged 7 weeks at the beginning of the experiment were subjected to UCMS or CNTRL conditions for 6 weeks. After UCMS exposure mice were subjected to behavioural testing battery, at the end of which blood was collected and mice were culled for brain tissue collection. 10 sections per brain were used in immunohistochemical staining for Iba1 as a marker of resident microglia **(A)** *Density of the Iba1+ cells in the granular zone (GZ) of the dentate gyrus (DG)* ***(B)*** *Density of Iba1+cells in the medial prefrontal cortex (mPFC)* ***(C)*** *Representative photomicrographs of the microglia in the GZ in CNTRL (top panel) and UCMS (bottom panel) groups, 10x magnification, scale bar = 500 µm* ***(D)*** *Representative photomicrographs of the microglia in the mPFC region in CNTRL (left panel) and UCMS (right panel) groups, scale bar = 500 µm. Top panels show region of interest were mPFC microglia was quantified at 2.5x magnification, between stereotaxic coordinates Bregma +1.70 and +1.90. Bottom panels show representative images at 10x. Data presented as mean±SEM, **p<0.01 derived from unpaired t-test CNTRL vs UCMS.*

5 Discussion

In this chapter, effect of UCMS on a number of parameters reflecting the state of AHN, as well as its relationship with hippocampal microglia and other neurobiological parameters was investigated.

5.1 Possible reasons for paradoxical neurogenic effects in the UCMS Experiment 2

In the UCMS Experiment 2 contrary to expectations, the DCX+ cell density was increased by UCMS exposure, an effect which was blocked by FLX treatment. There are a number of reasons which could have caused such an effect. Firstly, behavioural data suggested that the CNTRL group in this experiment also experienced a level of stress, potentially due to single housing and daily injections. Single housing has been shown previously to reduce AHN and impair negative feedback inhibition of the HPA axis (Evans et al., 2012; Spritzer et al., 2011). Indeed DCX+ cell density of CNTRL group in this experiment is strikingly similar to DCX+ cell density reported previously in UCMS-exposed BALB/c mice (Khemissi et al., 2014). On the other hand, UCMS-exposed animals were found to be hyperactive, and physical activity such as voluntary running has a very strong proneurogenic effect (Farioli-Vecchioli et al., 2014; van Praag et al., 1999). Therefore, it is possible that if these mice spent more time moving around the cage, it could have had a stimulating effect on their neurogenesis. If this is the case, it is unclear why FLX treatment reversed this effect, as FLX did not reverse UCMS-induced hyperactivity in other behavioural tests. One possible explanation could come from the understanding of the HPA axis state of these animals. As was shown in Chapter 2, both CNTRL and UCMS-exposed animals displayed hypoactive HPA axis which responded to acute stress with suppressed CORT elevation, and FLX was only able to restore normal HPA axis response in the CNTRL group. This hypoactive HPA axis profile resembles the profile of antidepressant-resistant mice in a previous UCMS study (Khemissi et al., 2014). In this study a subgroup of mice displayed similar hyporesponsive HPA axis, which coincided with absence of FLX effect on some behavioural deficits including anhedonia in the NSF, and on AHN, thereby suggesting that hyporesponsive HPA axis leads to antidepressant resistance. The level of DCX+ cell density in antidepressant resistant mice was comparable to that in the FLX-treated groups in UCMS Experiment 2. Moreover, a recent study also showed that in a group of mice with hyporesponsive HPA axis FLX reduced cell proliferation and caused a trend towards decline in DCX+ cells, resembling the present data (Surget et al., 2016). Therefore, it is possible to suggest that in the BALB/cAnNCrl strain of mice, UCMS induces a fluoxetine-resistant phenotype attributed to hypoactivity or hypersuppression of the HPA axis. Factors such as single housing and stress of daily injections in control groups additionally complicated this data, therefore another UCMS experiment with improved control conditions was necessary to disentangle observed effects.

5.2 AHN in the UCMS Experiment 3

In a UCMS Experiment 3 control animals were pair housed and no antidepressant treatment was applied to avoid effect of daily injections while a valid UCMS protocol was being established (for experimental design see p.93). This time, in line with previous studies, UCMS exposure reduced the number of DCX+ neuroblasts in the dentate gyrus. As DCX comprises a wide variety of neuronal progenitors at different stages of neuronal maturation, the DCX+ cells were classified into subtypes based on their dendritic morphology to estimate which stage of maturation was most affected by UCMS. Data analysis showed that UCMS selectively reduced the number of neuroblasts with more mature dendritic tree appearance (EF type), potentially corresponding to postmitotic type 3 progenitors. This finding is in line with two previous studies which also identified a reduction in DCX+ cell population with complex dendritic morphology following UCMS or chronic CORT exposure (Lussier et al., 2013; Vega-Rivera et al., 2016).

Several potential mechanisms might underlie the UCMS effect on EF-type DCX+ cell population. Low number of DCX+ cells with developing dendritic trees might be reflecting low rate of neuronal maturation, higher cell death among maturing neuroblasts, reduced dendritogenesis or dendritic atrophy. A number of previous studies showed a reduction in dendritic length or branching following chronic stress exposure in mature granule neurons of DG and in other areas, such as CA3 and the mPFC, suggesting that this effect is not specific to immature neurons and therefore is more likely to be a result of occurring atrophy rather than aberrant development (Bessa et al., 2009; Sousa et al., 2000). Moreover, in the latter study, mPFC was the only region where dendritic atrophy was also accompanied by a reduction of spine density, suggesting that chronic stress might have a stronger effect on synaptic plasticity in this region. To detect if EF-type cells also showed signs of dendritic deficit, their dendritic length and branching was measured by manual tracing of dendritic trees visualised by DCX staining. However, no difference in the number or length of branches was identified. The absence of effect could be due to methodological limitations of this study. It is possible that applied methodology did not allow to detect dendritic tree changes as it was limited to DCX+ cells, while many studies reporting dendritic deficit previously utilised Golgi impregnation method which allows tracing of dendrites of prenatally-born as well as adult-born mature neurons. Moreover, DAB staining and 40µm thickness of sections in our study did not allow to trace the most distal parts of the dendritic tree. Unfortunately, it was not possible to perform Golgi impregnation in this study as the tissue was perfused with formaldehyde.

5.3 UCMS effect on neuroblast migration in the GZ

A recent study of the pattern of cell migration in SGZ neuroblasts found that radial migration into the GZ was restricted to later stages of DCX expression most likely corresponding to EF type morphology (Sun et al., 2015). Therefore, we decided to assess if UCMS affected the migration pattern of DCX cells. For that, position of DCX+ cell bodies relative to the SGZ was estimated according to a method suggested by Han et al. (2016). The analysis showed that in the UCMS group, a significantly smaller percentage of cells remained in the SGZ, and a trend towards increase in the percentage of cells was observed in a number of deeper GZ layers. This data suggests that UCMS promoted radial migration of immature neuroblasts. While little is known regarding the effect of stress on neuroblast migration, a number of other pathological conditions have been shown to induce cell migration in the DG. The most well-characterised is the effect of kainic acid - induced seizures used to model temporal lobe epilepsy. Jessberger et al. (2007) showed that kainic acid injections induced appearance of ectopical granular neurons on the hilar/CA3 border, which were suggested to contribute to increased excitability. While this phenotype has little in common with those observed in our study, it provides evidence that pathological stimuli can promote neuroblast migration. In addition, chronic neuroinflammation induced by intraventricular administration of LPS has been shown to increase migration distance of newly born neurons (Belarbi et al., 2012). Interestingly, increased neuroblast migration was described in a number of gene knockout phenotypes, some of which are highly relevant for the present study. Fitzsimons et al. (2012) described GR knockdown in neural progenitors *in vivo*, which resulted in increased neuroblast migration into the GZ, accompanied by hippocampal-dependant contextual memory deficits. This parallels the potential involvement of glucocorticoid signalling in observed effects. Moreover, a knockdown of two schizophrenia-related genes, disrupted in schizophrenia 1 (DISC1) and phospholipase C-β1(PLC- β1), was also accompanied by increased neuroblast migration (Duan et al., 2007; Manning et al., 2012). Interestingly PLC-β1 knockdown also induced spatial memory impairment and hyperlocomotion, while mutations in DISC1 have been linked to mood disorders (Thomson et al., 2014). Therefore, evidence exists that increased migration in the DG could have negative consequences for hippocampal-dependent behaviour and might be linked to glucocorticoid signalling.

5.4 Microglial density and its possible link with AHN changes

As microglial activation has been implicated in the effect of chronic stress on adult hippocampal neurogenesis, we wanted to investigate if microglia might be involved in the observed effects of UCMS. As microglial activation frequently leads to increase in microglial

density due to proliferation of these cells or recruitment of macrophages from the bloodstream, the number of Iba1+ cells is often used as an estimate of the level of microglial activation. However, no significant change in microglial number in the dentate gyrus has been observed in this study. While several studies showed increase in microglial number upon chronic stress exposure (Farooq et al., 2012; Tynan et al., 2010), other studies report decrease in the number of microglial cells and appearance of dystrophic hyperramified phenotype which follows initial microglial activation, subsiding after weeks of chronic stress exposure (Hinwood et al., 2012; Kreisel et al., 2014). Walker et al. (2013) argues that these discrepancies could be due to the methodology used to assess the number of Iba1+ cells. Some studies employ thresholding method to quantify the immunostaining, as opposed to estimating cell density based on cell counts, as it was done in the UCMS Experiment 3. Unlike cell counting, threshold analysis does not distinguish between increase in the immunostained surface due to enlarged cell body or cell numbers, as it would be in case of microglial activation, and increases in the number and length of processes, as in the case of dystrophic hyperramification (Walker et al., 2013). Moreover, evidence exists that chronic stress paradigms involving heterotypic stressors as opposed to repeated stressors such as restraint or social defeat may not induce microglial activation (Kopp et al., 2013). This difference was attributed to a higher corticosterone levels induced by heterotypic stress, known to limit microglial activation upon stress (Sugama et al., 2013). Finally, some studies show that chronic stress exerts its main effect on microglial activation in areas other than dentate gyrus, such as nucleus accumbens, amygdala and the prefrontal cortex (Couch et al., 2013; Tynan et al., 2010). Indeed, the number of microglial cells was increased in the PFC of UCMS-exposed mice in this experiment, confirming that methodology used was capable of detecting stress-induced microglial proliferation. Previously chronic stress-induced microglial activation has been described to take place simultaneously in the hippocampus and the PFC (Wohleb et al., 2012), therefore it is somewhat surprising that microglial density was selectively increased in the PFC area. However, previous studies also suggested that the PFC is more sensitive to chronic stress than the hippocampus, as indicated by the suppression of glutamatergic transmission upon repeated stress which was present in the former but not the latter region (Yuen et al., 2012). At the same time PFC has been shown to be less prone to microglial dystrophy following chronic stress, which could be another reason why microglial increase was still present at the time of sacrifice in this area (Kreisel et al., 2014). Interestingly, dendritic atrophy in the PFC upon stress exposure is a well-described phenomenon (McEwen and Morrison, 2013; Radley et al., 2008). In light of this it is interesting to speculate if observed increase in microglial density could be related to this phenomenon

and if potential increase of proinflammatory signalling in the PFC could have indirectly influenced dendritic development in the hippocampal DG.

5.5 Contribution of systemic factors to the antineurogenic effects of UCMS

Next the combined predictive relationship and individual contributions of plasma measures reported in the previous chapter, microglial number and AHN has been evaluated using the explorative approach of a stepwise multiple linear regression. Stepwise multiple linear regression with backward method of predictor entry eliminates factors which do not improve the prediction of the dependant variable and presents the combination of factors which best explains changes in the outcome. UCMS exposure and neurobiological changes observed in this study, including CRP and leptin plasma levels, Iba1 hippocampal density and plasma levels of CORT measured in unstimulated animals and physically stressed animals were initially included into the model. However multiple regression showed that leptin and Iba1 did not contribute to the variation in the density of DCX+ cells, while UCMS exposure factor combined with unstimulated CORT and post physical stress CORT levels and plasma CRP significantly predicted almost 90% of variation in the density of DCX+ cells. Beta coefficients show that baseline CORT and CRP had negative relationship with DCX levels, which is line with the notion that inflammation and overactivation of the HPA axis negatively impact AHN. However positive relationship with post-physical stress CORT suggests that excessive suppression of the HPA in response to acute stress, potentially caused by UCMS, was detrimental for neurogenesis. This notion is line with the previous studies showing that some mice respond to UCMS exposure with a hypersuppression of the HPA axis, which has linked to inability of antidepressants to exert their proneurogenic effects (Khemissi et al., 2014). As for the lack of predictive effect of the microglial number, the involvement of the immune system activation was nonetheless confirmed by the predictive ability of the CRP levels. Therefore, it is possible that a factor more specifically reflecting microglial activation rather than proliferation, such as activation marker expression, would show a stronger role of microglia in these effects.

5.6 Limitations to the study of neurogenesis in UCMS experiments

In the studies described in this chapter density of DCX+ cells measured 7 to 9 days after the end of UCMS was used as an estimate of the level of adult neurogenesis, which presents a number of limitations. DCX is frequently used as a correlate of AHN, as its expression in the adult brain is almost exclusively confined to the immature neurons of the neurogenic regions (Ming and Song, 2005). However a single measure of DCX levels 7 days after the end of UCMS exposure might have a limited ability to reflect the changes in AHN which occurred during

previous weeks of UCMS. On the other hand, as DCX is expressed during different stages of neuronal differentiation, the population of DCX+ cells is likely to include a mixed population of cells which began differentiation 3 days to 4 weeks before the time of sacrifice (Kempermann, 2010). Importantly, DCX levels give only an indirect indication of the changes to the level of cell proliferation and survival in the dentate gyrus, as it is not possible to decipher from this data wether reduction in DCX levels was due to reduced proliferation, increased cell death or reduced commitment of cells to neuronal lineage. Bromohydroxyuridine (BrdU) administration during the UCMS exposure could have allowed to investigate these processes in more detail.

Another limitation to the study of adult neurogenesis is the absence of any behavioural data reflecting the state of neurogenesis-dependent cognitive functions. Indeed, it has been shown previously that reduction of neurogenesis in mouse models of depression is associated with behavioural deficit in spatial and associative memory tasks which have been shown to be neurogenesis-dependent (Darcet et al., 2016). For instance, Surget et al. (2016) showed improvement of spatial memory in the Morris water maze by fluoxetine treatment only in antidepressant responders which also displayed increased neurogenesis, but not in antidepressant-resistant UCMS exposed BALB/c mice. Darcet et al. (2014) showed cognitive deficits in mice exposed to the neuroendocrine model of depression (chronic corticosterone administration) in contextual fear conditioning and Barnes maze, which have been previously associated with AHN (Deng et al., 2010). Inclusion of these tests in our UCMS experiments could have demonstrated whether reduction in neurogenesis seen in Experiment 3 had behavioural consequences for neurogenesis-dependant cognitive functions.

6 Conclusions

Overall, these data show that behaviourally validated UCMS exposure compared to appropriate control conditions in BALB/cAnNCrl mice, reduced the level of immature neuroblasts, with the most mature population of the DCX+ cells being the most affected by the UCMS. As the maturity of the DCX+ cells was evaluated based on their dendritic tree morphology, this finding also goes in line with studies showing the detrimental effect of chronic stress on dendritic and spine density. Next the results of this chapter showed that UCMS stimulated migration of immature neuroblasts away from the SGZ into deeper layers of the GZ. While other detrimental factors such as LPS and kainic acid exposure, as well as GR and schizophrenia related gene knockouts have been previously shown to increase the distance of DCX+ cell migration (Belarbi et al., 2012; Fitzsimons et al., 2012; Jessberger et al., 2007), this effect has not been shown in UCMS before. This finding extends the range of antineurogenic

effects known to be exerted by the UCMS. In the future studies, analysis of dendritic morphology of mature neurons in the hippocampus as well as in other stress-responsive brain regions, such as PFC, could show if effects of UCMS on dendritic morphology extend beyond immature neurons. Antidepressant drugs administered via a non-injection route could also help to evaluate if indeed UCMS induced an antidepressant-resistant phenotype in BALB/cAnNCrl mice as suggested by the hypoactive HPA axis observed in these animals.

Chapter 4 Genome-wide gene expression changes in UCMS model

1 Introduction

Chapters 2 and 3 revealed a variety of behavioural and neurobiological phenotypes induced by UCMS protocols used, as distinct as hyperactivity and deficit in grooming behaviour, systemic proinflammatory changes and those localised to a particular brain area (PFC), reduction of hippocampal neurogenesis and in the level of appetite-regulating hormone leptin. Such a variety of changes suggested that UCMS might have affected multiple signalling pathways in different brain areas. Thus this chapter is dedicated to a study of these pathways and a search for common regulators interconnecting them to provide novel insights into the mechanisms of chronic stress response.

One of the ways to study neurobiological mechanisms in their full complexity is to utilise hypothesis-free explorative approach of a genome-wide transcriptome changes in selected tissues and brain regions. This approach is currently being widely utilised in clinical depression research to discover novel genes and pathways involved in the neurobiology of depression based on post-mortem brain tissue (Gao et al., 2015) and peripheral blood (Hepgul et al., 2016), and to detect biomarkers of depression subtypes (Xu et al., 2015) and of antidepressant response (Cattaneo et al., 2016) in peripheral blood cells.

1.1 Brain regions implicated in depression and in chronic stress research

The importance of a particular brain region in depression research is partly determined by the evidence of anatomical abnormalities in this region in depressed patients detected by neuroimaging studies. The majority of the research on depression focuses on the brain areas of the cortico-limbic circuit, which include the hippocampus, hypothalamus, amygdala, nucleus accumbens and the PFC (Wang et al., 2012). Reduction in hippocampal volume is one of the most consistent findings in the neuroimaging studies (Lorenzetti et al., 2009), however a number of post-mortem and imaging studies have reported decreased volume and activity in the PFC (Drevets et al., 1997; van Tol et al., 2014). The role of PFC in depression was further supported by the evidence from the deep brain stimulation (DBS) trials, showing that DBS over PFC and ACC produces an antidepressant effect (Berlim et al., 2014; Levkovitz et al., 2009). Investigation of PFC pathology in animal models of depression demonstrated that exposure to

chronic stress and increased glucocorticoid levels causes damage and neurodegenerative changes in the PFC, such as microglial activation (Hinwood et al., 2013), atrophy of pyramidal neurons (Cerqueira, 2005), dendritic atrophy (Dias-Ferreira et al., 2009; Liston et al., 2006) and reduction of synaptic proteins expression and synaptic currents (Li et al., 2011; Müller et al., 2011).

1.2 Gene expression changes induced by chronic stress in the rodent brain

A number of previous animal studies took advantage of the availability of the brain tissue to study gene expression changes in brain regions previously implicated in depression. Most transcriptomic studies of chronic stress effects in rodents focused on the consequence of stress on gene expression in the hippocampus. Hippocampus has been shown to be particularly sensitive to stress potentially due to a high expression of the glucocorticoid receptor activated by CORT hormone released in the course of stress response (McEwen, 1999). GR activation is thought to lead to an induction of long term potentiation observed in the hippocampus following stress (Datson et al., 2012). Taking into account hippocampal role in learning and memory it has been suggested that these changes underlie cognitive impairment and adaptive memory changes in response to stress exposure (Kim et al., 2006). In addition, gene expression in the hippocampus is investigated as a way to discover pathways involved the effect of chronic stress on adult hippocampal neurogenesis (Datson et al., 2012; Surget, Wang, et al., 2008).

Thus a number of datasets incorporating hippocampal gene expression changes upon chronic stress are available to date. While these studies differ significantly in their experimental design, from the species and types of chronic stress used, to the microarray analysis methods employed, some general patterns could be detected in these studies. The total number of genes for which their expression is significantly affected by stress exposure varies from below 50 to over 700, however fold changes reported rarely exceed 3-fold. Both rat and mouse studies find activation of immune response-related gene networks and signalling pathways often centred around nuclear factor kappa B (NF-kB). As such, Gray et al., (2014) showed that NF-kB pathway was activated in the hippocampi of adult male C57/BL6 subjected to 21 days of chronic restraint stress. Similar effect was observed in the hippocampi of four different mouse strains including BALB/c and C57/BL6 exposed to chronic mild stress, whereby weighted gene co-expression network analysis identified activation of a gene network regulated by NF-kB1 (Malki et al., 2013, 2015). The activation of inflammatory pathways could be related to the microglial activation described by some studies in this region upon chronic stress. A number of other studies investigating the effect of chronic mild or restraint stress on hippocampal gene

expression in rats and mice identified signalling pathways involved in cell fate, such as cell apoptosis (Bergström et al., 2007), proliferation and cell cycle control (Liu et al., 2010), axonal guidance and cell migration (Datson et al., 2012; Jungke et al., 2011; Zitnik et al., 2013). These findings go in line with dendritic atrophy and decrease in hippocampal neurogenesis known to be induced by chronic stress exposure.

Another region frequently assessed in gene expression studies of chronic stress effect is frontal and prefrontal cortex. Similar to the studies on the hippocampus, studies looking at the gene expression in the frontal and prefrontal cortex found a variation in the number of affected genes. Involvement of cell proliferation, differentiation and apoptosis pathways have also been described in rats and C57/BL6 and BALB/c strains of mice exposed to chronic mild and restraint stress (Liu et al., 2010; Orsetti et al., 2008; Tordera et al., 2011). Interestingly one study investigating gene expression changes in PFC of C57/BL6 mice exposed to chronic mild stress found a strong evidence for the involvement of the circadian rhythm pathway as many circadian rhythm genes, such as Clock, Period 1 (Per1) and Per2 were downregulated in this region (Erburu et al., 2015). Expression of circadian rhythm genes has been also investigated individually in a number of previous studies, which showed their downregulation in the PFC as well as in the hippocampus of rats exposed to chronic mild stress (Calabrese et al., 2016). In addition, reduced amplitude in the Per2 expression upon UCMS has been found in the suprachiasmatic nucleus (SCN) of the hypothalamus in C57/BL6 mice (Jiang et al., 2011; Logan et al., 2015a). These findings go in line with data obtained from post-mortem tissue of depressed patients, which showed that circadian fluctuation of many genes including the clock genes is decreased in depressed patients in a number of limbic regions, including dorsolateral PFC, ACC and the hippocampus.

Another region frequently included in gene expression analysis of chronic stress effects is the hypothalamus. The most obvious role of the hypothalamus in depression stems from the CRH-releasing function of its paraventricular nucleus and its reciprocal connections with the amygdala and the hippocampus. Hypothalamus also receives neuroendocrine input from the gut metabolic hormones ghrelin and leptin and sends it to the VTA implicated in reward-related behaviour (van Zessen et al., 2012). In addition, the SCN is a major regulator of the circadian clock, relevant for sleep disturbance and alteration of molecular circadian rhythms observed in depression (Li et al., 2013). Jungke et al. (2011) found 152 transcripts differentially expressed in the rat hypothalamus upon chronic restraint stress exposure, with neurotransmitter signalling, oxidative stress and immune pathways being implicated. Another study investigating the effect of 15 days of chronic restraint in ICR mice focused on the food

intake related genes, and found change in ghrelin and proopiomelanocortin gene expression, while decrease in plasma levels of leptin was not associated with gene expression changes in the hypothalamus (Jeong et al., 2013). Gene expression changes of ghrelin and leptin upon chronic stress exposure were also investigated in the PFC, where ghrelin and ghrelin receptor were found to be increased in contrast to leptin and leptin receptor which were decreased in UCMS-exposed rats (Liu et al., 2015). These findings implicate PFC in the weight and appetite changes induced by chronic stress in animal models of depression.

1.3 Comparison of gene expression changes in different brain regions

Very few genome-wide gene expression studies compared transcriptomic profiles of different brain regions upon chronic stress exposure. Surget et al. (2008) showed that in BALB/c exposed to UCMS more genes (292) were affected in the amygdala compared to 245 genes differentially expressed in the cingulate cortex and 158 in the hippocampal dentate gyrus. In the amydgala neurotransmitter signalling pathways such as GABA, glutamate and serotonin, as well as various kinase pathways were enriched among activated genes, while a strong enrichment of oligodendrocyte-related genes was observed among the downregulated transcripts. Interestingly, pathway analysis was inconclusive in other regions. Little overlap among the brain regions was observed in this study. Similarly Liu et al. (2010) described bigger gene expression changes in BALB/c mice upon UCMS in the cerebral cortex (102 genes) compared to the hippocampus (60 genes). However, in this study a bigger overlap than in the study by Surget et al. (2008) between the two areas was observed, with 14 genes changed in the same direction in the two areas. These genes included those involved in glutamate signalling, apoptosis, neuronal differentiation and immune response. Authors also highlighted an overlap in cholecystokinin (Cck) upregulation in both areas, which relevance stems from the implication of Cck signalling in depression in the previous literature (Becker et al., 2008; Vialou et al., 2014).

Many of the signalling pathways found to be involved in these studies are relevant for the behaviour and neurobiology observed in our UCMS experiments. This together with the behavioural and histopathological changes described in the previous chapters prompted us to study genome wide transcriptome of the three brain regions – the hippocampus, the PFC and the hypothalamus. The gene expression study was designed primarily as an explorative analysis aimed to identify novel molecular targets and pathways involved in UCMS effects in selected brain areas. However, a number of more specific questions were expected to be resolved by the transcriptomic assay. Firstly, the gene expression study was expected to expose the extent of the HPA axis alteration by revealing GR and GR related genes expression

changes in the hippocampus and CRH expression in the hypothalamus. Secondly, we hypothesised that in line with the previous studies and our findings, we would see activation of the immune pathways in some of these regions, which could partly explain CRP elevation and neurogenesis decline in UCMS-exposed animals. Third, alteration of factors which could affect neurogenesis, such as brain derived neurotrophic factor (Bdnf) and serotonergic and glutamatergic signalling were also expected to be revealed in the hippocampus.

2 Methods

2.1 Experimental design of the UCMS Experiment 4

In parallel to the UCMS Experiment 3, a separate cohort of animals was subjected to control (n=8) and UCMS (n=8) conditions as described in the UCMS Experiment 3 section 6.1.1 according to the UCMS schedule in Table 8 for 4 weeks as depicted in Figure 32. Behavioural testing for this group consisted of sucrose preference measured once weekly over 2 nights as described in section 3.3.2 of Chapter 2 and a short behavioural testing battery which included open field, splash test, light-dark box, novelty suppressed feeding and cookie test conducted as described in sections 3.3.4-3.3.7 and 3.3.10 of Chapter 2 according to the schedule in Table 10.

.

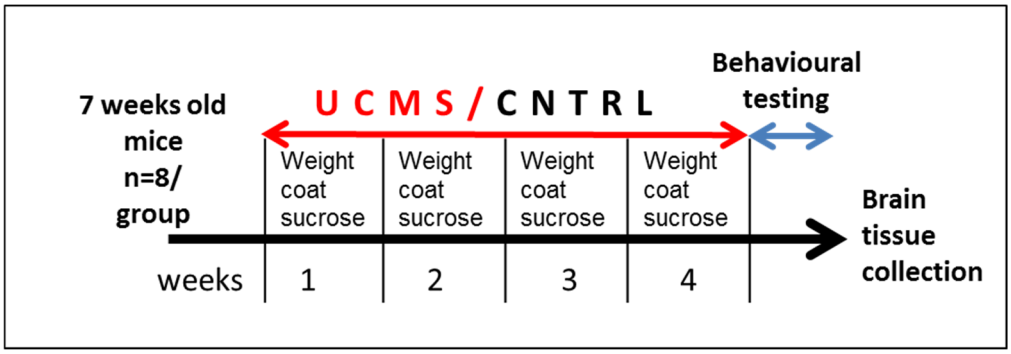

Figure 32 Experimental design of UCMS Experiment 4
Adult male BALB/c mice were exposed to unpredictable chronic mild stress (UCMS) or control (CNTRL) for 4 weeks (n=8/group) and subsequently tested in a short behavioural testing battery, after which fresh frozen brain tissue was collected and selected brain regions (hippocampus (HIP), hypothalamus (HYP) and prefrontal cortex (PFC) were subjected to a genome-wide transcriptomic analysis using Illumina microarray platform.

Table 10 Schedule of behavioural testing conducted in the UCMS Experiment 4
Adult male BALB/c mice were exposed to unpredictable chronic mild stress (UCMS) or control (CNTRL) for 4 weeks (n=8/group) and subsequently tested in a short behavioural testing battery shown, after which fresh frozen brain tissue was collected and selected brain regions (hippocampus (HIP), hypothalamus (HYP) and prefrontal cortex (PFC) were subjected to a genome-wide transcriptomic analysis using Illumina microarray platform.

	TESTING DAY	DAY1	DAY2	DAY2	DAY3	DAY4	DAY4
N	GROUP	Rest day	Open field	Splash test	NSF	LD box	Cookie test
1	CNTRL		8:58	13:12	14:00	10:14	12:30
2	UCMS		9:10	13:24	14:07	10:21	12:45
3	CNTRL		9:22	13:46	14:14	10:28	13:00
4	UCMS		9:34	13:58	14:21	10:35	13:15
5	CNTRL		9:46	14:10	14:28	10:42	13:30
6	UCMS		9:58	14:22	14:35	10:49	13:45
7	CNTRL		10:10	14:34	14:42	10:56	14:00
8	UCMS		10:22	14:46	14:49	11:03	14:15
9	CNTRL		10:34	14:58	14:56	11:10	14:30
10	UCMS		10:46	15:10	15:10	11:17	14:45
11	CNTRL		10:58	15:22	15:17	11:24	15:00
12	UCMS		11:10	15:34	15:24	11:31	15:15
13	CNTRL		11:22	15:46	15:31	11:38	15:30
14	UCMS		11:34	15:58	15:38	11:45	15:45
15	CNTRL		11:46	16:10	15:45	11:52	16:00
16	UCMS		11:58	16:22	15:52	11:59	16:15

2.2 RNA extraction

After completion of the UCMS protocol and application of the shortened behavioural testing battery (4 days) animals were anaesthetised with Euthatal i.p. (Merial Animal Health Ltd, Harlow, UK) at a dose of 40 mg/kg pentobarbital sodium. After confirmation of a deep anaesthesia by the loss of righting and pain reflexes and slowing of the rate of respiration, dislocation of the neck was performed. Following decapitation brains were removed from the skull and placed dorsal side down on a wetted filter paper on a petri dish kept on ice. First the brain was placed with the dorsal side facing down and the hypothalamus was dissected as a rectangle along the lateral border 2 mm from either side of the third ventricle from the optic chiasm to the posterior border of the mammillary bodies, and the thalamus dorsally (Quennell et al., 2011). Next the brain was placed with the ventral side facing down and cortex exposed. The cerebral halves were opened out from the midline, after cutting through the corpus

callosum. Approximately 3 mm^3 of tissue was cut from the anterior part of the frontal lobes (from 2.46 mm to 1.34 mm relative to bregma (Franklin and Paxinos, 2012), mainly containing the medial prefrontal cortex including some prelimbic cortex, infralimbic cortex, cingulate cortex and motor cortex (Spijker, 2011). For the hippocampal dissection, the cortical hemispheres were peeled laterally to expose the hippocampus, which was subsequently carefully rolled out with a brush. Whole hippocampi were used for RNA extraction. Right and left dissected areas were pooled for each sample, while brain tissue from each mouse was analysed as individual samples. Dissected brain areas were immediately flash frozen on dry ice. Total RNA was extracted from fresh frozen brain tissue by the guanidine isothiocyanate method (Chomczynski and Sacchi, 1987) with TRIzol reagent (Life Technologies, ThermoFisher Scientific Inc.) The tissue was homogenised using disposable tissue grinders before Trizol reagent was added to the sample tube. Next samples were transferred to Phase lock gel heavy tubes (Scientific Laboratory supplies, UK), and after short incubation at room temperature with chloroform (Sigma-Aldrich, UK) were centrifuged at 13000rpm to separate the nucleic acid phase. The top aqueous layer was transferred to a new tube and RNA was precipitated with isopropanol (Sigma-Aldrich, UK). After removal of isopropanol the precipitate was washed in ethanol and redissolved in DNA-RNAase free water. The quality of the extracted RNA was assessed using 1% agarose gel electrophoresis and spectrophotometry. The 260/280 ratio was over 2 in all samples indicating a high level of purity in the extracted nucleic acid samples. To remove contaminating DNA from RNA samples DNase digestion of samples was performed using the Qiagen Rnase-Free DNase Set (79254, Qiagen, UK) followed by column-based sample purification using RNeasy MinElute Cleanup Kit (74204, Qiagen, UK), both performed according to the manufacturer's instructions. Subsequently, RNA integrity numbers (RINs) were assessed using the Agilent 2100 Bioanalyzer (G2938-90034, Agilent Technologies, UK) according to the manufacturers' instructions. All samples had RINs of 8.8 or higher, indicating good quality of RNA. RNA concentrations were measured using the Quant-iT™ RiboGreen® RNA assay kit (R11490, ThermoFisher Scientific Inc.) following the manufacturer's instructions.

2.3 Running the microarray

Genome-wide gene expression was assessed using the MouseWG-6 BeadChip Kit (Illumina, US), which measures the expression of 45290 transcripts. This assay is based on direct hybridisation, whereby gene-specific probes are hybridised directly onto the complementary labelled cRNA in the samples, and their fluorescent intensity corresponding to the quantity of each transcript is subsequently measured by Illumina Scan System. Sample labelling, hybridisation and signal detection and imaging were performed according to manufacturer's

instructions. Briefly 300ng of sample RNA were prepared in 11µl nuclease-free H_20 to be used for labelling and amplification using the Ambion TotalPrep-96 RNA Amplification Kit (4393543, Illumina, US). The concentration of labelled RNA was assessed using Quant-iT™ RiboGreen® RNA assay kit (R11490, ThermoFisher Scientific Inc.) and 1.5ug was loaded onto bead chips for hybridisation. The hybridisation occurred in the Illumina Hybridisation Oven at 58°C for 15 hours 20 min. Next day the beads were washed in high temperature (55°C) buffer and ethanol, and Cy3-Streptavidin was added to bind the beads to allow for signal detection. Finally, laser-induced fluorescent signal from the beads was recorded by iScan System Reader.

2.4 Microarray data analysis

Images were analysed using the GenomeStudio software (Illumina, US), where the initial quality control did not detect any outliers based on average signal intensities. Signal intensity data generated by GenomeStudio was pre-processed using the R package Lumi (Du et al., 2008). Pre-processing included the following transformations using functions of the Lumi package. Background correction using bgAdjust function was applied to eliminate background signal intensity by subtracting an offset, which is estimated based on the quantile of the control probes. Variance stabilisation (vst function) transformed the expression values based on the model of the mean-variance relationship of the within-array technical replicates at the bead level of Illumina microarray, taking advantage of the high number of technical replicates available on the Illumina platform to reduce variance of high and low intensity values (Lin et al., 2008). Quantile normalisation (LumiN, method=quantile) normalised the expression values by calculating the empirical distribution of the average sample quantiles and using it to index the empirical distribution of each original array; log-transformation normalised distribution of intensity values (LumiT, method=log2). For the effect of pre-processing on the distribution of sample intensities see Figure 33.

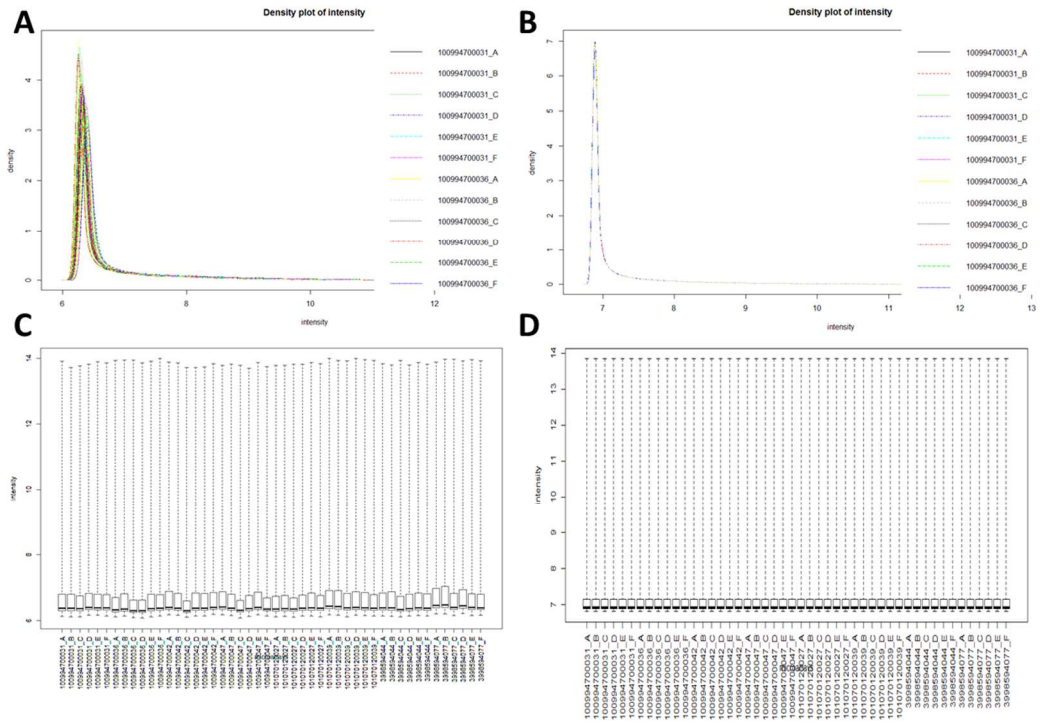

Figure 33 Distribution of Intensity in microarray samples normalised by the pre-processing steps
*RNA samples from the UCMS Experiment 4 were run on a MouseWG-6 BeadChip Kit (Illumina, US) and images analysed by GenomeStudio software. Intensity values were than transformed used LumiR pipeline of pre-processing steps. Density plot of fluorescent signal intensities before (**A**) and after (**B**) pre-processing steps (X axis – density, Y axis – intensity units). Boxplot of sample intensities (X axis) before (**C**) and after (**D**) pre-processing steps*

Only transcripts for which intensity values reached the detection threshold of p<0.01, and which were expressed in more than 4 samples to allow for individual variation in each treatment group were included into the final statistical analysis (19632 transcripts). Statistical analysis of differential expression was performed using the Statistical Analysis of Microarrays (SAM) method and R-based software (Tusher et al., 2001). This method identifies significant differential expression based on repeated permutations of the data to determine if expression of individual genes is related to the experimental group of the sample. It calculates gene-specific fluctuations of expression in the dataset, and then estimates the ratio of change in gene expression between experimental groups to the standard deviation of expression of that particular gene. This ratio is represented by the observed score in Figure 39 F, while expected score is calculated based on permutations of the data. For genes which expression is independent on the group factor the scores are equal, so when their correlation is plotted, they align to the equality line (see Figure 39). However, those genes which expression is determined by experimental group factor, deviate from the equality line by a varying distance. The user adjusts the distance threshold beyond which the genes will be deemed significantly differentially expressed. The threshold will therefore determine the false discovery rate (FDR),

a percentage of genes identified as significant by chance. For PFC data, the threshold was adjusted to achieve FDR of 0. For hippocampal and hypothalamic gene expression, the threshold allowed FDR of 0.095 which corresponds to 0.05% chance of a false-positive finding frequently used in genome-wide gene expression studies (see Figure 39) (Bagot et al., 2016; Malki et al., 2016). The dataset for each brain region was analysed separately as a two-class unpaired data.

2.5 Pathway analysis

Significant pathway, function and upstream regulator analysis was conducted through the use of QIAGEN's Ingenuity Pathway Analysis (IPA®, QIAGEN Redwood City USA, www.qiagen.com/ingenuity). IPA® utilised the right-tailed Fisher Exact Test to calculate the p-value of a pathway, function or an upstream regulator. In this method, the p-value for a given pathway or function annotation is calculated by considering the number of differentially expressed genes that participate in that pathway and the total number of genes that are known to be associated with a given pathway in the selected reference set. The significance level for pathways and functions was set at $p<0.05$. IPA software was also used to generate figures illustrating this analysis.

2.6 Microarray validation by quantitative real-time PCR

To verify microarray data analysis, expression of 10 individual genes was independently assessed in the same mRNA samples using real-time quantitative polymerase chain reaction (qPCR). The genes were selected based on their fold changes (a range from the top up- and down-regulated genes to allow for the future correlation analysis with qPCR expression values) and their functional relevance, that is affiliation with one of the top pathways identified to be activated by the pathway analysis (Myl4, Tnnc, Cam2A, Calb2, Slc32a1, Gad1) or association with chronic stress or depression by the previous studies (Cck, Cckbr, Per2, Gng7).

2.6.1 Reverse transcription of mRNA

For this, firstly mRNA was converted to cDNA by reverse transcription with Superscript III reverse transcriptase (Invitrogen Thermofisher Scientific Inc.) following manufacturer's instructions. Briefly 1µg of mRNA was combined with 250 ng of random hexamer primers (Life Technologies) and 1mM dNTP mix (Thermofisher Scientific Inc.), incubated for 5 minutes at 65°C on a heated block to denature RNA secondary structure and quenched on ice for 1 minute. Next, the following reagents were added to the reaction: 1x First Strand Buffer (Invitrogen), 5 mM dithithretiol (Life Technologies), 40 units RNaseOUT™ (Life Technologies) and 200 units SuperScript III Reverse Transcriptase. Samples were then incubated at 25ºC for 5

minutes, 50ºC for 1 hour, 55ºC for 30 minutes (to remove any secondary structures) and finally 70 ºC for 15 minutes to terminate the reaction.

2.6.2 qPCR primer design

qPCR primers were designed using Integrated DNA Technology (IDT) software (Http://www.idtdna.com/primerquest/home/index) based on target genes DNA sequences obtained from the NCBI Gene database (Http://www.ncbi.nlm.nih.gov/gene). The primers were designed to amplify the exon region targeted by the Beadchip in the microarray. Several conditions were met in primer design: forward and reverse primers were selected to have minimal GC content, similar length, minimal self-complementarity and no complementarity to each other. The length of the amplicon was limited to 70 to 130 base pairs; the amplicon sequence melting temperature was tested for single peak melting curves using uMelt software (Https://www.dna.utah.edu/umelt/umelt.html). The specificity of the primers to the gene of interest was tested in the In silico PCR online software (Http://genome.ucsc.edu/cgi-bin/hgPcr) – only primer pairs replicating a single product from the target gene sequence in the in silico PCR were selected. Specificity was further confirmed by the melting curve analysis – conducted along with the qPCR. Only primer pairs resulting in a single clear peak at predicted temperatures in all tested samples were used for the data analysis (for examples of melting curves see Figure 34B). The primer oligonucleotides were synthetized by IDT Custom oligo synthesis service. On arrival, the oligonucleotides were re-suspended in nuclease-free H_20 to a stock concentration of 100 µM and a working concentration of 2 µM. For primer sequences see Table 11.

Table 11 Primer sequences used for qPCR to validate the gene expression values derived from microarray analysis of RNA collected in the UCMS Experiment 4.
Mouse genome sequences were used for all primers

TARGET GENE	ACCESSION N	AMPLICON LENGTH (bp)	FORWARD PRIMER	REVERSE PRIMER
Myl4	NM_010858.4	103	TCTGGGTAAAGCACGTTTCTC	AGAAGCCATGTGAGTCCAATAC
Tnnc1	NM_009393.2	82	CCGTGGTAGGAGTGCAG	GGAGAGAAAGTCCGGAAGG
Cck	NM_001284508.2	85	GGAGGTGGAATGAGGAAACAA	GCACACTCTGGACAGATTTCA
Camk2a	NM_009792.3	102	CATCCTGAACCCTCACATCC	GCATCCAGGTACTGAGTGATG
Cckbr	NM_007627.5	94	TCTATAGTGCCCATAGCCTAGT	TTCAGTGCTGGATAAGGAAGG
Per2	NM_011066.3	94	GTAACAGGGAAGCCACAAGAG	TGAGAGGATGTCAGGAGAGATG
Calb2	NM_007586.1	75	GTGGATCTGGAAAGGAGAGATG	CGCAGGCACAACTGTCTAT
Gng7	NM_001038655.1	97	CCTTCCCTCTGCTTTGTGAA	CAATAGTAACACTGGGAGAGTGG
Slc32a1	NM_009508.2	116	GCGTTTCTGTCGTCCTTTCT	TTTGGTGGTGGTGGTGATG
Gad1	NM_008077.5	102	CCCTCTTTACAGAACCAGAATCA	CTTCAGTGAGATGGCCTAGATG
Atp5b	NM_016774.3	92	GCTGATAAGCTGGCAGAAGA	CCTGAGCTCTCGCTTGATATG
Cst3	NM_009976.4	97	GACTGACTGTCCTTTCCATGAC	CAGGGAGTGTGTGCCTTTC

2.6.3 qPCR and its data analysis

qPCR reaction master mix was assembled in white 96 well qPCR plates (AB-0900/W, ThermoFisher Scientific Inc.). All samples assayed for the same gene were included on the same plate. The master mix consisted of 5x HOT FIREPol® EvaGreen® qPCR Mix Plus (no ROX) (Solis BioDyne), containing DNA polymerase which incorporates EvaGreen fluorescent dye into double-stranded DNA; 0.2µM forward and reverse primer mix and nuclease-free water. cDNA template (31.25ng) or water was added to the duplicate wells. The reaction was performed on a Chromo4 Real-time PCR detector (Bio-Rad Laboratories Inc.) according to the following programme: initial denaturation at 95°C for 15 minutes, 45 cycles of denaturation at 95°C for 30 seconds, annealing at 60°C for 30 seconds, extension at 72°C for 30 seconds. Fluorescent signal was detected at the end of each cycle. At the end of the protocol a melting curve analysis was carried out by detecting the fluorescence during a heating step from 60°C to 95°C at every 1°C increment.

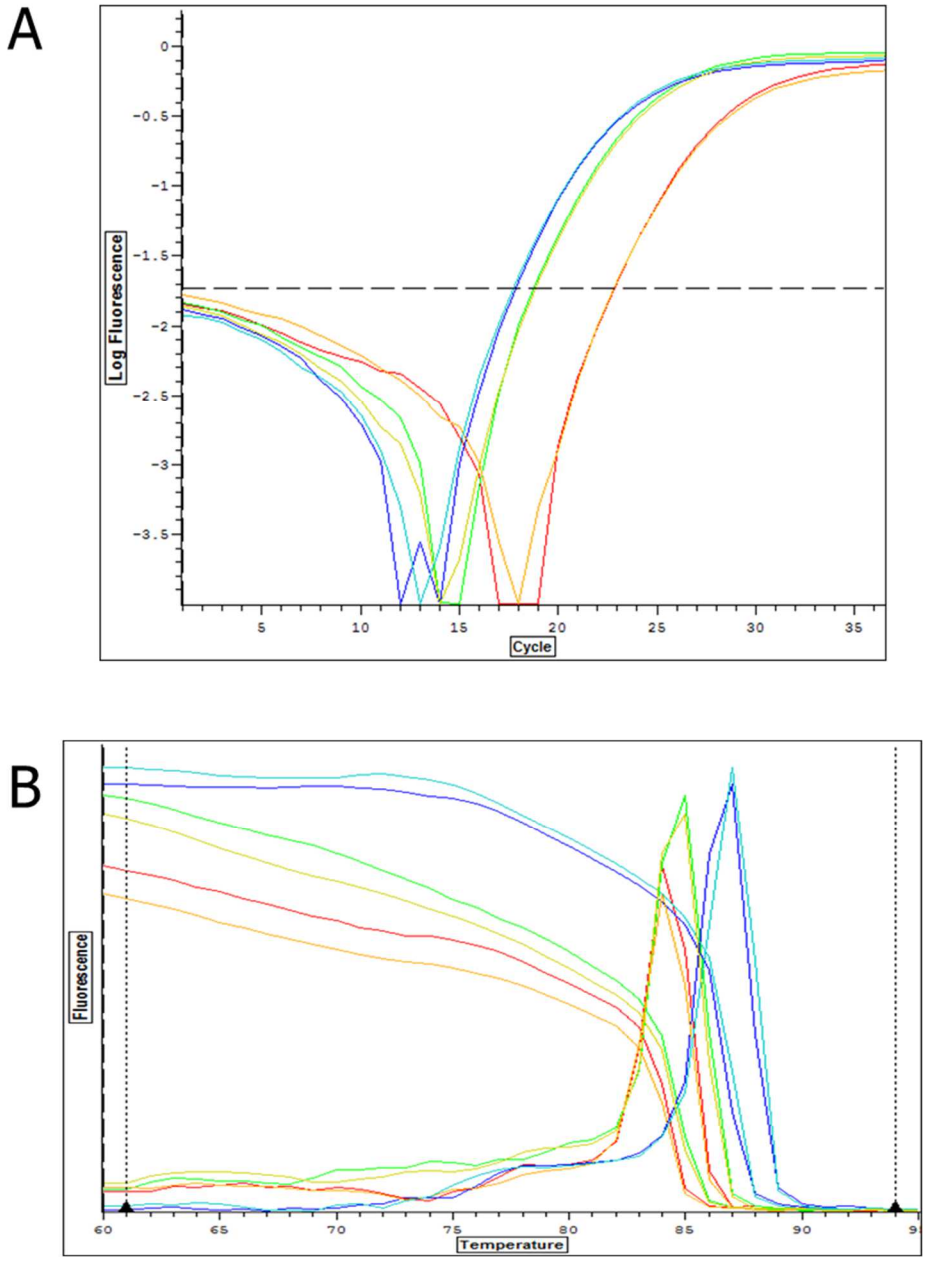

Figure 34 Example of an output of the quantitative polymerase chain reaction

Example of an output of qPCRs conducted with primers for Myl4 (in red and orange) and reference genes Atp5b (in light and dark blue) and Cst3 (in light and dark green) sequences with aliquots of the same cDNA sample in duplicate. (A) Y axis – Log fluorescence detected, X-cycle number, the curves for Myl4 primers cross the threshold (dotted line) at around 23rd cycle (Ct=23), the curves for Atp5b and Cst3 cross the threshold at around 17th and 18th cycle respectively (Ct_{Atp5b} = 17, Ct_{Cst3} = 18) (B) Melting curves for each qPCR showing distinct shapes and single peaks at separate temperatures for each primer pair confirming their specificity to target amplicons, Y axis - fluorescence, X axis - temperature

Data was extracted with Opticon Monitor 3 (Bio-Rad Laboratories Inc.) software. To calculate relative gene expression, cycle threshold (Ct) values for target genes were normalised to the reference genes Atp5b and Cst3, and expression ratio was calculated separately for each UCMS group sample relative to the average value of all CNTRL group samples using the Pfaffl

mathematical model according to the Equation 3 (Pfaffl, 2001). For examples of cycle threshold determination for target and housekeeping genes in a single sample see Figure 34A.

$$Ratio = \frac{E\ target^{\Delta Ct(control-sample)}}{E\ ref^{\Delta Ct(control-sample)}}$$

Equation 3 Pfaffl mathematical model used to quantify relative expression of target genes in the qPCR, where E target is efficiency of a target gene and E ref is efficiency of a reference gene; ΔCt was calculated by subtraction of the Ct value of a replicon of each UCMS group sample ("sample") from average Ct of this gene in all CNTRL group samples ("control")

For this analysis, 2 reference genes were selected based on low variation and high expression levels in the microarray dataset across all samples and regions accessed, as the reference gene is required to have a stable level of expression independent of treatment exposure. The variation of a gene's expression was estimated by calculating its CV in all samples. Among genes with low CV only genes with high levels of expression (intensity values ≥12 in all samples across all tissues, for distribution of intentisity values across all samples for all genes see Figure 33B) were considered for reference role to ensure stable PCR results. Based on these two parameters, Atp5b and Cst3 emerged as reasonable candidates. Moreover, Atp5b has been previously validated as a suitable reference gene for gene expression analysis in a mouse brain (Cleal et al., 2014), therefore these two genes were used as reference genes in the Pfaffl equation. Fluorescent intensities for both reference genes across all samples are shown in Table 12.

Table 12 Fluorescent intensity values for reference genes ATP5B and CST3 in all samples.
Adult male BALB/c mice were exposed to unpredictable chronic mild stress (UCMS) or control (CNTRL) for 4 weeks (n=8/group) and subsequently tested in a short behavioural testing battery shown, after which fresh frozen brain tissue was collected and selected brain regions (hippocampus (HIP), hypothalamus (HYP) and prefrontal cortex (PFC) were subjected to a genome-wide transcriptomic analysis using Illumina microarray platform.Table shows fluorescent intensity values across all samples for ATP5B and CST3 genes used as reference genes in 1PCR analysis due to their stable expression in all samples.

ILLUMINA SAMPLE ID	BRAIN REGION	GROUP	ATP5B	CST3
100994700031_A	HIPPOCAMPUS	UCMS	13.13213	12.87719
100994700031_B	HYPOTHALAMUS	UCMS	13.05731	12.96203
100994700031_C	PFC	UCMS	13.3127	12.93862
100994700031_D	HIPPOCAMPUS	CNTRL	13.15525	12.69969
100994700031_E	HYPOTHALAMUS	CNTRL	12.98834	12.78428
100994700031_F	PFC	CNTRL	13.13213	13.03099
100994700036_A	HIPPOCAMPUS	UCMS	13.10425	12.93862
100994700036_B	HYPOTHALAMUS	UCMS	12.93862	13.00695
100994700036_C	PFC	UCMS	12.96203	12.93862
100994700036_D	HIPPOCAMPUS	CNTRL	13.05731	13.00695
100994700036_E	HYPOTHALAMUS	CNTRL	12.80279	12.93862
100994700036_F	PFC	CNTRL	12.82541	12.93862
100994700042_A	HIPPOCAMPUS	UCMS	13.03099	12.84687
100994700042_B	HYPOTHALAMUS	UCMS	13.00695	12.82541
100994700042_C	PFC	UCMS	12.93862	13.03099
100994700042_D	HIPPOCAMPUS	CNTRL	13.18544	12.71966
100994700042_E	HYPOTHALAMUS	CNTRL	12.91753	12.84687

ILLUMINA SAMPLE ID	BRAIN REGION	GROUP	ATP5B	CST3
100994700042_F	PFC	CNTRL	13.03099	12.93862
100994700047_A	HIPPOCAMPUS	UCMS	13.03099	12.84687
100994700047_B	HYPOTHALAMUS	UCMS	12.96203	12.80279
100994700047_C	PFC	UCMS	12.98834	12.91753
100994700047_D	HIPPOCAMPUS	CNTRL	13.39013	12.93862
100994700047_E	HYPOTHALAMUS	CNTRL	13.03099	12.7431
100994700047_F	PFC	CNTRL	13.15525	12.84687
101070120027_A	HIPPOCAMPUS	UCMS	13.08105	12.96203
101070120027_B	HYPOTHALAMUS	UCMS	13.00695	12.93862
101070120027_C	PFC	UCMS	12.93862	12.89598
101070120027_D	HIPPOCAMPUS	CNTRL	13.08105	13.00695
101070120027_E	HYPOTHALAMUS	CNTRL	12.87719	13.03099
101070120027_F	PFC	CNTRL	13.08105	12.71966
101070120039_A	HIPPOCAMPUS	UCMS	13.10425	12.7431
101070120039_B	HYPOTHALAMUS	UCMS	12.75958	12.96203
101070120039_C	PFC	UCMS	13.13213	12.84687
101070120039_D	HIPPOCAMPUS	CNTRL	13.18544	12.87719
101070120039_E	HYPOTHALAMUS	CNTRL	12.96203	12.87719
101070120039_F	PFC	CNTRL	13.10425	12.98834
3998594044_A	HIPPOCAMPUS	UCMS	13.27599	12.82541
3998594044_B	HYPOTHALAMUS	UCMS	13.08105	13.05731
3998594044_C	PFC	UCMS	13.03099	12.71966
3998594044_D	HIPPOCAMPUS	CNTRL	13.21062	12.91753
3998594044_E	HYPOTHALAMUS	CNTRL	12.89598	12.75958
3998594044_F	PFC	CNTRL	13.27599	12.89598
3998594077_A	HIPPOCAMPUS	UCMS	13.00695	12.89598
3998594077_B	HYPOTHALAMUS	UCMS	13.00695	13.03099
3998594077_C	PFC	UCMS	13.03099	12.78428
3998594077_D	HIPPOCAMPUS	CNTRL	12.93862	12.7431
3998594077_E	HYPOTHALAMUS	CNTRL	12.82541	12.87719
3998594077_F	PFC	CNTRL	13.00695	12.80279

The average of ratios normalised to the two reference genes were used in statistical analysis. Average group ratio for each gene was compared to the relative control expression level set at 1 with a 1-sample t-test. To compare the expression values derived from the microarray from those obtained with a qPCR, Pearson's correlation has been conducted between microarray values for each target gene and corresponding qPCR-derived group average gene expression ratios.

3 Results

3.1 Behavioural characteristics of the gene expression cohort of the UCMS Experiment 4 were similar to that of the UCMS Experiment 3 cohort

To confirm the presence of behavioural changes in the UCMS Experiment 4 cohort used in the gene expression study, mice were subjected to selected behavioural tests from the UCMS Experiment 3 testing battery prior to fresh frozen tissue collection. Similar to the results described in Chapter 2, UCMS induced deterioration of the coat state and reduction of grooming in the splash test in the exposed mice, although in this cohort the onset of effect

occurred already after one week of UCMS exposure (Mann-Whitney U = 45, p>0.995 on week 0; U = 3, p = 0.0002 on week 1; U=5, p = 0.0003 on week 2; U=5, p=0.0002 on week 3; U=28.5 p = 0.181 on week 4) (see Figure 35B). Changes in coat state were not accompanied by group differences in weight (see Figure 35A).

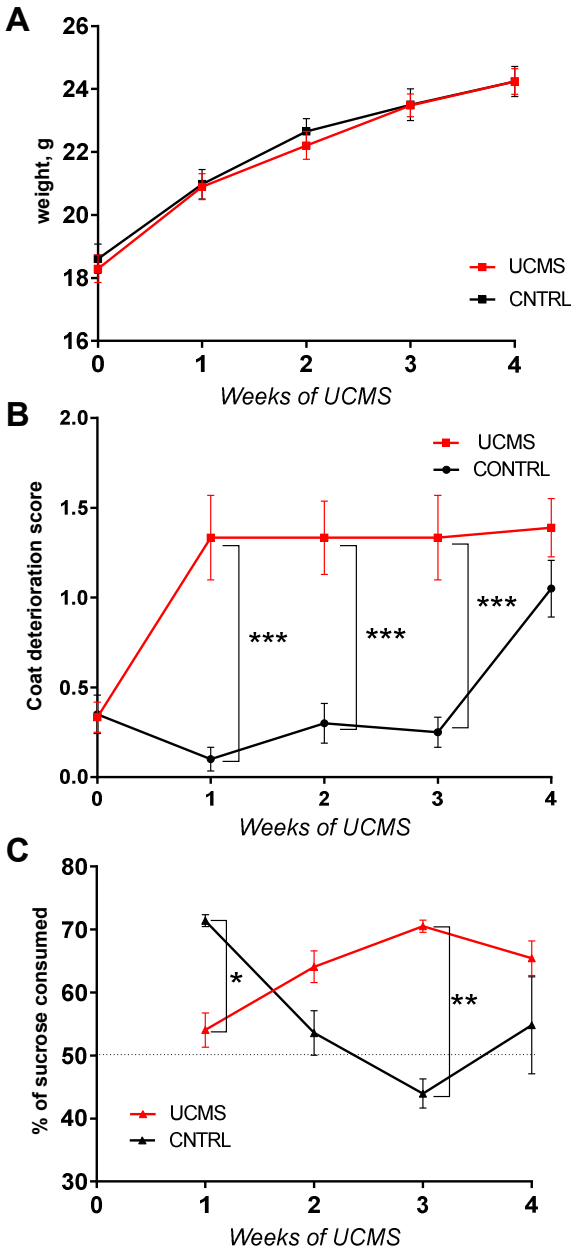

*Figure 35 Weekly measures of coat state, weight change and sucrose preference in the UCMS Experiment 4 Adult male BALB/c mice were exposed to unpredictable chronic mild stress (UCMS) or control (CNTRL) for 4 weeks (n=8/group) and subsequently tested in a short behavioural testing battery, after which fresh frozen brain tissue was collected and selected brain regions were subjected to a genome-wide transcriptomic analysis using Illumina microarray platform. (A) weekly weight measures in UCMS and CNTRL groups (B) weekly coat state measures in UCMS and CNTRL groups (C) average weekly sucrose preference measures taken over 2 consecutive nights to allow for sucrose bottle side change; *p<0.05, **p<0.01, ***p<0.001 CNTRL vs UCMS derived from Mann-Whitney U-test (coat state) or post-hoc Bonferroni multiple comparisons (sucrose preference). Data represents mean ± SEM*

Unlike the UCMS Experiment 3, UCMS-exposed group in Experiment 4 did not display differences in the locomotor activity measured by distance travelled in the open field arena (Student t-test t = 1.385 df = 17, p = 0.184) and in the anxiety measured in the open field test (Student t-test t = 0.4193 df = 17, p = 0.68; see Figure 36A,B). Similarly, no difference between CNTRL and UCMS groups was found in the anxiety-like behaviour in the light-dark box test (Student t-test of latency to enter the light box CNTRL vs UCMS t = 1.532, df = 170, p =0.144; Student t-test of time spent in the light box CNTRL vs UCMS t = 0.1437 df = 17, p = 0.887; see Figure 36C,D). However similarly to the UCMS Experiment 3, UCMS-exposed mice showed reduction of latency to start grooming (Student t-test CNTRL vs UCMS t = 2.67 df = 17, p = 0.016) and overall grooming time (Mann-Whitney U = 10, p = 0.003) in the splash test (see Figure 36E,F).

2-way repeated measures ANOVA of the sucrose preference showed significant effect of week x group interaction (Week X Stress F (3, 6) = 16.63, p = 0.003; Week F (3, 6) = 1.079, p = 0.426; Effect of Stress F (1, 2) = 5.759, p = 0.139). Interestingly in this experiment similarly to the UCMS Experiment 3 mice displayed weekly fluctuation of preference for sucrose. However unlike in the previous experiment, in the UCMS Experiment 4 anhedonia was detected already after 1 week of the UCMS exposure. However, upon repeated exposures to the same sucrose concentration (1%) the preference fluctuated during subsequent weeks, with UCMS group preference being significantly higher than the CNTRL group preference on week 3 (see Figure 35C).

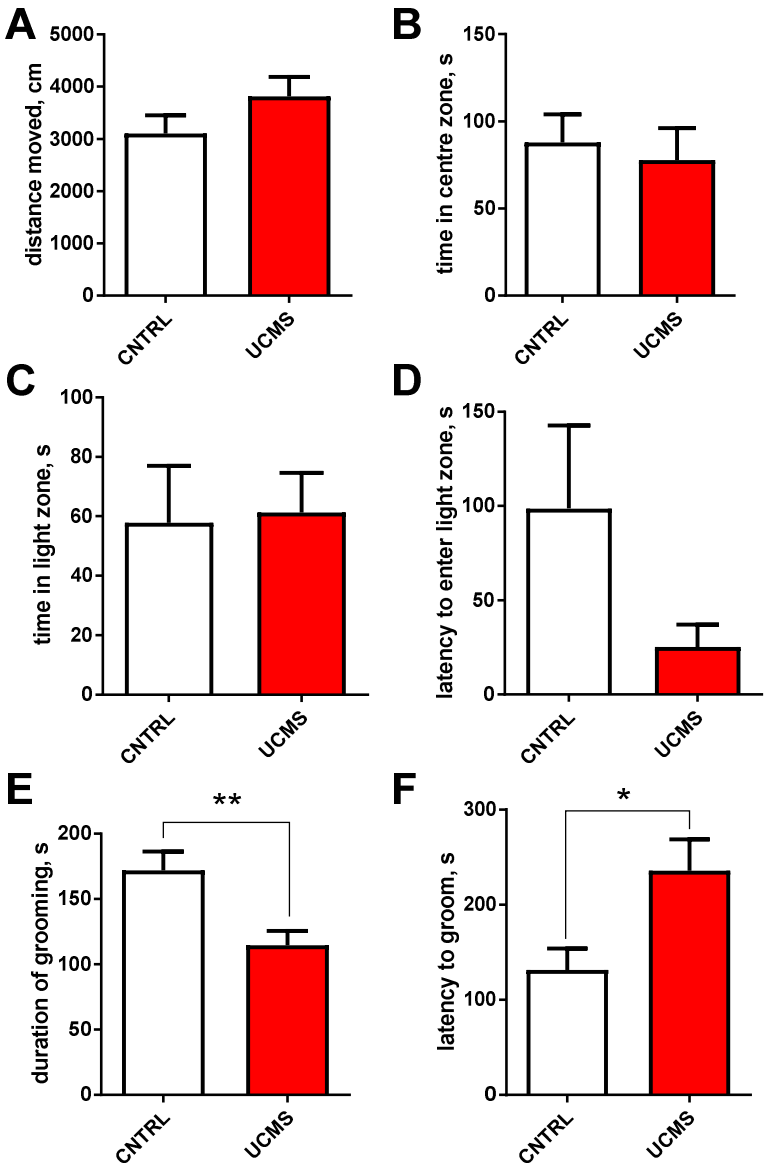

Figure 36 Anxiety and grooming behaviour in the UCMS Experiment 4

Adult male BALB/c mice were exposed to unpredictable chronic mild stress (UCMS) or control (CNTRL) for 4 weeks (n=8/group) and subsequently tested in a short behavioural testing battery, after which fresh frozen brain tissue was collected and selected brain regions were subjected to a genome-wide transcriptomic analysis using Illumina microarray platform. (A*) Total distance moved by mice (B) Time spent in the centre zone of the open field arena during 5 min test (C) Time spent in the light zone of the light-dark box during 5 min test (D) Latency to enter the light zone in the light-dark box test (E) Time spent grooming during 10 min splash test (F) Latency to start grooming in the splash; *p<0.05 derived from Mann-Whitney test CNTRL vs UCMS **p<0.05 derived from unpaired two-tailed Student t-test CNTRL vs UCMS. Data represents mean ± SEM*

In the novelty suppressed feeding test, UCMS group showed reduced latency to start eating the food pellet in the middle of the novel arena, identical to that observed in the UCMS Experiment 3 cohort described in Chapter 2 (Mann-Whitney CNTRL vs UCMS U=3, p = 0.0002; see Figure 37B). There was no significant difference in the amount of food mice consumed in the arena (Student t-test CNTRL vs UCMS t = 2.041, df = 17, p = 0.057) and during the first 10

minutes in the home cage (Student t-test CNTRL vs UCMS t = 1.119, df = 15, p = 0.281). UCMS-exposed mice also showed reduced latency to find and start eating the cookie in the cookie test (Student t-test CNTRL vs UCMS t=2.417 df=17, p = 0.027; see Figure 37A).

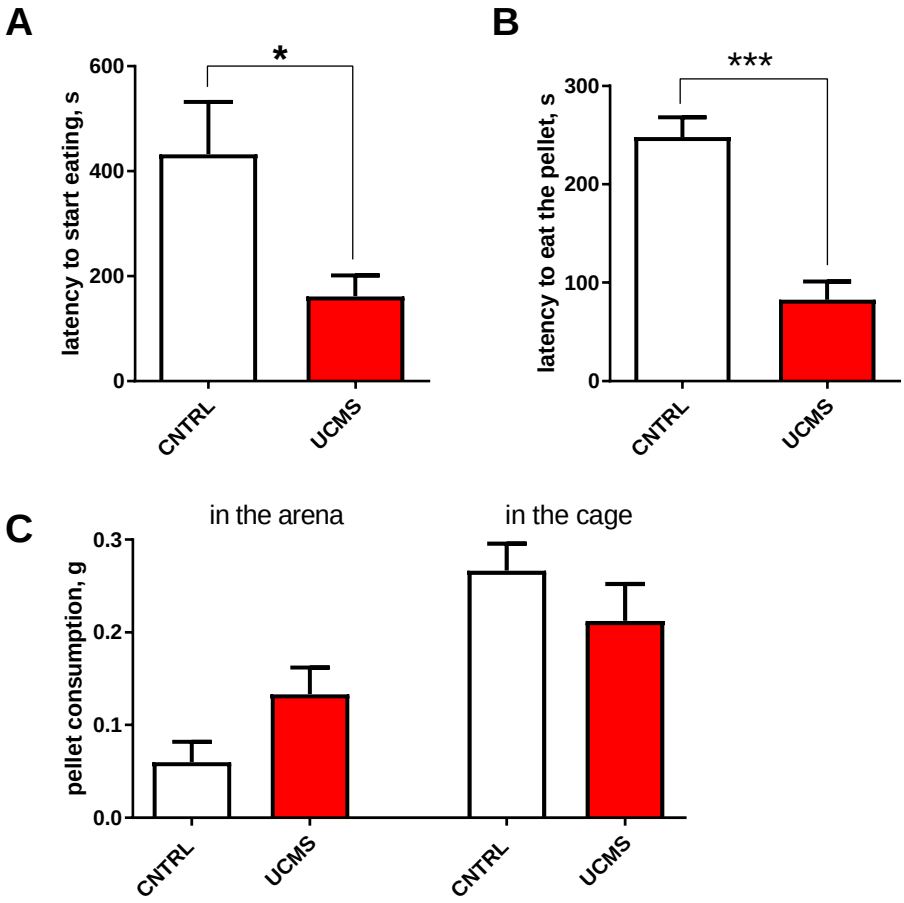

Figure 37 Behaviour in the novelty suppressed feeding and cookie test in the UCMS Experiment 4. Adult male BALB/c mice were exposed to unpredictable chronic mild stress (UCMS) or control (CNTRL) for 4 weeks (n=8/group) and subsequently tested in a short behavioural testing battery, after which fresh frozen brain tissue was collected and selected brain regions were subjected to a genome-wide transcriptomic analysis using Illumina microarray platform. (A*) Latency to start eating a hidden chocolate cookie in the cookie test (B) Latency to start eating the pellet in the middle of the anxiogenic novel arena in the novelty suppressed feeding test (C) Weight of pellet consumed by mice in the novel arena of the novelty suppressed feeding test and during the first 10 min on return to the home cage; *p<0.05 derived from unpaired two-tailed Student t-test CNTRL vs UCMS, ***p<0.05 derived from Mann-Whitney test CNTRL vs UCMS. Data represents mean ± SEM*

3.2 UCMS exerted the strongest effect on gene expression in the PFC

For initial data overview hierarchical cluster analysis based on the top 500 variable genes was conducted in the R environment. It showed that samples primarily clustered based on the brain region they derived from, while within the regions some treatment group – based clustering was observed. The PFC samples clustered based on the UCMS exposure, apart from 2 outlier samples which were excluded from subsequent analysis as can be seen in Figure 38.

In the hippocampus only a few control and UCMS-exposed samples clustered together, and no clear distinct pattern of expression could be seen on the heatmap for HIP UCMS and CNTRL samples. In the hypothalamus no clustering based on stress exposure was observed and the heatmap showed visibly uniform gene expression pattern among all hypothalamic samples indicating a very limited effect of the UCMS on gene expression in this area (see Figure 38).

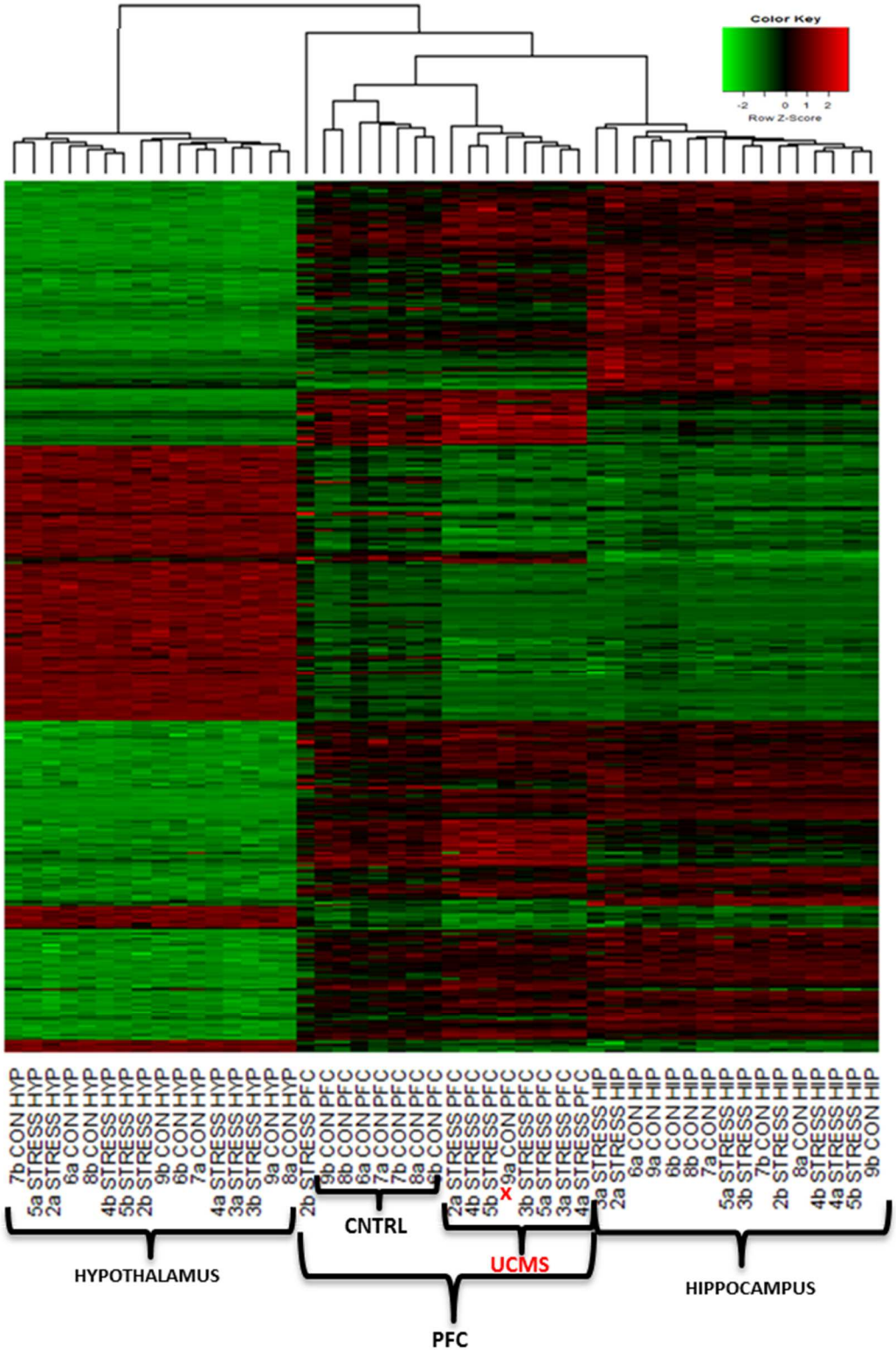

Figure 38 Heatmap of cluster analysis based on the top 500 variable genes.
Adult male BALB/c mice were exposed to unpredictable chronic mild stress (STRESS) or control (CON) for 4 weeks (n=8/group) after which fresh frozen brain tissue from selected brain regions (hippocampus (HIP), hypothalamus (HYP) and prefrontal cortex (PFC)) were subjected to a genome-wide transcriptomic analysis using Illumina microarray platform. The heatmap shows the clustering of samples (top connecting lines) and the heatmap pattern of expressionbased on intensity values of top 500 variable genes. The gradient of green and red represents the deviation of each sample intensity value for this gene from the mean intensity across all samples. Individual sample IDs and their groups highlighted at the bottom of the heatmap.

3.3 Differential expression analysis using SAM package yielded the highest number of significant genes in the PFC

Significance Analysis of Microarrays (SAM) method detected 467 differentially expressed genes between the UCMS and CNTRL groups in the PFC with FDR of 0. As such a low level of FDR was calling a very small number of genes in other regions, FDR level was relaxed to a recommended 0.1 for the hippocampus and the hypothalamus. Such settings called 46 and 27 differentially expressed genes in the hippocampus and in the hypothalamus respectively (see Figure 34).

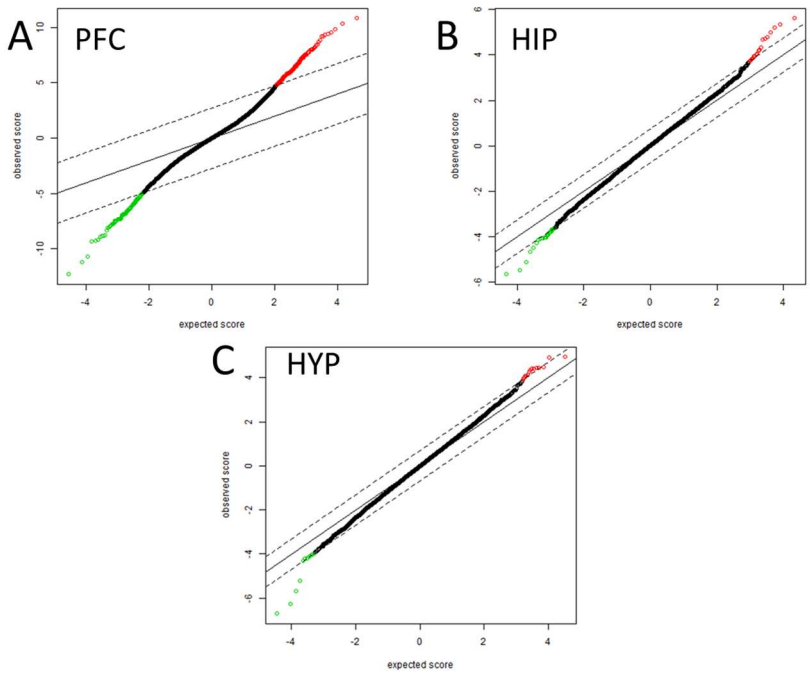

Figure 39 SAM plot of differentially expressed genes in the PFC (A), the hippocampus (B) and the hypothalamus (C). Adult male BALB/c mice were exposed to unpredictable chronic mild stress (UCMS) or control (CNTRL) for 4 weeks (n=8/group) and subsequently tested in a short behavioural testing battery shown, after which fresh frozen brain tissue was collected and selected brain regions (hippocampus (HIP), hypothalamus (HYP) and prefrontal cortex (PFC) were subjected to a genome-wide transcriptomic analysis using Illumina microarray platform. Figure shows plot of the expected (X axis) vs observed (Y axis) relative difference in expression of individual genes between CNTRL and UCMS conditions shows genes for which this relationship deviates from the equality line beyond the set threshold of false discovery rate (ΔFDR, broken line). FDR of 0 yielded 467 genes significantly increased (in red) or decreased (in green) in the PFC; FDR 0.1 yielded 46 significant genes in the hippocampus and 27 significant genes in the hypothalamus.

3.4 Pathway analysis revealed meaningful pathways, functions and predicted upstream regulators in the PFC dataset

All 467 significantly differentially expressed genes in the PFC derived from the SAM analysis were entered into the Ingenuity software for pathway and gene network analysis. Table 9 lists top up- and downregulated genes selected based on their fold change (all genes with expression increased 1.5 fold and above and all genes with expression decreased 0.65 fold and below).

Table 13 Top up and downregulated genes based on fold change estimation derived from SAM and annotated by Ingenuity based on Entrez gene database.
Adult male BALB/c mice were exposed to unpredictable chronic mild stress or control for 4 weeks (n=8/group) after which fresh frozen brain tissue from selected brain regions (hippocampus (HIP), hypothalamus (HYP) and prefrontal cortex (PFC)) were subjected to a genome-wide transcriptomic analysis using Illumina microarray platform. (For a complete list of the significantly differentially expressed genes, see Appendix Table 21).

	TOP UPREGULATED GENES IN THE PFC			TOP DOWNREGULATED GENES IN THE PFC		
	GENE	**Fold Change**	**Entrez gene name**	**GENE**	**Fold change**	**Entrez gene name**
1	Myl4	2.232	Myosin, light chain 4	Rgs9	0.285	Regulator of G-protein signalling 9
2	Tnnc1	2.149	Troponin C type 1 (slow)	Tac1	0.286	Tachykinin, precursor 1
3	Nrgn	2.071	Neurogranin	Pcp4l1	0.304	Purkinje cell protein 4-like 1
4	C17orf96	2.063	Chromosome 17 open reading frame 96	Calb2	0.346	Calbindin 2
5	Fezf2	2.019	FEZ family zinc finger 2	Cartpt	0.368	CART prepropeptide
6	Cpne9	1.965	Copine family member IX	Gng7	0.373	Guanine nucleotide binding protein (G protein), gamma 7
7	Mef2c	1.878	Myocyte enhancer factor 2C	Cartpt	0.481	CART prepropeptide
8	Dkk3	1.869	Dickkopf WNT signaling pathway inhibitor 3	Slc32a1	0.515	Solute carrier family 32 (GABA vesicular transporter), member 1
9	Ldb2	1.864	LIM domain binding 2	Chn2	0.521	Chimerin 2
10	Satb1	1.817	SATB homeobox 1	Cacng5	0.526	Calcium channel, voltage-dependent, gamma subunit 5
11	Stx1a	1.785	Syntaxin 1A (brain)	Lmo3	0.538	LIM domain only 3
12	Pvalb	1.765	Parvalbumin	Scg2	0.541	Secretogranin II
13	Nfix	1.737	Nuclear factor I/X (CCAAT-binding transcription factor)	Gad1	0.545	Glutamate decarboxylase 1 (brain, 67kda)
14	9130024f11rik	1.721	RIKEN cdna 9130024F11 gene	Hap1	0.547	Huntingtin-associated protein 1
15	Zbtb18	1.715	Zinc finger and BTB domain containing 18	Apod	0.560	Apolipoprotein D
16	Lamp5	1.708	Lysosomal-associated membrane protein family, member 5	Slc17a6	0.561	Solute carrier family 17 (vesicular glutamate transporter), member 6
17	Cck	1.672	Cholecystokinin	Slc17a6	0.568	Solute carrier family 17 (vesicular glutamate transporter), member 6

	TOP UPREGULATED GENES IN THE PFC			TOP DOWNREGULATED GENES IN THE PFC		
	GENE	**Fold Change**	**Entrez gene name**	**GENE**	**Fold change**	**Entrez gene name**
18	Galnt9	1.648	Polypeptide N-acetyl-galactosaminyltransferase 9	Gad1	0.569	Glutamate decarboxylase 1 (brain, 67kda)
19	Arhgap32	1.632	Rho gtpase activating protein 32	Tf	0.570	Transferrin
20	Ccl27a	1.627	Chemokine (C-C motif) ligand 27A	Zcchc12	0.571	Zinc finger, CCHC domain containing 12
21	Ddit4l	1.584	DNA-damage-inducible transcript 4-like	Pcp4l1	0.573	Purkinje cell protein 4-like 1
22	Tex40	1.584	Testis expressed 40	Adra2a	0.577	Adrenoceptor alpha 2A
23	Sytl2	1.576	Synaptotagmin-like 2	Mobp	0.581	Myelin-associated oligodendrocyte basic protein
24	Dgkz	1.574	Diacylglycerol kinase, zeta	Tiam1	0.587	T-cell lymphoma invasion and metastasis 1
25	Tshz3	1.568	Teashirt zinc finger homeobox 3	Bcl11b	0.592	B-cell CLL/lymphoma 11B (zinc finger protein)
26	Camk2a	1.565	Calcium/calmodulin-dependent protein kinase II α	Tpbg	0.593	Trophoblast glycoprotein
27	Pcsk2	1.561	Proprotein convertase subtilisin/kexin type 2	Mag	0.594	Myelin associated glycoprotein
28	Osbpl1a	1.550	Oxysterol binding protein-like 1A	Ppp1r2	0.596	Protein phosphatase 1, regulatory (inhibitor) subunit 2
29	Nuak1	1.547	NUAK family, SNF1-like kinase, 1	Strip2	0.598	Striatin interacting protein 2
30	Arpp19	1.544	Camp-regulated phosphoprotein, 19kda	Meis1	0.600	Meis homeobox 1
31	Cckbr	1.539	Cholecystokinin B receptor	Cacng5	0.604	Calcium channel, voltage-dependent, gamma subunit 5
32	Mapk11	1.538	Mitogen-activated protein kinase 11	Mbp	0.606	Myelin basic protein
33	Pvrl3	1.537	Poliovirus receptor-related 3	Zic1	0.612	Zic family member 1
34	Cobl	1.529	Cordon-bleu WH2 repeat protein	Clic6	0.617	Chloride intracellular channel 6
35	Slc17a7	1.528	Solute carrier family 17 (vesicular glutamate transporter), member 7	H3f3a/H3f3b	0.626	H3 histone, family 3A
36	Ccdc3	1.522	Coiled-coil domain containing 3	Btg1	0.634	B-cell translocation gene 1, anti-proliferative
37	Arhgef25	1.514	Rho guanine nucleotide exchange factor (GEF) 25	Tmem255a	0.638	Transmembrane protein 255A
38	Extl1	1.508	Exostosin-like glycosyltransferase 1	Cntnap2	0.650	Contactin associated protein-like 2
39				Sez6	0.650	Seizure related 6 homolog (mouse)

3.4.1 Canonical pathway analysis identified 17 pathways significantly activated in the PFC

Canonical pathway analysis conducted by IPA™ mapped the differentially expressed genes on known canonical pathways, among which 17 were statistically significant ($p<0.05$) based on Fisher's exact test analysis utilised by IPA. Table 14 lists the significant pathways relevant for the brain ordered by their significance level with the ratio showing the proportion of genes included in the pathways which were differentially expressed in the dataset, and z-score predicting up or downregulation whenever such a prediction could have been made based on fold changes of individual genes involved in the pathway.

Table 14 Canonical pathways deemed significant in the PFC dataset by IPA pathway analysis
Adult male BALB/c mice were exposed to unpredictable chronic mild stress or control for 4 weeks (n=8/group) after which fresh frozen brain tissue from selected brain regions (hippocampus (HIP), hypothalamus (HYP) and prefrontal cortex (PFC)) were subjected to a genome-wide transcriptomic analysis using Illumina microarray platform. The table shows canonical pathways deemed significant in the PFC dataset ordered by the log (p-value) derived from Fisher's exact test, with dataset genes/pathway genes ratio and z-score of predicted pathway up or downregulation, calculated for pathways where differential gene expression showed consistent direction of change

INGENUITY CANONICAL PATHWAYS	-LOG (P-VALUE)	RATIO	Z-SCORE	ASSOCIATED DIFFERENTIALLY EXPRESSED GENES
Axonal Guidance Signalling	2.61	0.05	-	Ephb2, Tuba4a, Gng13, Sema4f, Robo3, Gng7, Tubb2b, Ephb6, Sema6d, Mag, Wnt10a, Efna5, Arhgef6, Lingo1, Mras, Myl4, Fzd5, Sema7a, Adamts4
Glutamate Receptor Signalling	2.12	0.10	-	Slc17a7, Slc17a6, Homer1, Grm4, Gng7
Calcium Signalling	2.03	0.06	2.45	Camk2a, Tnnc1, Myh3, Rcan3, Myl4, Mef2c, Itpr1, Camkk2, Camk2g
Wnt/β-catenin Signalling	2.01	0.06	0.33	Csnk2a2, Nlk, Wnt10a, Dkk3, Sox10, Fzd5, Acvr2b, Sox11, Tcf7l2
GABA Receptor Signalling	1.94	0.09	-	Slc32a1, Gabrg1, Gad1, Mras, Ap2s1
Paxillin Signalling	1.65	0.07	0.45	Actn2, Actb, Arhgef6, Mras, Itgb4, Mapk11
Thrombin Signalling	1.64	0.05	1.89	Camk2a, Arhgef6, Mras, Myl4, Gng13, Itpr1, Mapk11, Gng7, Camk2g
Gαq Signalling	1.63	0.06	1.13	Napepld, Adrbk1, Mras, Gng13, Arhgef25, Itpr1, Chrm3, Gng7
Ephrin B Signalling	1.50	0.07	-	Ephb6, Ephb2, Mras, Gng13, Gng7
RhoGDI Signalling	1.49	0.05	-0.82	Dgkz, Arhgdig, Actb, Arhgef6, Mras, Myl4, Gng13, Gng7
B Cell Receptor Signalling	1.40	0.05	2.12	Synj2, Map3k10, Camk2a, Inpp5f, Mras, Mef2c, Mapk11, Camk2g
CCR5 Signalling in Macrophages	1.35	0.08	-	Mras, Gng13, Mapk11, Gng7
G Protein Signalling Mediated by Tubby	1.34	0.09	-	Mras, Gng13, Gng7
Triacylglycerol Degradation	1.33	0.14	-	Faah, Mgll
α-Adrenergic Signalling	1.31	0.06	-	Adra2a, Mras, Gng13, Itpr1, Gng7
Glutamate Dependent Acid Resistance	1.30	0.50	-	GAD1

3.4.2 Pathway analysis predicted a number of relevant upstream regulators

Next, the predicted upstream regulators analysis was conducted using the IPA software. Table 15 lists the top 15 predicted upstream regulators connected to 2 or more differentially expressed genes. In some cases, the software could also make a prediction of the direction and magnitude of up- or downregulation based on the fold changes data available for target genes (activation z-score).

Table 15 Upstream regulators of differentially expressed genes in the PFC dataset predicted by the IPA software. Adult male BALB/c mice were exposed to unpredictable chronic mild stress or control for 4 weeks (n=8/group) after which fresh frozen brain tissue from selected brain regions (hippocampus (HIP), hypothalamus (HYP) and prefrontal cortex (PFC)) were subjected to a genome-wide transcriptomic analysis using Illumina microarray platform. IPA pathway analysis predicted upstream regulators in the PFC dataset shown in the table

	UPSTREAM REGULATOR	GENE NAME	ACTIVATION Z-SCORE	P-VALUE	N OF TARGET GENES
1	Htt	huntingtin	-0.004	0.0000	25
2	Lep	leptin	-0.970	0.0000	8
3	Myrf	myelin regulatory factor		0.0001	3
4	Mecp2	methyl-CpG binding protein 2	1.126	0.0001	7
5	Bdnf	brain-derived neurotrophic factor	-0.181	0.0001	9
6	Hdac4	histone deacetylase 4		0.0001	8
7	Kmt2a	lysine methyltransferase 2A	1.342	0.0002	5
8	Ntrk2	neurotrophic receptor tyrosine kinase 2		0.0011	3
9	Dcc	DCC netrin 1 receptor		0.0018	2
10	Pou4f1	POU class 4 homeobox 1		0.0022	4
11	Comt	catechol-O-methyltransferase		0.0035	2
12	Mtor	mechanistic target of rapamycin		0.0054	3
13	Arntl	aryl hydrocarbon receptor nuclear translocator like		0.0117	2
14	Ascl1	achaete-scute family bHLH transcription factor 1		0.0123	3
15	Bckdk	branched chain ketoacid dehydrogenase kinase		0.0153	2

The relationships between the main upstream regulators and their differentially expressed target genes are presented in Figure 40.

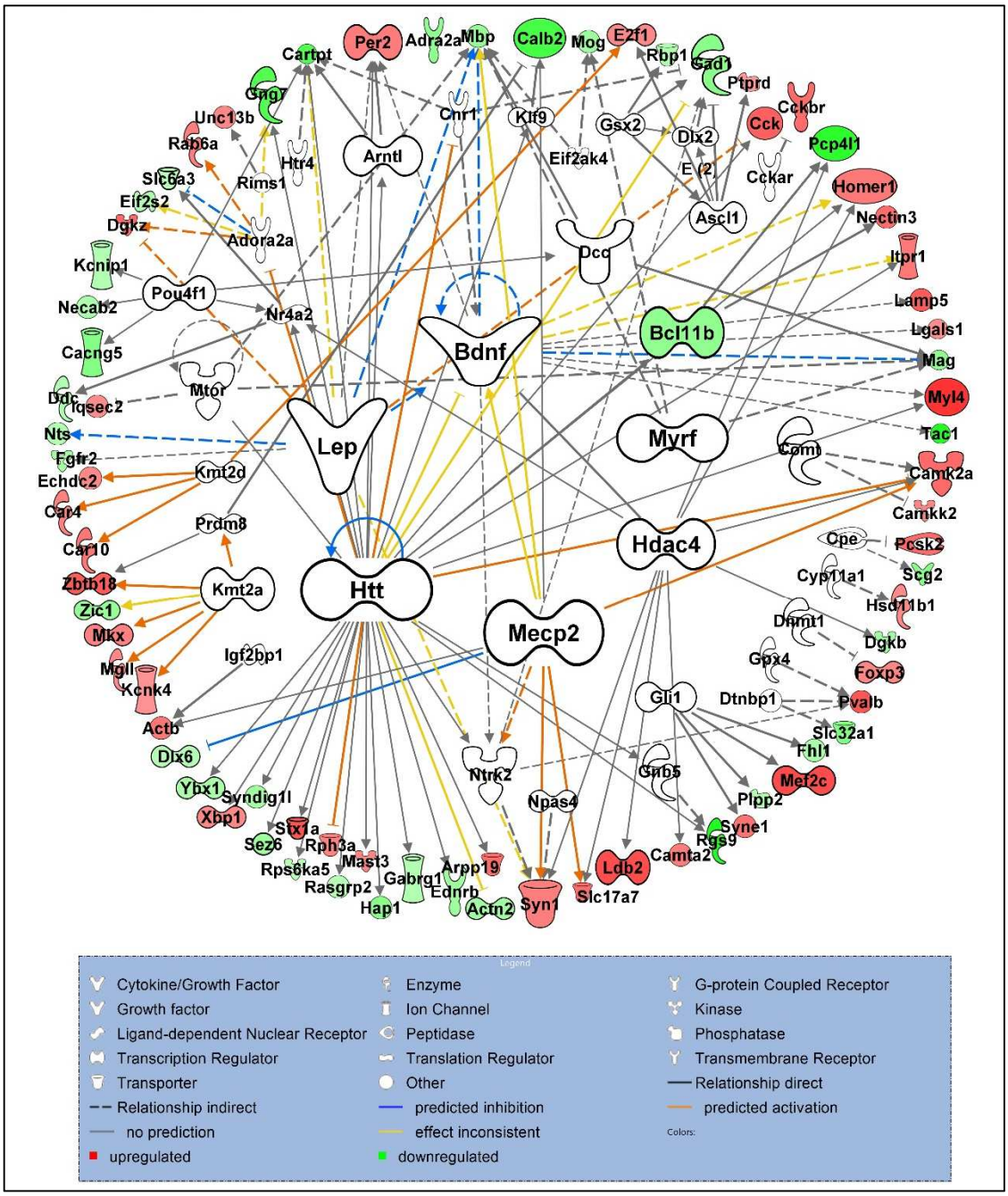

Figure 40 The predicted network of upstream regulators and their target differentially expressed genes in the PFC, designed by the IPA software based on the upstream regulator analysis.

Adult male BALB/c mice were exposed to unpredictable chronic mild stress or control for 4 weeks (n=8/group) after which fresh frozen brain tissue from selected brain regions (hippocampus (HIP), hypothalamus (HYP) and prefrontal cortex (PFC)) were subjected to a genome-wide transcriptomic analysis using Illumina microarray platform. The diagram shows the network of upstream regulators linked to genes differentially expressed in the PFC dataset. The relative size of the upstream regulator molecules reflects their significance ranking with Huntingtin (Htt), Leptin (Lep), myelin regulatory factor (Myrf), methyl-CpG binding protein 2 (Mecp2) and brain derived neurotrophic factor (Bdnf) being the top 5 predicted upstream regulators.

3.4.3 Functional analysis identified functions related to dendritic morphology

Next, we assessed if differentially expressed genes in the PFC dataset were linked to particular functions in the IPA database. IPA functional analysis recognised over a 100 significant functions related to the dataset genes, however some of them were not relevant for the brain or were based on only 1 gene. Table 16 lists only brain-relevant functions based on 2 or more

genes, for which the software could make a prediction regarding its up- or downregulation. These functions fell in mostly 3 functional groups: those related to synaptic plasticity, such as long-term potentiation or synaptic depression, those related to dendritic morphology, such as neurite formation or neuritogenesis and branching of neurites, and those related to cell fate such as cell proliferation, differentiation and migration.

Table 16 Predicted functions associated with the differentially expressed genes in the PFC dataset.
Adult male BALB/c mice were exposed to unpredictable chronic mild stress or control for 4 weeks (n=8/group) after which fresh frozen brain tissue from selected brain regions (hippocampus (HIP), hypothalamus (HYP) and prefrontal cortex (PFC)) were subjected to a genome-wide transcriptomic analysis using Illumina microarray platform.Pathway analysis in the PFC dataset was conducted using IPA software. The listed functions were selected based on their relevance for the brain, number of genes related to each function and the ability of the software to make a prediction regarding the direction of change (activation z-score). Functions related to synaptic plasticity, dendritic morphology and cell fate were overrepresented in the list.

CATEGORIES	FUNCTIONS ANNOTATION	P-value	Activation z-score	N of genes
Cell-To-Cell Signaling &Interaction	long-term potentiation of brain	0.005	-1.177	9
	long-term potentiation of cerebral cortex	0.007	-0.923	8
	neurotransmission	0.009	-0.164	8
	long-term potentiation	0.013	-0.978	10
	release of neurotransmitter	0.016	-1.718	4
	synaptic depression	0.031	-0.527	6
Cell Morphology, Cellular Assembly & Organization, Cellular Development, Cellular Function & Maintenance, Cellular Growth & Proliferation, Embryonic Development, Nervous System Development & Function, Tissue Development	branching of neurites	0.004	-0.250	13
	Neuritogenesis	0.004	-0.250	15
	dendritic growth/branching	0.008	-1.342	11
	outgrowth of neurites	0.050	1.898	6
Cellular Assembly & Organization, Cellular Development, Cellular Growth & Proliferation, Nervous System Development & Function, Tissue Development	microtubule dynamics	0.003	-0.346	17
	growth of neurites	0.039	2.129	8
Cellular Development, Cellular Growth & Proliferation, Nervous System Development & Function, Tissue Development	proliferation of neuronal cells	0.013	0.995	11
	development of neurons	0.001	0.017	20
Cellular Growth & Proliferation	proliferation of cells	0.002	0.512	27
	generation of cells	0.000	0.101	22
Cellular Development	differentiation of cells	0.001	0.460	19
Lipid Metabolism, Molecular Transport, Small Molecule Biochemistry	concentration of lipid	0.007	-2.400	7
Nervous System Development & Function, Tissue Morphology	density of neurons	0.014	-2.213	7
Developmental Disorder, Neurological Disease, Organismal Injury & Abnormalities	cerebral dysgenesis	0.024	0.931	4
Behavior	Behavior	0.037	0.687	8
Cellular Movement, Nervous System Development & Function	migration of neurons	0.050	-0.124	6

3.5 qPCR data replicated the microarray analysis for 10 genes selected from the PFC dataset

10 genes selected from the top differentially expressed genes in the PFC have been also measured using qPCR to validate the results of the microarray analysis. The average UCMS group relative expression of all 10 selected genes calculated against the expression of two reference genes Apt5b and Cst3 significantly differed from CNTRL (see Figure 41A). Moreover, relative expression values showed a strong correlation with fold change data derived from the microarray analysis (see Figure 41 B).

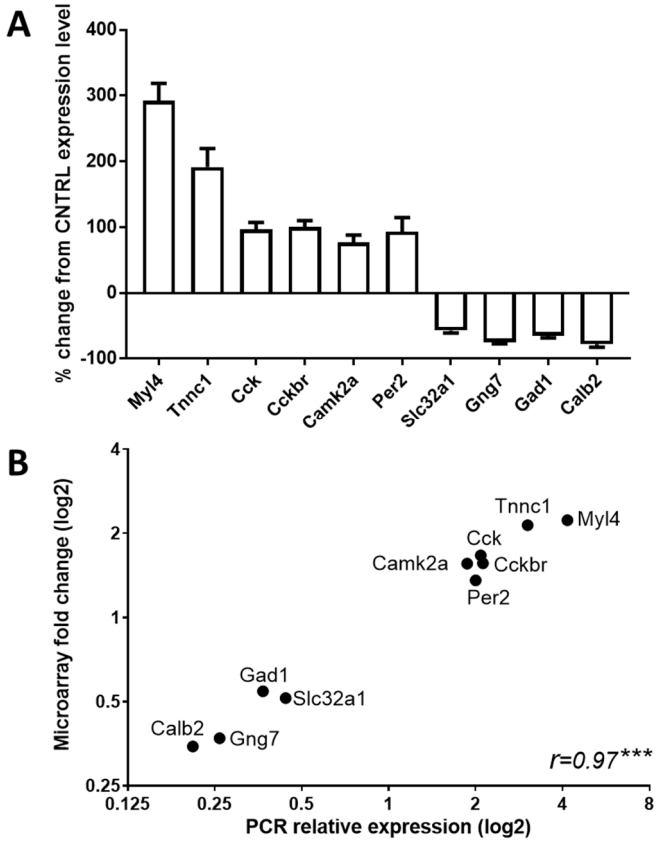

Figure 41 Validation of microarray analysis by qPCR gene expression data

Adult male BALB/c mice were exposed to unpredictable chronic mild stress or control for 4 weeks (n=8/group) after which fresh frozen brain tissue from selected brain regions (hippocampus (HIP), hypothalamus (HYP) and prefrontal cortex (PFC)) were subjected to a genome-wide transcriptomic analysis using Illumina microarray platform. (A) Relative gene expression of 10 genes selected from the list of significantly differentially expressed genes in the microarray was evaluated using qPCR by Pfaffl method, normalised to the expression of 2 housekeeping genes Atp5b and Cst3. Average relative expression of each gene was significantly different from the control level ($p<0.05$ for all genes, derived from 1-sample t-test) (B) For the 10 genes selected for validation by qPCR, there was a strong correlation between the microarray (Y axis) and qPCR (X axis) – derived relative expression levels (Pearson's $r=0.97$, $p***<0.001$).

3.6 Small number of differentially expressed genes in the hippocampus and the hypothalamus datasets limited the use of the pathway analysis

In the hippocampus only 12 genes were significantly differentially expressed with FDR=0 (8 upregulated and 4 downregulated), while in the hypothalamus only 4 downregulated genes were significant with FDR=0. As it is possible to adjust significance criteria in SAM, the datasets for hippocampus and the hypothalamus were analysed with FDR set at 0.095, which deems significant all genes with a q-value up to 9.95%. Such analysis settings yielded 46 significantly differentially expressed genes in the hippocampus and 26 in the hypothalamus (for the full list of genes see Appendix Table 22). However, such a small number of genes was not sufficient to produce meaningful results in the pathway analysis, thus it is not presented in this chapter.

4 Discussion

4.1 Overview of gene expression changes across the three regions

One of the main findings of the microarray analysis was the observation that UCMS affected the expression of an overwhelmingly larger number of genes in the PFC than in the hippocampus and the hypothalamus. The PFC has been previously shown to be affected by the chronic stress exposure on structural and molecular levels, and is thought to play a crucial role in the response of the brain to chronic stress (Arnsten, 2015; McEwen and Morrison, 2013). However most previous gene expression studies in animal chronic stress models focused on the hippocampal changes, therefore a moderate response in this area was somewhat surprising.

While only a handful of studies compared gene expression upon chronic stress in these two areas, some of them show results similar to those described above. At least two studies described in the Introduction section 1.3 above looking at the gene expression in the cerebral cortex and the hippocampus upon UCMS in BALB/c mice showed that more genes were affected in the cerebral cortex and the amygdala then in the dentate gyrus or in the whole hippocampus (Liu et al., 2010; Surget, Wang, et al., 2008). Kaastrup Muller et al. (2011) showed that chronic restraint stress predominantly affected the expression of synaptic proteins involved in the exocytosis of synaptic vesicles in the prefrontal cortex with little effect in the hippocampus, reflecting the higher stress sensitivity of this region in chronic stress response. Similarly Yuen et al. (2012) showed that chronic restrained stress caused suppression of the glutamatergic neurotransmission in the PFC but not in the CA1 region of the hippocampus, which also prompted the authors to claim lower sensitivity of the hippocampus to chronic stress.

While the role of the hippocampus in chronic stress is undeniable, it is possible that the lack of gene expression response comes from the heterogeneity of the hippocampal tissue. Indeed, dorsal and ventral hippocampi are thought to be functionally and molecularly distinct regions. Expression pattern of certain genes have been shown to map onto the anatomical boundaries of the hippocampal regions (Fanselow and Dong, 2010). Moreover, some studies show that the two regions differ in their gene expression response to chronic stress. For example, the expression of HPA axis related genes Fkbp5 and GR has been shown to be affected by the UCMS in the ventral, but not in the dorsal hippocampus (Guidotti et al., 2013). At the same time maternal separation affected Bdnf expression in the dorsal, but not in the ventral region (Hill et al., 2014). Thus it is possible that the use of the total hippocampal tissue might have masked some of the gene expression effects which were present only in one of the hippocampal regions.

The hypothalamus is another region which has been implicated in the chronic stress response due to its role in the HPA axis and the regulation of circadian rhythm. Jungke et al. (2011) found over 150 genes differentially expressed in the hypothalamus upon exposure to chronic restraint stress. Therefore it is also surprising that only a very small number of genes were affected in this area in our analysis. However it is possible that the distinct nature of restraint stress (physical repeated inescapable stress) could cause changes in this region specific to this type of chronic stress. At the same time, changes in the expression of clock genes following UCMS have been found specifically in the suprachiasmatic nucleus (SCN) of the hypothalamus and might not be apparent in total hypothalamic tissue (Jiang et al., 2011; Logan et al., 2015b). Interestingly, the clock gene Per2 was differentially expressed in the PFC as well as in the hippocampus as shown by the microarray analysis and the qPCR, suggesting that the circadian rhythm could nonetheless have been affected in the UCMS-exposed mice. This finding is in line with previous studies showing a change in Per2 expression in the PFC after UCMS (Calabrese et al., 2016; Erburu et al., 2015). Moreover, the translational value of this finding comes from a human post-mortem study which also showed that in depressed patients expression of clock genes is affected by the disorder in brain areas other than the SCN (Li et al., 2013).

4.2 Pathway and functional analysis of the PFC dataset suggests ongoing dendritic remodelling

Pathway analysis is a useful tool to utilise for exploratory hypothesis-free approach. As a large number of genes were found to be differentially expressed in the PFC, pathway analysis was essential to gain insight into the potential systemic changes driving the expression of individual genes. Ingenuity canonical pathway analysis identified 16 significantly activated pathways

relevant for the brain. The top three canonical pathways identified by the pathway analysis were axonal guidance, glutamate signalling and calcium signalling. Differential expression of some of the genes belonging to these pathways (Tnnc1, Gng7, Myl4, Camk2a, Calb1) has been confirmed by qPCR. Involvement of axonal guidance pathway points out towards dendritic remodelling, which might be ongoing in the PFC as a consequence of the UCMS exposure. Indeed dendritic atrophy is perhaps one of the best-described consequences of chronic stress in the PFC (McEwen and Morrison, 2013; Qiao et al., 2016). For example, chronic restraint stress has been shown to reduce the length of apical dendrites of pyramidal neurons and the size of dendritic spines in the dorsal and medial PFC (Liston et al., 2006; Radley et al., 2008). Similarly chronic unpredictable stress with moderate stressors (rotation on shaker, placement at 4°C, food and water deprivation) in rats was shown to reduce spine density and expression of synaptic proteins in the mPFC (Li et al., 2011). The latter study implicated glutamate signalling in the mechanism of spine loss, as this effect of the chronic stress was rapidly reversed by administration of NMDA channel blocker ketamine. Indeed repeated stress is known to cause suppressed glutamate receptor expression and signalling in the PFC, which is thought to be linked to dendritic atrophy (Yuen et al., 2012). Many recent studies have explored the antidepressant potential of ketamine in chronic stress animal models of depression, strengthening the glutamatergic theory of depression (Sun et al., 2016; X Zhu et al., 2015). Therefore glutamate signalling pathway involvement is in line with this hypothesis.

Interestingly, calcium signalling has also been implicated in dendrite remodelling via its effect on protein kinase A (PKA) and protein kinase C (PKC). Calcium is a necessary cofactor in the activation of PKA and PKC, and it has been shown that pharmacological suppression of the PKA and PKC activation prevented spine atrophy following chronic stress exposure (Hains et al., 2009, 2015). PKA and PKC activation are thought to promote spine loss via their stimulatory effect on actin disassembly in the spine cytoskeleton (Arnsten, 2015). In light of these hypotheses it is interesting to note that calcium signalling was one of the few pathways for which strong activation was predicted by the Ingenuity pathway analysis software, as reflected by its positive z-score 2.45 (see Table 14). In addition, over 1.5 fold increase in Camk2a expression is confirmed by qPCR. Moreover, calcium and PKC signalling is supposed to be activated by stress via activation of alpha adrenoreceptors (αAR), while αAR signalling was also deemed a significant pathway in the PFC. Therefore, pathway analysis points towards dendritic and/or spine remodelling as a primary pathology occurring in the PFC upon chronic stress. Indeed, neurite morphology related functions, such as growth of neurites and microtubule dynamics, appeared most frequently in the list of Ingenuity pathway analysis predicted functions (see Table 16). The other two groups dominating functional analysis were synaptic

plasticity and functions related to neural cell fate, such as neuronal proliferation, differentiation, migration and neuronal density. It is interesting to draw a parallel between this analysis and the effect of UCMS on adult hippocampal neurogenesis described in Chapter 3, where a reduction in the number of neuroblasts with developed dendritic trees and their increased migration was observed in the UCMS-exposed group. The fact that signalling pathways relevant for these effects appeared to be altered in the PFC but not in the hippocampus might be suggesting that UCMS exerts its antineurogenic effect on the hippocampus indirectly, potentially via its PFC neuronal connections through the enthorinal cortex (Canto et al., 2008).

4.3 Predicted upstream regulators are highly relevant for observed UCMS-induced pathology

Additional insight into molecular changes occurring in the PFC was provided by the upstream regulators analysis. This type of analysis helps to approach a large pool of differentially expressed genes in a systemic way. Recently a transcriptomic study of chronic stress susceptibility in mice showed that so called hub genes can play an important role in the chronic stress response (Bagot et al., 2016). Similar to upstream regulators, these hub genes were defined as highly connected within the differentially expressed genes pool and capable of predicting the expression of many other target genes. In this study researchers selected three of such hub genes from a gene expression microarray analysis exploring differences between control, chronic social defeat stress-resilient and stress-susceptible mice for overexpression in the PFC and the ventral hippocampus. Even though one of these genes, Sdk1, was not differentially expressed in the original microarray, its overexpression affected animals' susceptibility to chronic social defeat stress. This study verified the importance of regulatory genes in stress response regardless of the effect of stress on their own expressions levels. Therefore the most significant upstream regulators ($p \leq 0.0001$) and their potential role in the chronic stress response are discussed below.

4.3.1 Htt and Bdnf

In my dataset, Ingenuity pathway analysis predicted several highly relevant genes to be upstream regulators, even though most of them were not differentially expressed in the microarray analysis. Htt, the top regulator in the list, is thought to protect neurons against excitotoxicity-induced apoptosis (Leavitt et al., 2006). It is present at pre- and post-synaptic terminals, where it interacts with the proteins controlling exo- and endocytosis of synaptic vesicles, and consequently plays a role in neurotransmitter release and receptor activation (Zuccato et al., 2010). Htt also acts as an activator of the production and transport of Bdnf,

another highly significant upstream regulator in our analysis (Zuccato, 2001). It is noteworthy that in Huntington disease, caused by Htt mutation and loss of function, depression is very common and often precedes motor symptoms characteristic of this disease (Pla et al., 2014). It has been observed that in HD mouse models anxiety-like behaviour can also be detected. Importantly, a study by Pla et al. (2013) showed that targeted knockout of Htt in mature cortical and hippocampal neurons results in anxious phenotype accompanied by a decline in adult hippocampal neurogenesis. More specifically, Htt knockout in mature neurons was associated with reduced survival and dendritic arborisation in immature DCX+ neuroblasts. This effect was partly attributed to a reduction of Bdnf secretion and transport in hippocampal neurons. Bdnf on its own has been strongly implicated into the neurobiology of depression and of antidepressant action (Bjorkholm and Monteggia, 2016). It has been shown to be reduced in the hippocampus and the PFC in post-mortem tissue of depressed patients and upon chronic stress in preclinical models (Autry and Monteggia, 2012). In adult brain Bdnf affects synaptic plasticity and has been shown to increase spine density in hippocampal neurons (M Alonso et al., 2004), as well as to promote neuroblast differentiation and maturation in the dentate gyrus (Waterhouse et al., 2012). In light of these findings it is interesting to point out that in my dataset both Htt and Bdnf were predicted to be downregulated (see z-scores in Table 15 Upstream regulators of differentially expressed genes in the PFC dataset predicted by the IPA software.Table 15), while in parallel UCMS experiment the number of DCX+ neuroblasts with mature dendritic tree was reduced. In fact, one previous study of gene expression upon CRS showed activation of Huntingtin disease related genes in the hippocampus (Andrus et al., 2012). Although it is not clear why in our study these highly interrelated findings were not localised in the same brain region, they do support that the results of microarray analysis corroborate a vast majority of existing literature on neurobiology of chronic stress and depression.

4.3.2 Leptin

The predicted upstream regulator leptin hints at the involvement of metabolic pathways in the effect of UCMS exposure. In the brain leptin mostly acts via leptin receptors in the hypothalamic neurons where it suppresses the release of orexigenic factors and induces the release of anorexigenic factors, which eventually leads to a reduction in food intake *(Reichelt et al., 2015)*. However, leptin effects extend beyond hypothalamus. Leptin plays a role in the mesolimbic dopamine reward system by regulating the excitation of dopaminergic neurons projecting from the ventral tegmental area into the nucleus accumbens, the PFC, the hippocampus and the amygdala (van Zessen et al., 2012). Leptin receptors are also present in the PFC and the hippocampus (Wada et al., 2014). Leptin has been previously implicated in the

effect of chronic stress and its reversal. Various chronic stress paradigms were shown to reduce plasma and brain tissue leptin levels, while leptin administration has been shown to have an antidepressant effect (Liu et al., 2015; Lu et al., 2006). Moreover, leptin has also been shown to reverse the detrimental effect of stress and glucocorticoids on adult hippocampal neurogenesis (Garza et al., 2008, 2012), and to have a stimulating effect on dendritic branching in the hippocampus (O'Malley et al., 2007). These observations support the relevance of leptin signaling for the effect of UCMS. It is noteworthy that leptin signaling was predicted to be downregulated in our PFC analysis, which goes in line with reduced plasma levels of leptin described post UCMS in Chapter 2 UCMS model (see Figure 24).

4.3.3 Myelin regulatory factor Myrf

While upstream regulators discussed above have already been linked to chronic stress in previous literature, little is known about the role of 3rd regulator in the list, the myelin regulatory factor or Myrf (see Figure 40). The few studies on Myrf describe its role in myelination processes occurring in the CNS during development and adulthood (Bujalka et al., 2013). Myrf is an oligodendrocyte-specific target of Sox10, transcription factor which regulates myelination of axonal terminals. Upon Sox10 stimulation Myrf induces a myelinating program in the oligodendrocytes (Hornig et al., 2013). Interestingly, several studies report myelination deficit upon chronic stress. Yang et al. (2016) report reduced maturation of oligodendrocytes and myelination in the mPFC of mice subjected to chronic unpredictable stress. A diffusion tensor imaging (DTI) study found signs of demyelination upon UCMS in rats in the wide range of brain regions, including frontal cortex, hippocampus and the hypothalamus (Hemanth Kumar et al., 2014). Another study found shortening of myelin-formed nodes of Ranvier and in the corpus callosum of chronically stressed mice, which corresponded to the DTI data showing signs of white matter damage in the corpus callosum of depressed patients (Miyata et al., 2016). Taken together, these findings suggest that prediction of Myrf as an upstream regulator could be pointing towards myelination deficit known to be induced by UCMS in animals and by clinical depression in patients.

4.3.4 Epigenetic factors

Another interesting finding from the upstream regulator analysis was the presence of two proteins playing key roles in the mechanisms of epigenetic regulation, methyl-CpG binding protein 2 (Mecp2) and histone deacetylase 4 (Hdac4), involved in DNA methylation and histone deacetylation, respectively. Both mechanisms, if acting on a promoter or other regulatory region of a given gene, reduce expression of that gene, however the functional consequences of such regulation depend of course on a function of the gene in question. Nonetheless, it has been observed that chornic social defeat stress increases histone

acetylation in the limbic areas including the hippocampus and the PFC, and that administration of HDAC inhibitors produces an antidepressant effect on chronic social defeat-induced behavioural deficits (Iii et al., 2015). DNA methylation of various target genes has been extensively studied in early life stress research in an attempt to uncover mechanisms through which early life adversity predisposes individuals to psychiatric disorders including depression. Indeed DNA methylation of genes encoding such crucial for psychopathology proteins as GR, CRH and Bdnf has been shown to be modified by prenatal or early life stress exposure, often with behavioural consequences in adulthood (Provençal and Binder, 2014). While limited data exist on the effect of chronic stress on DNA methylation in adulthood, few studies set the precedent for the ability of chronic stress to modify methylation of individual genes and the genome-wide methylation levels. For instance, chronic social defeat was found to increase the level of DNA methyltransferases, enzymes catalysing DNA methylation, in the nucleus accumbens (LaPlant et al., 2010). On the individual gene level UCMS has been shown to alter DNA methylation of CRF gene promoter (Sterrenburg et al., 2011). Moreover, post-mortem study provided clinical evidence for the involvement of DNA methylation in depression, by demonstrating increased levels of GABAA receptor methylation in limbic brain regions of suicide completers (Poulter et al., 2008). Therefore, evidence of UCMS activating molecular networks involved in epigenetic regulation also goes in line with existing literature and suggest long-term consequences of UCMS exposure.

4.4 Cholecystokinine and its receptor were increased in the PFC

One group of differentially expressed genes was not highlighted by the pathway analysis, however deserves special attention due to its relevance for chronic stress and some particular behaviours observed in this experiment. Both cholecystokinine (Cck) and cholecystokinine receptor B (Cckbr) were upregulated in the PFC of UCMS-exposed mice as shown by the microarray and the qPCR analysis. Cck is a gastropeptide and a neurotransmitter. Its CckA receptors are located in the gut and are thought to play a role in food intake regulation via its effect on vagal nerve terminals (Dockray, 2012). CckB receptors are located predominantly in the brain where they form a part of Cck signalling system, spread out across the prefrontal cortex, the amygdala, the hippocampus and the hypothalamus (Zwanzger et al., 2012). Cck signalling has been implicated in the fear and anxiety responses, and in the development of the panic disorder. Administration of the Cck agonist has been shown to induce panic attacks in healthy volunteers as well as in depressed patients (Koszycki et al., 2004). Cck is increased in the frontal cortex of animals subjected to chronic social defeat (CSD) (Becker et al., 2008). In the same study Cckbr antagonist has been shown to prevent development of behavioural deficit in the FST and the sucrose preference tests in socially defeated mice. Moreover,

blockade of Cckbr reversed a reduction of cell proliferation in the hippocampal dentate gyrus induced by this chronic stress paradigm. Another chronic social defeat study went on to show that the low level of Cckbr expression in the prefrontal cortex predicts animals' resilience, while a high expression level was observed in mice susceptible to the effect of chronic social defeat (Vialou et al., 2010). Therefore, the observed increase in the expression levels of Cck and the Cckbr in our study supports the role of this neurotransmitter in the neurobiological changes induced by chronic stress and supports the induction of expression profile previously described in the PFC in chronic stress studies. Also the role of Cck in food intake control and the gut-brain axis suggests an intriguing possibility of the link between anxiety and appetitive behaviours.

4.5 Absence of HPA axis and immune pathways

The additional aims of the gene expression study were to detect activation of the immune and HPA axis related signalling, which has been detected in the hippocampus in previous UCMS studies. However, the list of differentially expressed genes in the hippocampus and the hypothalamus did not include any GR or immune response related genes, such as NFkB or cytokines and their receptors. Moreover, a small number of differentially expressed genes in these regions limited the use of pathway analysis. It is possible that these negative results are related to the timing of tissue collection, as it has been done after the end of the UCMS protocol and thus might not reflect some of the short-term changes occurring earlier in the course of UCMS exposure. In addition, analysis of the whole region tissue instead of its subregions, such as dorsal or ventral hippocampus or separate hypothalamic nuclei, might have prevented the detection of significant differences. On the other hand, the absence of GR or immune response signalling pathways activation goes in line with the absence of microglial activation in the hippocampus and activation of the HPA axis in UCMS-exposed groups. At the same time microglial activation in the PFC collocated with a large number of differentially expressed genes in this area, suggesting an association between the two phenomena.

5 Conclusions

To summarise, the genome wide gene expression analysis provided a lot of insights into the molecular mechanisms involved in UCMS effects. It indicated that the gene expression changes were most apparent in the PFC among the 3 regions investigated. Many target genes, upstream regulators and signalling pathways involved could be linked to one of the well described effects of chronic stress on the PFC, dendritic remodelling and spine atrophy. Among them glutamatergic, calcium and Cck signalling, and Htt and Bdnf centred networks stood out as the most significantly involved. In addition, Cck and leptin signalling suggested a potential

modulation of anxiety and food reward related pathways. Evidence of circadian rhythm alteration was also present in the PFC as well as in the hippocampus. The limited number of differentially expressed genes in the hippocampus did not allow any hypotheses to be tested regarding the mechanisms affecting adult neurogenesis in this region. However, it is possible that signalling pathways affecting dendritic morphology in the PFC could be indirectly influencing hippocampal neurons via PFC-hippocampal connections. This notion is also supported by the enrichment of cell proliferation, differentiation and migration functions in the functional analysis of the PFC dataset. Dendritic tree and dendritic spine density measurements in the PFC and the hippocampus could show if these molecular changes led to dendritic morphology alteration in adult neurons in these two regions. Finally, genome wide gene expression analysis suggested the involvement of two mechanisms not predicted from the behavioural or immunohistochemical experiments carried out in this project, namely the modulation of myelination and epigenetic pathways. Future myelin measurements and DNA methylation and histone acetylation assays could show if indeed UCMS caused any functional changes in these domains.

However, there are a number of limitations to the gene expression study. The conclusions drawn from the gene expression data need to be taken with caution, as hypothesis-free pathway analysis is interpreted based on already available evidence of the involvement of processes in question in the chronic stress response. In addition, the observed effects are limited to the time window of tissue collection, and therefore do not represent changes which might have occurred earlier during UCMS. Future experiments could address this issue by collecting the tissue at different time points during the UCMS exposure. The analysis could also benefit from separating the tissue into specific subregions based on their anatomical and functional significance in chronic stress response.

Chapter 5 LPS-based model

1 Introduction

As clinical evidence of the importance of the immune system in depression accumulated to form the neuroinflammatory hypothesis of the disease neurobiology (Hodes et al., 2015; Raison and Miller, 2011), the need to study neuroimmune mechanisms and their influence on depression-like behaviour in model organisms became apparent. While evidence exists that some chronic stress models are capable of inducing neuroimmune alterations, such as elevation of peripheral and CNS proinflammatory cytokines levels and microglial activation in the brain (Lu et al., 2016; Tynan et al., 2010), our study of the UCMS effects showed that neuroinflammatory changes were not a major part of the neurobiological phenotype induced by UCMS. Therefore, another type of manipulation was required to reproduce immune aspects of depression neurobiology.

1.1 The behavioural effects of lipopolysaccharide (LPS)

LPS exposure in animals has long been used to model depressive-like behaviour and relevant neurobiology. LPS is a glycolipid set in the outer membrane of Gram negative bacteria. Extracted from a bacterial culture, LPS acts as a proinflammatory agent which induces a behavioural and neurobiological inflammatory response similar to that seen in bacterial infection, but in absence of living pathogen (Alexander and Rietschel, 2001). Upon administration, LPS is recognized by leukocytes and other immunocompetent cell types via a surface toll-like receptor 4 (TLR4). Binding of LPS causes TLR4 dimerization and activation, which initiates downstream signalling via adaptor protein myeloid differentiation factor 88 (MyD88) and Toll/IL-1 receptor homology domain-containing adaptor protein (TRIF). Recruitment of MyD88 to TLR4 results in the activation of a signalling cascade involving the IL-1-receptor-associated kinases (IRAKs) and mitogen-activated protein kinases (MAPK), that in turn facilitate activation of the nuclear factor kappa B (NF-κB) pathway (Murphy et al., 2011). NF-κB translocates to the nucleus where it stimulates transcription of pro-inflammatory cytokines such as TNFα, IL-6 and IL-1β, as well as inducible nitric oxide synthase (Bohannon et al., 2013). TRIF on the other hand activates interferon regulatory factor 3 which ultimately leads to the activation of interferon-β (IFNβ) and related genes (Morris et al., 2015) (see Figure 42).

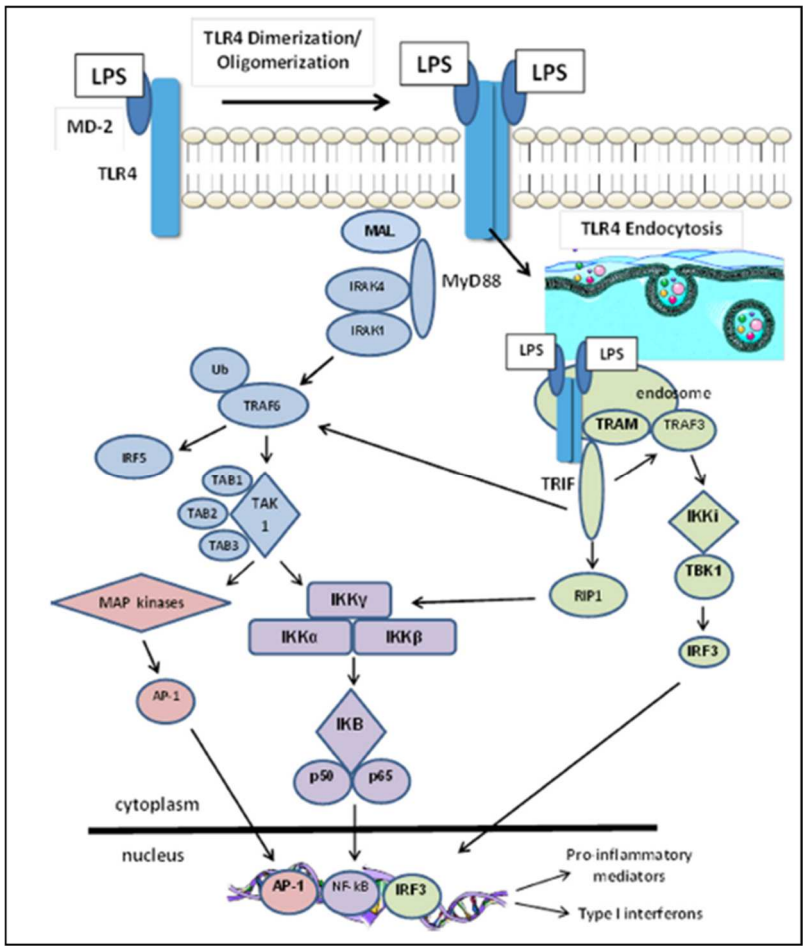

Figure 42 Signalling pathways downstream of TLR4 activated by LPS.
Presentation of lipopolysaccharide (LPS) induces Toll-like receptor 4 (TLR4) dimerization and subsequent activation of the MyD88-depedent signaling pathways, including Toll/IL-1 receptor homology domain-containing adaptor protein (TRIF) pathway and IL-1-receptor-associated kinases (IRAKs) and mitogen-activated protein kinases (MAPK) pathways. The signalling cascade eventually leads to activation of the nuclear factor kappa B (NF-κB), which translocates to the nucleus where it stimulates transcription of pro-inflammatory factors such as cytokines TNFα, IL-6 and IL-1β and interferons such as IFNγ. From Bohannon et al., Shock 2013 40(6): 451–462

Therefore, response to a single dose of LPS involves elevation of plasma cytokine levels, which have been shown to act within the brain tissue via several mechanisms, including transport across permeable regions of the BBB such as in the vasculature of the lateral ventricles (Banks, 2007), transport aacross the leaky BBB induced by systemic inflammation(D'Mello et al., 2009) or by activating the cells forming the barrier, such as endothelial cells, perivascular macrophages and astrocytes (Hodes et al., 2015) (see Figure 5 in Chapter 1 section 2.4.2.2). Once transmitted to the brain, LPS signal triggers inflammation-like responses and behavioural changes commonly described as sickness behaviour. These behavioural changes include reduced food intake, weight loss, fever and hypolocomotion (Biesmans et al., 2013). While some of these behaviours already carry a degree of resemblance to symptoms of depression, LPS exposure also is known to potentiate depression-like behaviour in relevant behavioural tests. Yirmiya (1996) was one of the first to show that injection of 1mg/kg LPS induced anhedonia in a sucrose consumption and sexual behaviour test, conducted within the 4 to 12

hr time period after injection in LPS-exposed rats. Behavioural despair in the FST and tail suspension tests 24 hours after 0.33 mg/kg LPS injections was shown in BALB/c mice by Godbout et al. (2008). However in these two studies early behavioural assessment meant that these changes simply could be a result of sickness-induced hypolocomotion, which was documented to coincide with the behavioural testing in both studies. To disentangle these effects, Frenois et al. (2007) showed that ICR mice displayed hypolocomotion at 6, but not 24 hours after exposure to 0.83mg/kg dose of LPS, while behavioural despair was detected in FST and TST at the 24-hour time point. While the time gap between sickness and depressive-like behaviour is now being widely used to demonstrate the independence of depressive-like changes from the physical sickness induced by LPS (O'Connor et al., 2009; Park et al., 2011), the short time window in which these behaviours occur limits its use for modelling chronic disease and testing chronic antidepressant therapy. However, a limited number of studies showed that LPS challenge can result in long-term consequences. For example, Painsipp et al. (2011) showed that group-housed female C57BL6 mice displayed increased immobility 28 days after 0.83mg/kg LPS injection. However, this effect was strain-dependent, as CD1 mice displayed only a short-term (24 hours) increase in immobility following LPS exposure.

1.2 Neurobiological effects of LPS

In addition to behavioural changes, LPS also mimics some aspects of depression neurobiology observed in clinical studies or other animal models of the disease. Some studies implicated the elevation of indolamine 2,3-dioxygenase (IDO) metabolism, stimulated by proinflammatory cytokines, in the mechanism of depressive LPS effects. O'Connor et al. (2009) showed that blockade of IDO elevation following acute 0.83 mg/kg LPS administration also blocks increases in FST immobility in LPS-exposed CD1 mice. As IDO plays a key role in serotonin/kynurenine metabolism, a process already implicated in depression, behavioural changes in this study were attributed to the neurotransmitter imbalance. Interestingly, to block IDO in this study authors used pre-treatment with minocycline, a semisynthetic derivative of the antibiotic drug tetracycline, known to inhibit macrophage and microglial activation. Minocycline treatment has been previously shown to prevent development of sickness behaviour and anhedonia in the sucrose preference test in BALB/c mice repeatedly injected i.p. with 0.33mg/kg LPS (Henry et al., 2008). While in this study effect of minocycline was also attributed to blockade of IDO increase, it is possible that inhibition of microglial activation also played a role in minocycline's mechanism of action.

Indeed, it has been shown that systemic LPS exposure is capable of inducing microglial activation in the brain. Buttini et al. (1996) was the first to show morphological transition of resting ramified microglia to a round, CD11b-positive activated-like state in the rat

hypothalamus, thalamus and the brainstem during first 7 days following peripheral injections with 2.5 and 5 mg/kg LPS. Increases in activated Iba1-positive microglia also were described in the hippocampus and frontal cortex of C57BL/6J mice 2 hours after an injection with 1mg/kg LPS (Qin et al., 2007). The same dose induced an increase in the number of Iba1-positive microglia in the hypothalamus of BALB/c mice 28 hours after injections (Clark et al., 2015). This dose has been also shown to increase another microglial activation marker density, CD68, in the hippocampal dentate gyrus of rats (Monje, 2003). This study was also one of the first to show that peripheral LPS injection can reduce the density of DCX positive cells in the hippocampus.

Indeed, a decrease in the level of adult hippocampal neurogenesis is another neurobiological aspect which converges mechanisms of depression and LPS effects literature. LPS has been shown to reduce the level of neural stem cell proliferation, differentiation and survival in the hippocampus. For example, cell proliferation was shown to be reduced in the DG 24 hours after 1mg/kg LPS injections in rats (Fujioka and Akema, 2010). Neuronal differentiation was shown to be reduced in the DG 7 and 28 days after a 5mg/kg LPS injection to C57BL6 mice (Ormerod et al., 2013) (Ekdahl et al., 2003; Graciarena et al., 2013; Ormerod et al., 2013). Long-term effects of a single 1mg/kg LPS injection were investigated in a study where C57BL6 mice were sacrificed 6 weeks after injections (Valero et al., 2014). At this time point cell proliferation was found to be increased in the DG, but proliferating cells expressed microglial CD11b rather than neuronal NeuN marker. At the same time the number of DCX+ cells was decreased, specifically the population with more mature dendritic tree structure ("EF" type). In addition, DCX+ dendritic tree volume, dendritic length and postsynaptic density (PSD95) puncta were decreased in LPS-exposed animals. Thus the last two studies showed that effect of LPS on AHN could be long-lasting.

1.3 Limitations in the use of LPS to model depression

Despite this extensive evidence for the value of LPS as a model for inducing depression-like behaviour and relevant neurobiology in rodents, there are a number of issues regarding the dose and duration of exposure to LPS. Firstly, many studies used very high doses of LPS (3-5mg/kg) resulting in a drastic elevation in proinflammatory cytokines, as might be seen in sepsis, which might not be relevant for the more subtle increases seen in depressed patients (Anderson et al., 2016; Erickson and Banks, 2011). Secondly, most behavioural and neurobiological effects of LPS are short-lived (24 hours or less) and therefore their relevance as a model of a chronic disorder is limited (Godbout et al., 2007; Graciarena et al., 2013). Chronicity is an important aspect in depression neurobiology, as over half of all patients do not recover within 2 years and it is estimated that about 80% of patients experience at least one

relapse in their lifetime (Otte et. al., 2016). Moreover, existing evidence suggests that chronic inflammation years before the disease onset might be an important risk factor for depression, such as the Whitehall II study of over 3000 cases which showed that increased peripheral blood CRP and IL-6 concentrations significantly predicted depressive symptoms occurring 12 years later (Gimeno et al., 2009).

Therefore to prolong the effects of LPS some studies had employed a protocol involving repeated LPS injections at various time intervals. For example, ICR mice subjected to 16 daily injections with 0.83mg/kg of LPS displayed immobility in the FST and anhedonia in the NSF test, which was accompanied by increased IL-1β expression and decreased BDNF expression in the hippocampus and cortex (Guo et al., 2014). Another study compared the effect of a single 0.6mg/kg LPS injection with 8 weeks of daily injection with the same dose in rats, and showed that chronically injected rats also displayed hypolocomotion and increased immobility in the FST. Behavioural results were accompanied by an increase in IL-1β and IFNγ in the hypothalamus, although no change in cytokine level was detected in the blood serum (Fischer et al., 2015). A different approach was used in a study by Kubera et al. (2013), where female C57BL6 mice were injected with a dose of LPS fluctuating between 0.75 and 1.25 mg/kg for five consecutive days each month for 4 months. Sucrose preference measurements showed that every month mice took progressively longer to recover from anhedonic effects of LPS injections with no recovery observed on the last month. However chronic fluoxetine treatment was able to reverse this effect. While such protocols induced more relevant long-lasting phenotypes, repeated exposure is also known to result in a suppressed reaction of the immune system, known as LPS or endotoxin tolerance.

LPS tolerance is a hyporesponsive state of the immune system in which there is an attenuated cellular and endocrine response to repeated LPS challenges, also leading to reduced sickness behaviour (López-Collazo and Del Fresno, 2013). This phenomenon was first described in patients who developed sepsis, and later replicated in animals injected with sublethal doses of proinflammatory agents, which survived subsequent exposures to doses known to be lethal to naïve animals (reviewed in López-Collazo and del Fresno, 2013). However similar modifications in response, or tolerance, are known to be induced by milder stimuli. For example, Rosenthal et al. (1996) showed attenuation of the fever response to a second and third LPS injections in rats, either injected with the same 0.02mg/kg or changed to higher or lower doses compared to the first injections. Attenuation of hypolocomotion and anxiety compared to the first exposure was observed in CD1 mice after a second injection with 0.025mg/kg LPS. In the immune system LPS tolerance is characterised by reduced proinflammatory cytokine (TNFα, IL-1β and IL-6) expression and increased expression of anti-inflammatory cytokines, such as IL-10

(Biswas and Lopez-Collazo, 2009). The mechanism behind this reaction is thought to be linked to the downregulation of a signalling pathway downstream of TLR4 (Morris et al., 2015) by inhibitors of MyD88 signalling pathway. For example, MAPK phosphatase-1 supresses the activation of MAPKs, IRAK-M disrupts the function of IRAKs, and inhibitor of NF-κB (IκB) reduces nuclear translocation and decreases production of LPS-induced gene products (Bohannon et al., 2013). Such state of the immune system differs dramatically from the chronic activation seen in depression.

To summarise, both single and repeated LPS exposure models have their advantages and disadvantages for modelling immune changes seen in depressed patients. More specifically, single injections with moderate doses induce very short-lived depression-like phenotypes sometimes indistinguishable from physical sickness. In contrast, repeated injections might result in more long-lasting changes, but can also lead to the development of LPS tolerance, a supressed state of the immune system response which has little in common with immune changes seen in depressed patients. Therefore, the main aims of the experiments described in this chapter were firstly, to establish the time line of sickness and depression-like behaviours following a single, moderate and frequently used dose of LPS and to evaluate if it causes any long-lasting behavioural and neurobiological changes relevant for depression, comparable to the timescale of the UCMS model. The second aim was to develop a model of repeated injections which would induce long-term depression-like behavioural and immune changes, as well as affect neurobiological processes relevant for depression pathology, such as microglial activation and neuronal differentiation in the hippocampal dentate gyrus, but not trigger a supressed state of the immune system known as LPS tolerance.

2 Methods

2.1 Animals

7-week old male BALB/cAnNCrl mice were obtained from Charles River (Margate, Kent, U.K.). .). All animals were housed in the Biological Services Unit (BSU) at the Institute of Psychiatry, Psychology & Neuroscience in standard conditions (19-22°C, humidity 55%, 12h:12h light:dark cycle with lights on at 7.30am, food [Rat and Mouse No. 1 Diet; Special Diet Services, Essex, UK] and water ad libitum). Mice were pair-housed with their litter mates in large cages 45x28x13cm with environmental enrichment (small plastic and cardboard houses, cardboard tube, paper sizzle nest material; Datesand Ltd, Manchester, UK). Housing with litter mates was implemented to prevent fighting of cage mates observed in this strain in previous experiments (such as in CON group of UCMS Experiment 1).

2.2 LPS injections

For all injections LPS from *E.Coli* Serotype O127:B8 (L3129, Sigma Aldrich, Poole, UK) was used. LPS powder was freshly dissolved prior to injections in sterile 0.9% saline (Aquapharm, Argyll, UK). All injections were administered i.p. in all experiments. In Experiment 1: Single LPS exposure mice from LPS group were injected with 0.33 mg/kg LPS, VEH group was injected with saline at a volume of 8 ml/kg calculated for an average 25g mouse (100 µL) (for experimental design see Figure 43).

In Experiment 2: Repeated LPS exposure control group (SAL; n=10) received 100 µL of 0.9% saline each week; 0.1 LPS group (n=8) received 0.1mg/kg of LPS each week; escalating LPS (0.33-0.83) group (n=8) received 0.33 mg/kg of LPS on weeks one and two, 0.53 mg/kg of LPS on week three, 0.63 mg/kg on week four, 0.73 mg/kg on week five, 0.83 mg/kg on week six; single LPS group (n=8) received 0.83 mg/kg on week one, and 100 µL saline on weeks 2-6 (for experimental design see Figure 46).

2.3 Behavioural testing

Body and food weight were measured immediately before the injections and at time points of interest post injections. The difference between the two data points was used as weight gain or food intake measures respectively. Open field test and forced swim test were performed as described in Chapter 2 (see p62 and 63). For home cage activity tests, enrichment materials were removed from the cages and clear, acrylic lids were placed on top of the cage to allow video recording and subsequent activity tracking. The movements were recorded for 5 minutes. Distance travelled was measured using the automated tracking system (Ethovision, Noldus Information Technologies, Wageningen, The Netherlands).

2.4 Blood collection

Blood was collected by incision method from the lateral tail vein (Sadler and Bailey, 2013). Whole blood (30-50µL) was collected into EDTA microvette CB 300 tubes (Sarstedt, Leicester, UK) and separated by centrifugation for 10min at 3000 rpm (4^{o}C), after which plasma was manually transferred into a new sterile tube (1.5ml 'Crystal clear' microcentrifuge tube sterile, Starlab UK Ltd) and stored at -80°C. Cytokine analaysis was conducted using the multiplex screening assay based on magnetic Luminex® xMAP® technology as described in Chapter 2 Section 3.6.

Another blood collection by method of cardiac puncture was utilised in Experiment 2: Repeated LPS. This collection occured after the terminal general anaesthesia had been induced by the injection of 40mg/kg of pentobarbital sodium i.p. (Euthatal, Merial Animal Health Ltd,

Harlow, UK). 100-200 µL of whole blood was collected using syringe injected into the cardiac cavity and subsequently processed as described above to measure corticosterone levels.

2.5 Immunohistochemistry and microscopy

For brain tissue collection, mice were anesthetised with 40mg/kg of pentobarbital sodium i.p. (Euthatal, Merial Animal Health Ltd, Harlow, UK) and subsequently transcardially perfused with saline and 4% paraformaldehyde (Paraformaldehyde, prills, 95%, 441244, Sigma-Aldrich, Poole, UK) in phosphate-buffered saline (pH = 7.4 from PBS tablets, 18912-014, Gibco by Life Technologies, Paisley, UK) through the left cardiac ventricle. Brains were post-fixed overnight in 4% PFA at 4°C, and subsequently stored at 4°C in 30% sucrose (Sigma-Aldrich, Poole, UK) in PBS.

Brain tissue was cut on a HM430 sliding microtome (Thermo Scientific) into serial 40µm thick coronal sections and stored in tris-buffered saline (TBS, pH=7.4) with 30% v/v glycerol, 15% w/v sucrose and 0.05% w/v sodium azide (all Sigma Aldrich, UK) to prevent bacterial growth and for cryoprotection at 4°C. For immunohistochemistry on free floating sections, every 6th section was washed in PBS 3x5min, incubated in 1% hydrogen peroxide (Sigma Aldrich, UK) for 30 mins with subsequent washing in PBS. Non-specific antibody binding was blocked by incubating sections in 10% NGS (Normal goat serum, S1000, Vector laboratories, UK) in PBST (PBS with 0.25% TritonX (Sigma Aldrich, UK) for 1hr. Sections were incubated in primary antibodies (anti- doublecortin (DCX) diluted 1:1000, ab18723, Abcam; Anti-Iba1 diluted 1:500, 019-19741, Wako; anti CD68 diluted 1:2000, MCA 1957, ABD Serotec, Anti-Ki67 diluted 1:200, ab15580, Abcam; all made in rabbit) diluted in PBST with 10% NGS at 4°C, agitated on orbital shaker overnight. The next day sections were washed in PBS 3x5min and incubated in secondary antibody, biotinylated anti-Rabbit IgG made in goat (BA1000, Vector Laboratories, UK) for 2hrs at room temperature on an orbital shaker. Subsequently, sections were incubated in a solution containing avidin-biotin complex (Vectastain Elite ABC Kit, PK6100, Vector Laboratories, UK) for signal amplification. The staining was visualised with diaminobenzidine (DAB, Sigma Aldrich, UK). Sections were rinsed PBS 3x5min, mounted on Superfrost Plus microscope slides (Thermo Scientific), air-dried, dehydrated in serial ethanol dilutions, cleared in xylene (Sigma Aldrich, UK) and coverslipped using Distyrene Plasticizer Xylene (DPX) (Sigma-Aldrich, UK).

Stereological analysis

Stereological method was used to quantify the density of immunopositive cells as described previously (Thuret et al., 2009). An Axioskop 2 MOT Zeiss microscope and a semiautomatic stereology system (StereoInvestigator, Microbrightfield Inc.) were used to estimate the volume

of the region of interest (ROI) and the total number of immunopositive cells in the ROI. For this estimation, the optical fractionator method in the StereoInvestigator software was used. The optical fractionator estimates the total volume of the ROI using the sectional ROI volume manually traced at x2.5 magnification and known intersection intervals (240µm). To estimate the number of positive cells, the software extrapolates the number of manually counted cells in the areas of chosen size (50 µm x50 µm counting frames placed over grid with chosen size of X: 94.59µm and Y: 182.53 µm) of the ROI selected by systematic random sampling to the sectional volume of the region of interest. A chosen set number of average sampling sites per section was 50, while for each brain, 11 sections between stereotactic coordinates -1.06mm and -3.80 relative to bregma (Franklin and Paxinos, 2012) were included into the optical fractionator analysis. The density of Iba1 and DCX positive cells was calculated by dividing the estimated cell number by the estimated volume of the ROI.

Classification of DCX positive cells by dendritic morphology

The DCX positive cells were visually classified according to the categorization of Plumpe and co-workers (Plümpe et al., 2006). The AB group included cells with no or short plump processes, the CD group included cells with medium length processes without branching, and the EF group comprised cells with long branching dendrite(s) reaching the molecular layer. The density of each type of cells was determined using stereology as described in the previous section.

Quantification of CD68 surface area

For quantification of CD68 staining, digital images were taken using Zeiss Axioimager microscope and Zeiss AxioCam MR Rev3 camera at 40X magnification. Per each brain area (CA1, CA3, DG) identified using the Allen Mouse Brain reference coronal atlas, 1 image was taken from every 2nd section between stereotactic coordinates -1.06mm and -3.80 relative to bregma (Franklin and Paxinos, 2012) to achieve equal intersection intervals (80µm). ImageJ software (Schneider et al., 2012) and macros code were kindly provided by Lianne Hoeijmakers and Dr Aniko Korosi (Center for Neuroscience, Swammerdam Institute for Life Sciences, University of Amsterdam, Amsterdam, the Netherlands) were used to quantify the % surface area immunopositive for CD68.

2.6 Statistical analysis

In Experiment 1 repeated measures two-way ANOVA was used to analyse the timeline of sickness behaviour in the LPS compared to VEH group. Repeated measures one-way ANOVA was used to analyse the timeline of cytokine elevations in the LPS group compared to baseline

levels. Where single measures were taken, two-tailed unpaired t-test was used to analyse the difference between 0.33LPS and VEH groups.

In Experiment 2 repeated measures two-way ANOVA was used to compare mean differences in weight gain, food intake and cytokine levels among treatment groups over weeks of injections. One-way ANOVA was used to compare mean differences in DCX and Iba1 hippocampal cell density among treatment groups.

The Bonferroni multiple comparisons method was applied for post-hoc analyses to determine individual differences between treatment groups and the control group. Normality of distribution within the datasets was confirmed by Kolmogorov-Smirnov test.

3 Results

3.1 Experiment 1: Single LPS exposure

In this experiment, acute and long-term effects of a single exposure to 0.33mg/kg LPS injection were investigated. This dose was chosen as it has been consistently described to induce moderate sickness and depressive-like behaviour in BALB/c mice (Burton et al., 2011; Fenn et al., 2014; Godbout et al., 2007). Firstly, the dynamics of the sickness behaviour and plasma cytokine elevation was investigated following LPS injection over the first hours and days following exposure. For this mice were injected with either 0.33mg/kg LPS or saline (n=12/group) and locomotor activity in the home cage was assessed at baseline (5 min before the injections) and at 2, 4, 48 and 72 hours post injections (for schedule of experimental procedures see Table 17). Body weight change and food intake were assessed at 24, 48 and 72 hours post injections. Immobility in the forced swim test was assessed at 24 and 48 hours post injections. A separate cohort of mice (n=6/group) injected at the same times was used for blood collection at 2, 4, 24 and 48 hours according to the schedule used for sickness behaviour assessment.

Table 17 Schedule of behavioural testing of acute effects in the Experiment 1: Single LPS exposure
8 week old male BALB/cAnNCrl mice were injected with 0.33mg/kg LPS (0.33 LPS) or saline (VEH) i.p. and their locomotion was assessed in their home cages (HC) immediately before the injections (Baseline) and at 2, 4, 48 and 72 hours after the injections according to schedules shown. Immobility in the forced swim test (FST) was also assessed at 24 and 48 hour timepoints post injections.

	Time point	Baseline	2 hours	4 hours	24 hours	48 hours	48 hours	72 hours
ID	GROUP	HC	HC	HC	FST	HC	FST	HC
1	VEH	09:24	11:29	13:30	09:30	09:24	09:30	09:24
2	0.33 LPS	09:34	11:42	13:40	09:40	09:34	09:40	09:34
3	VEH	09:44	11:53	13:50	09:50	09:44	09:50	09:44
4	0.33 LPS	09:54	12:05	14:00	10:00	09:54	10:00	09:54
5	VEH	10:04	12:10	14:10	10:10	10:04	10:10	10:04
6	0.33 LPS	10:14	12:20	14:20	10:20	10:14	10:20	10:14
7	VEH	10:24	12:30	14:30	10:30	10:24	10:30	10:24
8	0.33 LPS	10:34	12:40	14:40	10:40	10:34	10:40	10:34
9	VEH	10:44	12:50	14:50	10:50	10:44	10:50	10:44
10	0.33 LPS	10:54	13:00	15:00	11:00	10:54	11:00	10:54
11	VEH	11:04	13:10	15:10	11:10	11:04	11:10	11:04
12	0.33 LPS	11:14	13:20	15:20	11:20	11:14	11:20	11:14
13	VEH	11:22	13:30	15:30	11:30	11:24	11:30	11:24
14	0.33 LPS	11:35	13:40	15:40	11:40	11:34	11:40	11:34
15	VEH	11:47	13:50	15:50	11:50	11:44	11:50	11:44
16	0.33 LPS	11:59	14:00	16:00	12:00	11:54	12:00	11:54
17	VEH	12:04	14:10	16:10	12:10	12:04	12:10	12:04
18	0.33 LPS	12:14	14:20	16:20	12:20	12:14	12:20	12:14
19	VEH	13:24	15:30	17:30	13:25	13:19	13:25	13:19
20	0.33 LPS	13:34	15:40	17:40	13:35	13:29	13:35	13:29
21	VEH	13:49	15:50	17:50	13:45	13:39	13:45	13:39
22	0.33 LPS	14:04	16:00	18:00	14:00	13:54	14:00	13:54
23	VEH	14:19	16:10	18:10	14:15	14:09	14:15	14:09
24	0.33 LPS	14:34	16:20	18:20	14:30	14:24	14:30	14:24

In the second part of the experiment, long-term consequences of LPS exposure for depressive-like behaviour, HPA axis regulation, plasma cytokine levels and adult hippocampal neurogenesis were studied 8 weeks after injections. For the timeline of the experimental design see Figure 43.

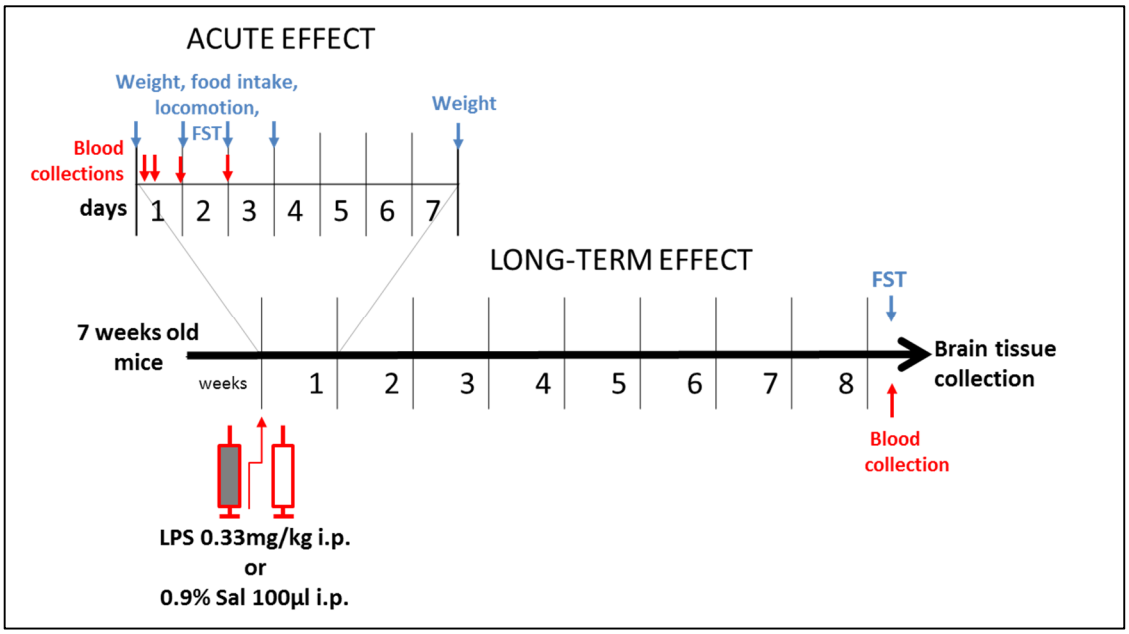

Figure 43 Experimental design of Experiment 1: Single LPS exposure
8 week old male BALB/cAnNCrl mice were injected with 0.33mg/kg LPS (0.33 LPS) or saline (VEH) i.p. (n=12/group) and the dynamics of the sickness behaviour, depression-like behaviour and cytokine response were assessed during the next 7 days (Acute effect) and 8 weeks later (Long-term effect).

3.1.1 Single LPS exposure produces acute sickness behaviour-like response, depressive-like behaviour, and elevation of plasma cytokines levels

The dynamics of sickness behaviour parameters in the first cohort of mice were analysed by repeated measures two-way ANOVA. The results showed that single 0.33 LPS exposure induced weight loss within the first 24 hours, which returned to normal during the next 7 days (Effect of LPS X Time F (4, 88) = 30.24, p<0.0001, Effect of Time F (4, 88) = 25.29, p<0.0001, Effect of LPS F (1, 22) = 2.094, p = 0.162) (see Figure 44A). Single 0.33 LPS exposure also reduced food intake in the first 24 hours after injection which returned to control levels by 48 hours (Effect of LPS X Time F (3, 63) = 6.456, p = 0.0007, Effect of Time F (3, 63) = 11.50, p < 0.0001, Effect of LPS F (2, 125) = 1.555, p = 0.215) (see Figure 44B). Home cage locomotion was reduced in LPS injected group 2 and 4 hours post injection, but returned to normal by 48 hours (Effect of LPS X Time F (4, 32) = 4.316, p = 0.007, Effect of Time F (4, 32) = 2.94, p = 0.035, Effect of LPS F (1, 8) = 9.13, p = 0.017) (see Figure 44C). LPS-exposed mice showed increased immobility in the FST 24 but not 48 hours post injections (Effect of LPS x Time F (1, 22) = 0.044, p = 0.837, Effect of Time F (1, 22) = 0.974, p = 0.334, Effect of LPS F (1, 22) = 6.851, p = 0.016) (see Figure 44D).

The second cohort injected with 0.33 mg/kg LPS (n=6/group) was used to measure plasma cytokine levels at 2, 4, 24 and 48 hours post injections. One-way repeated measures ANOVA of results showed that all 10 cytokines measured were elevated at 2 and 4 hrs time points, but most cytokine levels apart from IL-6 returned to baseline levels at 24hrs (see Figure 44E and

Table 18 for details of statistical analysis). IL-6 was still elevated at this time point, but also returned to baseline by 48 hrs.

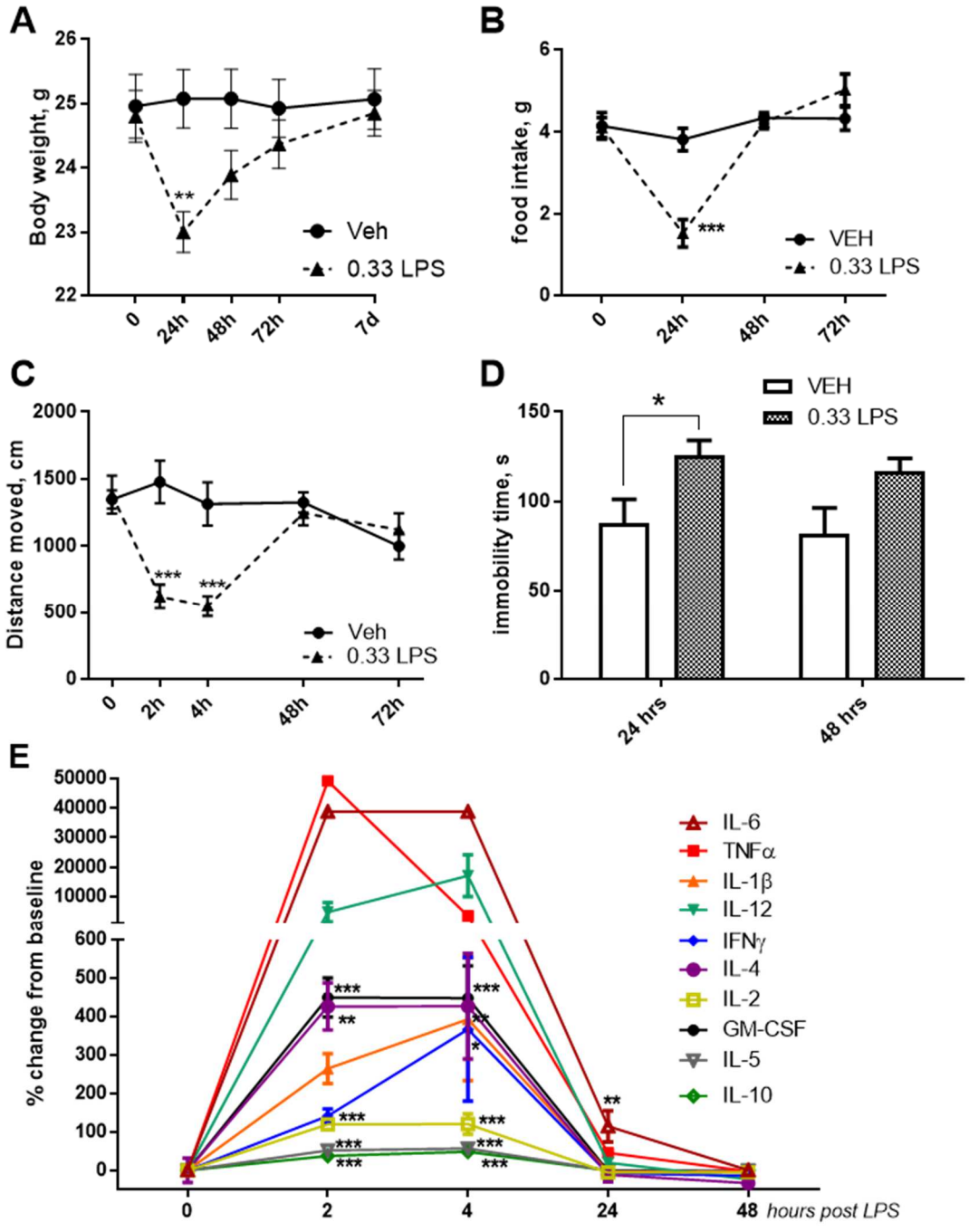

Figure 44 Acute effects of a single LPS exposure

*8 week old male BALB/cAnNCrl mice were injected with 0.33mg/kg LPS (0.33 LPS) or saline (VEH) i.p. (n=12/group) and the dynamics of the sickness behaviour, depression-like behaviour and cytokine response were assessed during the next 3 days. (A)body weight measured at 0, 24, 48 and 72 hours and 7 days following injections (B) Food intake within 24 hours measured at 0, 24, 48 and 72 hours post injections (C) locomotion was assessed in the home cages (HC) at 0, 2, 4, 48 and 72 hours after the injections (D) immobility in the forced swim test (FST) at 24 and 48 hrs post injections; (E) plasma cytokine levels measured at 0, 2, 4, 24 and 48 hours post injection, (measures which were above or below of the sensitivity range of the assay substituted with highest/lowest points of the standard curve for representation; for statistical analysis details see Table 18, n=6, data presented as %change from baseline). Data represents mean±SEM, *p<0.05, **p<0.01, ***p<0.001 derived from post-hoc Bonferroni multiple comparisons test 0.33LPS vs VEH*

Table 18 One-way RM ANOVA and post-hoc Bonferroni multiple comparisons of plasma cytokine measures during first 48 hours post LPS injections.
8 week old male BALB/cAnNCrl mice were injected with 0.33mg/kg LPS (0.33 LPS) or saline (VEH) i.p. (n=6) and peripheral plasma levels of a panel of 10 cytokines were assessed at 0,2, 24 and 48 hours post injections using Luminex technology and data analysed using repeated measures one-way ANOVA as shown in the table

	One-way ANOVA				Bonferroni multiple comparisons			
Cytokine		df	F	p	Baseline, pg/ml	Time points, hrs	Mean, pg/ml	p
IL-6	Between Groups	2	6.341	**.017**	41.2200	2	above range	
	Within Groups	5				4	above range	
	Residual	10				24	88.38	0.2113
	Total	17				48	41.52	> 0.9999
IL-4	Between Groups	4	16.820	**.007**	155.5000	2	817.5000	**.002**
	Within Groups	5				4	818.7000	.082
	Residual	20				24	137.3000	> 0.9999
	Total	29				48	104.0000	> 0.9999
IFN-γ	Between Groups	4	3.914	**.017**	58.0700	2	140.3000	.963
	Within Groups	5				4	270.8000	**.021**
	Residual	20				24	53.3600	> 0.9999
	Total	29				48	50.0200	> 0.9999
IL-12	Between Groups	4	12.250	**.000**	120.5000	2	5820.0000	0.962
	Within Groups	5				4	above range	
	Residual	20				24	144.2000	> 0.9999
	Total	29				48	92.9900	> 0.9999
IL-1β	Between Groups	4	6.948	**.000**	118.4000	2	431.5000	.063
	Within Groups	5				4	583.0000	**0.004**
	Residual	20				24	113.3000	> 0.9999
	Total	29				48	113.4000	> 0.9999
TNFα	Between Groups	4	26.860	**.001**	23.0700	2	above range	
	Within Groups	5				4	819.7000	> 0.9999
	Residual	20				24	33.6100	> 0.9999
	Total	29				48	22.5100	> 0.9999
IL-5	Between Groups	2	21.640	**.003**	32.3800	2	159.5000	**.001**
	Within Groups	5				4	175.4000	**.013**
	Residual	10				24	below range	
	Total	17				48	below range	
IL-2	Between Groups	4	27.900	**.000**	20.1100	2	44.2100	**< 0.0001**
	Within Groups	5				4	44.2400	**< 0.0001**
	Residual	20				24	18.8900	> 0.9999
	Total	29				48	19.0700	> 0.9999
IL-10	Between Groups	2	8.517	**.023**	36.6000	2	102.8000	**.010**
	Within Groups	5				4	131.9000	.056
	Residual	10				24	below range	
	Total	17				48	below range	
GM-CSF	Between Groups	4	38.290	**.000**	20.2300	2	111.1000	**< 0.0001**
	Residual	20				4	110.7000	**< 0.0001**
	Within Groups	5				24	19.8200	> 0.9999
	Total	29				48	19.3900	> 0.9999

3.1.2 Single LPS exposure did not induce long-lasting changes in depressive behaviour, HPA axis and adult hippocampal neurogenesis

Long-term effects of a single LPS exposure was investigated 8 weeks after an injection with 0.33 mg/kg LPS. To assess if the acute effect of LPS on immobility in the FST remained after 8 weeks, FST test was conducted in the long-term cohort, however no difference was observed

between VEH and LPS groups (Student t-test t=0.1013, df=21, p=0.92) (see Figure 45A). Assessment of CORT levels before and after FST also showed that LPS did not have a long-lasting effect on the HPA axis (Effect of LPS x FST F (1, 17) = 0.025, p = 0.876; Effect of LPS F (1, 17) = 0.148, p = 0.706; Effect of FST F (1, 17) = 51.49, p < 0.0001) (see Figure 45B). To measure long-lasting plasma cytokine level changes, plasma was analysed using a 10-plex cytokine assay. However only two cytokines, IL-12 and IL-2, were detectable in the samples, and their were not affected by LPS (IL-12 Student t-test t=0.1298 df=12, p=0.9; IL-2 t=0.6084 df=18, p=0.5 t test) (see Figure 45D). Finally, density of DCX+ neuroblasts in the hippocampal dentate gyrus was analysed using immunohistochemistry. LPS did not significantly affect the level of DCX+ cells, but a trend towards increase (Student t-test t=2.051, df=9, p=0.07) was observed in the LPS-exposed group (see Figure 45C).

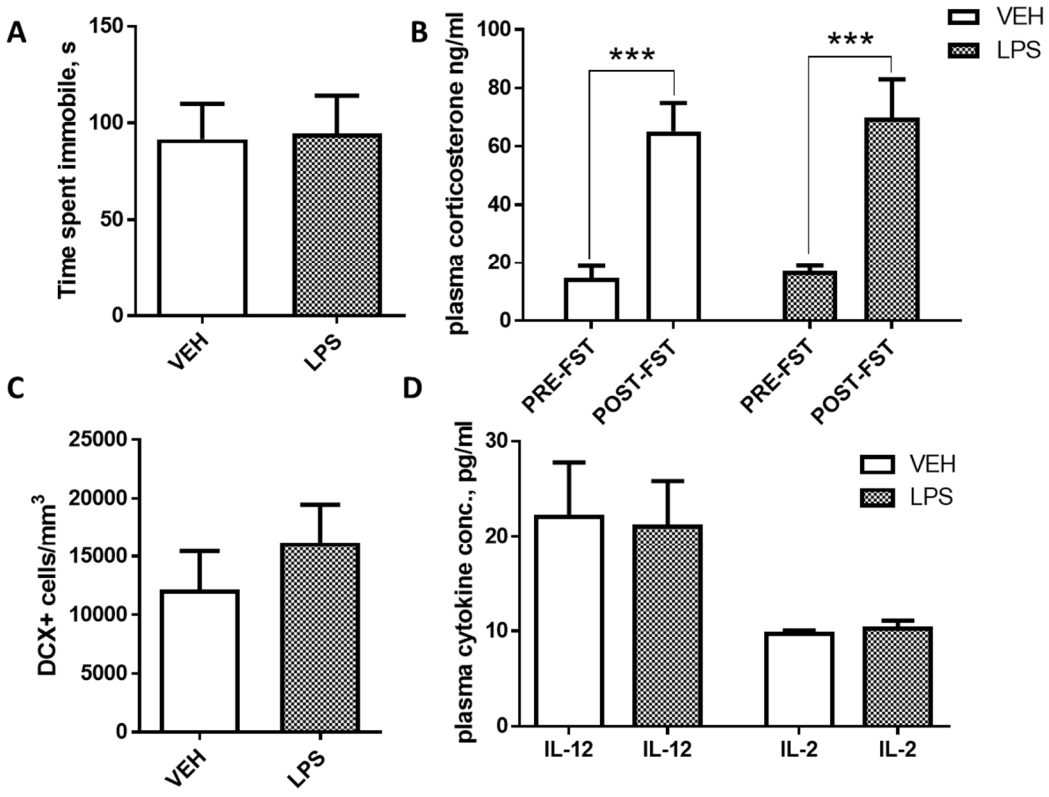

Figure 45 Long-term effects of a single LPS exposure
*8 week old male BALB/cAnNCrl mice were injected with 0.33mg/kg LPS (0.33 LPS) or saline (VEH) i.p. (n=12/group) and long-term effects of a single exposure to 0.33 mg/kg were investigated 7 weeks later (A) LPS did not have a long-term effect on immobility in the forced swim test (FST) (B) LPS did not have a long-term effect on baseline and post-FST CORT levels, ***p<0.001 derived from Bonferroni multiple comparisons VEH vs LPS (C) the density of DCX+ cells, n=6/group (D) plasma leves of 2 out of 10 cytokines which could be detected in the Luminex assay, IL-2 and IL-12, n=6/group*

3.1.3 Discussion of Experiment 1 results

Thus this experiment showed that injection with 0.33mg/kg of LPS induces strong but transient response which included components of sickness behaviour, such as decreased locomotor

activity, food intake and weight loss. However most of these parameters returned to normal within 3 days. LPS exposure also stimulated a significant elevation of plasma cytokines levels in the first hours after injection, with the majority of cytokines returning to baseline levels at 24 hrs post-injection. Yet at this time point LPS-exposed mice showed increased immobility in the FST, a behavioural change commonly interpreted as depression-like behavioural despair. However, 24 hours later (48 hours after injections) this effect was no longer significant, although a strong trend towards reduced immobility remained in LPS exposed group. An assessment of the long-term effects of the single LPS injection showed that no behavioural despair was present in exposed mice 8 weeks later. Also single LPS exposure did not have any long-lasting effects on neurobiological parameters relevant for depression, such as plasma CORT levels, CORT response to acute stress and the level of neuronal differentiation in the hippocampal dentate gyrus. In addition, no plasma cytokine level changes were detected at this time point. Taken together, this data showed that single injections with 0.33 mg/kg LPS can stimulate transient sickness behaviour and plasma cytokine changes, but do not induce any long-term effects on depression-related behaviour and neurobiology. Therefore, its use in modelling chronic immune system activation described in depressed patients and its potential behavioural and neurobiological consequences is limited by the short lifespan of its effects. These findings prompted the need to develop a mode of injections which would better model chronic inflammatory-like changes observed in depression.

3.2 Experiment 2: Repeated LPS exposure

The aim of Experiment 2 was to develop a protocol to induce long-lasting effects on immune and central nervous systems, which would make it suitable for studying the biological processes mediating depression and the role of the immune system in mood disorders.

To develop such a protocol, we tested two different models of repeated LPS injections compared to a single injection of a relatively high dose of 0.83mg/kg LPS (single LPS group), a dose which has already been utilised in a model of depression (Painsipp et al., 2011). As repeated LPS injections are known to induce tolerance to LPS, several measures were taken to avoid its development: a weekly interval between injections was included to allow for immune system recovery; a relatively low dose 0.1 mg/kg of LPS was used in 0.1 LPS group; a weekly increment from initial 0.33 mg/kg to a final 0.83 mg/kg dose was used in the escalating LPS (0.33-0.83) group as dose increase has been shown to avoid habituation of immune response (Wickens et al., 2014). Sickness behaviour, plasma cytokine profile, and the state of adult hippocampal neurogenesis and microglial activation in the hippocampus were assessed weekly or at the end of six weekly injections in each group, compared to a control group injected with saline (SAL).

Sibling pairs were randomly assigned to one of the 4 treatment groups, which received the following intraperitoneal (i.p.) injections once a week for 6 weeks: Control group (SAL; N=10), received 100 µL of 0.9% saline each week; 0.1 LPS group (N=8), received 0.1mg/kg of LPS each week; escalating LPS (0.33-0.83) group (N=8), received 0.33 mg/kg of LPS on weeks 1 and 2, 0.53 mg/kg of LPS on week 3, 0.63 mg/kg on week 4, 0.73 mg/kg on week 5, 0.83 mg/kg on week 6; single LPS group (N=8), received 0.83 mg/kg on week 1, and 100 µL saline on weeks 2-6. For an overview of experimental design see Figure 46.

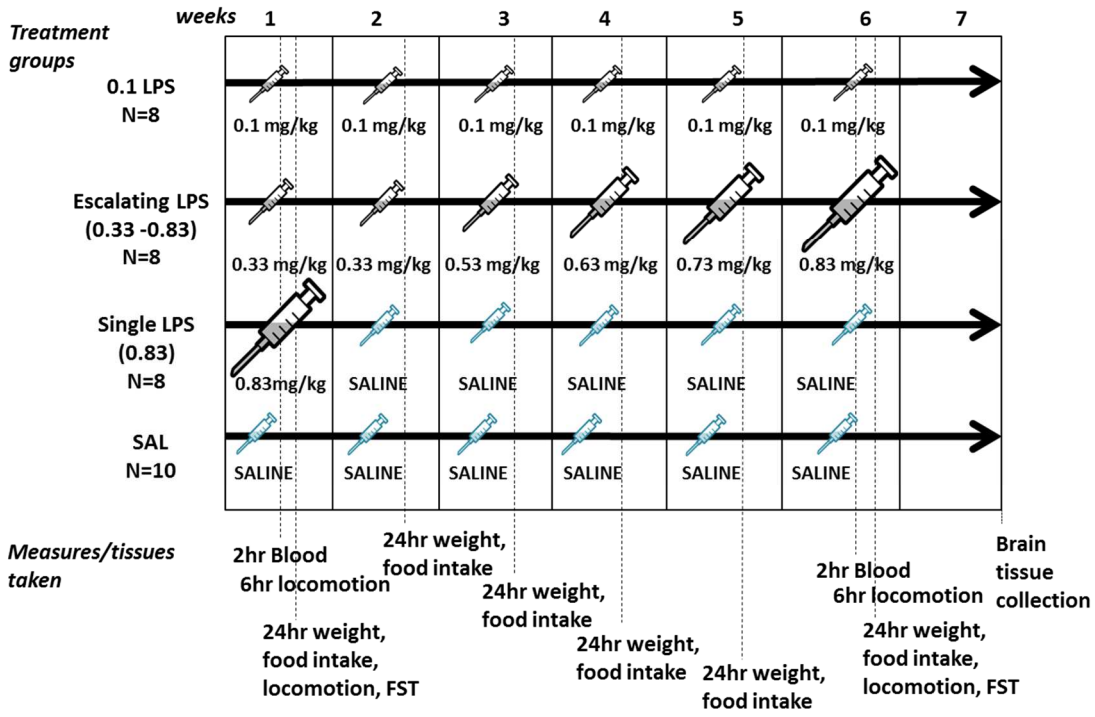

Figure 46 Experimental design of Experiment 2: Repeated LPS exposure
8 week old male BALB/cAnNCrl mice were injected with LPS or saline i.p. once a week for 6 weeks . Experimental conditions included: 0.1 LPS group injected with 0.1 mg/kg LPS once weekly; Escalating LPS group injected with 0.33mg/kg on weeks 1 and 2, 0.53mg/kg on week 3, 0.63 mg/kg on week 4, 0.73 mg/kg on week 5 and 0.83 mg/kg on week 6; Single LPS group injected with 0.83 mg/kg on week 1 and Saline on weeks 2-6; SAL group was injected weekly with 0.9% saline solution. Blood was collected 2 hours after LPS injections on weeks 1 and 6; locomotion was measured 6 hours after LPS injections on weeks 1 and 6; weight change and food intake were measured during a 24-hour period after the LPS injections

3.2.1 Repeated LPS injections induced sickness behaviour each week for 6 weeks

Body weight change and food intake were measured 24 hours after LPS injections to assess the suppressant effects of the sickness behaviour response on feeding (Biesmans et al., 2013). Both the dose and chronicity of LPS affected the change in weight gain and food intake (see Figure 47 and Table 19)

Table 19 Two-way repeated measures ANOVA outcomes for weight gain and food intake measures taken each week 24hrs after either LPS or saline injections for six weeks.
8 week old male BALB/cAnNCrl mice were injected with LPS or saline i.p. once a week for 6 weeks. Experimental conditions (n=8-10/group) included: 0.1 LPS group injected with 0.1 mg/kg LPS once weekly; Escalating (0.33-0.83) LPS group injected with 0.33mg/kg on weeks 1 and 2, 0.53mg/kg on week 3, 0.63 mg/kg on week 4, 0.73 mg/kg on week 5 and 0.83 mg/kg on week 6; Single LPS group injected with 0.83 mg/kg on week 1 and saline on weeks 2-6; SAL group was injected weekly with 0.9% saline solution.

Factor	Effect size (% of total variation)	F	DF	DF Residual	p
Weight gain					
Dose	12.33	24.66	3	30	< 0.0001
Time	18.36	11.29	5	150	< 0.0001
Interaction	16.3	3.341	15	150	< 0.0001
Food intake					
Dose	34.45	24.6	3	13	< 0.0001
Time	13.92	11.04	5	65	< 0.0001
Interaction	30.74	8.122	15	65	< 0.0001

On week 1, LPS treated animals showed significantly reduced body weight gain and/or reduced food intake compared to the saline control group, with the magnitude of effect dependant on the dose of LPS injected (see Figure 47). On week 2, only the 0.1 LPS group had a significant reduction in body weight gain. There was no significant difference in body weight gain in any LPS groups at week 3 but from week 4 through to 6, there was a significant, reduction in body weight gain in the group receiving escalating doses (0.33-0.83) of LPS. The effect of LPS on food intake remained significant each subsequent week for the escalating LPS (0.33-0.83) group, while 0.1 LPS group displayed a significant reduction again only on the 6th week. Locomotor activity also was assessed in the open field arena 6 hours after the LPS or saline injections on week 1 and week 6. On week 1, the escalating (0.33-0.83) LPS group displayed statistically significant hypolocomotion (effect of dose $F(3,28)=3.19$, $p=0.039$), but on week 6 the reduction in locomotor activity did not reach significance in comparison with SAL group (effect of dose $F(2,23)=1.6$, $p=0.22$, Figure 47C).

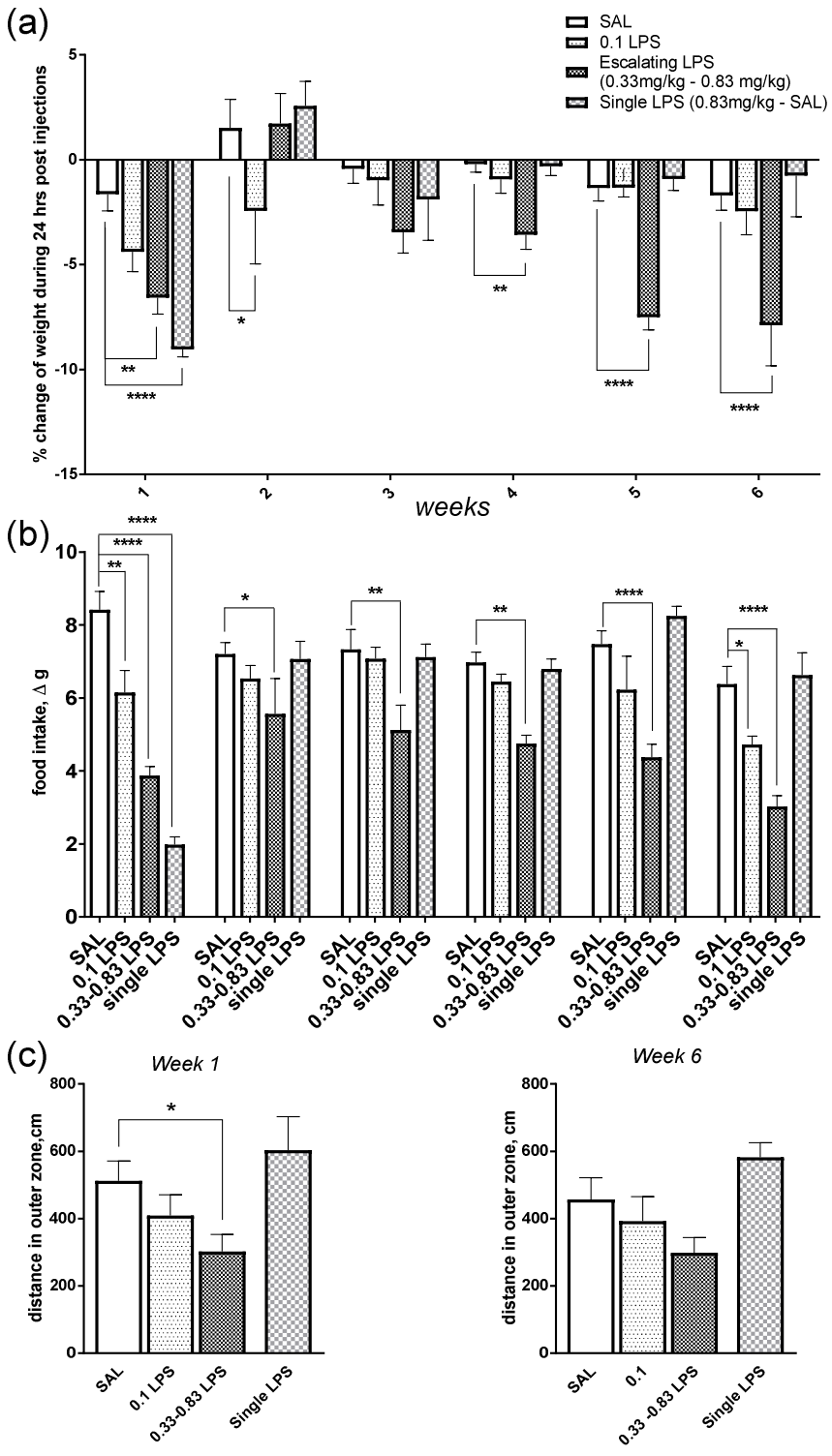

Figure 47 Short-term sickness behaviour induced by weekly LPS injections

*8 week old male BALB/cAnNCrl mice were injected with LPS or saline i.p. once a week for 6 weeks. Experimental conditions included: 0.1 LPS group injected with 0.1 mg/kg LPS once weekly; Escalating LPS group injected with 0.33mg/kg on weeks 1 and 2, 0.53mg/kg on week 3, 0.63 mg/kg on week 4, 0.73 mg/kg on week 5 and 0.83 mg/kg on week 6; Single LPS group injected with 0.83 mg/kg on week 1 and saline on weeks 2-6; SAL group was injected weekly with 0.9% saline solution (a) Weight change measured during first 24hrs after injections each week expressed as % change from a baseline measured immediately before the LPS injections. (b) Food intake during first 24hrs after weekly injections. (c) locomotor activity on weeks 1 and 6 measured 6hrs after LPS or SAL injections in the open field arena; p values derived from Bonferroni multiple comparisons test SAL vs 0.1LPS/Escalating LPS/Single LPS, *p<0.05, **p<0.01, ***p<0.001, ****p<0.0001. Data represents mean±SEM, n=8-10/group.*

3.2.2 Depressive-like behaviour diminished on week 6 in the Escalating LPS (0.33-0.83) group

As 0.33-0.83 LPS group showed sustained sickness behaviour across the 6 weeks, in a separate cohort (N=10/group) of mice depressive-like behaviour in the FST was investigated on weeks 1 and 6, 24 hrs after injections to assess the influence of repeated exposure on the development of behavioural despair. Repeated measures 2-way ANOVA of results showed that LPS injection on week 1 induced increase in immobility, while on week 6 the difference between 0.33-0.83 LPS and SAL was no longer significant, although a trend towards increased immobility was still present in LPS-exposed group(Effect of Week X Dose F (1, 18) = 0.802, p=0.382; Effect of Week F (1, 18) = 6.866, p = 0.017; Effect of LPS F (1, 18) = 9.448, p = 0.007 (see Figure 48A). Locomotion in the open field arena did not differ between groups at both timepoints although was affected by week of inejctions (Week X Dose effect F (1, 36) = 7.38; p = 0.01, Effect of Week F (1, 36) = 8.66, p = 0.006; Effect of LPS F (1, 36) = 2.76, p = 0.105 (see Figure 48B).

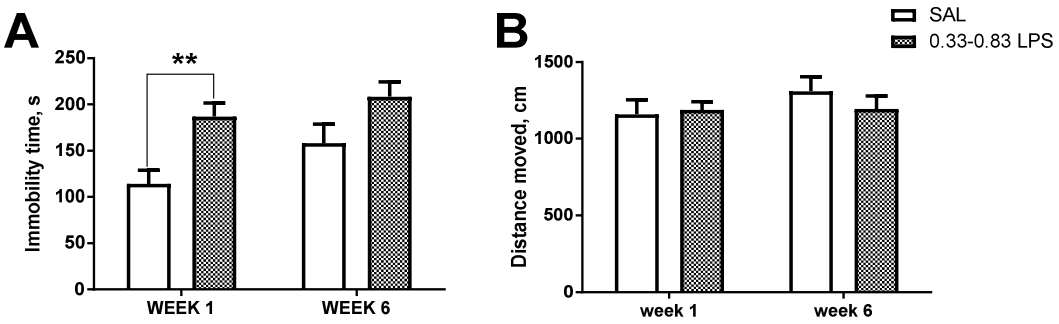

Figure 48 FST Immobility and locomotion in the Escalating LPS (0.33-0.83) group on weeks 1 and 6
*8 week old male BALB/cAnNCrl mice were injected with LPS or saline i.p. once a week for 6 weeks (n=8). FST was performed on week 1 and 6 24 hours after injections in 0.33-0.83 LPS group injected with LPS at a dose escalating from 0.33mg/kg to 0.83 mg/kg weekly and SAL group injected with saline (A) Immobility in the FST performed 24 hrs after injections (B) Locomotion in the open field arena measured at the same time point. Data represents mean±SEM, *p<0.05, **p<0.01, ***p<0.001 derived from post-hoc Bonferroni multiple comparisons SAL vs 0.33-0.83 LPS*

3.2.3 Repeated exposure modified cytokine response to LPS challenge

To detect systemic cytokine response to LPS challenge, selected cytokines were measured in the peripheral blood collected 2hrs after injection on weeks 1 and 6. The time point of blood collection was chosen based on previous studies which showed that in mice exposed to LPS blood levels of most cytokines peak within the first two hours after exposure and subside at later time points (Biesmans et al., 2013; Browne et al., 2012). Animals responded to acute LPS exposure on week 1 with a profound elevation of pro-inflammatory cytokines IL-6 and TNFα. More specifically, IL-6 was elevated up to 700 fold compared to control levels depending on the dose of LPS injected, while TNFα showed elevations in the range of 20 to 35 fold (see

Figure 49 and Table 20). Interestingly, some other cytokines and inflammatory markers were not elevated at this time point, including CRP, IL-5 and IL-2, while others did not reach detection levels of the assay used (IL-4, IFNγ, IL-1β). IL-10 showed an elevation on week 1, which reached significance in the escalating LPS (0.33-0.83) and single LPS groups. GM-CSF also significantly increased in response to all doses of LPS on week 1. In response to the 6th injection the elevation of IL-6 and particularly TNFα was much reduced compare to week 1. However, the levels of these pro-inflammatory cytokines were still over 570 fold (IL-6) and over 9 fold (TNFα) increased in the escalating LPS (0.33-0.83) group compared to levels observed in the control group (see Figure 49). In contrast, IL-2 was over 4 fold elevated exclusively in response to the escalating LPS (0.33-0.83) group, accompanied by an increase in GM-CSF levels in this group even more robust than on week 1 (20-fold on week 1 vs 30-fold on week 6). Interestingly, CRP was 0.44 fold decreased compared to control in response to the final LPS dose in the escalating LPS (0.33-0.83) group. Moreover, when the cytokine levels were measured in the cardiac blood collected 7 days after the last injection, it appeared that CRP was decreased in all LPS-injected animals compared to control group, including the single LPS group (see Figure 49). No other cytokines were detected at this time point.

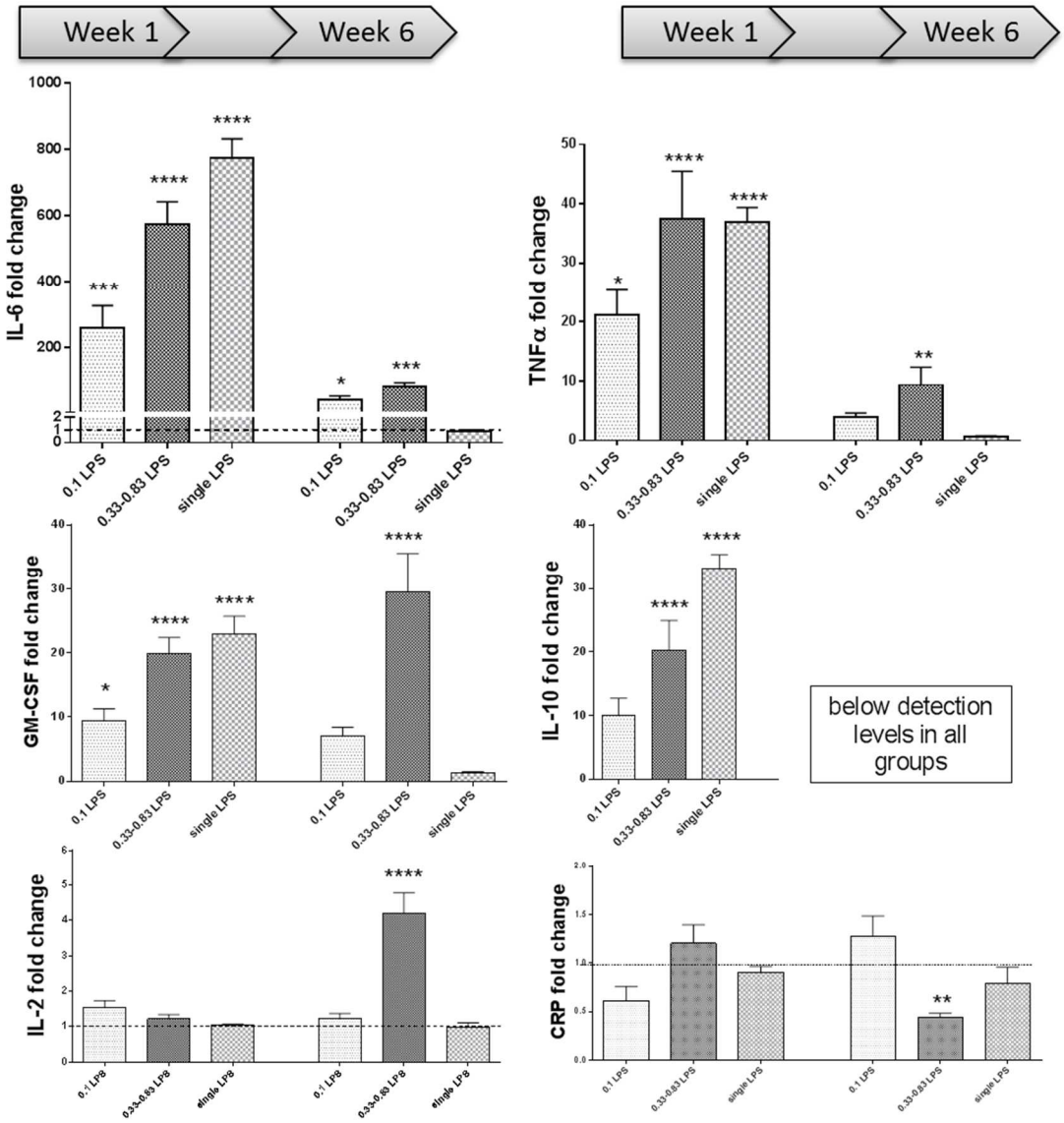

Figure 49 Plasma cytokine profile in response to LPS injections 2hrs after exposure on weeks one and six.
*8 week old male BALB/cAnNCrl mice were injected with LPS or saline i.p. once a week for 6 weeks. Experimental conditions included: 0.1 LPS group injected with 0.1 mg/kg LPS once weekly; Escalating LPS group injected with 0.33mg/kg on weeks 1 and 2, 0.53mg/kg on week 3, 0.63 mg/kg on week 4, 0.73 mg/kg on week 5 and 0.83 mg/kg on week 6; Single LPS group injected with 0.83 mg/kg on week 1 and saline on weeks 2-6; SAL group was injected weekly with 0.9% saline solution. Data shown as percentage change from control (SAL). P values derived from Bonferroni multiple comparisons test SAL vs 0.1LPS/Escalating LPS/Single LPS, *p<0.05, **p<0.01, ***p<0.001 compared to the SAL control group. Data represents mean±SEM, n=8-10/group.*

Table 20 One-way ANOVA and post-hoc Bonferroni multiple comparisons of plasma cytokine measures taken 2hrs after LPS/SAL exposure on weeks one and six.
8 week old male BALB/cAnNCrl mice were injected with LPS or saline i.p. once a week for 6 weeks. Experimental conditions (n=8-10/group) included: 0.1 LPS group injected with 0.1 mg/kg LPS once weekly; Escalating (0.33-0.83) LPS group injected with 0.33mg/kg on weeks 1 and 2, 0.53mg/kg on week 3, 0.63 mg/kg on week 4, 0.73 mg/kg on week 5 and 0.83 mg/kg on week 6; Single LPS group injected with 0.83 mg/kg on week 1 and Saline on weeks 2-6; SAL group was injected weekly with 0.9% saline solution.

	One-way ANOVA				Bonferroni multiple comparisons			
Cytokine_week		df	F	p	SAL group mean, pg/ml	LPS groups	Mean, pg/ml	p
IL-6_w1	Between Groups	3	43.400	**.000**	52.1680	0.1LPS	13517.7875	**.008**
	Within Groups	30				0.33-0.83 LPS	29908.7500	**.000**
	Total	33				Single LPS	40395.0000	**.000**
IL-6_w6	Between Groups	3	23.003	**.000**	65.1300	0.1LPS	2749.1429	**.039**
	Within Groups	28				0.33-0.83 LPS	5292.8750	**.000**
	Total	31				Single LPS	58.7529	1.000
TNFα_w1	Between Groups	3	14.457	**.000**	14.5209	0.1LPS	125.1339	**.032**
	Within Groups	30				0.33-0.83 LPS	221.6500	**.000**
	Total	33				Single LPS	218.5625	**.000**
TNFα_w6	Between Groups	3	6.953	**.001**	7.9657	0.1LPS	31.2271	1.000
	Within Groups	28				0.33-0.83 LPS	74.4538	**.002**
	Total	31				Single LPS	5.4520	1.000
CRP_w1	Between Groups	3	1.470	.242	87759.0000	0.1LPS	112317.5000	
	Within Groups	30				0.33-0.83 LPS	105770.0000	
	Total	33				Single LPS	79503.7500	
CRP_w6	Between Groups	3	4.857	**.008**	90505.0000	0.1LPS	55210.0000	.124
	Within Groups	28				0.33-0.83 LPS	40051.2500	**.006**
	Total	31				Single LPS	71444.2857	1.000
GM-CSF_w1	Between Groups	3	27.083	**.000**	1.7687	0.1LPS	16.7850	**.024**
	Within Groups	30				0.33-0.83 LPS	35.1038	**.000**
	Total	33				Single LPS	40.4513	**.000**
GM-CSF_w6	Between Groups	3	20.109	**.000**	1.7108	0.1LPS	12.0094	1.000
	Within Groups	28				0.33-0.83 LPS	50.5975	**.000**
	Total	31				Single LPS	2.1879	1.000
IL-2_w1	Between Groups	3	1.251	.309	15.0474	0.1LPS	18.3475	
	Within Groups	30				0.33-0.83 LPS	18.3050	
	Total	33				Single LPS	15.6600	
IL-2_w6	Between Groups	3	24.972	**.000**	17.9410	0.1LPS	27.6700	1.000
	Within Groups	28				0.33-0.83 LPS	75.3138	**.000**
	Total	31				Single LPS	17.6369	1.000
IL-10_w1	Between Groups	3	26.273	**.000**	8.2000	0.1LPS	81.4938	.151
	Within Groups	30				0.33-0.83 LPS	165.9275	**.000**
	Total	33				Single LPS	272.3875	**.000**
IL-5_w1	Between Groups	3	1.259	0.306	27.3370	0.1LPS	31.7650	
	Within Groups	30				0.33-0.83 LPS	32.4338	
	Total	33				Single LPS	29.9950	
IL-5_w6	Between Groups	3	1.336	0.283	28.0840	0.1LPS	30.1771	
	Within Groups	28				0.33-0.83 LPS	32.9788	
	Total	31				Single LPS	29.5943	

3.2.4 Hippocampal microglia was not affected by LPS exposure

The estimation of the number of Iba1 positive cells in neurogenic granular zone of the dentate gyrus, as well as in the whole hippocampus showed that the number of microglia was not altered in long term (7 days later) by LPS injections (Kruskal-Wallis one-way anova Effect of

treatment F(3,20)=0.45,p=0.72, see Fig.4A). The level of microglial activation was assessed by the density of CD68-positive puncta in the tissue. One-way ANOVA of results showed that LPS exposure did not have a long-term effect on microglial activation in any of the areas analysed (DG (F (3, 25) = 4.783, p = 0.009, CA1 F (3, 25) = 2.209, p = 0.112 and CA3 F (3, 25) = 2.918, p = 0.054 (see Figure 50B). Additionally, we investigated whether systemic LPS exposure affected the level of plasma corticosterone. For this purpose blood was collected via cardiac puncture 7 days after the last LPS injections as described in Methods section 2.4. High individual variability was observed in the systemic corticosterone levels and no statistical difference was detected among mean group levels by one-way ANOVA (F (3, 25) = 0.371, p = 0.775 (see Figure 50C).

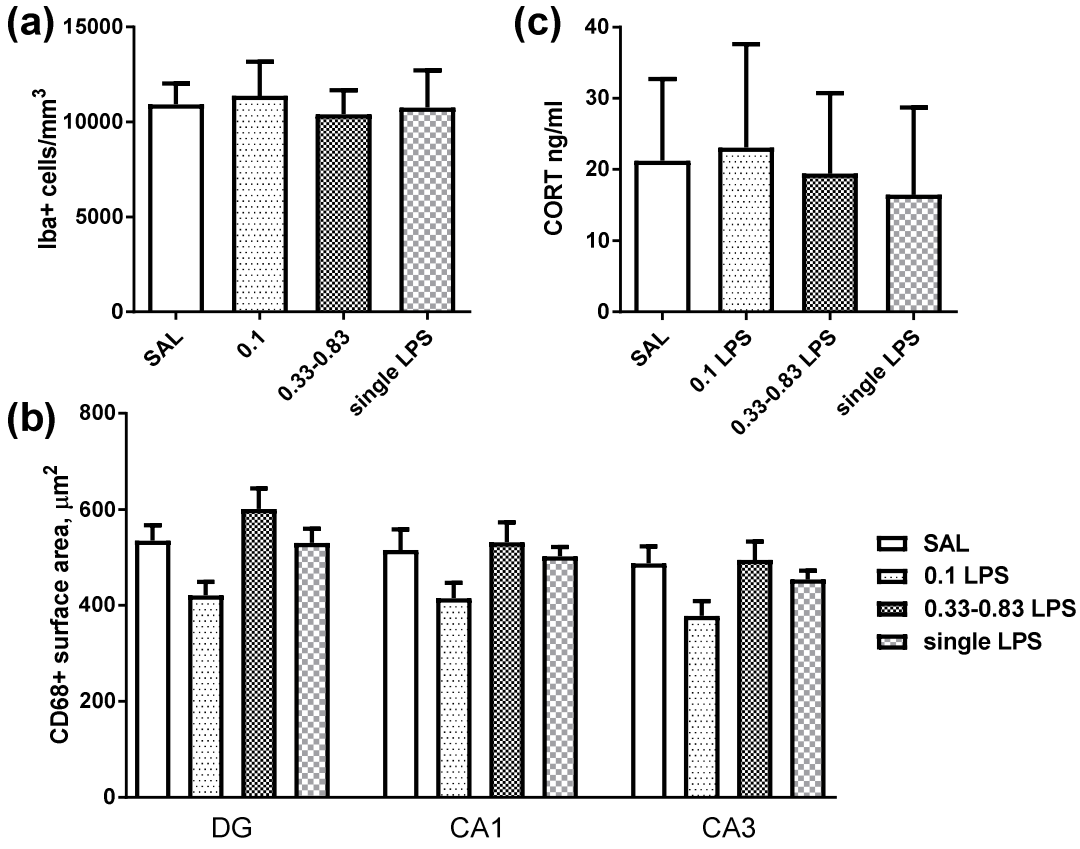

Figure 50 Hippocampal microglia and corticosterone levels in mice exposed to chronic LPS/SAL injections. 8 week old male BALB/cAnNCrl mice were injected with LPS or saline i.p. once a week for 6 weeks. Experimental conditions (n=8-10/group) included: 0.1 LPS group injected with 0.1 mg/kg LPS once weekly; Escalating (0.33-0.83) LPS group injected with 0.33mg/kg on weeks 1 and 2, 0.53mg/kg on week 3, 0.63 mg/kg on week 4, 0.73 mg/kg on week 5 and 0.83 mg/kg on week 6; Single LPS group injected with 0.83 mg/kg on week 1 and saline on weeks 2-6; SAL group was injected weekly with 0.9% saline solution. (a) Number of Iba1 positive cells in the dentate gyrus of the hippocampus was unaffected by LPS exposure, ns (b) CD68 positive surface area, detected in images taken from different regions of the hippocampus, also was unchanged by LPS exposure (DG – dentate gyrus, CA1 and CA3 – Cornu Ammonis areas), ns (c) Corticosterone levels detected in the cardiac blood 7 days after last LPS injections. Data represents mean±SEM.

3.2.5 LPS injections affected the number of postmitotic immature neurons in the hippocampal dentate gyrus.

One-way ANOVA of Ki67-positive cell density showed that in the tissue collected 7 days after the last injections, the level of proliferating Ki67 positive cells was not altered ($F(3, 22) = 0.146$, $p=0.931$ (see Figure 51A). Also, it showed that the density of DCX positive immature neurons was also not affected by LPS injections according to the One-way ANOVA ($F(3, 26) = 1.862$, $p = 0.161$). However, weekly LPS injections affected the number of "EF" type postmitotic DCX positive neurons (Effect of treatment $F(3,26) =15.46$, $p<0.0001$, RM one-way ANOVA). The density of other morphological types was not affected by treatment (Type AB $F(3, 26) = 1.845$, $p=0.164$, type CD $F(3, 26) = 0.67$, $p=0.579$, RM one-way ANOVA) (see Figure 51B for representative microphotographs and Figure 51C for data analysis).

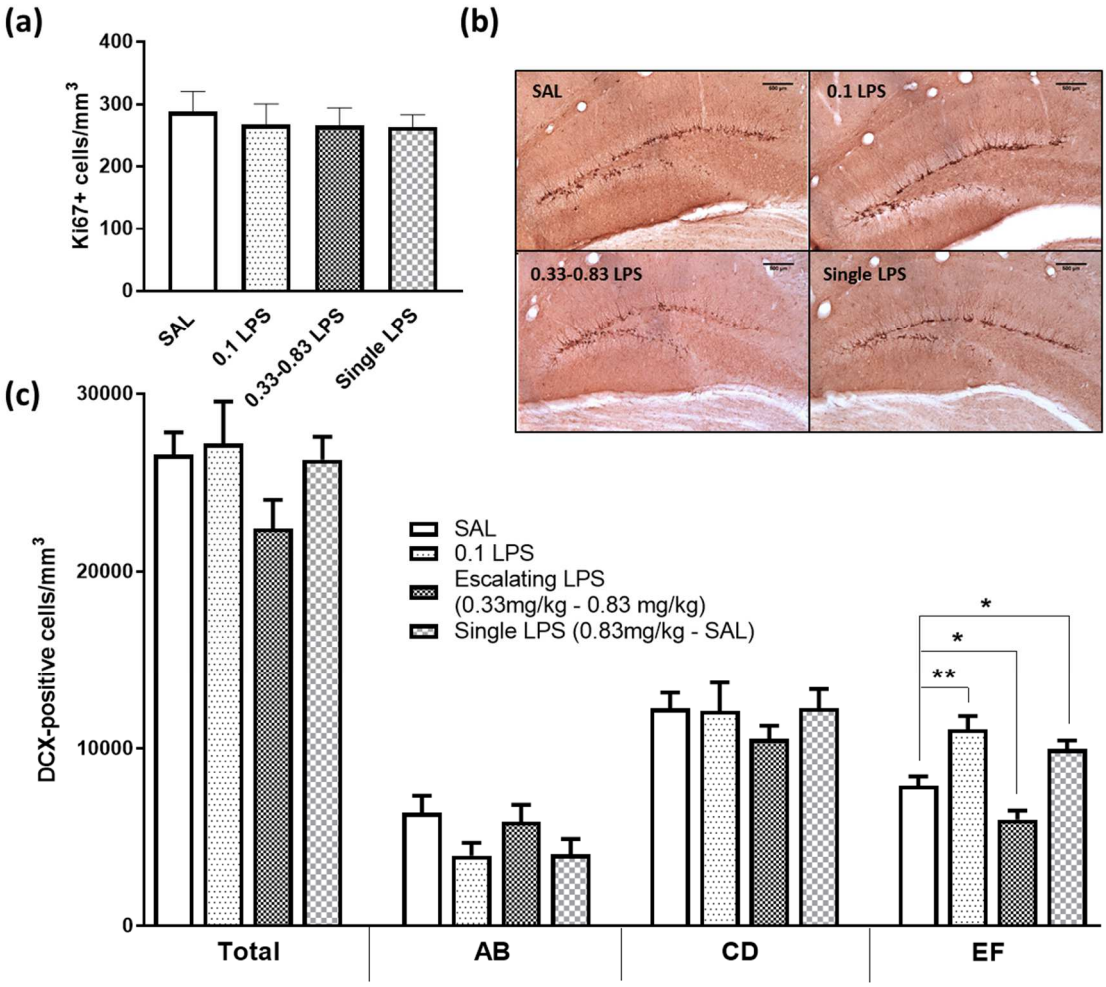

Figure 51 Adult hippocampal neurogenesis in the LPS-exposed animals
*8 week old male BALB/cAnNCrl mice were injected with LPS or saline i.p. once a week for 6 weeks. Experimental conditions (n=8-10/group) included: 0.1 LPS group injected with 0.1 mg/kg LPS once weekly; Escalating (0.33-0.83) LPS group injected with 0.33mg/kg on weeks 1 and 2, 0.53mg/kg on week 3, 0.63 mg/kg on week 4, 0.73 mg/kg on week 5 and 0.83 mg/kg on week 6; Single LPS group injected with 0.83 mg/kg on week 1 and saline on weeks 2-6; SAL group was injected weekly with 0.9% saline solution. (a) Number of proliferating Ki67 positive cells in the dentate gyrus of the hippocampus was unchanged by LPS injections, ns (b) Representative micrographs of DG show DCX+ cells with their dendritic trees (in dark-brown), scale bar = 500 µm (c) Total number of DCX+ cells was not significantly changed by LPS injections; DCX+ cells were then classified according to their dendritic morphology: AB – no or short dendrites, CD – medium length dendrites without branching; EF – long branching dendrites reaching the molecular layer. Data represents mean±SEM; P values derived from Bonferroni multiple comparisons test SAL vs 0.1LPS/Escalating LPS/Single LPS, *p<0.05, **p<0.01*

3.2.6 Discussion of Experiment 2 results

This experiment showed that systemic exposure to escalating dose of LPS administered once a week for 6 weeks repeatedly induced main aspects of sickness behaviour, such as reduced food intake and weight gain. The significance of this finding stems from previous studies which show that LPS tolerance manifests with a reduction of sickness behaviour, such as absence of reduced food intake or hypolocomotion (Banasikowski et al., 2015). In contrast, the effect induced by the repeated 0.1 mg/kg LPS dose was present only intermittently, while a single injection of 0.83 mg/kg of LPS did not induce any long-lasting effect on behavioural parameters studied. However, locomotor activity data suggests that hypolocomotion displayed in the

escalating LPS (0.33-0.83) group on week 1 was absent on week 6. It is important to note that locomotor activity data was collected in a novel environment of an open field test arena 6 hours after injections. Such comparatively late timing of assessment and repeated (second) exposure to the arena could have affected the outcome of this test. Equally, this data could indicate that a degree of tolerance in the effect of LPS on locomotor activity developed following repeated LPS challenge. However the presence of reduced food intake and weight loss at this time point suggests that if indeed present, this apparent tolerance was not substantial enough to affect all aspects of sickness behaviour response. Nonetheless, a loss of significant difference in depressive-like behaviour from week 1 to week 6 showed that the escalating dose of LPS was not sufficient to maintain depression-like state in exposed mice.

Assessment of peripheral cytokine levels in response to LPS showed that chronic exposure to escalating LPS doses induced a distinct cytokine profile, while single and low dose of LPS did not induce any long-lasting changes in the blood cytokine levels. In naïve animals LPS injections induced elevation of pro-inflammatory cytokines, such as IL-6, TNFα, GM-CSF and anti-inflammatory IL-10. Chronic injections with the escalating dose induced a rather distinct profile of cytokine response. On week 6, IL-6 and TNFα remained elevated, but the magnitude of effect was reduced. While this finding might suggest a certain degree of developing tolerance, a moderate elevation of these cytokines is in fact even more relevant for modelling depression, as depressed patients usually present with small elevation of IL-6 and TNFα levels (Dowlati et al., 2010). Surprisingly, some cytokines were modulated exclusively by chronic exposure. CRP was unchanged on week 1 in all groups but reduced in escalating LPS (0.33-0.83) group on week 6. As CRP is an acute-phase protein and is commonly used as a biomarker of inflammation, its reduction after 6 weeks might be suggestive of an increase in the anti-inflammatory state of the immune system, perhaps in response to the large increase in pro-inflammatory mediators observed on week 1. Subsequently this anti-inflammatory state may have been responsible for the reduction in pro-inflammatory markers observed at week 6. Interestingly IL-2 and GM-CSF appeared to be elevated by chronic exposure, with IL-2 being exclusively modulated by escalating LPS. IL-2 is known for its ability to stimulate proliferation of T-cells (Lemoine et al., 2009). IL-2 signalling has been shown to play an important role in the regulation of effector and regulator T-cells functioning, and its anti-autoimmune properties are currently being tested in the treatment of some autoimmune diseases (Bayer et al., 2013). GM-CSF stimulates proliferation of many leukocytes including macrophages and dendritic cells, as well as differentiation and immune response of T-cells, and has been historically considered to be a pro-inflammatory cytokine (Shi et al., 2006). The increase of these two cytokines in response to chronic injections may reflect an alternative state of immune system activation,

distinct from the conventional response to single LPS exposure. Of particular importance is the absence of an elevation in the anti-inflammatory IL-10 on week 6, as anti-inflammatory IL-10 upregulation has been implicated in a classical endotoxin tolerance (Biswas and Lopez-Collazo, 2009). Therefore, while this alternative profile possesses some features of supressed immune response, such as attenuated IL-6 and TNFα elevations and decrease in CRP levels, it does not fully resemble the previously described endotoxin tolerance. For example, a previous study which induced LPS tolerance in rats by way of repeated injections showed that blood levels of IL-6 and TNFα were at control levels 2 hours after an injection of 32mg/kg of LPS (Chen et al., 2005). This substantially differs from the data in my study were a much lower dose still induced a significant elevation of these cytokines in the blood. Another aspect of the cytokine profile described above which differs from previous studies of LPS tolerance is the absence of elevation of the anti-inflammatory IL-10, as for example has been shown previously in a mouse model of tolerance induced by intraplantar injection of LPS prior to intravenous challenge with 0.35mg/kg (Bosnar et al., 2013). Next the elevation of IL-2 observed in escalating LPS group has been previously associated with a mutation in NF-kB pathway enzyme A20 which led to a 100% mortality of mutant mice in response to a challenge with 10mg/kg LPS, a dose which did not induce deaths in wild type mice (Xuan et al., 2015). These differences between the cytokine profile of escalating LPS group and cytokine response previously described in LPS tolerance studies suggest a distinct state of the immune system induced by escalating dose LPS injections.

Elevation of IL-2 is of particular importance as IL-2 has been previously implicated in psychiatric conditions, including depression. Maes et al. (1995) found that depressed patients have elevated plasma levels of soluble IL-2 receptor, and later a consensus paper of the World Federation of Societies of Biological Psychiatry included soluble serum IL-2 receptor elevation into the list of depression biomarkers (Mössner et al., 2007). This status was not subsequently confirmed in the later meta-analysis mainly due to appearance of a number of studies showing the opposite change in IL-2 levels (Dowlati et al., 2010). However more recent reports show elevation of IL-2 levels in the blood of bipolar patients during a manic episode (Brietzke et al., 2009), as well as in chronic obstructive pulmonary disease patients with comorbid depression (Rybka et al., 2016). The involvement of IL-2 activation in psychopathology is further confirmed by the observation that IL-2 therapy in cancer patients is capable of inducing neuropsychiatric toxicity (Kammula et al., 1998). Interestingly, single 0.83 mg/kg dose did not induce any long-lasting changes in the cytokine levels albeit this dose inducing long-lasting depression-like behaviour in a previous study (Painsipp et al., 2011). However, it is important to note that plasma cytokine levels might not be representative of the cytokine content in the brain. Indeed

several studies showed that after repeated LPS injections levels of peripheral blood pro-inflammatory cytokines might return to control levels while the level of cytokine expression in the brain remains high (Chen et al., 2005; Fischer et al., 2015; Norden et al., 2016).

Due to the suggested role of adult hippocampal neurogenesis in depression neurobiology and in the mechanism of antidepressant action the effect of systemic chronic LPS exposure on the rate of AHN was investigated. It is important to note that the effects that are occurring in the tissue collected 7 days after the last LPS injections were studied, therefore the immediate effects of LPS would not be reflected in this analysis. While LPS did not affect cell proliferation in the DG in accordance with previously published studies (Belarbi et al., 2012; Ormerod et al., 2013), LPS exposure altered the level of postmitotic maturation of neuroblasts in the dentate gyrus, with escalating dose causing a decrease in contrast with a potentially compensatory increase seen in the low dose and single LPS groups. It has already been shown that LPS can disrupt the morphological maturation of DCX positive cells (Valero et al., 2014). Interestingly, in this experiment LPS injections had an effect on the number of postmitotic, almost mature "EF"-type DCX positive neurons with multiple dendritic branching reaching the molecular layer. The number of these cells was significantly higher than control in 0.1 LPS and single LPS groups. This data might be suggesting a compensatory increase in maturation of DCX positive progenitors. It is possible that a single 0.83 mg/kg LPS dose, as well as repeated 0.1 mg/kg LPS doses allow the neurogenic niche to recover from the insult and compensate for the damage occurring immediately after exposure with an increase in maturation rate of DCX+ neurons. Indeed previous studies described the acute (within first 24 hours) reduction in cell proliferation following LPS treatment (Fujioka and Akema, 2010), while other studies described an increase in the number of proliferating cells in the hippocampus 7 days after LPS injections (Valero et al., 2014). Therefore it is possible that during the first week after LPS insult, an initial decline in cell proliferation gives way to a compensative increase, which subsequently results in an increase in the number of postmitotic immature neurons. Importantly considering the timeline of neuroblast maturation to the postmitotic "EF" morphological stage (approximately 2-4 weeks according to Zhao et al. 2006), this group of DCX+ neurons most likely represents the neuroblasts which were generated on weeks 3 to 5 of the LPS treatment, which seems a likely time window for a compensatory effect. However, in the escalating LPS (0.33-0.83) group we observed a trend towards decline in the total number of DCX+ and a significant decrease in the number of postmitotic DCX+ neuroblasts in this group compared to control. These findings suggest that weekly increase of LPS dose from 0.33 to 0.83 mg/kg might be producing a damage for which compensation is no longer effective. It is possible that the dose range used in our study was not sufficiently high to induce changes which would also significantly reduce

the total number of DCX+ cells, as many studies which previously demonstrated the reduction of cell differentiation employed higher doses, such as 1 mg/kg or more (Graciarena et al., 2013; Monje, 2003; Ormerod et al., 2013). Yet the effect on the postmitotic morphology is of importance, as it replicates the effect which chronic mild stress, another depression-modelling intervention in animals, exerts on dendritic branching of DCX-positive hippocampal cells (Vega-Rivera et al., 2016). Moreover, it has been shown by previous studies that chronic stress and other models of depression in animals can cause similar changes in dendritic morphology of mature hippocampal neurons, such as dendritic atrophy and debranching (Qiao et al., 2016; Sousa et al., 2000; Vyas et al., 2002). Importantly this effect is thought to underlie the reduction of hippocampal volume described in neuroimaging studies of depressed patients (Lorenzetti et al., 2009). As dendritic morphology is a form of neural plasticity, this effect could also be involved in a cognitive decline frequently observed in clinical depression (Femenía et al., 2012). Therefore observed changes in dendritic morphology emphasise the relevance of described LPS exposure for modelling depression-related neurobiology. However, experimental design limited the ability to follow the dynamics of neurogenic changes. Inclusion of groups injected with 0.83mg/kg and 0.1mg/kg shortly before tissue collection would permit a direct test of whether the neurogenic decline occurs acutely after exposure to these doses, and subsequently gives way to a compensatory increase observed in this experiment.

Next the state of hippocampal microglia was assessed. It has been commonly described that systemic LPS exposure induces microglial activation in the hippocampus (Ho et al., 2015; Noh et al., 2014). Microglia in turn are known to have the ability to modulate neurogenesis during an inflammatory insult (Belarbi and Rosi, 2013; Ekdahl, 2012) potentially through a release of pro-inflammatory cytokines, which have been shown to exert a detrimental effect on neural stem cells proliferation and differentiation (Koo and Duman, 2008; Zunszain et al., 2012). However, in this experiment LPS exposure did not have a long-lasting effect on the hippocampal microglia. Indeed, no change in the number of Iba1 positive microglia neither in the whole hippocampus, nor in the neurogenic granular zone was observed. While some studies report an increase in the proliferation of microglia in response to LPS (Borges et al., 2012), most of these effects have been observed shortly after LPS exposure. Importantly the change in population number does not necessary reflect the state of microglial activation, the commonly observed response of microglia to inflammatory stimuli. Indeed many studies describe activation of microglia in response to LPS without reporting any change in microglial number (Aid et al., 2010; Qin et al., 2007). Activation of microglia usually involves morphological changes in the shape and size of microglial soma and processes (Stence et al., 2001), as well as increase in expression of activation markers, such as CD68 and CD11b (Ekdahl

et al., 2003; Sugama et al., 2009). In this experiment the average level of activation in the microglial population was assessed by determining the surface area of CD68 positive puncta. No change was observed in CD68 expression 7 days after the last LPS challenge in the DG, CA1 and CA3 areas of the hippocampus, regions frequently shown to be responsive to systemic LPS. It is possible that the future morphological analysis could uncover signs of microglial activation not reflected by CD68 expression. At the same time it has been reported in the literature that the morphological state highlighted by the Iba1 marker might not coincide with the expression of proinflammatory genes by activated microglial cells (Norden et al., 2016). Therefore histological assessment of microglial activation used in this experiment might have its limitations in reflecting the functional activation of microglial cells. Future experiments determining the cytokine content in relevant brain areas could give a deeper insight into the effect of repeated LPS injections on intracerebral immune state. Moreover, measurements of IDO expression could have shown if LPS affected serotonin/kynurenine metabolism relevant for depression, as it has been shown in previous LPS studies (Godbout et al., 2008; O'Connor et al., 2009).

Another notable finding in the biological parameters is the absence of an increase in blood corticosterone levels, which has been previously reported in response to acute (Browne et al., 2012) and chronic LPS administration (Elgarf et al., 2014). The lack of hypercortisolism could account for the absence of decline in the hippocampal neurogenesis, as this has been attributed to the glucocorticoid receptor activation (Anacker et al., 2011). It also highlights the limited ability of the current chronic LPS administration paradigm to model depression neurobiology. Another important limitation of this study is the absence of data reflecting depression-like behaviour induced by LPS administration, which prevents us from drawing final conclusions on the relevance of this model for depression research. However, based on neurobiological phenotype, it is reasonable to suggest that whist this paradigm might be used to induce inflammatory aspects of depression neurobiology, it is likely to require co-exposure with other stimuli to produce a full depression-like phenotype in mice.

4 Conclusions

These experiments investigated the effect of single and repeated LPS injections at doses relevant for modelling mood disorders on systemic immune response and on adult hippocampal neurogenesis. Experiment 1 showed that the effects of a single 0.33 mg/kg LPS injection are transient and thus do not provide insight into chronic aspects of depression neurobiology. Therefore, in Experiment 2 we tested a new mode of injections designed to bypass the development of LPS tolerance and to induce neurobiological changes similar to

those seen in clinical depression. The results showed that the escalating LPS (0.33-0.83) group did not develop signs of LPS tolerance in sickness behaviour, although a loss of significant increase in FST immobility, which was present after the first injection, was observed 6 weeks later. The peripheral blood cytokine profile induced by escalating LPS suggested a mode of immune system activation distinct from an acute activation induced by single LPS exposure, with only minor signs of LPS tolerance importantly lacking the anti-inflammatory cytokine elevation. A comparison to a cytokine profile of a group specifically treated to induce tolerance could have allowed to draw more definitive conclusions regarding its presence. In addition, an investigation of molecular correlates of LPS tolerance, such as TLR4 expression, activation of MyD88 pathways inhibitors and nuclear translocation of NF-kB, would have provided extra insight into its presence and underlying mechanisms.

Assessment of adult hippocampal neurogenesis, considered to play an important role in depression neurobiology, showed that exposure to escalating dose led to a reduction of neuroblast maturation in the dentate gyrus, in contrast to a compensatory increase seen in low dose 0.1 LPS group or a group exposed to a single 0.83mg/kg LPS injection. However the observed changes in neurogenesis were not accompanied by a change in microglial proliferation or activation around neurogenic regions. Therefore the lack of sickness behaviour tolerance and increase of anti-inflammatory cytokines, as well as changes observed in hippocampal neurogenesis suggest that weekly injections of LPS with dose increment might be a suitable model to utilise in future studies looking into immunological aspects of mood disorders. However, the loss of depressive effect of a single LPS exposure triggered by repeated injections shows that LPS on its own is not an intervention sufficient to solely induce depressive-like behavioural phenotype.

Chapter 6 Discussion and Conclusions

1 Suitability of the mouse BALB/c strain for the use in animal models of depression

This project was dedicated to the study and advancement of animal models of depression, with a specific focus on neurobiological changes including adult hippocampal neurogenesis and immune system markers. Initially most depression models and behavioural assessments of their outcome were developed in rats, however recent advances in mouse genetics and genetic tools arising from them demand the development of models suitable for the mouse. Moreover, mice present an advantage of relative ease and low cost of breeding and housing. To contribute to the advancement of mouse models, all experiments in this project were conducted in mice. A choice of the strain was directed by the known characteristics of BALB/c mice, that is high prevalence of anxiety–like behaviour in approach-avoidance tests, high sensitivity to UCMS and good responsiveness to antidepressant treatment. However behavioural assessments conducted throughout this project showed that some charachteristics of BALB/c response to chronic stress exposure are suboptimal for the use in depression model studies. Indeed hyperlocomotion induced by UCMS exposure acted as a limitation for evaluating the results of behavioural tests of anxiety, such as the open field, light-dark box and novelty-suppressed feeding, as anxiety in these tests is measured based on the time mice spend moving around potentially threatening areas.

Another important aspect of BALB/c sensitivity to chronic stress is their response to chronic injections. The comparison between undisturbed mice and those chronically i.p. injected with saline in the UCMS Experiment 1 showed that chronic injections affected their coat state and behaviour in the FST. These findings suggest that peripheral injection route of drug administration is not suitable for chronic stress studies in this strain as it acts as an additional stressful factor. This conclusion further limits the use of BALB/c strain preclinical studies of depression which often employ i.p. injections to administer therapeutic compounds.

2 Reproducability of the UCMS and new insights into its outcomes

The UCMS - dedicated chapters of this thesis which described the setup of the UCMS model demonstrated the challenges of this process. Indeed, it became apparent that the UCMS protocol needs to be carefully adjusted to a particular strain and facilities of the laboratory.

Nonetheless, the outcome of the optimisation process confirmed that an aetiologically relevant protocol which does not include physical stressors, such as food or water deprivation, restraint or footshock, most closely resembling the protocol by Nollet et al. (2013) can be effective in 8-week old male BALB/cAnNCrl to induce some behavioural changes relevant for depression. However due to high reactivity of this strain, control mice need to be housed in large cages with their siblings to avoid social isolation and cage mate fighting. The use of sibling pairs also additionally reduces genetic and environmental variability among animals, which has a potential to reduce individual variability known to be high in behavioural responses. At the same time it can be argued that sibling pairs do not represent true biological replicates. However animals from the same litters are often used in rodent studies, whether they are bred in house or by a supplier laboratory. Therefore the use of sibling pairs is unlikely to significantly modify the outcome compared to previous studies. Experimentation with a schedule of stressors during UCMS showed that 2 stressors per day are not sufficient to induce significant behavioural changes, while 4 stressors can successfully affect behavioural outcome. Overlapping of stressors is not recommended as it appeared to be too severe, increasing the risk of death in the stress-exposed group. Such comparison among protocols also demonstrated that even small changes in the schedule of stress exposure can lead to significantly different outcomes, which could also explain variability seen among UCMS studies. Moreover, a comparison between UCMS Experiments 3 and 4 which employed identical protocol showed that some response variability exists between different cohorts of the same inbred strain mice.

The behavioural phenotypes induced by our protocol included a reduction of grooming and a novelty-induced hyperactivity discussed above. Potently due to hyperactivity UCMS-exposed animals displayed paradoxical reduced anxiety in approach-avoidance tasks, which has been described by some previous studies (Couch et al., 2016; Schweizer et al., 2009). On the other hand it is possible that this reduced anxiety was not solely a result of hyperactivity, as some of these tests are known to be less dependent on activity levels, such as light-dark box and novelty suppressed feeding). If so, one could speculate that reduced anxiety behaviour in these animals stems from the lack of environmental awareness or an increase in impulsivity, which could be tested in tasks specific for these behaviours. Otherwise, it has been shown previously that mouse response in the novelty suppressed feeding test is dependent on the ambiguity of the previous experience of aversive stimuli and the state of adult hippocampal neurogenesis. Glover et al., (2017) demonstrated that neurogenesis-deficient mice which went through cued fear conditioning training where the cue was only 50% predictive of footshock, appeared less anxious in the novelty suppressed feeding than those exposed to training with a

100% cue – footshock association. This effect was attributed to the failure of neurogenesis deficient mice to generalise the aversive experience to novel environments. As UCMS-exposed mice did show a reduction in adult hippocampal neurogenesis in the UCMS Experiment 3, it is possible to argue that their response in the novelty suppressed feeding test arena, as well as in other anxiety test could be related to such deficiency of fear generalisation. This point brings up the complexity of interpretation of some of the available behavioural tests. Indeed in most mood and anxiety-related tests, a lot of behavioural aspects such as fearfullness, spatial memory and attention might affect the outcome and thus complicate the interpretation of results.

In addition, gene expression data provided some indirect evidence for the disturbance of the molecular regulation of circadian rhythm in UCMS-exposed animals, which could have led to hyperactivity in these animals detected in the light phase compared to undisturbed controls. Therefore, in future experiments, manipulations which do not cause circadian rhythm shift, such as application of stressors as well as behavioural testing in the active phase, could be advised to avoid the confound of hyperactivity. However, sleep disturbances are typical for clinical depression (Motivala et al., 2005), therefore circadian rhythm alterations could be considered advantageous if this phenotype is of importance for the study design.

Another controversy arose from the interpretation of the tests of anhedonic behaviour which involved appetitive rewards. Contrary to expectations, sucrose preference test measurements showed that mouse response to this test can fluctuate significantly during the UCMS procedure and in control groups, and is rather sensitive to the concentration of sucrose used. 2% sucrose solution successfully discriminated between UCMS and CNTRL groups in Experiment 3, but serial assessments showed that BALB/cAnNCrl mice show a level of habituation upon repeated exposure. At the same time, this habituation showed a different dynamic between CNTRL and UCMS mice, which was corroborated by some indirect evidence pointing at a possible imbalance in the appetite-regulating system of UCMS-exposed animals. This evidence consisted of a decrease in the plasma level of leptin detected in stressed animals, accompanied by a differential expression of some of the leptin-regulated genes. This effect became apparent via the pathway analysis of the gene expression data, which suggested that leptin is a significant upstream regulator of the genes found to be altered by UCMS. Leptin deficiency is usually associated with increased appetite which would be expected to lead to weight changes, not observed in our studies experiments. A supposed shift in circadian rhythms which could have been induced by UCMS also could have played a role in these effects, if daily disturbance of mice by stressors shifted their resting time towards the night and feeding time towards the day. This could also explain why an apparent increase in appetite

was not accompanied by weight change. In this case either measurements taken separately in light and dark phases, or a reversal of light/dark cycle and application of stressors during the dark phase should be considered in the future experiments.

Another explanation of the observed changes is a selective increase in the appetite for palatable food rewards, which was only apparent in the sucrose preference and cookie tests and therefore did not lead to a considerable weight change. Importantly, a behavioural phenotype of increased drive towards pleasurable food rewards could be of translational value for modelling increase in refined sugar consumption observed in some depressed patients (Davison and Kaplan, 2012; Gangwisch et al., 2015). Moreover such observation could be of relevance to the observation that there is an increased risk of type 2 diabetes in the depressed population (Vancampfort et al., 2015).

These considerations bring up an important point of appetite and appetitive motivation as a potential confounding factor in tests of anhedonia which involve palatable stimuli. As these tests are designed to measure mouse motivation for food rewards, a behavioural change in these tests might be driven by both change in motivation towards any rewarding stimuli (anhedonia) or appetite-affected specific motivation towards palatable stimuli. To disentangle these, assessment of motivation towards another rewarding stimuli, such as for example sexual cue, could have proven helpful and should be considered in the future experiments.

In addition, some behavioural domains which could have been affected by UCMS were not assessed in the behavioural batteries employed. Cognitive functions have been previously shown to be affected in animal models of depression, which corresponds to cognitive deficit seen in depressed patients. Moreover, observed changes seen in adult hippocampal neurogenesis might be pointing at the deficit in hippocampus- and hippocampal neurogenesis-dependent functions, such as spatial memory and pattern separation. Inclusion of relevant tests, such as Morris water maze and contextual fear discrimination learning, could have provided more insight into deficit in these behavioural domains.

2.1 UCMS affected adult hippocampal neurogenesis but the PFC emerged as the primary region of UCMS-induced gene expression changes

In line with multiple previous studies, a successful protocol of UCMS exposure induced a decrease in the number of adult-born DCX-positive neuroblasts in our experiments. While the effect size in this study (15%) was somewhat lower than in previously reported UCMS studies, it is important to point out that the magnitude of suppressing effect of UCMS on adult hippocampal neurogenesis varies from study to study and is likely to be dependent on the

measure of adult neurogenesis used. For example, Mineur et al. (2007) reported about 50% reduction in proportion of BrdU/NeuN – positive cells upon UCMS exposure in BALB/c mice, a measure which represents combined effect of neuronal differentiation and survival. Several years later the same group reported around 35% decrease in the density of DCX+ cells in dorsal hippocampus and 65% decrease in ventral hippocampus after 9 weeks of UCMS exposure in BALB/c mice (Nollet et al., 2012). While this measure is analogous to the one used in the UCMS experiment 3, the baseline level of DCX+ cell density in this study is much lower than described here (11000 cells/mm^3 vs 26000 cells/mm^3). Regardless of the potential source of such difference (substrain differences, control conditions, methodological variations in immunohistochemistry or quantification methods), it is very probable that such variation might have affected the effect size.

It is also interesting to compare the effect observed in my experiments to previously reported data from human subjects. Two studies have reported around 30% decline in neurogenic markers in depressed subjects compared to non-depressed controls (Boldrini et al., 2012; Lucassen et al., 2010). However both studies looked at cell proliferation and the density of nestin-positive proliferating neural progenitors rather than neuronal differentiation. It is likely that different progenitor populations would be differently affected by depression. Thus, it would be benefitial to assess the effect of UCMS on the pool of Nestin-positive type 1 progenitors to see if the effect observed in clinical studies could be replicated in the current UCMS model. On the other hand is has now been shown that the overall rate of adult hippocampal neurogenesis in humans is likely to be higher than in rodents (Spalding et al., 2013), therefore even a small decline in a mouse model might be of translational value for human disease research. Nonetheless, the sole use of DCX as a neurogenesis marker is a limitation to this study. Certain controversy over its ability to reliably reflect the state of AHN currently exists in the scientific community (Merz and Lie, 2013), therefore future studies should also employ other markers of immature neurons, such as Prox1 and NeuroD1, as well as assessment of the adult-born neurons population by BrdU/NeuN double-labelling (Nicola et al., 2015).

However a significant advantage of using DCX is the fact that DCX+ cell population comprises a wide variety of progenitors at different stages of neuronal maturation. Thus to get some insight into the effect of UCMS on stage of neuronal maturation, further classification of DCX+ cells based on dendritic morphology according to Plümpe et al. (2006) was used to detect a stage of neuroblast maturation most susceptible to UCMS effects. The results showed that UCMS specifically depleted the pool of neuroblasts with the most mature dendritic tree. This finding is in line with two previous studies which also identified a reduction in DCX+ cell

population with complex dendritic morphology following UCMS or chronic CORT exposure (Lussier et al., 2013; Vega-Rivera et al., 2016). However, this assessment does not clarify whether a number of neuroblasts with a more developed dendritic tree was lower in the UCMS-exposed hippocampi due to slower maturation of neuroblasts, increase in their apoptosis or dendritic atrophy or remodelling induced by UCMS. Immunohistochemistry using markers of cell death such as caspase 3, as well as stage 3 progenitor markers such as calretinin and NeuN could have helped to disentangle this effect, however such analysis was not included in our initial experimental design.

An indirect suggestion for potential dendritic atrophy came from the assessment of gene expression in the hippocampus and the PFC of UCMS-exposed animals. The decrease in DCX+ cells was indeed accompanied by a small reduction in the DCX gene expression in the hippocampus. While the hippocampal gene expression was otherwise not strongly affected by the UCMS, pathway analysis of a large number of genes differentially expressed in the PFC suggested activation of pathways involved in dendritic remodelling. These included glutamate receptor and calcium signalling, as well as the axonal guidance pathway. In addition, functional analysis of the gene expression dataset predicted many dendritic morphology-related functions to be affected by UCMS. Neurodegenerative changes in the PFC are well-described in chronic stress research and include not only dendritic atrophy (Dias-Ferreira et al., 2009; Liston et al., 2006), but also microglial activation (Hinwood et al., 2013) and atrophy of pyramidal neurons (Cerqueira, 2005). Moreover, it is in agreement with a number of post-mortem and neuroimaging studies, which reported decreased PFC volume and activity in depressed patients (Drevets et al., 1997; van Tol et al., 2014). While assessment of the dendritic structure of PFC neurons was not included in the original aims of our study, analysis of microglial density showed an increased number of Iba+ microglia in the PFC, considered to be one of the signs of microglial activation. Therefore, available gene expression and immunohistochemical data suggest a degree of neurodegeneration occurring in the PFC. It is possible that this neurodegenerative signalling was then transmitted to the hippocampus and affected the maturation of adult-born neurons in the DG. Interestingly, increased hippocampal functional connectivity with dorsolateral PFC has been shown in older depressed patients by a resting-state functional connectivity MRI study (Goveas et al., 2011), suggesting that hippocampal-PFC connection might indeed be activated in depression.

The question remains as to why UCMS did not induce more profound gene expression changes in the hippocampus along with the PFC. A number of transcriptomic studies of chronic stress effects described significant changes in the hippocampal gene expression (Bergström et al., 2007; Gray et al., 2014; Malki et al., 2013). However some previous studies already showed

more gene expression changes in other brain regions than in the hippocampus upon UCMS in BALB/c mice (Liu et al., 2010; Surget, Wang, et al., 2008). Moreover, the PFC has been shown to be more sensitive to chronic stress than the hippocampus in studies of synaptic neurotransmission changes (Müller et al., 2011; Yuen et al., 2012). It is possible that the use of the total hippocampal tissue might have masked some of the gene expression effects because of transcriptomic and functional heterogeneity of hippocampal regions. Indeed, dorsal and ventral hippocampus are thought to be functionally and molecularly distinct (Fanselow and Dong, 2010), and the two regions have been shown to differ in their gene expression response to chronic stress (Guidotti et al., 2013; Hill et al., 2014).

The results of the neuroblast assessment also showed that UCMS stimulated migration of immature neuroblasts from the SGZ into deeper layers of the GZ. An increase in neuroblast migration distance has been previously shown to be induced by detrimental factors including neuroinflammation and ablation of the GR (Belarbi et al., 2012; Fitzsimons et al., 2012). However, this is the first time this effect is shown to be induced by chronic stress, providing further insight into the antineurogenic effects of UCMS. In future studies, analyses of the dendritic morphology of mature neurons in the hippocampus as well as in other stress-responsive brain regions, such as the PFC, will show if the effects of UCMS on dendritic morphology extend beyond adult-born neurons.

Lastly, the design of the UCMS experiments neither aimed nor allowed asnwering the question of the causality of adult neurogenesis decline in depression. The data shown here confirms the hypothesis that a major risk factor for depression, chronic stress exposure, leads to a reduction in neuronal differentiation in the hippocampal dentate gyrus, however its role in depression neurobiology remains unclear. To address this issue experiments involving specific manipulation of the level of adult neurogenesis, such as its ablation or stimulation along with stress exposure, would be required. However, the current state of the neurogenesis hypothesis of depression prioritises its role in antidepressant mechanism of action over its potential causality, which so far has not been confirmed (Miller and Hen, 2015). Thus a successful depression model would primarily require adult neurogenesis as a correlate of behavioural decline and recovery.

2.2 HPA axis was not overactivated by UCMS

The assessment of the HPA axis activity provided some unexpected results. Plasma CORT measures did not show an increase in HPA axis activity previously shown to be induced by UCMS in the literature. In fact, the opposite trend towards a blunted HPA response to acute stress was observed, resembling a hypoactive state of HPA axis regulation. The hypoactive

response of the HPA axis to chronic stress has been linked to strain differences, individual variability and the effect of social isolation (Ibarguen-Vargas et al., 2008; Ieraci et al., 2016). Moreover, a hypoactive HPA axis is routinely observed in a chronic CORT injection model (David et al., 2009; Hill et al., 2015). Interestingly, in the UCMS model a hypoactive HPA axis has been linked to antidepressant resistance in behavioural and neurogenesis domains (Khemissi et al., 2014; Surget et al., 2016). In line with this, FLX was not able to improve AHN in the UCMS-exposed animals in the UCMS Experiment 2. In addition, investigation of the predictive factors affecting AHN in the UCMS Experiment 3s also provided evidence for a negative effect of low CORT response to acute stress. Moreover, indirect support of a hypoactive HPA axis hypothesis came from the gene expression analysis, which again contrary to expectations did not show any activation of the HPA axis or GR-dependent pathways in the hippocampus.

Therefore, it is possible to suggest that the BALB/cAnNCrl strain of mice responds to UCMS with a hypoactivity or hypersuppression of the HPA axis. Such a profile of HPA axis response resembles the reduced HPA axis activity seen in some depressed patients with comorbid cardiac conditions (Nikkheslat et al., 2015) and those with atypical depression (Gold, 2015). Further evaluation of antidepressant resistance in the future experiments with our UCMS setup would also confirm the validity of this model to study the mechanisms of antidepressant resistance seen in clinical practice, which currently presents a serious challenge in the treatment of depression (Thomas et al., 2013).

Future experiments will be able to refine the assessment of the HPA axis, which was limited in our experiments. The single CORT measure taken during the light phase could be replaced with a series of measures taken at various time points during the 24 hours to draw a comprehensive picture of the alterations in the CORT diurnal rhythm. Assessment of post-acute stress CORT could also be extended to additional earlier and later time points to capture the dynamics of the acute stress response. A dexamethasone suppression test would be able to confirm if UCMS resulted in altered suppression of the HPA axis by the negative feedback regulation.

2.3 UCMS induced limited signs of the immune system activation

One of the aims of the UCMS experiments was to evaluate the extent of immune changes induced by UCMS. Previous studies described elevation of blood proinflammatory biomarkers, increased cytokine gene expression and protein levels in the brain, as well as microglial activation in various brain areas. However, in our experiments only limited signs of immune system involvement were detected. Among the plasma inflammatory biomarkers only CRP was

increased in UCMS-exposed group, which could partly be attributed to the lack of sensitivity in the assays ran in this thesis. CRP elevation is widely used in the clinic as a biomarker of inflammation and therefore can serve as a sufficient proinflammatory evidence. However, the use of hypersensitive plasma cytokine assays in the future might be able to detect subtle changes in cytokine levels and therefore provide a more comprehensive picture of the blood proinflammatory profile.

Yet gene expression data corroborated the plasma profile, as no increase in cytokine gene expression was found in the PFC or the hippocampus. This finding was also consistent with the absence of microglial activation in the dentate gyrus. At the same time the density of microglial cells was increased in the PFC, suggesting a level of microglial activation occurring in this area. While chronic stress has been shown to induce activation of microglia in the hippocampus and the PFC (Wohleb et al. 2012; Tynan et al. 2010), hippocampus has been shown to be more prone to microglial dystrophy which replaces initial microglial activation in the course of a prolonged chronic stress exposure (Hinwood et al., 2012; Kreisel et al., 2014). The occurring dystrophy could have counterbalanced the original rise in microglial numbers and therefore result in no change in the final microglial density. At the same time, it is interesting to relate the absence of microglial activation in the hippocampus to the absence of HPA axis activation. Glucocorticoids have been shown to be responsible for the priming and proliferation of microglia upon stress exposure (Frank et al., 2014; Nair and Bonneau, 2006). Therefore, one could speculate if HPA axis resistance to chronic stress also prevented microglial activation specifically in the hippocampus, known for its high GR expression levels and involvement in the HPA axis regulation.

The limitation to the current study is the fact that microglial activation was only estimated via the evaluation of the microglial density. In future studies, assessment of the morphological signs of activation or dystrophy, as well as detection of activation-specific markers will improve the precision of the analysis of the microglial state.

3 LPS – based model induced long-term neurobiological changes

The limited evidence for proinflammatory changes induced by UCMS challenged its suitability to model neuroinflammatory aspects of depression neurobiology. Therefore, a separate intervention was required to model the proinflammatory changes seen in depressed patients, to allow future testing of the novel compounds designed to target this aspect of depression pathology. LPS is widely used to study the depression-inducing effects of the inflammatory

processes, however many studies focus on short-term phenotypes, whereby a distinction between sickness and depression-like behavioural changes is hard to define. As has been shown in the UCMS-dedicated chapters, parameters such as appetite and locomotor activity can significantly affect the outcome of tests designed to assess depression-like behaviour, and these parameters are known to be affected by ongoing inflammation. Thus, the interpretation of behavioural phenotypes in LPS-induced models is apriori confounded. Therefore, the LPS experiments described in this thesis were aimed to specifically attempt a model of long-term changes with a focus on neurobiology rather than the behavioural phenotypes.

Experiments showed that a single injection of LPS is not sufficient to induce chronic change, therefore a new mode of repeated injections was proposed and tested. The results showed that weekly injections with an escalating dose of LPS (from 0.33mg/kg to 0.83mg/kg) induced a distinct profile of blood proinflammatory biomarkers with some cytokines showing lower and some higher elevation compared to the effect of a single dose. Repeated exposure to LPS is known to induce a reduction of inflammatory response known as LPS tolerance. Although measures were taken to avoid the development of LPS tolerance, some signs of tolerance were observed to be induced by this protocol. Importantly one of them was the loss of behavioural despair in the FST observed on the first, but not on the last week of injections.

AHN assessment showed that exposure to escalating doses led to a reduction in neuroblast maturation in the hippocampal DG similar to that induced by the UCMS. However, our protocol was not able to significantly reduce the total number of DCX+ cells. Moreover, the repeated LPS injections did not increase microglial proliferation or activation in the hippocampus. Therefore, the repeated injections with escalating dose of LPS proved to be suitable to induce elevation of some proinflammatory biomarkers, but were not sufficient to induce depression-like changes in the hippocampus or in the forced swim test for behavioural despair.

The study design provided some limitations to the LPS study. Treatment groups included did not allow a comparison with LPS tolerant mice needed to draw definitive conclusions on the presence and extent of the tolerance to LPS. The depressive-like behaviour evaluated was limited to behavioural despair, therefore it is not known if other behavioural domains were affected by single or repeated LPS injections. AHN was assessed 7 days after the last LPS injections as long-term changes were the focus of this study, however this approach resulted in immediate effects of LPS most frequently described in the literature not be reflected in the current analysis.

4 Conclusions and future directions

The experiments described in this thesis have contributed towards the advancement of the knowledge and the methodology of the two commonly used models of depression, the UCMS model and the LPS exposure based model in BALB/c mice. Multiple UCMS experiments showed that following careful protocol optimisation for the substrain used, UCMS can be a reliable model to induce some of the depression-like behaviours and alterations in adult hippocampal neurogenesis. However, currently available depression and anxiety- related behavioural tests can be confounded by factors such as locomotor activity and appetite also affected by UCMS, and thus need to be interpreted with caution. Importantly, in male BALB/cAnNCrl mice UCMS is not associated with a profile of systemic inflammatory changes seen in depressed patients, even though some evidence of inflammatory processes has been collected. Interestingly, it appeared that the PFC but not the hippocampus responds to UCMS with profound gene expression changes and microglial activation, suggesting higher susceptibility of this region to chronic stress. In fact, hippocampal resistance to stress was further corroborated by the absence of HPA axis overactivation in response to the UCMS protocol, as HPA axis function is thought to depend on the GR signalling in the hippocampus. Some evidence of antidepressant resistance accompanying these changes was collected for this thesis, but further experiments incorporating antidepressant treated groups are needed to confirm this suggestion. These findings support an existing notion that other brain areas apart from the hippocampus play an important role in chronic stress response and perhaps deserve more attention in preclinical depression research (Willner et al., 2014). At the same time, observed hippocampal resistance might be suggesting that additional interventions are needed to increase susceptibility of mice to chronic stress effects and to achieve the desired depression-like response.

The LPS experiments described in this thesis attempted to design a model of neurobiological changes typical for depression, specifically chronic inflammatory alterations and decline in adult hippocampal neurogenesis, potentially accompanied by some depression-like behaviours. While the mode of chronic escalating dose injections proposed did induce weekly elevations of proinflammatory biomarkers, it was not associated with a significant decline in AHN or neuroinflammation in the hippocampus. At the same time some detrimental changes in the neuroblast populations, resembling those induced by UCMS, have been observed. This suggests that LPS insult was targeting the pathways of interest, but perhaps was not sufficiently potent to cause tangible damage. In addition, this mode of injections did not cause a sustained behavioural despair response in the FST.

Therefore, both models induced some aspects of neurobiology relevant for inflammatory and neurogenic theories of depression, however none achieved the comprehensive phenotype required to fully test novel drugs targeting factors derived from these theories. It is possible that the combination of two models might be more successful in achieving this aim in the future. Indeed few previous studies showed that co-administration with LPS during the UCMS exposure triggered an exaggerated elevation of proinflammatory cytokines in the blood as well as in the hippocampus (Elgarf et al., 2014; Espinosa-Oliva et al., 2011). The combination of manipulations also was associated with microglial activation and profound neurodegenerative changes in this key region (Espinosa-Oliva et al., 2011). At the same time exposure to chronic stress before LPS or polyI:C injections prolonged the duration of depression-like behaviour in affected animals (Chijiwa et al., 2015; Couch et al., 2016). Thus it is possible to suggest that a double hit model combining manipulations of the stress and immune systems will trigger a required level of susceptibility to induce depression-like behaviour, as well as inflammatory and neurogenic changes sufficient to test novel antidepressant compounds targeting these aspects of depression neurobiology in the future experiments.

References

Aggarwal A, Jethani SL, Rohatgi RK and Kalra J (2016) Selective serotonin re-uptake inhibitors (SSRIs) induced weight changes: A dose and duration dependent study on albino rats. *Journal of Clinical and Diagnostic Research* 10(3): AF01-AF03.

Ahima RS and Osei SY (2004) Leptin signaling. *Physiology and Behavior* 81(2): 223–241.

Aid S, Parikh N, Palumbo S and Bosetti F (2010) Neuronal overexpression of cyclooxygenase-2 does not alter the neuroinflammatory response during brain innate immune activation. *Neuroscience Letters*, Elsevier Ireland Ltd 478(3): 113–118.

Aimone JB, Li Y, Lee SW, Clemenson GD, Deng W and Gage FH (2014) Regulation and Function of Adult Neurogenesis: From Genes to Cognition. *Physiological Reviews* 94(4): 991–1026.

Alexander C and Rietschel ET (2001) Invited review: Bacterial lipopolysaccharides and innate immunity. *Journal of Endotoxin Research* 7(3): 167–202.

Alonso M, Medina JH and Pozzo-miller L (2004) ERK1 / 2 Activation Is Necessary for BDNF to Increase Dendritic Spine Density in Hippocampal CA1 Pyramidal Neurons. *Learning & Memory* 11: 172–178.

Alonso R, Griebel G, Pavone G, Stemmelin J, Le Fur G and Soubrié P (2004) Blockade of CRF(1) or V(1b) receptors reverses stress-induced suppression of neurogenesis in a mouse model of depression. *Molecular psychiatry* 9(3): 278–86, 224.

Ambrogini P, Lattanzi D, Ciuffoli S, Agostini D, Bertini L, Stocchi V, Santi S and Cuppini R (2004) Morpho-functional characterization of neuronal cells at different stages of maturation in granule cell layer of adult rat dentate gyrus. *Brain Research* 1017(1–2): 21–31.

Anacker C, Zunszain PA, Cattaneo A, Carvalho LA, Garabedian MJ, Thuret S, Price J and Pariante CM (2011) Antidepressants increase human hippocampal neurogenesis by activating the glucocorticoid receptor. *Molecular psychiatry*, Nature Publishing Group 16(7): 738–50.

Anacker C, Zunszain PA, Carvalho LA and Pariante CM (2011) The glucocorticoid receptor: Pivot of depression and of antidepressant treatment? *Psychoneuroendocrinology*, Elsevier Ltd 36(3): 415–425.

Anderson ST, Commins S, Moynagh P and Coogan AN (2016) Chronic fluoxetine treatment attenuates post-septic affective changes in the mouse. *Behavioural Brain Research* 297: 112–115.

Andrus BM, Blizinsky K, Vedell PT, Dennis K, Shukla PK, Schaffer DJ, Radulovic J, Churchill GA and Redei EE (2012) Gene expression patterns in the hippocampus and amygdala of endogenous depression and chronic stress models. *Molecular Psychiatry*, Nature Publishing Group 17(1): 49–61.

Anisman H, Zaharia MD, Meaney MJ and Merali Z (1998) Do early-life events permanently alter behavioral and hormonal responses to stressors? *International Journal of Developmental Neuroscience* 16(3–4): 149–164.

Anisman H, Hayley S, Kelly O, Borowski T and Merali Z (2001) Psychogenic, neurogenic, and systemic stressor effects on plasma corticosterone and behavior: mouse strain-dependent outcomes. *Behavioral Neuroscience* 115(2): 443–454.

Arnsten AFT (2015) Stress weakens prefrontal networks: molecular insults to higher cognition. *Nature Neuroscience* 18(10): 1376–1385.

Aslani S, Harb MR, Costa PS, Almeida OFX, Sousa N and Palha JA (2014) Day and night: diurnal phase influences the response to chronic mild stress. *Frontiers in Behavioral Neuroscience* 8: 82.

Autry AE and Monteggia LM (2012) Brain-derived neurotrophic factor and neuropsychiatric disorders. *Pharmacological Reviews* 64(2): 238–258.

Ayensu WK, Pucilowski O, Mason GA, Overstreet DH, Rezvani AH and Janowsky DS (1995) Effects of chronic mild stress on serum complement activity, saccharin preference, and corticosterone levels in Flinders lines of rats. *Physiology and Behavior* 57(1): 165–169.

Bagot RCC, Cates HMM, Purushothaman I, Lorsch ZSS, Walker DMM, Wang J, Huang X, Schlüter OMM, Maze I, Peña CJJ, Heller EAA, Issler O, Wang M, Song W min, Stein JL, Liu X, Doyle MAA, … Nestler EJJ (2016) Circuit-wide Transcriptional Profiling Reveals Brain Region-Specific Gene Networks Regulating Depression Susceptibility. *Neuron* 90(5): 969–983.

Bai J, Ramos RL, Ackman JB, Thomas AM, Lee R V and LoTurco JJ (2003) RNAi reveals doublecortin is required for radial migration in rat neocortex. *Nature Neuroscience* 6(12): 1277–1283.

Banasikowski TJ, Cloutier CJ, Ossenkopp KP and Kavaliers M (2015) Repeated exposure of male mice to low doses of lipopolysaccharide: Dose and time dependent development of behavioral sensitization and tolerance in an automated light-dark anxiety test. *Behavioural Brain Research* 286: 241–248.

Banasr M, Hery M, Printemps R and Daszuta A (2004) Serotonin-Induced Increases in Adult Cell Proliferation and Neurogenesis are Mediated Through Different and Common 5-HT Receptor Subtypes in the Dentate Gyrus and the Subventricular Zone. *Neuropsychopharmacology*, American College of Neuropsychopharmacology 29(3): 450–460.

Banasr M, Soumier A, Hery M, Mocaër E and Daszuta A (2006) Agomelatine, a New Antidepressant, Induces Regional Changes in Hippocampal Neurogenesis. *Biological Psychiatry* 59(11): 1087–1096.

Banks WA (2007) Blood-Brain Barrier Transport of Cytokines: a mechanism for neuropathology. *Current Pharmaceutical Design* 6(C): 93-107.

Bannerman DM, Deacon RMJ, Offen S, Friswell J, Grubb M and Rawlins JNP (2002) Double dissociation of function within the hippocampus: Spatial memory and hyponeophagia. *Behavioral Neuroscience* 116(5): 884–901.

Bayer AL, Pugliese A and Malek TR (2013) The IL-2/IL-2R system: From basic science to therapeutic applications to enhance immune regulation. *Immunologic Research* 57(1–3): 197–209.

Beattie EC (2002) Control of Synaptic Strength by Glial TNFalpha. *Science* 295(5563): 2282–2285.

Becker C, Zeau B, Rivat C, Blugeot A, Hamon M and Benoliel J-J (2008) Repeated social defeat-induced depression-like behavioral and biological alterations in rats: involvement of cholecystokinin. *Molecular Psychiatry* 13(12): 1079–1092.

Bekris S, Antoniou K, Daskas S and Papadopoulou-Daifoti Z (2005) Behavioural and neurochemical effects induced by chronic mild stress applied to two different rat strains. *Behavioural Brain Research* 161(1): 45–59.

Belarbi K and Rosi S (2013) Modulation of adult-born neurons in the inflamed hippocampus. *Frontiers in Cellular Neuroscience* 7(September): 145.

Belarbi K, Arellano C, Ferguson R, Jopson T and Rosi S (2012) Chronic neuroinflammation impacts the recruitment of adult-born neurons into behaviorally relevant hippocampal networks. *Brain, Behavior, and Immunity* 26(1): 18–23.

Bellavance MA and Rivest S (2014) The HPA - immune axis and the immunomodulatory actions of glucocorticoids in the brain. *Frontiers in Immunology* 5(MAR): 136.

Belozertseva IV, Kos T, Popik P, Danysz W and Bespalov AY (2007) Antidepressant-like effects of mGluR1 and mGluR5 antagonists in the rat forced swim and the mouse tail suspension tests. *European Neuropsychopharmacology* 17(3): 172–179.

Belzung C and Billette de Villemeur E (2010) The design of new antidepressants: can formal models help? A first attempt using a model of the hippocampal control over the HPA-axis based on a review from the literature. *Behavioural Pharmacology* 21(8): 677–689.

Bergmann O, Liebl J, Bernard S, Alkass K, Yeung MSY, Steier P, Kutschera W, Johnson L, Landén M, Druid H, Spalding KL and Frisén J (2012) The Age of Olfactory Bulb Neurons in Humans. *Neuron* 74(4): 634–639.

Bergström A, Jayatissa MN, Thykjær T and Wiborg O (2007) Molecular Pathways Associated with Stress Resilience and Drug Resistance in the Chronic Mild Stress Rat Model of Depression—a Gene Expression Study. *Journal of Molecular Neuroscience* 33(2): 201–215.

Berlim MT, McGirr A, Van Den Eynde F, Fleck MPA and Giacobbe P (2014) Effectiveness and acceptability of deep brain stimulation (DBS) of the subgenual cingulate cortex for treatment-resistant depression: A systematic review and exploratory meta-analysis. *Journal of Affective Disorders* 159: 31–38.

Bernet CZ and Stein MB (1999) Relationship of childhood maltreatment to the onset and course of major depression in adulthood. *Depression and Anxiety* 9(4): 169–174.

Besnard A and Sahay A (2016) Adult Hippocampal Neurogenesis, Fear Generalization, and Stress. *Neuropsychopharmacology*, Nature Publishing Group 41(1): 24–44.

Bessa JM, Ferreira D, Melo I, Marques F, Cerqueira JJ, Palha JA, Almeida OFX and Sousa N (2009) The mood-improving actions of antidepressants do not depend on neurogenesis but are associated with neuronal remodeling. *Molecular Psychiatry*, Nature Publishing Group 14(8): 764–773, 739.

Bessa JM, Morais M, Marques F, Pinto L, Palha J a, Almeida OFX and Sousa N (2013) Stress-induced anhedonia is associated with hypertrophy of medium spiny neurons of the nucleus accumbens. *Translational Psychiatry*, Nature Publishing Group 3(6): e266.

Bienvenu J, Monneret G, Fabien N and Revillard JP (2000) The Clinical Usefulness of the Measurement of Cytokines. *Clinical Chemistry and Laboratory Medicine* 38(4): 267–285.

Biesmans S, Meert TF, Bouwknecht JA, Acton PD, Davoodi N, De Haes P, Kuijlaars J, Langlois X,

Matthews LJR, Ver Donck L, Hellings N and Nuydens R (2013) Systemic immune activation leads to neuroinflammation and sickness behavior in mice. *Mediators of Inflammation* 2013: 14.

Biesmans S, Acton PD, Cotto C, Langlois X, Ver Donck L, Bouwknecht JA, Aelvoet SA, Hellings N, Meert TF and Nuydens R (2015) Effect of stress and peripheral immune activation on astrocyte activation in transgenic bioluminescent Gfap-luc mice. *Glia* 63(7): 1126–1137.

Biesmans S, Matthews LJR, Bouwknecht JA, De Haes P, Hellings N, Meert TF, Nuydens R and Ver Donck L (2016) Systematic Analysis of the Cytokine and Anhedonia Response to Peripheral Lipopolysaccharide Administration in Rats. *BioMed Research International* 2016: 1–14.

Bilbo SD, Levkoff LH, Mahoney JH, Watkins LR, Rudy JW and Maier SF (2005) Neonatal Infection Induces Memory Impairments Following an Immune Challenge in Adulthood. *Behavioral Neuroscience* 119(1): 293–301.

Biswas SK and Lopez-Collazo E (2009) Endotoxin tolerance: new mechanisms, molecules and clinical significance. *Trends in Immunology* 30(10): 475-487.

Bjorkholm C and Monteggia LM (2016) BDNF - A key transducer of antidepressant effects. *Neuropharmacology* 102: 72–79.

Blanchard DC, Canteras NS, Markham CM, Pentkowski NS and Blanchard RJ (2005) Lesions of structures showing FOS expression to cat presentation: Effects on responsivity to a Cat, Cat odor, and nonpredator threat. *Neuroscience and Biobehavioral Reviews* 29(8): 1243–1253.

Bohannon JK, Hernandez A, Enkhbaatar P, Adams WL and Sherwood ER (2013) The immunobiology of toll-like receptor 4 agonists: from endotoxin tolerance to immunoadjuvants. *Shock* 40(6): 451–62.

Boldrini M, Underwood MD, Hen R, Rosoklija GB, Dwork AJ, John Mann J and Arango V (2009) Antidepressants increase neural progenitor cells in the human hippocampus. *Neuropsychopharmacology* 34(11): 2376–2389.

Boldrini M, Hen R, Underwood MD, Rosoklija GB, Dwork AJ, Mann JJ and Arango V (2012) Hippocampal angiogenesis and progenitor cell proliferation are increased with antidepressant use in major depression. *Biological Psychiatry*, Elsevier Inc. 72(7): 562–571.

Borges BC, Rorato R, Antunes-Rodrigues J, Elias LLK, Borges BC, Rorato R and Elias LLK (2012) Glial cell activity is maintained during prolonged inflammatory challenge in rats. *Brazilian Journal of Medical and Biological Research* 45(8): 784–791.

Bosnar M, Dominis-Kramarić M, Nujić K, Stupin Polančec D, Marjanović N, Glojnarić I and Eraković Haber V (2013) Immunomodulatory effects of azithromycin on the establishment of lipopolysaccharide tolerance in mice. *International Immunopharmacology* 15(3): 498–504.

Boyle MP, Brewer JA, Funatsu M, Wozniak DF, Tsien JZ, Izumi Y and Muglia LJ (2005) Acquired deficit of forebrain glucocorticoid receptor produces depression-like changes in adrenal axis regulation and behavior. *Proceedings of the National Academy of Sciences of the United States of America* 102(2): 473–8.

Brandt MD, Jessberger S, Steiner B, Kronenberg G, Reuter K, Bick-Sander A, Von Der Behrens W and Kempermann G (2003) Transient calretinin expression defines early postmitotic step of neuronal differentiation in adult hippocampal neurogenesis of mice. *Molecular and Cellular Neuroscience* 24(3): 603–613.

Brietzke E, Stertz L, Fernandes BS, Kauer-Sant'Anna M, Mascarenhas M, Escosteguy Vargas A, Chies JA and Kapczinski F (2009) Comparison of cytokine levels in depressed, manic and euthymic patients with bipolar disorder. *Journal of Affective Disorders*, Elsevier B.V. 116(3): 214–217.

Brummelte S and Galea LAM (2010) Chronic high corticosterone reduces neurogenesis in the dentate gyrus of adult male and female rats. *Neuroscience*, Elsevier Inc. 168(3): 680–690.

Bujalka H, Koenning M, Jackson S, Perreau VM, Pope B, Hay CM, Mitew S, Hill AF, Lu QR, Wegner M, Srinivasan R, Svaren J, Willingham M, Barres BA and Emery B (2013) MYRF Is a Membrane-Associated Transcription Factor That Autoproteolytically Cleaves to Directly Activate Myelin Genes. *PLoS Biology* 11(8): e1001625.

Burton MD, Sparkman NL and Johnson RW (2011) Inhibition of interleukin-6 trans-signaling in the brain facilitates recovery from lipopolysaccharide-induced sickness behavior. *Journal of Neuroinflammation* 8(1): 54.

Buttini M, Limonta S and Boddeke HWG. (1996) Peripheral administration of lipopolysaccharide induces activation of microglial cells in rat brain. *Neurochemistry International* 29(1): 25–35.

Cacci E, Claasen JH and Kokaia Z (2005) Microglia-derived tumor necrosis factor-alpha exaggerates death of newborn hippocampal progenitor cells in vitro. *Journal of Neuroscience Research* 80(6): 789–797.

Calabrese F, Savino E, Papp M, Molteni R and Riva MA (2016) Chronic mild stress-induced alterations of clock gene expression in rat prefrontal cortex: Modulatory effects of prolonged lurasidone treatment. *Pharmacological Research*, Elsevier Ltd 104: 140–150.

Camara M Lou, Corrigan F, Jaehne EJ, Jawahar MC, Anscomb H and Baune BT (2015) Effects of Centrally Administered Etanercept on Behavior, Microglia, and Astrocytes in Mice Following a Peripheral Immune Challenge. *Neuropsychopharmacology* 40(2): 502–512.

Campbell S, Marriott M, Nahmias C and MacQueen GM (2004) Lower Hippocampal Volume in Patients Suffering from depression: A Meta-Analysis. *American Journal of Psychiatry* 161(4): 598-607.

Canto CB, Wouterlood FG and Witter MP (2008) What does the anatomical organization of the entorhinal cortex tell us? *Neural Plasticity* 2008:18.

Capuron L, Neurauter G, Musselman DL, Lawson DH, Nemeroff CB, Fuchs D and Miller AH (2003) Interferon-alpha-induced changes in tryptophan metabolism: Relationship to depression and paroxetine treatment. *Biological Psychiatry* 54(9): 906–914.

Capuron L, Fornwalt FB, Knight BT, Harvey PD, Ninan PT and Miller AH (2009) Does cytokine-induced depression differ from idiopathic major depression in medically healthy individuals? *Journal of Affective Disorders* 119(1–3): 181–185.

Carpenter LL, Gawuga CE, Tyrka AR, Lee JK, Anderson GM and Price LH (2010) Association between plasma IL-6 response to acute stress and early-life adversity in healthy adults. *Neuropsychopharmacology : official publication of the American College of Neuropsychopharmacology* 35(13): 2617–23.

Carrillo-de Sauvage MÁ, Maatouk L, Arnoux I, Pasco M, Sanz Diez A, Delahaye M, Herrero MT, Newman TA, Calvo CF, Audinat E, Tronche F and Vyas S (2013) Potent and multiple regulatory actions of microglial glucocorticoid receptors during CNS inflammation. *Cell Death and Differentiation* 20(11): 1546–1557.

Caspi A (2003) Influence of Life Stress on Depression: Moderation by a Polymorphism in the 5-HTT Gene. *Science* 301(5631): 386–389.

Cattaneo A, Ferrari C, Uher R, Bocchio-Chiavetto L, Riva MA and Pariante CM (2016) Absolute

measurements of macrophage migration inhibitory factor and interleukin-1-β mRNA levels accurately predict treatment response in depressed patients. *International Journal of Neuropsychopharmacology* 19(10): 1–10.

Cepeda MS, Stang P and Makadia R (2016) Depression Is Associated With High Levels of C-Reactive Protein and Low Levels of Fractional Exhaled Nitric Oxide. *The Journal of Clinical Psychiatry* 77(12): 1666–1671.

Cerqueira JJ (2005) Morphological Correlates of Corticosteroid-Induced Changes in Prefrontal Cortex-Dependent Behaviors. *Journal of Neuroscience* 25(34): 7792–7800.

Chen R, Zhou H, Beltran J, Malellari L and Chang SL (2005) Differential expression of cytokines in the brain and serum during endotoxin tolerance. *Journal of Neuroimmunology* 163(1–2): 53–72.

Chijiwa T, Oka T, Lkhagvasuren B, Yoshihara K and Sudo N (2015) Prior chronic stress induces persistent polyI: C-induced allodynia and depressive-like behavior in rats: Possible involvement of glucocorticoids and microglia. *Physiology and Behavior*, Elsevier Inc. 147: 264–273.

Chomczynski P and Sacchi N (1987) Single-step method of RNA isolation by acid guanidinium thiocyanate-phenol-chloroform extraction. *Analytical Biochemistry*, Academic Press 162(1): 156–159.

Clark SM, Michael KC, Klaus J, Mert A, Romano-Verthelyi A, Sand J and Tonelli LH (2015) Dissociation between sickness behavior and emotionality during lipopolysaccharide challenge in lymphocyte deficient Rag2-/- mice. *Behavioural Brain Research* 278: 74–82.

Cleal JK, Shepherd JN, Shearer JL, Bruce KD and Cagampang FR (2014) Sensitivity of housekeeping genes in the suprachiasmatic nucleus of the mouse brain to diet and the daily light-dark cycle. *Brain Research* 1575(1): 72–77.

Clelland CD, Choi M, Romberg C, Clemenson GD, Fragniere A, Tyers P, Jessberger S, Saksida LM, Barker RA, Gage FH and Bussey TJ (2009) A Functional Role for Adult Hippocampal Neurogenesis in Spatial Pattern Separation. *Science* 325(5937): 210–213.

Colgin LL, Moser EI and Moser MB (2008) Understanding memory through hippocampal remapping. *Trends in Neurosciences* 31(9): 469-477.

Colla M, Kronenberg G, Deuschle M, Meichel K, Hagen T, Bohrer M and Heuser I (2007) Hippocampal volume reduction and HPA-system activity in major depression. *Journal of*

Psychiatric Research 41(7): 553–560.

Colton CA (2009) Heterogeneity of microglial activation in the innate immune response in the brain. *Journal of Neuroimmune Pharmacology* 4(4): 399-418.

Cornwell BR, Salvadore G, Colon-Rosario V, Latov DR, Holroyd T, Carver FW, Coppola R, Manji HK, Zarate CA and Grillon C (2010) Abnormal hippocampal functioning and impaired spatial navigation in depressed individuals: Evidence from whole-head magnetoencephalography. *American Journal of Psychiatry*, American Psychiatric Association 167(7): 836–844.

Couch Y, Anthony DC, Dolgov O, Revischin A, Festoff B, Santos AI, Steinbusch HW and Strekalova T (2013) Microglial activation, increased TNF and SERT expression in the prefrontal cortex define stress-altered behaviour in mice susceptible to anhedonia. *Brain, Behavior, and Immunity* 29: 136–146.

Couch Y, Trofimov A, Markova N, Nikolenko V, Steinbusch HW, Chekhonin V, Schroeter C, Lesch K-P, Anthony DC and Strekalova T (2016) Low-dose lipopolysaccharide (LPS) inhibits aggressive and augments depressive behaviours in a chronic mild stress model in mice. *Journal of Neuroinflammation*, 13(1): 108.

Crawley J and Goodwin FK (1980) Preliminary report of a simple animal behavior model for the anxiolytic effects of benzodiazepines. *Pharmacology Biochemistry and Behavior* 13(2): 167–170.

Cryan JF and Holmes A (2005) Model organisms: The ascent of mouse: advances in modelling human depression and anxiety. *Nature Reviews Drug Discovery* 4(9): 775–790.

Cryan JF and Mombereau C (2004) In search of a depressed mouse: utility of models for studying depression-related behavior in genetically modified mice. *Molecular Psychiatry* 9(4): 326–357.

Cryan JF, Mombereau C and Vassout A (2005) The tail suspension test as a model for assessing antidepressant activity: Review of pharmacological and genetic studies in mice. *Neuroscience and Biobehavioral Reviews* 29(4–5): 571–625.

Cunningham C, Campion S, Teeling J, Felton L and Perry VH (2007) The sickness behaviour and CNS inflammatory mediator profile induced by systemic challenge of mice with synthetic double-stranded RNA (poly I:C). *Brain, Behavior, and Immunity* 21(4): 490–502.

D'Aquila PS, Brain P and Willner P (1994) Effects of chronic mild stress on performance in

behavioural tests relevant to anxiety and depression. *Physiology and Behavior* 56(5): 861–867.

D'Mello C, Le T and Swain MG (2009) Cerebral Microglia Recruit Monocytes into the Brain in Response to Tumor Necrosis Factor Signaling during Peripheral Organ Inflammation. *Journal of Neuroscience* 29(7): 2089–2102.

Dahl J, Ormstad H, Aass HCD, Malt UF, Bendz LT, Sandvik L, Brundin L and Andreassen OA (2014) The plasma levels of various cytokines are increased during ongoing depression and are reduced to normal levels after recovery. *Psychoneuroendocrinology* 45: 77–86.

Danese A, Moffitt TE, Pariante CM, Ambler A, Poulton R and Caspi A (2008) Elevated Inflammation Levels in Depressed Adults With a History of Childhood Maltreatment. *Archives of General Psychiatry* 65(4): 409.

Darcet F, Gardier AM, David DJ and Guilloux JP (2016) Chronic 5-HT4 receptor agonist treatment restores learning and memory deficits in a neuroendocrine mouse model of anxiety/depression. *Neuroscience Letters*, Elsevier Ireland Ltd 616: 197–203.

Darcet F, Gardier AM, Gaillard R, David DJ and Guilloux JP (2016a) Cognitive dysfunction in major depressive disorder. A translational review in animal models of the disease. *Pharmaceuticals*.

Datson NA, Speksnijder N, Mayer JL, Steenbergen PJ, Korobko O, Goeman J, de Kloet ER, Joëls M and Lucassen PJ (2012) The transcriptional response to chronic stress and glucocorticoid receptor blockade in the hippocampal dentate gyrus. *Hippocampus* 22(2): 359–371.

David D, Samuels BA, Rainer Q, Wang JW, Marsteller D, Mendez I, Drew M, Craig DA, Guiard BP, Guilloux JP, Artymyshyn RP, Gardier AM, Gerald C, Antonijevic IA, Leonardo ED and Hen R (2009) Neurogenesis-Dependent and -Independent Effects of Fluoxetine in an Animal Model of Anxiety/Depression. *Neuron* 62(4): 479–493.

Davison KM and Kaplan BJ (2012) Food intake and blood cholesterol levels of community-based adults with mood disorders. *BMC Psychiatry* 12(1): 10.

de Kloet ER, Joëls M and Holsboer F (2005) Stress and the brain: from adaptation to disease. *Nature Reviews Neuroscience* 6(6): 463–475.

Deisseroth K, Singla S, Toda H, Monje M, Palmer TD and Malenka RC (2004) Excitation-Neurogenesis Coupling in Adult Neural Stem/Progenitor Cells. *Neuron*, Elsevier 42(4):

535–552.

Deng W, Aimone JB and Gage FH (2010) New neurons and new memories: how does adult hippocampal neurogenesis affect learning and memory? *Nature Reviews Neuroscience* 11(5): 339–350.

Déry N, Pilgrim M, Gibala M, Gillen J, Martin Wojtowicz J, MacQueen G and Becker S (2013) Adult hippocampal neurogenesis reduces memory interference in humans: Opposing effects of aerobic exercise and depression. *Frontiers in Neuroscience* 7(7 APR): 66.

Dias-Ferreira E, Sousa JC, Melo I, Morgado P, Mesquita AR, Cerqueira JJ, Costa RM and Sousa N (2009) Chronic Stress Causes Frontostriatal Reorganization and Affects Decision-Making. *Science* 325(5940): 621–625.

Dias GP, Bevilaqua MC do N, Da Luz ACDS, Fleming RL, De Carvalho LA, Cocks G, Beckman D, Hosken LC, De Sant'Anna Machado W, Corrêa-e-Castro AC, Mousovich-Neto F, De Castro Gomes V, Bastos G de NT, Kubrusly RCC, Da Costa VMC, Srivastava D, Landeira-Fernandez J, … Gardino PF (2014) Hippocampal biomarkers of fear memory in an animal model of generalized anxiety disorder. *Behavioural Brain Research* 263: 34–45.

Dias GP, Hollywood R, Do Nascimento Bevilaqua MC, Da Silveira Da Luz ACD, Hindges R, Nardi AE and Thuret S (2014) Consequences of cancer treatments on adult hippocampal neurogenesis: Implications for cognitive function and depressive symptoms. *Neuro-Oncology* 16(4): 476-492.

Dinarello CA (2000) Proinflammatory Cytokines. *Chest* 118(2): 503–508.

Dockray GJ (2012) Cholecystokinin. *Current Opinion in Endocrinology & Diabetes and Obesity* 19(1): 8–12.

Doosti MH, Bakhtiari A, Zare P, Amani M, Majidi-Zolbanin N, Babri S and Salari AA (2013) Impacts of early intervention with fluoxetine following early neonatal immune activation on depression-like behaviors and body weight in mice. *Progress in Neuro-Psychopharmacology and Biological Psychiatry*, Elsevier Inc. 43: 55–65.

Dournes C, Beeské S, Belzung C and Griebel G (2013) Deep brain stimulation in treatment-resistant depression in mice: Comparison with the CRF1 antagonist, SSR125543. *Progress in Neuro-Psychopharmacology and Biological Psychiatry*, Elsevier Inc. 40: 213–220.

Dowlati Y, Herrmann N, Swardfager W, Liu H, Sham L, Reim EK and Lanctôt KL (2010) A Meta-Analysis of Cytokines in Major Depression. *Biological Psychiatry* 67(5): 446–457.

Drevets WC, Price JL, Simpson JR, Todd RD, Reich T, Vannier M and Raichle ME (1997) Subgenual prefrontal cortex abnormalities in mood disorders. *Nature* 386(6627): 824–7.

Drude S, Geißler A, Olfe J, Starke A, Domanska G, Schuett C and Kiank-Nussbaum C (2011) Side effects of control treatment can conceal experimental data when studying stress responses to injection and psychological stress in mice. *Laboratory Animals*, Nature Publishing Group 40(4): 119–128.

Drugan RC, Basile AS, Ha JH, Healy D and Ferland RJ (1997) Analysis of the importance of controllable versus uncontrollable stress on subsequent behavioral and physiological functioning. *Brain Research Protocols* 2(1): 69–74.

DSM-5 (2013) *Diagnostic and Statistical Manual of Mental Disorders: DSM-5*. 5th ed. Arlington, VA: American Psychiatric Association.

Du P, Kibbe WA and Lin SM (2008) lumi: A pipeline for processing Illumina microarray. *Bioinformatics* 24(13): 1547–1548.

Duan X, Chang JH, Ge S, Faulkner RL, Kim JY, Kitabatake Y, Liu X bo, Yang CH, Jordan JD, Ma DK, Liu CY, Ganesan S, Cheng HJ, Ming G li, Lu B and Song H (2007) Disrupted-In-Schizophrenia 1 Regulates Integration of Newly Generated Neurons in the Adult Brain. *Cell* 130(6): 1146–1158.

Ducottet C, Griebel G and Belzung C (2003) Effects of the selective nonpeptide corticotropin-releasing factor receptor 1 antagonist antalarmin in the chronic mild stress model of depression in mice. *Progress in Neuro-Psychopharmacology* 27: 625–631.

Ducottet C, Aubert A and Belzung C (2004) Susceptibility to subchronic unpredictable stress is related to individual reactivity to threat stimuli in mice. *Behavioural Brain Research* 155(2): 291–299.

Ducottet C and Belzung C (2005) Correlations between behaviours in the elevated plus-maze and sensitivity to unpredictable subchronic mild stress: Evidence from inbred strains of mice. *Behavioural Brain Research* 156(1): 153–162.

Dulawa SC, Holick KA, Gundersen B and Hen R (2004) Effects of chronic fluoxetine in animal models of anxiety and depression. *Neuropsychopharmacology*, American College of Neuropsychopharmacology 29(7): 1321–1330.

Dulawa SC and Hen R (2005) Recent advances in animal models of chronic antidepressant effects: The novelty-induced hypophagia test. *Neuroscience & Biobehavioral Reviews*

29(4): 771–783.

Egeland M, Zhang X, Millan MJ, Mocaer E and Svenningsson P (2012) Pharmacological or genetic blockade of the dopamine D3 receptor increases cell proliferation in the hippocampus of adult mice. *Journal of Neurochemistry* 123(5): 811–823.

Egeland M, Zunszain PA and Pariante CM (2015) Molecular mechanisms in the regulation of adult neurogenesis during stress. *Nature reviews. Neuroscience*, Nature Publishing Group 16(4): 189–200.

Ekdahl CT, Claasen J-H, Bonde S, Kokaia Z and Lindvall O (2003) Inflammation is detrimental for neurogenesis in adult brain. *Proceedings of the National Academy of Sciences* 100(23): 13632–13637.

Ekdahl CT (2012) Microglial activation-tuning and pruning adult neurogenesis. *Frontiers in Pharmacology*, Frontiers 3 MAR: 41.

Elgarf ASA, Aboul-Fotouh S, Abd-Alkhalek H a, El Tabbal M, Hassan AN, Kassim SK, Hammouda GA, Farrag KA and Abdel-Tawab AM (2014) Lipopolysaccharide repeated challenge followed by chronic mild stress protocol introduces a combined model of depression in rats: Reversibility by imipramine and pentoxifylline. *Pharmacology Biochemistry and Behavior*, Elsevier Inc. 126: 152–162.

Elhwuegi AS (2004) Central monoamines and their role in major depression. *Progress in Neuro-Psychopharmacology and Biological Psychiatry* 28(3): 435-451.

Engler H, Bailey MT, Engler A, Stiner-Jones LM, Quan N and Sheridan JF (2008) Interleukin-1 receptor type 1-deficient mice fail to develop social stress-associated glucocorticoid resistance in the spleen. *Psychoneuroendocrinology* 33(1): 108–117.

Epp JR, Beasley CL and Galea LA (2013) Increased Hippocampal Neurogenesis and p21 Expression in Depression: Dependent on Antidepressants, Sex, Age, and Antipsychotic Exposure. *Neuropsychopharmacology*, Nature Publishing Group 38(11): 2297–2306.

Epp JR, Silva Mera R, Köhler S, Josselyn SA and Frankland PW (2016) Neurogenesis-mediated forgetting minimizes proactive interference. *Nature Communications* 7: 10838.

Erburu M, Cajaleon L, Guruceaga E, Venzala E, Munoz-Cobo I, Beltran E, Puerta E and Tordera RM (2015) Chronic mild stress and imipramine treatment elicit opposite changes in behavior and in gene expression in the mouse prefrontal cortex. *Pharmacology Biochemistry and Behavior*, Elsevier Inc. 135: 227–236.

Erickson MA and Banks WA (2011) Cytokine and chemokine responses in serum and brain after single and repeated injections of lipopolysaccharide: Multiplex quantification with path analysis. *Brain, Behavior, and Immunity* 25(8): 1637–1648.

Ernst A, Alkass K, Bernard S, Salehpour M, Perl S, Tisdale J, Possnert G, Druid H and Frisen J (2014) Neurogenesis in the striatum of the adult human brain. *Cell* 156(5): 1072–1083.

Ernst A and Frisen J (2015) Adult Neurogenesis in Humans- Common and Unique Traits in Mammals. *PLoS Biology* 13(1): e1002045.

Espinosa-Oliva AM, de Pablos RM, Villarán RF, Argüelles S, Venero JL, Machado A and Cano J (2011) Stress is critical for LPS-induced activation of microglia and damage in the rat hippocampus. *Neurobiology of Aging* 32(1): 85–102.

Evans J, Sun Y, McGregor A and Connor B (2012) Allopregnanolone regulates neurogenesis and depressive/anxiety-like behaviour in a social isolation rodent model of chronic stress. *Neuropharmacology*, Elsevier Ltd 63(8): 1315–1326.

Fanselow MS and Dong HW (2010) Are the Dorsal and Ventral Hippocampus Functionally Distinct Structures? *Neuron*, Elsevier Inc. 65(1): 7–19.

Farioli-Vecchioli S, Mattera A, Micheli L, Ceccarelli M, Leonardi L, Saraulli D, Costanzi M, Cestari V, Rouault JP and Tirone F (2014) Running rescues defective adult neurogenesis by shortening the length of the cell cycle of neural stem and progenitor cells. *Stem Cells* 32(7): 1968–1982.

Farooq KR, Isingrini E, Tanti A, Guisquet A Le, Arlicot N, Minier F, Leman S, Chalon S, Belzung C, Camus V, Farooq RK, Isingrini E, Tanti A, Le Guisquet AM, Arlicot N, Minier F, Leman S, … Camus V (2012) Is unpredictable chronic mild stress (UCMS) a reliable model to study depression-induced neuroinflammation ? *Behavioural Brain Research*, Elsevier B.V. 231(1): 130–137.

Fava M and Kendler KS (2000) Major depressive disorder. *Neuron* 28(2): 335–41.

Fava M (2003) Diagnosis and definition of treatment-resistant depression. *Biological Psychiatry* 53(8):649-659.

Feld JJ and Hoofnagle JH (2005) Mechanism of action of interferon and ribavirin in treatment of hepatitis C. *Nature* 436(7053): 967–72.

Femenía T, Gómez-Galán M, Lindskog M and Magara S (2012) Dysfunctional hippocampal

activity affects emotion and cognition in mood disorders. *Brain Research*, Elsevier B.V. 1476:58-70

Fenn AM, Gensel JC, Huang Y, Popovich PG, Lifshitz J and Godbout JP (2014) Immune activation promotes depression 1 month after diffuse brain injury: A role for primed microglia. *Biological Psychiatry* 76(7): 575–584.

Ferrari AJ, Charlson FJ, Norman RE, Patten SB, Freedman G, Murray CJ, Vos T and Whiteford HA (2013) Burden of depressive disorders by country, sex, age, and year: findings from the global burden of disease study 2010. *PLoS Medicine* 10(11): e1001547.

Fischer CW, Elfving B, Lund S and Wegener G (2015) Behavioral and systemic consequences of long-term inflammatory challenge. *Journal of Neuroimmunology*, Elsevier B.V. 288: 40–46.

Fitzsimons CP, van Hooijdonk LW a, Schouten M, Zalachoras I, Brinks V, Zheng T, Schouten TG, Saaltink DJ, Dijkmans T, Steindler D a, Verhaagen J, Verbeek FJ, Lucassen PJ, de Kloet ER, Meijer OC, Karst H, Joels M, … Vreugdenhil E (2012) Knockdown of the glucocorticoid receptor alters functional integration of newborn neurons in the adult hippocampus and impairs fear-motivated behavior. *Molecular Psychiatry*, Nature Publishing Group 18(9): 993–1005.

Fournier JC, Derubeis RJ, Hollon SD, Dimidjian S, Amsterdam JD, Shelton RC and Fawcett J (2010) Antidepressant Drug effects and Depression Severity: A Patient- Level Meta-Analysis. *Journal of American Medical Association* 6(3031): 47–53.

Fournier NM and Duman RS (2012) Role of vascular endothelial growth factor in adult hippocampal neurogenesis: Implications for the pathophysiology and treatment of depression. *Behavioural Brain Research* 227(2): 440-449.

Franceschelli A, Sens J, Herchick S, Thelen C and Pitychoutis PM (2015) Sex differences in the rapid and the sustained antidepressant-like effects of ketamine in stress-naïve and 'depressed' mice exposed to chronic mild stress. *Neuroscience*, IBRO 290: 49–60.

Frank MG, Hershman SA, Weber MD, Watkins LR and Maier SF (2014) Chronic exposure to exogenous glucocorticoids primes microglia to pro-inflammatory stimuli and induces NLRP3 mRNA in the hippocampus. *Psychoneuroendocrinology* 40(1): 191–200.

Frankland PW, Köhler S and Josselyn SA (2013) Hippocampal neurogenesis and forgetting. *Trends in Neurosciences* 36(9): 497-503.

Franklin KBJ and Paxinos G (2012) *The mouse brain in stereotaxic coordinates*. 4th ed. London: Academic Press.

Frenois F, Moreau M, O'Connor J, Lawson M, Micon C, Lestage J, Kelley KW, Dantzer R and Castanon N (2007) Lipopolysaccharide induces delayed FosB/DeltaFosB immunostaining within the mouse extended amygdala, hippocampus and hypothalamus, that parallel the expression of depressive-like behavior. *Psychoneuroendocrinology* 32(5): 516–531.

Fujioka H and Akema T (2010) Lipopolysaccharide acutely inhibits proliferation of neural precursor cells in the dentate gyrus in adult rats. *Brain Research*, Elsevier B.V. 1352: 35–42.

Fukuda S, Kato F, Tozuka Y, Yamaguchi M, Miyamoto Y and Hisatsune T (2003) Two distinct subpopulations of nestin-positive cells in adult mouse dentate gyrus. *The Journal of Neuroscience* 23(28): 9357–9366.

Fulton S (2010) Appetite and reward. *Frontiers in Neuroendocrinology*, Elsevier Inc. 31(1): 85–103.

Gangwisch JE, Hale L, Garcia L, Malaspina D, Opler MG, Payne ME, Rossom RC and Lane D (2015) High glycemic index diet as a risk factor for depression: Analyses from the Women's Health Initiative. *American Journal of Clinical Nutrition* 102(2): 454–463.

Gao L, Gao Y, Xu E and Xie J (2015) Microarray Analysis of the Major Depressive Disorder mRNA Profile Data. *Psychiatry Investigation* 12(3): 388–396.

Garcia-Oscos F, Salgado H, Hall S, Thomas F, Farmer GE, Bermeo J, Galindo LC, Ramirez RD, D'Mello S, Rose-John S and Atzori M (2012) The stress-induced cytokine interleukin-6 decreases the inhibition/excitation ratio in the rat temporal cortex via trans-signaling. *Biological Psychiatry* 71(7): 574–582.

Garcia LSB, Comim CM, Valvassori SS, Réus GZ, Stertz L, Kapczinski F, Gavioli EC and Quevedo J (2009) Ketamine treatment reverses behavioral and physiological alterations induced by chronic mild stress in rats. *Progress in Neuro-Psychopharmacology and Biological Psychiatry* 33(3): 450–455.

Garza JC, Guo M, Zhang W and Lu X-Y (2012) Leptin restores adult hippocampal neurogenesis in a chronic unpredictable stress model of depression and reverses glucocorticoid-induced inhibition of GSK-3β/β-catenin signaling. *Molecular Psychiatry* 17(8): 790–808.

Garza JC, Guo M, Zhang W and Lu XY (2008) Leptin increases adult hippocampal neurogenesis

in vivo and in vitro. *Journal of Biological Chemistry* 283(26): 18238–18247.

Ge JF, Qi CC and Zhou JN (2013) Imbalance of leptin pathway and hypothalamus synaptic plasticity markers are associated with stress-induced depression in rats. *Behavioural Brain Research*, Elsevier B.V. 249: 38–43.

Geschwind DH and Flint J (2015) Genetics and genomics of psychiatric disease. *Science* 349(6255): 1489–94.

Gimeno D, Kivimäki M, Brunner EJ, Elovainio M, De Vogli R, Steptoe A, Kumari M, Lowe GDO, Rumley A, Marmot MG and Ferrie JE (2009) Associations of C-reactive protein and interleukin-6 with cognitive symptoms of depression: 12-year follow-up of the Whitehall II study. *Psychological medicine*, NIH Public Access 39(3): 413–23.

Girotti M, Pace TWW, Gaylord RI, Rubin BA, Herman JP and Spencer RL (2006) Habituation to repeated restraint stress is associated with lack of stress-induced c-fos expression in primary sensory processing areas of the rat brain. *Neuroscience* 138(4): 1067–81.

Global Burden of Disease Study 2013 Collaborators (2015) Global, regional, and national incidence, prevalence, and years lived with disability for 301 acute and chronic diseases and injuries in 188 countries, 1990-2013: a systematic analysis for the Global Burden of Disease Study 2013. *Lancet* 386(9995): 743–800.

Glover LR, Schoenfeld TJ, Karlsson R-M, Bannerman DM, Cameron HA and Reynolds R (2017) Ongoing neurogenesis in the adult dentate gyrus mediates behavioral responses to ambiguous threat cues. *PLOS Biology* 15(4): e2001154.

Godbout JP, Moreau M, Lestage J, Chen J, Sparkman NL, Connor JO, Castanon N, Kelley KW, Dantzer R and Johnson RW (2007) Aging Exacerbates Depressive-like Behavior in Mice in Response to Activation of the Peripheral Innate Immune System. *Neuropsychopharmacology* 33(10): 2341–2351.

Gold PW (2015) The organization of the stress system and its dysregulation in depressive illness. *Molecular Psychiatry* 20(1): 32–47.

Gottesman II and Gould TD (2003) The endophenotype concept in psychiatry: Etymology and strategic intentions. *American Journal of Psychiatry* 160(4): 636–645.

Gould E, Cameron HA a, Daniels DCC, Woolley CSS and McEwen BSS (1992) Adrenal hormones suppress cell division in the adult rat dentate gyrus. *The Journal of Neuroscience* 12(September): 3642–3650.

Gould E, McEwen BSS, Tanapat P, Galea LAMA and Fuchs E (1997) Neurogenesis in the dentate gyrus of the adult tree shrew is regulated by psychosocial stress and NMDA receptor activation. *The Journal of Neuroscience* 17(7): 2492–2498.

Gould E, Tanapat P, McEwen BS, Flügge G and Fuchs E (1998) Proliferation of granule cell precursors in the dentate gyrus of adult monkeys is diminished by stress. *Proceedings of the National Academy of Sciences of the United States of America* 95(6): 3168–3171.

Gould NF, Holmes MK, Fantie BD, Luckenbaugh DA, Pine DS, Gould TD, Burgess N, Manji HK ZCJ (2007) Gould 2007 Performance on a virtual reality spatial memory navigation task in depressive patients. *American Journal of Psychiatry*, American Psychiatric Association 164(March): 516–519.

Gould TD (2009) *Mood and anxiety related phenotypes in mice*. Gould TD (ed.), *Neuromethods*. 42:297-326

Goveas J, Xie C, Wu Z, Douglas Ward B, Li W, Franczak MB, Jones JL, Antuono PG, Yang Z and Li SJ (2011) Neural correlates of the interactive relationship between memory deficits and depressive symptoms in nondemented elderly: Resting fMRI study. *Behavioural Brain Research* 219(2): 205–212.

Graciarena M, Roca V, Mathieu P, Depino AM and Pitossi FJ (2013) Differential vulnerability of adult neurogenesis by adult and prenatal inflammation: Role of TGF-β1. *Brain, Behavior, and Immunity*, Elsevier Inc. 34(null): 17–28.

Gray JD, Rubin TG, Hunter RG and McEwen BS (2014) Hippocampal gene expression changes underlying stress sensitization and recovery. *Molecular Psychiatry*, Nature Publishing Group 19(11): 1171–1178.

Grayton HM, Missler M, Collier DA and Fernandes C (2013) Altered Social Behaviours in Neurexin 1α Knockout Mice Resemble Core Symptoms in Neurodevelopmental Disorders. *PLoS ONE* 8(6): e67114.

Griebel G, Belzung C, Perrault G and Sanger DJ (2000) Differences in anxiety-related behaviours and in sensitivity to diazepam in inbred and outbred strains of mice. *Psychopharmacology*, Springer-Verlag 148(2): 164–170.

Griebel G, Simiand J, Serradeil-Le Gal C, Wagnon J, Pascal M, Scatton B, Maffrand J-P and Soubrie P (2002) Anxiolytic- and antidepressant-like effects of the non-peptide vasopressin V1b receptor antagonist, SSR149415, suggest an innovative approach for the

treatment of stress-related disorders. *Proceedings of the National Academy of Sciences of the United States of America* 99(9): 6370–5.

Guan XT, Lin WJ and Tang MM (2015) Comparison of stress-induced and LPS-induced depressive-like behaviors and the alterations of central proinflammatory cytokines mRNA in rats. *Chinese Psychology Journal* 4(3): 113–122.

Guidotti G, Calabrese F, Anacker C, Racagni G, Pariante CM and Riva MA (2013) Glucocorticoid Receptor and FKBP5 Expression Is Altered Following Exposure to Chronic Stress: Modulation by Antidepressant Treatment. *Neuropsychopharmacology*, Nature Publishing Group 38(4): 616–627.

Gundersen HJG (1977) Notes on the estimation of the numerical density of arbitrary profiles: the edge effect. *Journal of Microscopy* 111(2): 219–223.

Guo J, Lin P, Zhao X, Zhang J, Wei X, Wang Q and Wang C (2014) Etazolate abrogates the lipopolysaccharide (LPS)-induced downregulation of the cAMP/pCREB/BDNF signaling, neuroinflammatory response and depressive-like behavior in mice. *Neuroscience* 263: 1–14.

Hains AB, Vu MAT, Maciejewski PK, van Dyck CH, Gottron M and Arnsten AFT (2009) Inhibition of protein kinase C signaling protects prefrontal cortex dendritic spines and cognition from the effects of chronic stress. *Proceedings of the National Academy of Sciences of the United States of America* 106(42): 17957–62.

Hains AB, Yabe Y and Arnsten AFT (2015) Chronic stimulation of alpha-2A-adrenoceptors with guanfacine protects rodent prefrontal cortex dendritic spines and cognition from the effects of chronic stress. *Neurobiology of Stress* 2: 1–9.

Hamilton JP, Etkin A, Furman DJ, Lemus MG, Johnson RF and Gotlib IH (2012) Functional neuroimaging of major depressive disorder: A meta-analysis and new integration of baseline activation and neural response data. *American Journal of Psychiatry* 169(7): 693-703.

Han J, Kim HJ, Schafer ST, Paquola A, Clemenson GD, Toda T, Oh J, Pankonin AR, Lee BS, Johnston ST, Sarkar A, Denli AM and Gage FH (2016) Functional Implications of miR-19 in the Migration of Newborn Neurons in the Adult Brain. *Neuron*, Elsevier Inc. 91(1): 79–89.

Hardeveld F, Spijker J, Vreeburg SA, De Graaf R, Hendriks SM, Licht CMM, Nolen WA, Penninx BWJH and Beekman ATF (2014) Increased cortisol awakening response was associated

with time to recurrence of major depressive disorder. *Psychoneuroendocrinology* 50: 62–71.

Harrison NA, Brydon L, Walker C, Gray MA, Steptoe A and Critchley HD (2009) Inflammation Causes Mood Changes Through Alterations in Subgenual Cingulate Activity and Mesolimbic Connectivity. *Biological Psychiatry* 66(5): 407–414.

Hemanth Kumar BS, Mishra SK, Trivedi R, Singh S, Rana P and Khushu S (2014) Demyelinating evidences in CMS rat model of depression: A DTI study at 7T. *Neuroscience*, IBRO 275: 12–21.

Henry CCJ, Huang Y, Wynne A, Hanke M, Himler J, Bailey MT, Sheridan JF, Godbout JPJ, Kelley K, Bluthe R, Dantzer R, Zhou J, Shen W, Johnson RR, Broussard S, Konsman J, Luheshi G, … Johnson RR (2008) Minocycline attenuates lipopolysaccharide (LPS)-induced neuroinflammation, sickness behavior, and anhedonia. *Journal of Neuroinflammation* 5(1): 15.

Hepgul N, Cattaneo A, Agarwal K, Baraldi S, Borsini A, Bufalino C, Forton DM, Mondelli V, Nikkheslat N, Lopizzo N, Riva MA, Russell A, Hotopf M and Pariante CM (2016) Transcriptomics in Interferon-α-Treated Patients Identifies Inflammation-, Neuroplasticity- and Oxidative Stress-Related Signatures as Predictors and Correlates of Depression. *Neuropsychopharmacology* 41(10): 2502–2511.

Hill AS, Sahay A and Hen R (2015) Increasing Adult Hippocampal Neurogenesis is Sufficient to Reduce Anxiety and Depression-Like Behaviors. *Neuropsychopharmacology* 40(10): 2368–2378.

Hill MN, Hellemans KGC, Verma P, Gorzalka BB and Weinberg J (2012) Neurobiology of chronic mild stress: Parallels to major depression. *Neuroscience and Biobehavioral Reviews*, Elsevier Ltd 36(9): 2085-2117.

Hill RA, Klug M, Kiss Von Soly S, Binder MD, Hannan AJ and van Den Buuse M (2014) Sex-specific disruptions in spatial memory and anhedonia in a 'two hit' rat model correspond with alterations in hippocampal brain-derived neurotrophic factor expression and signaling. *Hippocampus* 24(10): 1197–1211.

Hinwood M, Morandini J, Day TA and Walker FR (2012) Evidence that microglia mediate the neurobiological effects of chronic psychological stress on the medial prefrontal cortex. *Cerebral Cortex* 22(6): 1442–1454.

Hinwood M, Tynan RJ, Charnley JL, Beynon SB, Day TA and Walker FR (2013) Chronic stress induced remodeling of the prefrontal cortex: Structural re-organization of microglia and the inhibitory effect of minocycline. *Cerebral Cortex* 23(8): 1784–1797.

Hiscott J and Ware C (2011) Cytokines. *Current Opinion in Immunology* 23(5): 561–3.

Ho Y-H, Lin Y-T, Wu C-WJ, Chao Y-M, Chang AYW and Chan JYH (2015) Peripheral inflammation increases seizure susceptibility via the induction of neuroinflammation and oxidative stress in the hippocampus. *Journal of Biomedical Science* 22(1): 46.

Hodes GE, Kana V, Menard C, Merad M and Russo SJ (2015) Neuroimmune mechanisms of depression. *Nature Neuroscience* 18(10): 1386–1393.

Holsboer F (2000) The corticosteroid receptor hypothesis of depression. *Neuropsychopharmacology* 23(5): 477-501.

Hornig J, Fröb F, Vogl MR, Hermans-Borgmeyer I, Tamm ER and Wegner M (2013) The Transcription Factors Sox10 and Myrf Define an Essential Regulatory Network Module in Differentiating Oligodendrocytes. *PLoS Genetics* 9(10): e1003907.

Horowitz MA, Zunszain PA, Anacker C, Musaelyan K and Pariante CM (2013) Glucocorticoids and Inflammation: A Double-Headed Sword in Depression? In: *Modern trends in pharmacopsychiatry*, pp. 127–143.

Hu F, Pace TWW and Miller AH (2009) Interferon-alpha inhibits glucocorticoid receptor-mediated gene transcription via STAT5 activation in mouse HT22 cells. *Brain, Behavior, and Immunity* 23(4): 455–463.

Husain MI, Chaudhry IB, Rahman RR, Hamirani MM, Qurashi I, Khoso AB, Deakin JF, Husain N and Young AH (2015) Minocycline as an adjunct for treatment-resistant depressive symptoms: study protocol for a pilot randomised controlled trial. *Trials* 16(1): 410.

Hye A, Riddoch-Contreras J, Baird AL, Ashton NJ, Bazenet C, Leung R, Westman E, Simmons A, Dobson R, Sattlecker M, Lupton M, Lunnon K, Keohane A, Ward M, Pike I, Zucht HD, Pepin D, … Lovestone S (2014) Plasma proteins predict conversion to dementia from prodromal disease. *Alzheimer's and Dementia* 10(6): 799–807.

Hyman S (2014) Mental health: depression needs large human-genetics studies. *Nature* 515(7526): 189–91.

Ibarguen-Vargas Y, Surget A, Touma C, Palme R and Belzung C (2008) Multifaceted strain-

specific effects in a mouse model of depression and of antidepressant reversal. *Psychoneuroendocrinology* 33(10): 1357–1368.

Ieraci A, Mallei A and Popoli M (2016) Social Isolation Stress Induces Anxious-Depressive-Like Behavior and Alterations of Neuroplasticity-Related Genes in Adult Male Mice. *Neural Plasticity* 2016: 6212983.

Iii HEC, Maze I, Vialou V and Nestler EJ (2015) Antidepressant action of hdac inhibition in the prefrontal cortex. *Neuroscience*, IBRO 298: 329–335.

Incollingo Rodriguez AC, Epel ES, White ML, Standen EC, Seckl JR and Tomiyama AJ (2015) Hypothalamic-pituitary-adrenal axis dysregulation and cortisol activity in obesity: A systematic review. *Psychoneuroendocrinology*, Elsevier Ltd 62: 301–318.

Ito H, Nagano M, Suzuki H and Murakoshi T (2010) Chronic stress enhances synaptic plasticity due to disinhibition in the anterior cingulate cortex and induces hyper-locomotion in mice. *Neuropharmacology*, Elsevier Ltd 58(4–5): 746–757.

Jacobs BL, van Praag H and Gage FH (2000) Adult brain neurogenesis and psychiatry: a novel theory of depression. *Molecular psychiatry* 5(November 1999): 262–269.

Jayatissa MN, Bisgaard C, Tingström A, Papp M and Wiborg O (2006) Hippocampal Cytogenesis Correlates to Escitalopram-Mediated Recovery in a Chronic Mild Stress Rat Model of Depression. *Neuropsychopharmacology* 31(11): 2395–2404.

Jayatissa MN, Henningsen K, West MJ and Wiborg O (2009) Decreased cell proliferation in the dentate gyrus does not associate with development of anhedonic-like symptoms in rats. *Brain Research*, Elsevier B.V. 1290: 133–141.

Jeon CJ, Strettoi E and Masland RH (1998) The major cell populations of the mouse retina. *Journal of Neuroscience* 18(21): 8936–8946.

Jeong JY, Lee DH and Kang SS (2013) Effects of chronic restraint stress on body weight, food intake, and hypothalamic gene expressions in mice. *Endocrinology and Metabolism* 28(4): 288–96.

Jessberger S, Zhao C, Toni N, Clemenson GD, Li Y and Gage FH (2007) Seizure-Associated, Aberrant Neurogenesis in Adult Rats Characterized with Retrovirus-Mediated Cell Labeling. *Journal of Neuroscience* 27(35): 9400–9407.

Jessberger S and Kempermann G (2003) Adult-born hippocampal neurons mature into activity-

dependent responsiveness. *European Journal of Neuroscience*, Blackwell Science Ltd 18(10): 2707–2712.

Jiang WG, Li SX, Zhou SJ, Sun Y, Shi J and Lu L (2011) Chronic unpredictable stress induces a reversible change of PER2 rhythm in the suprachiasmatic nucleus. *Brain Research*, Elsevier B.V. 1399: 25–32.

Jungke P, Ostrow G, Li JL, Norton S, Nieber K, Kelber O and Butterweck V (2011) Profiling of hypothalamic and hippocampal gene expression in chronically stressed rats treated with St. John's wort extract (STW 3-VI) and fluoxetine. *Psychopharmacology* 213(4): 757–772.

Kaiser RH, Andrews-Hanna JR, Wager TD and Pizzagalli DA (2015) Large-Scale Network Dysfunction in Major Depressive Disorder: A Meta-analysis of Resting-State Functional Connectivity. *JAMA psychiatry* 72(6): 603–11.

Kammula US, White DE and Rosenberg SA (1998) Trends in the safety of high dose bolus interleukin-2 administration in patients with metastatic cancer. *Cancer* 83(4): 797–805.

Kas MJH, Fernandes C, Schalkwyk LC and Collier D a (2007) Genetics of behavioural domains across the neuropsychiatric spectrum; of mice and men. *Molecular psychiatry* 12(4): 324–30.

Katz RJ (1982) Animal model of depression: Pharmacological sensitivity of a hedonic deficit. *Pharmacology, Biochemistry and Behavior* 16(6): 965–968.

Kempermann G (2003) Early determination and long-term persistence of adult-generated new neurons in the hippocampus of mice. *Development* 130(2): 391–399.

Kempermann G (2010) Adult Hippocampal Neurogenesis. 2nd ed. In: *Adult Neurogenesis*, Oxford University Press, pp. 1–85.

Kendler KS, Karkowski LM and Prescott CA (1999) Causal Relationship Between Stressful Life Events and the Onset of Major Depression. *Psychiatry Interpersonal and Biological Processes* 156(June): 837–841.

Kettner NM, Mayo SA, Hua J, Lee C, Moore DD and Fu L (2015) Circadian dysfunction induces leptin resistance in mice. *Cell Metabolism*, NIH Public Access 22(3): 448–459.

Khemissi W, Farooq RK, Le Guisquet A-M, Sakly M and Belzung C (2014) Dysregulation of the hypothalamus-pituitary-adrenal axis predicts some aspects of the behavioral response to chronic fluoxetine: association with hippocampal cell proliferation. *Frontiers in Behavioral*

Neuroscience 8(September): 1–9.

Kim I-J, Beck HN, Lein PJ and Higgins D (2002) Interferon gamma induces retrograde dendritic retraction and inhibits synapse formation. *The Journal of Neuroscience* 22(11): 4530–4539.

Kim JJ, Song EY, Kim JJ, Song EY and Kosten TA (2006) Stress effects in the hippocampus: Synaptic plasticity and memory. *Stress* 9(1): 1–11.

Kim S, Lee S, Ryu S, Suk J and Park C (2002) Comparative analysis of the anxiety-related behaviors in four inbred mice. *Behavioural Processes* 60(2): 181–190.

Kinoshita C, Miyazaki K and Ishida N (2012) Chronic stress affects PERIOD2 expression through glycogen synthase kinase-3β phosphorylation in the central clock. *NeuroReport* 23(2): 98–102.

Knorr U, Vinberg M, Kessing L V and Wetterslev J (2010) Salivary cortisol in depressed patients versus control persons: a systematic review and meta-analysis. *Psychoneuroendocrinology* 35(9): 1275–86.

Kocabas NA, Antonijevic I, Faghel C, Forray C, Kasper S, Lecrubier Y, Linotte S, Massat I, Mendlewicz J, Noro M, Montgomery S, Oswald P, Snyder L, Zohar J and Souery D (2011) Brain-derived neurotrophic factor gene polymorphisms: influence on treatment response phenotypes of major depressive disorder. *International Clinical Psychopharmacology* 26(1): 1–10.

Kohman RA and Rhodes JS (2013) Neurogenesis, inflammation and behavior. *Brain, Behavior, and Immunity*, Elsevier Inc. 27(1): 22–32.

Kondo S, Kohsaka S and Okabe S (2011) Long-term changes of spine dynamics and microglia after transient peripheral immune response triggered by LPS in vivo. *Molecular Brain* 4(1): 27.

Koo JW and Duman RS (2008) IL-1beta is an essential mediator of the antineurogenic and anhedonic effects of stress. *Proceedings of the National Academy of Sciences of the United States of America* 105(2): 751–6.

Kopp BL, Wick D and Herman JP (2013) Differential effects of homotypic vs. heterotypic chronic stress regimens on microglial activation in the prefrontal cortex. *Physiology and Behavior* 122: 246–252.

Kopp C, Vogel E, Rettori M-C, Delagrange P, Guardiola-Lemaître B and Misslin R (1999) Effects of Melatonin on Neophobic Responses in Different Strains of Mice. *Pharmacology Biochemistry and Behavior* 63(4): 521–526.

Kopp C, Vogel E, Rettori MC, Delagrange P and Misslin R (1999a) The effects of melatonin on the behavioural disturbances induced by chronic mild stress in C3H/He mice. *Behavioural Pharmacology* 10(1): 73–83.

Korosi A, Naninck EFG, Oomen CA, Schouten M, Krugers H, Fitzsimons C and Lucassen PJ (2012) Early-life stress mediated modulation of adult neurogenesis and behavior. *Behavioural Brain Research* 227(2): 400-409.

Koszycki D, Copen J and Bradwejn J (2004) Sensitivity to cholecystokinin-tetrapeptide in major depression. *Journal of Affective Disorders* 80(2–3): 285–290.

Kreisel T, Frank MG, Licht T, Reshef R, Ben-Menachem-Zidon O, Baratta M V, Maier SF and Yirmiya R (2014) Dynamic microglial alterations underlie stress-induced depressive-like behavior and suppressed neurogenesis. *Molecular Psychiatry* 19(6): 699–709.

Krishnan V and Nestler EJ (2008) The molecular neurobiology of depression. *Nature* 455(7215): 894–902.

Kroeze Y, Peeters D, Boulle F, van den Hove DLA, van Bokhoven H, Zhou H and Homberg JR (2015) Long-term consequences of chronic fluoxetine exposure on the expression of myelination-related genes in the rat hippocampus. *Translational Psychiatry*, Nature Publishing Group 5(9): e642.

Kronenberg G, Reuter K, Steiner B, Brandt MD, Jessberger S, Yamaguchi M and Kempermann G (2003) Subpopulations of Proliferating Cells of the Adult Hippocampus Respond Differently to Physiologic Neurogenic Stimuli. *Journal of Comparative Neurology* 467(4): 455–463.

Kubera M, Basta-Kaim A, Holan V, Simbirtsev A, Roman A, Pigareva N, Prokopieva E and Sham J (1998) Effect of mild chronic stress, as a model of depression, on the immunoreactivity of C57BL/6 mice. *International Journal of Immunopharmacology* 20(12): 781–9.

Kubera M, Curzytek K, Duda W, Leskiewicz M, Basta-Kaim A, Budziszewska B, Roman A, Zajicova A, Holan V, Szczesny E, Lason W and Maes M (2013) A new animal model of (chronic) depression induced by repeated and intermittent lipopolysaccharide administration for 4 months. *Brain Behaviour Immunity*, Elsevier Inc. 31: 96–104.

Kuwabara T, Hsieh J, Muotri A, Yeo G, Warashina M, Lie DC, Moore L, Nakashima K, Asashima M, Fred H and Gage FH (2009) NIH Public Access. *Nature Neuroscience*, Nature Publishing Group 12(9): 1097–1105.

Lad HV, Liu L, Paya-Cano JL, Parsons MJ, Kember R, Fernandes C and Schalkwyk LC (2010) Behavioural battery testing: Evaluation and behavioural outcomes in 8 inbred mouse strains. *Physiology and Behavior* 99(3): 301–316.

Lagace DC, Donovan MH, DeCarolis NA, Farnbauch LA, Malhotra S, Berton O, Nestler EJ, Krishnan V and Eisch AJ (2010) Adult hippocampal neurogenesis is functionally important for stress-induced social avoidance. *Proceedings of the National Academy of Sciences of the United States of America*, National Academy of Sciences 107(9): 4436–41.

Lanquillon S, Krieg JC, Bening-Abu-Shach U and Vedder H (2000) Cytokine production and treatment response in major depressive disorder. *Neuropsychopharmacology* 22(4): 370–379.

LaPlant Q, Vialou V, Covington HE, Dumitriu D, Feng J, Warren BL, Maze I, Dietz DM, Watts EL, Iñiguez SD, Koo JW, Mouzon E, Renthal W, Hollis F, Wang H, Noonan MA, Ren Y, … Nestler EJ (2010) Dnmt3a regulates emotional behavior and spine plasticity in the nucleus accumbens. *Nature Neuroscience* 13(9): 1137–1143.

Law J, Ibarguen-Vargas Y, Belzung C and Surget A (2016) Decline of hippocampal stress reactivity and neuronal ensemble coherence in a mouse model of depression. *Psychoneuroendocrinology*, Elsevier Ltd 67: 113–123.

Le François B, Czesak M, Steubl D and Albert PR (2008) Transcriptional regulation at a HTR1A polymorphism associated with mental illness. *Neuropharmacology* 55(6): 977–85.

Leavitt BR, Van Raamsdonk JM, Shehadeh J, Fernandes H, Murphy Z, Graham RK, Wellington CL, Raymond LA and Hayden MR (2006) Wild-type huntingtin protects neurons from excitotoxicity. *Journal of Neurochemistry* 96(4): 1121–1129.

Lemoine FM, Cherai M, Giverne C, Dimitri D, Rosenzwajg M, Trebeden-Negre H, Chaput N, Barrou B, Thioun N, Gattegnio B, Selles F, Six A, Azar N, Lotz JP, Buzyn A, Sibony M, Delcourt A, … Lacave R (2009) Massive expansion of regulatory T-cells following interleukin 2 treatment during a phase I-II dendritic cell-based immunotherapy of metastatic renal cancer. *International Journal of Oncology* 35(3): 569–581.

Levkovitz Y, Harel E V, Roth Y, Braw Y, Most D, Katz LN, Sheer A, Gersner R and Zangen A

(2009) Deep transcranial magnetic stimulation over the prefrontal cortex: Evaluation of antidepressant and cognitive effects in depressive patients. *Brain Stimulation* 2(4): 188–200.

Lewis SR, Ahmed S, Dym C, Khaimova E, Kest B and Bodnar RJ (2005) Inbred mouse strain survey of sucrose intake. *Physiology & Behavior* 85(5): 546–556.

Li JZ, Bunney BG, Meng F, Hagenauer MH, Walsh DM and Vawter MP (2013) Circadian patterns of gene expression in the human brain and disruption in major depressive disorder. *Proceedings of the National Academy of Sciences of the United States of America* 110: 9950–9955.

Li N, Liu RJ, Dwyer JM, Banasr M, Lee B, Son H, Li XY, Aghajanian G and Duman RS (2011) Glutamate N-methyl-D-aspartate receptor antagonists rapidly reverse behavioral and synaptic deficits caused by chronic stress exposure. *Biological Psychiatry* 69(8): 754–761.

Lim DA and Alvarez-Buylla A (2016) The Adult Ventricular – Subventricular Zone and Olfactory bulb Neurogenesis. *Cold Spring Harbor perspectives in biology* 8(a018820).

Lin SM, Du P, Huber W and Kibbe WA (2008) Model-based variance-stabilizing transformation for Illumina microarray data. *Nucleic Acids Research* 36(2): e11.

Liston C, Miller MM, Goldwater DS, Radley JJ, Rocher AB, Hof PR, Morrison JH and Mcewen BS (2006) Stress-Induced Alterations in Prefrontal Cortical Dendritic Morphology Predict Selective Impairments in Perceptual Attentional Set-Shifting. *Journal of Neuroscience* 26(30): 7870–7874.

Liu D, Xie K, Yang X, Gu J, Ge L, Wang X and Wang Z (2014) Resveratrol reverses the effects of chronic unpredictable mild stress on behavior, serum corticosterone levels and BDNF expression in rats. *Behavioural Brain Research* 264: 9–16.

Liu J, Dupree JL, Gacias M, Frawley R, Sikder T, Naik P and Casaccia P (2016) Clemastine Enhances Myelination in the Prefrontal Cortex and Rescues Behavioral Changes in Socially Isolated Mice. *Journal of Neuroscience* 36(3): 957–962.

Liu W, Wang H, Wang Y, Li H and Ji L (2015) Metabolic factors-triggered inflammatory response drives antidepressant effects of exercise in CUMS rats. *Psychiatry Research* 228(3): 257–264.

Liu Y, Ho RC-M and Mak A (2012) Interleukin (IL)-6, tumour necrosis factor alpha (TNF-α) and soluble interleukin-2 receptors (sIL-2R) are elevated in patients with major depressive

disorder: a meta-analysis and meta-regression. *Journal of affective disorders* 139(3): 230–9.

Liu Y, Yang N and Zuo P (2010) CDNA microarray analysis of gene expression in the cerebral cortex and hippocampus of BALB/c mice subjected to chronic mild stress. *Cellular and Molecular Neurobiology* 30(7): 1035–1047.

Logan RW, Edgar N, Gillman AG, Hoffman D, Zhu X and McClung CA (2015a) Chronic Stress Induces Brain Region-Specific Alterations of Molecular Rhythms that Correlate with Depression-like Behavior in Mice. *Biological Psychiatry*, Elsevier 78(4): 249–258.

Logan RW, Edgar N, Gillman AG, Hoffman D, Zhu X and McClung CA (2015b) Supplemental Information: Chronic Stress Induces Brain Region Specific Alterations of Molecular Rhythms in Mice that Correlate with Depression-Like Behavior. *Biological Psychiatry* 78(4): 1–11.

López-Collazo E and Del Fresno C (2013) Pathophysiology of endotoxin tolerance: mechanisms and clinical consequences. *Critical Care* 17(6): 242.

Lopez-Munoz F and Alamo C (2009) Monoaminergic Neurotransmission: The History of the Discovery of Antidepressants from 1950s Until Today. *Current Pharmaceutical Design* 15(14): 1563–1586.

Lorenzetti V, Allen NB, Fornito A and Yucel M (2009) Structural brain abnormalities in major depressive disorder: A selective review of recent MRI studies. *Journal of Affective Disorders*, Elsevier B.V. 117(1–2): 1–17.

Lu J, Shao R-H, Hu L, Tu Y and Guo J-Y (2016) Potential antiinflammatory effects of acupuncture in a chronic stress model of depression in rats. *Neuroscience Letters* 618: 31–38.

Lu M, Yang J-Z, Geng F, Ding J-H and Hu G (2014) Iptakalim confers an antidepressant effect in a chronic mild stress model of depression through regulating neuro-inflammation and neurogenesis. *The International Journal of Neuropsychopharmacology*, The Oxford University Press 17(9): 1501–1510.

Lu S, Gao W, Huang M, Li L and Xu Y (2016) In search of the HPA axis activity in unipolar depression patients with childhood trauma: Combined cortisol awakening response and dexamethasone suppression test. *Journal of Psychiatric Research* 78: 24–30.

Lu X-Y, Kim CS, Frazer A and Zhang W (2006) Leptin: a potential novel antidepressant. *Proceedings of the National Academy of Sciences of the United States of America* 103(5):

1593–8.

Lucassen PJ, Stumpel MW, Wang Q and Aronica E (2010) Decreased numbers of progenitor cells but no response to antidepressant drugs in the hippocampus of elderly depressed patients. *Neuropharmacology*, Elsevier Ltd 58(6): 940–949.

Lucki I, Dalvi A and Mayorga AJ (2001) Sensitivity to the effects of pharmacologically selective antidepressants in different strains of mice. *Psychopharmacology* 155(3): 315–22.

Luo Y, Cao Z, Wang D, Wu L, Li Y, Sun W and Zhu Y (2014) Dynamic study of the hippocampal volume by structural MRI in a rat model of depression. *Neurological Sciences* 35(11): 1777–1783.

Lussier AL, Lebedeva K, Fenton EY, Guskjolen A, Caruncho HJ and Kalynchuk LE (2013) The progressive development of depression-like behavior in corticosterone-treated rats is paralleled by slowed granule cell maturation and decreased reelin expression in the adult dentate gyrus. *Neuropharmacology*, Elsevier Ltd 71: 174–183.

Maes M, Meltzer HY, Bosmans E, Bergmans R, Vandoolaeghe E, Ranjan R and Desnyder R (1995) Increased plasma concentrations of interleukin-6, soluble interleukin-6, soluble interleukin-2 and transferrin receptor in major depression. *Journal of Affective Disorders* 34(4): 301–309.

Maier SF and Watkins LR (2010) Role of the medial prefrontal cortex in coping and resilience. *Brain Research*, Elsevier B.V. 1355: 52–60.

Malberg JE and Duman RS (2003) Cell Proliferation in Adult Hippocampus is Decreased by Inescapable Stress: Reversal by Fluoxetine Treatment. *Neuropsychopharmacology* 28(9): 1562–1571.

Malberg JE, Eisch AJ, Nestler EJ and Duman RS (2000) Chronic antidepressant treatment increases neurogenesis in adult rat hippocampus. *The Journal of Neuroscience* 20(24): 9104–9110.

Malki K, Tosto MG, Pain O, Sluyter F, Mineur YS, Crusio WE, de Boer S, Sandnabba KN, Kesserwani J, Robinson E, Schalkwyk LC and Asherson P (2016) Comparative mRNA analysis of behavioral and genetic mouse models of aggression. *American Journal of Medical Genetics, Part B: Neuropsychiatric Genetics* 171(3): 427–436.

Malki K, Tosto MG, Jumabhoy I, Lourusamy A, Sluyter F, Craig IW, McGuffin P, Schalkwyk LC, Lourdusamy A, Sluyter F, Craig IW, Uher R, McGuffin P, Schalkwyk LC, Lourusamy A,

Sluyter F, Craig IW, … Schalkwyk LC (2013) Integrative mouse and human mRNA studies using WGCNA nominates novel candidate genes involved in the pathogenesis of major depressive disorder. *Pharmacogenomics* 14(16): 1979–1990.

Malki K, Mineur YS, Tosto MG, Campbell J, Karia P, Jumabhoy I, Sluyter F, Crusio WE and Schalkwyk LC (2015) Pervasive and opposing effects of Unpredictable Chronic Mild Stress (UCMS) on hippocampal gene expression in BALB/cJ and C57BL/6J mouse strains. *BMC Genomics* 16(1): 262.

Manning EE, Ransome MI, Burrows EL and Hannan AJ (2012) Increased adult hippocampal neurogenesis and abnormal migration of adult-born granule neurons is associated with hippocampal-specific cognitive deficits in phospholipase C-β1 knockout mice. *Hippocampus* 22(2): 309–319.

Marino F and Cosentino M (2013) Adrenergic modulation of immune cells: An update. *Amino Acids*.

Matsubara T, Funato H, Kobayashi A, Nobumoto M and Watanabe Y (2006) Reduced glucocorticoid receptor expression in mood disorder patients and first-degree relatives. *Biological Psychiatry* 59(8): 689–695.

Mayer JL, Klumpers L, Maslam S, de Kloet ER, Joels M and Lucassen PJ (2006) Brief treatment with the glucocorticoid receptor antagonist mifepristone normalises the corticosterone-induced reduction of adult hippocampal neurogenesis. *Journal of Neuroendocrinology* 18(8): 629–631.

McEwen B and Morrison J (2013) The Brain on Stress: Vulnerability and Plasticity of the Prefrontal Cortex over the Life Course. *Neuron*, Elsevier Inc. 79(1): 16–29.

McEwen BS (1999) Stress and hippocampal plasticity. *Annual Review of Neuroscience* 22(1): 105–122.

McGowan PO, Sasaki A, D'Alessio AC, Dymov S, Labonté B, Szyf M, Turecki G and Meaney MJ (2009) Epigenetic regulation of the glucocorticoid receptor in human brain associates with childhood abuse. *Nature Neuroscience* 12(3): 342–348.

McKay MS and Zakzanis KK (2010) The impact of treatment on HPA axis activity in unipolar major depression. *Journal of Psychiatric Research* 44(3):183-192.

McKinney WTWT and Bunney WE (1969) Animal Model of Depression. *Archives of General Psychiatry*, American Medical Association 21(2): 240.

Meijer MK, Spruijt BM, van Zutphen LFM and Baumans V (2006) Effect of restraint and injection methods on heart rate and body temperature in mice. *Laboratory Animals*, SAGE PublicationsSage UK: London, England 40(4): 382–391.

Meijering E, Jacob M, Sarria JCF, Steiner P, Hirling H and Unser M (2004) Design and validation of a tool for neurite tracing and analysis in fluorescence microscopy images. *Cytometry. Part A: The Journal of the International Society for Analytical Cytology* 58A(2): 167–176.

Merz K and Lie DC (2013) Evidence that Doublecortin Is Dispensable for the Development of Adult Born Neurons in Mice. *PLoS ONE* 8(5): e62693.

Miles J and Shelvin M (2001) *Applying regression and correlation : a guide for students and researchers*. London: SAGE Publications.

Milior G, Lecours C, Samson L, Bisht K, Poggini S, Pagani F, Deflorio C, Lauro C, Alboni S, Limatola C, Branchi I, Tremblay ME and Maggi L (2016) Fractalkine receptor deficiency impairs microglial and neuronal responsiveness to chronic stress. *Brain, Behavior, and Immunity*, Elsevier Inc. 55: 114–125.

Miller AH, Maletic V and Raison CL (2009) Inflammation and Its Discontents: The Role of Cytokines in the Pathophysiology of Major Depression. *Biological Psychiatry* 65(9): 732-741.

Miller BR and Hen R (2015) The current state of the neurogenic theory of depression and anxiety. *Current Opinion in Neurobiology* 30: 51–58.

Mineur YS, Belzung C and Crusio WE (2006) Effects of unpredictable chronic mild stress on anxiety and depression-like behavior in mice. *Behavioural Brain Research* 175(1): 43–50.

Mineur YS, Belzung C and Crusio WE (2007) Functional implications of decreases in neurogenesis following chronic mild stress in mice. *Neuroscience* 150(2): 251–259.

Ming G and Song H (2005) Adult neurogenesis in the mammalian central nervous system. *Annual Review of Neuroscience* 28(1): 223–250.

Miyaoka T, Wake R, Furuya M, Liaury K, Ieda M, Kawakami K, Tsuchie K, Taki M, Ishihara K, Araki T and Horiguchi J (2012) Minocycline as adjunctive therapy for patients with unipolar psychotic depression: An open-label study. *Progress in Neuropsychopharmacology & Biological Psychiatry*, Elsevier Inc. 37(2): 222–226.

Miyata S, Taniguchi M, Koyama Y, Shimizu S, Tanaka T, Yasuno F, Yamamoto A, Iida H, Kudo T,

Katayama T and Tohyama M (2016) Association between chronic stress-induced structural abnormalities in Ranvier nodes and reduced oligodendrocyte activity in major depression. *Scientific Reports*, Nature Publishing Group 6(February): 23084.

Monje ML (2003) Inflammatory Blockade Restores Adult Hippocampal Neurogenesis. *Science* 302(5651): 1760–1765.

Moreau M, André C, O'Connor JC, Dumich SA, Woods JA, Kelley KW, Dantzer R, Lestage J and Castanon N (2008) Inoculation of Bacillus Calmette-Guerin to mice induces an acute episode of sickness behavior followed by chronic depressive-like behavior. *Brain, Behavior, and Immunity* 22(7): 1087–1095.

Morris MC, Gilliam EA and Li L (2015) Innate immune programing by endotoxin and its pathological consequences. *Frontiers in Immunology* 6(JAN): 1-8.

Mössner R, Mikova O, Koutsilieri E, Saoud M, Ehlis A-C, Müller N, Fallgatter AJ and Riederer P (2007) Consensus paper of the WFSBP Task Force on Biological Markers: biological markers in depression. *The World Journal of Bological Psychiatry* 8(3): 141–74.

Motivala SJ, Sarfatti A, Olmos L and Irwin MR (2005) Inflammatory Markers and Sleep Disturbance in Major Depression. *Psychosomatic Medicine* 67(2): 187–194.

Mrazek DA, Rush AJ, Biernacka JM, O'Kane DJ, Cunningham JM, Wieben ED, Schaid DJ, Drews MS, Courson VL, Snyder KA, Black JL and Weinshilboum RM (2011) SLC6A4 variation and citalopram response. *Pharmacogenetics and Genomics* 21(1): 1–9.

Mu Y, Lee SW and Gage FH (2010) Signaling in adult neurogenesis. *Current Opinion in Neurobiology* 20(4): 416-423.

Müller HK, Wegener G, Popoli M and Elfving B (2011) Differential expression of synaptic proteins after chronic restraint stress in rat prefrontal cortex and hippocampus. *Brain Research*, Elsevier B.V. 1385: 26–37.

Murphy K, Travers P and Walport M (2011) Innate Immunity : The First Lines of Defense. In: *Janeway's Immunobiology*, pp. 37–73.

Musselman DL, Lawson DH, Gumnick JF, Manatunga AK, Penna S, Goodkin RS, Greiner K, Nemeroff CB and Miller AH (2001) Paroxetine for the Prevention of Depression Induced by High-Dose Interferon Alfa. *New England Journal of Medicine* 344(13): 961–966.

Mutlu O, Gumuslu E, Ulak G, Komsuoglu I, Kokturk S, Maral H, Akar F and Erden F (2012)

Effects of fluoxetine , tianeptine and olanzapine on unpredictable chronic mild stress-induced depression-like behavior in mice. *Life Sciences*, Elsevier Inc. 91(25–26): 1252–1262.

Naert A, Callaerts-Vegh Z and D'Hooge R (2011) Nocturnal hyperactivity, increased social novelty preference and delayed extinction of fear responses in post-weaning socially isolated mice. *Brain Research Bulletin*, Elsevier Inc. 85(6): 354–362.

Nair A and Bonneau RH (2006) Stress-induced elevation of glucocorticoids increases microglia proliferation through NMDA receptor activation. *Journal of Neuroimmunology* 171(1–2): 72–85.

Nemeroff CB, Widerlöv E, Bissette G, Walléus H, Karlsson I, Eklund K, Kilts CD, Loosen PT and Vale W (1984) Elevated concentrations of CSF corticotropin-releasing factor-like immunoreactivity in depressed patients. *Science* 226(4680): 1342–1344.

Nestler EJ and Hyman SE (2010) Animal models of neuropsychiatric disorders. *Nature Neuroscience*, Nature Publishing Group, a division of Macmillan Publishers Limited. All Rights Reserved. 13(10): 1161–1169.

Nestler EJ, Gould E and Manji H (2002) Preclinical models: Status of basic research in depression. *Biological Psychiatry* 52(6): 503–528.

Nicola Z, Fabel K and Kempermann G (2015) Development of the adult neurogenic niche in the hippocampus of mice. *Frontiers in Neuroanatomy* 9(May): 53.

Nikkheslat N, Zunszain PA, Horowitz MA, Barbosa IG, Parker JA, Myint AM, Schwarz MJ, Tylee AT, Carvalho LA and Pariante CM (2015) Insufficient glucocorticoid signaling and elevated inflammation in coronary heart disease patients with comorbid depression. *Brain, Behavior, and Immunity* 48: 8–18.

Noh H, Jeon J and Seo H (2014) Systemic injection of LPS induces region-specific neuroinflammation and mitochondrial dysfunction in normal mouse brain. *Neurochemistry International* 69(1): 35–40.

Nollet M, Guisquet A Le and Belzung C (2013) Models of Depression: Unpredictable Chronic Mild Stress in Mice. In: *Current Protocols in Pharmacology*, John Wiley & Sons, Inc., pp. 1–17.

Nollet M, Gaillard P, Minier F, Tanti A, Belzung C and Leman S (2011) Activation of orexin neurons in dorsomedial/perifornical hypothalamus and antidepressant reversal in a

rodent model of depression. *Neuropharmacology*, Elsevier Ltd 61(1–2): 336–346.

Nonogaki K, Nozue K, Takahashi Y, Yamashita N, Hiraoka S, Kumano H, Kuboki T and Oka Y (2007) Fluvoxamine, a selective serotonin reuptake inhibitor, and 5-HT2C receptor inactivation induce appetite-suppressing effects in mice via 5-HT1B receptors. *The international journal of neuropsychopharmacology / official scientific journal of the Collegium Internationale Neuropsychopharmacologicum (CINP)* 10(5): 675–681.

Norden DM, Trojanowski PJ, Villanueva E, Navarro E and Godbout JP (2016) Sequential activation of microglia and astrocyte cytokine expression precedes increased iba-1 or GFAP immunoreactivity following systemic immune challenge. *Glia* 64(2): 300–316.

O'Brien SM, Scully P, Fitzgerald P, Scott L V and Dinan TG (2007) Plasma cytokine profiles in depressed patients who fail to respond to selective serotonin reuptake inhibitor therapy. *Journal of Psychiatric Research* 41(3–4): 326–331.

O'Connor JC, Lawson MA, André C, Moreau M, Lestage J, Castanon N, Kelley KW and Dantzer R (2009) Lipopolysaccharide-induced depressive-like behavior is mediated by indoleamine 2,3-dioxygenase activation in mice. *Molecular Psychiatry* 14(5): 511–522.

O'Malley D, MacDonald N, Mizielinska S, Connolly CN, Irving AJ and Harvey J (2007) Leptin promotes rapid dynamic changes in hippocampal dendritic morphology. *Molecular and Cellular Neuroscience*, Elsevier Inc. 35(4): 559–572.

Okada R, Fujiwara H, Mizuki D, Araki R, Yabe T and Matsumoto K (2015) Involvement of dopaminergic and cholinergic systems in social isolation-induced deficits in social affiliation and conditional fear memory in mice. *Neuroscience*, IBRO 299: 134–145.

Oomen CA, Soeters H, Audureau N, Vermunt L, van Hasselt FN, Manders EMM, Joels M, Lucassen PJ and Krugers H (2010) Severe Early Life Stress Hampers Spatial Learning and Neurogenesis, but Improves Hippocampal Synaptic Plasticity and Emotional Learning under High-Stress Conditions in Adulthood. *Journal of Neuroscience* 30(19): 6635–6645.

Oomen CA, Mayer JL, De Kloet ER, Joëls M and Lucassen PJ (2007) Brief treatment with the glucocorticoid receptor antagonist mifepristone normalizes the reduction in neurogenesis after chronic stress. *European Journal of Neuroscience* 26(12): 3395–3401.

Orikasa C, Nagaoka K, Katsumata H, Sato M, Kondo Y, Minami S and Sakuma Y (2015) Social isolation prompts maternal behavior in sexually naive male ddN mice. *Physiology and Behavior*, Elsevier B.V. 151: 9–15.

Ormerod BK, Hanft SJ, Asokan A, Haditsch U, Lee SW and Palmer TD (2013) PPARγ activation prevents impairments in spatial memory and neurogenesis following transient illness. *Brain, Behavior, and Immunity*, Elsevier Inc 29:28-38.

Orsetti M, Di Brisco F, Canonico PL, Genazzani AA and Ghi P (2008) Gene regulation in the frontal cortex of rats exposed to the chronic mild stress paradigm, an animal model of human depression. *European Journal of Neuroscience* 27(8): 2156–2164.

Otte C, Gold SM, Penninx BW, Pariante CM, Etkin A, Fava M, Mohr DC and Schatzberg AF (2016) Major depressive disorder. *Nature Reviews Disease Primers*, Nature Publishing Group 2: 16065.

Pace TWW, Hu F and Miller AH (2007) Cytokine-effects on glucocorticoid receptor function: Relevance to glucocorticoid resistance and the pathophysiology and treatment of major depression. *Brain, Behavior, and Immunity* 21(1): 9-19.

Painsipp E, Köfer MJ, Sinner F and Holzer P (2011) Prolonged depression-like behavior caused by immune challenge: Influence of mouse strain and social environment. *PLoS ONE* 6(6): e20719.

Palmer TD, Willhoite AR and Gage FH (2000) Vascular niche for adult hippocampal neurogenesis. *Journal of Comparative Neurology*, John Wiley & Sons, Inc. 425(4): 479–494.

Pan Y, Wang FM, Qiang LQ, Zhang DM and Kong LD (2010) Icariin attenuates chronic mild stress-induced dysregulation of the LHPA stress circuit in rats. *Psychoneuroendocrinology* 35(2): 272–283.

Paolicelli RC, Bolasco G, Pagani F, Maggi L, Scianni M, Panzanelli P, Giustetto M, Ferreira TA, Guiducci E, Dumas L, Ragozzino D and Gross CT (2011) Synaptic Pruning by Microglia Is Necessary for Normal Brain Development. *Science*, New York: American Association for the Advancement of Science 72(1): 1-17.

Papp M, Gruca P, Lason-Tyburkiewicz M and Willner P (2013) Rivastigmine causes antidepressant, anxiolytic and procognitive effects in the chronic mild stress model in rats. *European Neuropsychopharmacology* 23: S190.

Pariante CM, Hye A, Williamson R, Makoff A, Lovestone S and Kerwin RW (2003) The antidepressant clomipramine regulates cortisol intracellular concentrations and glucocorticoid receptor expression in fibroblasts and rat primary neurones.

Neuropsychopharmacology 28(9): 1553–61.

Pariante CM and Miller AH (2001) Glucocorticoid receptors in major depression: Relevance to pathophysiology and treatment. *Biological Psychiatry* 49(5): 391-404.

Park S-E, Lawson M, Dantzer R, Kelley KW and McCusker RH (2011) Insulin-like growth factor-I peptides act centrally to decrease depression-like behavior of mice treated intraperitoneally with lipopolysaccharide. *Journal of Neuroinflammation* 8(1): 179.

Pawlby S, Hay D, Sharp D, Cerith S W and Pariante CM (2011) Antenatal depression and offspring psychopathology: The influence of childhood maltreatment. *British Journal of Psychiatry* 199(2): 106–112.

Petit-Demouliere B, Chenu F and Bourin M (2005) Forced swimming test in mice: A review of antidepressant activity. *Psychopharmacology* 177(3):245-255.

Pfaffl MW (2001) A new mathematical model for relative quantification in real-time RT-PCR. *Nucleic Acids Research* 29(9): 45e–45.

Pitkänen A, Pikkarainen M, Nurminen N and Ylinen A (2006) Reciprocal Connections between the Amygdala and the Hippocampal Formation, Perirhinal Cortex, and Postrhinal Cortex in Rat: A Review. *Annals of the New York Academy of Sciences* 911(1): 369–391.

Pizzagalli DA, Holmes AJ, Dillon DG, Goetz EL, Birk JL, Bogdan R, Dougherty DD, Iosifescu D V, Rauch SL and Fava M (2009) Reduced caudate and nucleus accumbens response to rewards in unmedicated individuals with major depressive disorder. *American Journal of Psychiatry* 166(6): 702–710.

Pla P, Orvoen S, Benstaali C, Dodier S, Gardier AM, David DJ, Humbert S and Saudou F (2013) Huntingtin Acts Non Cell-Autonomously on Hippocampal Neurogenesis and Controls Anxiety-Related Behaviors in Adult Mouse. *PLoS ONE* 8(9): 1–12.

Pla P, Orvoen S, Saudou F, David DJ and Humbert S (2014) Mood disorders in Huntington's disease: from behavior to cellular and molecular mechanisms. *Frontiers in Behavioral Neuroscience* 8(April): 135.

Plümpe T, Ehninger D, Steiner B, Klempin F, Jessberger S, Brandt M, Römer B, Rodriguez GR, Kronenberg G and Kempermann G (2006) Variability of doublecortin-associated dendrite maturation in adult hippocampal neurogenesis is independent of the regulation of precursor cell proliferation. *BMC Neuroscience* 7: 77.

Porsolt RD, Le Pichon M and Jalfre M (1977) Depression: a new animal model sensitive to antidepressant treatments. *Nature* 266(5604): 730–732.

Porsolt RD, Bertin A and Jalfre M (1978) 'Behavioural despair' in rats and mice: Strain differences and the effects of imipramine. *European Journal of Pharmacology* 51(3): 291–294.

Pothion S, Bizot JC, Trovero F and Belzung C (2004) Strain differences in sucrose preference and in the consequences of unpredictable chronic mild stress. *Behavioural Brain Research* 155(1): 135–146.

Potter M (1985) The BALB/c Mouse: Genetics and Immunology. *Current Topics in Microbiology and Immunology*, Springer-Verlag 122: 1–253.

Poulter MO, Du L, Weaver ICG, Palkovits M, Faludi G, Merali Z, Szyf M and Anisman H (2008) GABAA Receptor Promoter Hypermethylation in Suicide Brain: Implications for the Involvement of Epigenetic Processes. *Biological Psychiatry* 64(8): 645–652.

Powell TR, Fernandes C and Schalkwyk LC (2012) Depression-Related Behavioral Tests. *Current* 2(June): 119–127.

Prather AA, Rabinovitz M, Pollock BG and Lotrich FE (2009) Cytokine-induced depression during IFN-alpha treatment: the role of IL-6 and sleep quality. *Brain, behavior, and immunity* 23(8): 1109–16.

Price A, Rayner L, Okon-Rocha E, Evans A, Valsraj K, Higginson IJ and Hotopf M (2011) Antidepressants for the treatment of depression in neurological disorders: a systematic review and meta-analysis of randomised controlled trials. *Journal of Neurology, Neurosurgery & Psychiatry* 82(8): 914–923.

Procaccini C, Aitta-aho T, Jaako-Movits K, Zharkovsky A, Panhelainen A, Sprengel R, Linden A-M and Korpi ER (2011) Excessive novelty-induced c-Fos expression and altered neurogenesis in the hippocampus of GluA1 knockout mice. *The European journal of neuroscience* 33(1): 161–74.

Provençal N and Binder EB (2014) The effects of early life stress on the epigenome: From the womb to adulthood and even before. *Experimental Neurology* 268:10-20.

Qiao H, Li MX, Xu C, Chen H Bin, An SC and Ma XM (2016) Dendritic Spines in Depression: What We Learned from Animal Models. *Neural Plasticity* 2016:8056370.

Qin L, Wu X, Block ML, Liu Y, Breese GR, Hong JS, Knapp DJ and Crews FT (2007) Systemic LPS causes chronic neuroinflammation and progressive neurodegeneration. *Glia* 55(5): 453–462.

Quennell JH, Howell CS, Roa J, Augustine RA, Grattan DR and Anderson GM (2011) Leptin Deficiency and Diet-Induced Obesity Reduce Hypothalamic Kisspeptin Expression in Mice. *Endocrinology*, Oxford University Press 152(4): 1541–1550.

Radley JJ, Rocher AB, Rodriguez A, Ehlenberger DB, Dammann M, McEwen BS, Morrison JH, Wearne SL and Hof PR (2008) Repeated stress alters dendritic spine morphology in the rat medial prefrontal cortex. *The Journal of Comparative Neurology* 507(1): 1141–1150.

Raison CL, Borisov AS, Broadwell SD, Capuron L, Woolwine BJ, Jacobson IM, Nemeroff CB and Miller AH (2005) Depression during pegylated interferon-alpha plus ribavirin therapy: prevalence and prediction. *The Journal of clinical psychiatry* 66(1): 41–48.

Raison CL, Woolwine BJ, Demetrashvili MF, Borisov AS, Weinreib R, Staab JP, Zajecka JM, Bruno CJ, Henderson MA, Reinus JF, Evans DL, Asnis GM and Miller AH (2007) Paroxetine for prevention of depressive symptoms induced by interferon-alpha and ribavirin for hepatitis C. *Alimentary Pharmacology and Therapeutics* 25(10): 1163–1174.

Raison CL, Borisov AS, Woolwine BJ, Massung B, Vogt G and Miller AH (2010) Interferon-α effects on diurnal hypothalamic–pituitary–adrenal axis activity: relationship with proinflammatory cytokines and behavior. *Molecular Psychiatry* 15(5): 535–547.

Raison CL and Miller AH (2011) Is depression an inflammatory disorder? *Current Psychiatry Reports* 13(6): 467–475.

Raison CL and Miller AH (2013) Role of inflammation in depression: Implications for phenomenology, pathophysiology and treatment. *Modern Trends in Pharmacopsychiatry* 28: 33–48.

Raison CL, Rutherford MD, Woolwine BJ, Chen Shuo MS, Schettler P, Drake DF, Haroon E and Miller AH (2013) A Randomized Controlled Trial of the Tumor Necrosis Factor- alpha Antagonist Infliximab in Treatment Resistant Depression: Role of Baseline Inflammatory Biomarkers. *JAMA Psychiatry* 70(1): 31–41.

Rakic P (2009) Evolution of the neocortex: Perspective from developmental biology. *Nature reviews. Neuroscience*, NIH Public Access 10(10): 724.

Reader BF, Jarrett BL, McKim DB, Wohleb ES, Godbout JP and Sheridan JF (2015) Peripheral

and central effects of repeated social defeat stress: Monocyte trafficking, microglial activation, and anxiety. *Neuroscience* 289: 429–442.

Reichelt AC, Westbrook RF and Morris MJ (2015) Integration of reward signalling and appetite regulating peptide systems in the control of food-cue responses. *British Journal of Pharmacology* 172(22): 5225–5238.

Reichenberg A, Yirmiya R, Schuld A, Kraus T, Haack M, Morag A and Pollmächer T (2001) Cytokine-Associated Emotional and Cognitive Disturbances in Humans. *Archives of General Psychiatry*, American Medical Association 58(5): 445.

Reif A, Fritzen S, Finger M, Strobel A, Lauer M, Schmitt A and Lesch K-P (2006) Neural stem cell proliferation is decreased in schizophrenia, but not in depression. *Molecular Psychiatry* 11(5): 514–522.

Ripke S, Wray NR, Lewis CM, Hamilton SP, Weissman MM, Breen G, Byrne EM, Blackwood DHR, Boomsma DI, Cichon S, Heath AC, Holsboer F, Lucae S, Madden PAF, Martin NG, McGuffin P, Muglia P, … Sullivan PF (2013) A mega-analysis of genome-wide association studies for major depressive disorder. *Molecular Psychiatry* 18(4): 497–511.

Rohleder N, Marin TJ, Ma R and Miller GE (2009) Biologic cost of caring for a cancer patient: Dysregulation of pro- and anti-inflammatory signaling pathways. *Journal of Clinical Oncology* 27(18): 2909–2915.

Rolls ET and Kesner RP (2006) A computational theory of hippocampal function, and empirical tests of the theory. *Progress in Neurobiology* 79(1): 1-48.

Rosenthal M, Roth J, Storr B and Zeisberger E (1996) Fever response in lean (Fa/-) and obese (fa/fa) Zucker rats and its lack to repeated injections of LPS. *Physiology and Behavior* 59(4–5): 787–793.

Rybka J, Korte SM, Czajkowska-Malinowska M, Wiese M, Kędziora-Kornatowska K and Kędziora J (2016) The links between chronic obstructive pulmonary disease and comorbid depressive symptoms: role of IL-2 and IFN-γ. *Clinical and Experimental Medicine* 16(4): 493–502.

Sadler AM and Bailey SJ (2013) Validation of a refined technique for taking repeated blood samples from juvenile and adult mice. *Laboratory Animals* 47(4): 316–319.

Sadler AM and Bailey SJ (2016) Repeated daily restraint stress induces adaptive behavioural changes in both adult and juvenile mice. *Physiology and Behavior*, Elsevier B.V. 167: 313–

323.

Sahay A, Scobie KN, Hill AS, O'Carroll CM, Kheirbek MA, Burghardt NS, Fenton AA, Dranovsky A and Hen R (2011) Increasing adult hippocampal neurogenesis is sufficient to improve pattern separation. *Nature* 472(7344): 466–470.

Sahin TD, Karson A, Balci F, Yazir Y, Bayramgurler D and Utkan T (2015) TNF-alpha inhibition prevents cognitive decline and maintains hippocampal BDNF levels in the unpredictable chronic mild stress rat model of depression. *Behavioural Brain Research* 292: 233–240.

Samuels BA, Anacker C, Hu A, Levinstein MR, Pickenhagen A, Tsetsenis T, Madroñal N, Donaldson ZR, Drew LJ, Dranovsky A, Gross CT, Tanaka KF and Hen R (2015) 5-HT1A receptors on mature dentate gyrus granule cells are critical for the antidepressant response. *Nature Neuroscience*, Nature Publishing Group, a division of Macmillan Publishers Limited. All Rights Reserved. 18(11): 1606–1616.

Santarelli L (2003) Requirement of Hippocampal Neurogenesis for the Behavioral Effects of Antidepressants. *Science* 301(5634): 805–809.

Scherrer JF, Chrusciel T, Garfield LD, Freedland KE, Carney RM, Hauptman PJ, Bucholz KK, Owen R and Lustman PJ (2012) Treatment-resistant and insufficiently treated depression and all-cause mortality following myocardial infarction. *British Journal of Psychiatry* 200(2): 137–142.

Schildkraut J. (1965) The catecholamine hypothesis of affective disorders: a review of the evidence. *American Journal of Psychiatry* 4(122): 509–522.

Schmaal L, Veltman DJ, van Erp TGM, Sämann PG, Frodl T, Jahanshad N, Loehrer E, Tiemeier H, Hofman A, Niessen WJ, Vernooij MW, Ikram MA, Wittfeld K, Grabe HJ, Block A, Hegenscheid K, Völzke H, … Hibar DP (2016) Subcortical brain alterations in major depressive disorder: findings from the ENIGMA Major Depressive Disorder working group. *Molecular Psychiatry*, Nature Publishing Group 21(6): 806–812.

Schmidt M V, Sterlemann V, Wagner K, Niederleitner B, Ganea K, Liebl C, Deussing JM, Berger S, Schütz G, Holsboer F and Müller MB (2009) Postnatal glucocorticoid excess due to pituitary glucocorticoid receptor deficiency: differential short- and long-term consequences. *Endocrinology* 150(6): 2709–16.

Schneider CA, Rasband WS and Eliceiri KW (2012) NIH Image to ImageJ: 25 years of image analysis. *Nature Methods*, Nature Publishing Group, a division of Macmillan Publishers

Limited. All Rights Reserved. 9(7): 671–675.

Schreiber G, Tsykin A, Alfred AR, Thomas T, Fung W-PP, Dickson PW, Cole T, Birch H, De Jong F a and Milland J (1989) The acute phase response in the rodent. *Annals of the New York Academy of Sciences* 557(1): 61-85–6.

Schrodl W, Bichler R, Wendler S, Reinhold P, Muckova P, Reindl J and Rhode H (2016) Acute phase proteins as promising biomarkers: Perspectives and limitations for human and veterinary medicine. *Proteomics - Clinical Applications* 10(11): 1077-1092.

Schwarcz R (2002) Manipulation of Brain Kynurenines: Glial Targets, Neuronal Effects, and Clinical Opportunities. *Journal of Pharmacology and Experimental Therapeutics* 303(1): 1–10.

Schweizer MC, Henniger MSH and Sillaber I (2009) Chronic mild stress (CMS) in mice: Of anhedonia, 'anomalous anxiolysis' and activity. *PLoS ONE* 4(1): e4326.

Seguin JA, Brennan J, Mangano E and Hayley S (2009) Proinflammatory cytokines differentially influence adult hippocampal cell proliferation depending upon the route and chronicity of administration. *Neuropsychiatric Disease and Treatment* 5(1): 5–14.

Seligman ME and Maier SF (1967) Failure to escape traumatic shock. *Journal of Experimental Psychology* 47(1): 1–9.

Seri B, Garcia-Verdugo JM, McEwen BS and Alvarez-Buylla A (2001) Astrocytes give rise to new neurons in the adult mammalian hippocampus. *The Journal of Neuroscience* 21(18): 7153–7160.

Setiawan E, Wilson AA, Mizrahi R, Rusjan PM, Miler L, Rajkowska G, Suridjan I, Kennedy JL, Rekkas PV, Houle S and Meyer JH (2015) Role of translocator protein density, a marker of neuroinflammation, in the brain during major depressive episodes. *JAMA psychiatry* 72(3): 268–75.

Shansky RM, Hamo C, Hof PR, McEwen BS and Morrison JH (2009) Stress-induced dendritic remodeling in the prefrontal cortex is circuit specific. *Cerebral Cortex* 19(10): 2479–2484.

Shelton DJ and Kirwan CB (2013) A possible negative influence of depression on the ability to overcome memory interference. *Behavioural Brain Research*, Elsevier B.V. 256: 20–26.

Sher L, Oquendo MA, Burke AK, Cooper TB and John Mann J (2013) Combined dexamethasone suppression-corticotrophin-releasing hormone stimulation test in medication-free major

depression and healthy volunteers. *Journal of Affective Disorders* 151(3): 1108–1112.

Shi Y, Liu CH, Roberts AI, Das J, Xu G, Ren G, Zhang Y, Zhang L, Yuan ZR, Tan HSW, Das G and Devadas S (2006) Granulocyte-macrophage colony-stimulating factor (GM-CSF) and T-cell responses: what we do and don't know. *Cell Research* 16(2): 126–133.

Sierra A, Encinas JM, Deudero JJP, Chancey JH, Enikolopov G, Overstreet-Wadiche LS, Tsirka SE and Maletic-Savatic M (2010) Microglia shape adult hippocampal neurogenesis through apoptosis-coupled phagocytosis. *Cell Stem Cell*, Elsevier Inc. 7(4): 483–495.

Sierra A, Beccari S, Diaz-Aparicio I, Encinas JM, Comeau S and Tremblay MÈ (2014) Surveillance, phagocytosis, and inflammation: How never-resting microglia influence adult hippocampal neurogenesis. *Neural Plasticity* 2014:610343.

Silverman MN, Pearce BD, Biron CA and Miller AH (2005) Immune Modulation of the Hypothalamic-Pituitary-Adrenal (HPA) Axis during Viral Infection. *Viral Immunology* 18(1): 41–78.

Silverman MN and Sternberg EM (2012) Glucocorticoid regulation of inflammation and its functional correlates: From HPA axis to glucocorticoid receptor dysfunction. *Annals of the New York Academy of Sciences* 1261(1): 55–63.

Simon NM, McNamara K, Chow CW, Maser RS, Papakostas GI, Pollack MH, Nierenberg AA, Fava M and Wong KK (2008) A detailed examination of cytokine abnormalities in Major Depressive Disorder. *European Neuropsychopharmacology* 18(3): 230–233.

Slomianka L and West MJ (2005) Estimators of the precision of stereological estimates: An example based on the CA1 pyramidal cell layer of rats. *Neuroscience* 136(3): 757–767.

Smith DJ, Nicholl BI, Cullen B, Martin D, Ul-Haq Z, Evans J, Gill JMR, Roberts B, Gallacher J, Mackay D, Hotopf M, Deary I, Craddock N and Pell JP (2013) Prevalence and characteristics of probable major depression and bipolar disorder within UK biobank: cross-sectional study of 172,751 participants. *PloS one* 8(11): e75362.

Snyder JS, Soumier A, Brewer M, Pickel J and Cameron HA (2011) Adult hippocampal neurogenesis buffers stress responses and depressive behaviour. *Nature*, Nature Publishing Group, a division of Macmillan Publishers Limited. All Rights Reserved. 476(7361): 458–461.

Song J, Zhong C, Bonaguidi MA, Sun GJ, Hsu D, Gu Y, Meletis K, Huang ZJ, Ge S, Enikolopov G, Deisseroth K, Luscher B, Christian KM, Ming G and Song H (2012) Neuronal circuitry

mechanism regulating adult quiescent neural stem-cell fate decision. *Nature*, Nature Publishing Group, a division of Macmillan Publishers Limited. All Rights Reserved. 489(7414): 150–4.

Sorrells SF, Caso JR, Munhoz CD and Sapolsky RM (2009) The Stressed CNS: When Glucocorticoids Aggravate Inflammation. *Neuron*, Elsevier Inc. 64(1): 33–39.

Sousa N, Lukoyanov NV, Madeira MD, Almeida OFX and Paula-Barbosa MM (2000) Reorganization of the morphology of hippocampal neurites and synapses after stress-induced damage correlates with behavioral improvement. *Neuroscience* 97(2): 253–266.

Spalding KL, Bergmann O, Alkass K, Bernard S, Salehpour M, Huttner HB, Boström E, Westerlund I, Vial C, Buchholz BA, Possnert G, Mash DC, Druid H and Frisén J (2013) Dynamics of Hippocampal Neurogenesis in Adult Humans. *Cell* 153(6): 1219–1227.

Spijker S (2011) Neuroproteomics: Dissection of Rodent Brain Regions. *Neuromethods* 57: 13–27.

Spritzer MD, Ibler E, Inglis W and Curtis MG (2011) Testosterone and social isolation influence adult neurogenesis in the dentate gyrus of male rats. *Neuroscience*, Elsevier Inc. 195: 180–190.

Spruijt BM, Van Hooff JARAM and Gispen WH (1992) Ethology and neurobiology of grooming behavior. *Physiological Review* 72(3): 825–852.

Srivastava DP, Copits BA, Xie Z, Huda R, Jones KA, Mukherji S, Cahill ME, VanLeeuwen JE, Woolfrey KM, Rafalovich I, Swanson GT and Penzes P (2012) Afadin is required for maintenance of dendritic structure and excitatory tone. *Journal of Biological Chemistry* 287(43): 35964–35974.

Steiner B, Klempin F, Wang L, Kott M, Kettenmann H and Kempermann G (2006) Type-2 cells as link between glial and neuronal lineage in adult hippocampal neurogenesis. *Glia* 54(8): 805–14.

Stence N, Waite M and Dailey ME (2001) Dynamics of microglial activation: A confocal time-lapse analysis in hippocampal slices. *Glia* 33(3): 256–266.

Sterrenburg L, Gaszner B, Boerrigter J, Santbergen L, Bramini M, Elliott E, Chen A, Peeters BWMM, Roubos EW and Kozicz T (2011) Chronic stress induces sex-specific alterations in methylation and expression of corticotropin-releasing factor gene in the rat. *PLoS ONE*, Public Library of Science 6(11): e28128.

Steru L, Chermat R, Thierry B and Simon P (1985) The tail suspension test: a new method for screening antidepressants in mice. *Psychopharmacology* 85(3): 367–70.

Strekalova T, Spanagel R, Dolgov O and Bartsch D (2005) Stress-induced hyperlocomotion as a confounding factor in anxiety and depression models in mice. *Behavioural Pharmacology* 16(3): 171–80.

Strekalova T, Gorenkova N, Schunk E, Dolgov O and Bartsch D (2006) Selective effects of citalopram in a mouse model of stress-induced anhedonia with a control for chronic stress. *Behavioural Pharmacology* 17(3): 271–287.

Strekalova T, Couch Y, Kholod N, Boyks M, Malin D, Leprince P and Steinbusch HM (2011) Update in the methodology of the chronic stress paradigm: internal control matters. *Behavioral and Brain Functions*, BioMed Central Ltd 7(1): 9.

Sugama S, Takenouchi T, Fujita M, Conti B and Hashimoto M (2009) Differential microglial activation between acute stress and lipopolysaccharide treatment. *Journal of Neuroimmunology* 207(1–2): 24–31.

Sugama S, Takenouchi T, Fujita M, Kitani H, Conti B and Hashimoto M (2013) Corticosteroids limit microglial activation occurring during acute stress. *Neuroscience* 232: 13–20.

Sun GJ, Zhou Y, Stadel RP, Moss J, Yong JH, Ito S, Kawasaki NK, Phan AT, Oh JH, Modak N, Reed RR, Toni N, Song H and Ming GL (2015) Tangential migration of neuronal precursors of glutamatergic neurons in the adult mammalian brain. *Proceedings of the National Academy of Sciences* 112(30): 9484–9489.

Sun H-L, Zhou Z-Q, Zhang G-F, Yang C, Wang X-M, Shen J-C, Hashimoto K and Yang J-J (2016) Role of hippocampal p11 in the sustained antidepressant effect of ketamine in the chronic unpredictable mild stress model. *Translational Psychiatry* 6(2): e741.

Surget A, Saxe M, Leman S, Ibarguen-Vargas Y, Chalon S, Griebel G, Hen R and Belzung C (2008) Drug-Dependent Requirement of Hippocampal Neurogenesis in a Model of Depression and of Antidepressant Reversal. *Biological Psychiatry* 64(4): 293–301.

Surget A, Wang Y, Leman S, Ibarguen-Vargas Y, Edgar N, Griebel G, Belzung C and Sibille E (2008a) Corticolimbic Transcriptome Changes are State-Dependent and Region-Specific in a Rodent Model of Depression and of Antidepressant Reversal. *Neuropsychopharmacology*, Nature Publishing Group 34(6): 1363–138076.

Surget A and Belzung C (2009) Unpredictable chronic mild stress in mice. In: Kalueff A.V. and

LaPorte J.L. (eds), *Experimental Animal Models in Neurobehavioral Research*, New York: Nova Science Publishers, pp. 79–112.

Surget A, Tanti A, Leonardo ED, Laugeray A, Rainer Q, Touma C, Palme R, Griebel G, Ibarguen-Vargas Y, Hen R and Belzung C (2011) Antidepressants recruit new neurons to improve stress response regulation. *Molecular Psychiatry*, Nature Publishing Group 16(12): 1177–1188.

Surget A, Van Nieuwenhuijzen PS, Heinzmann JM, Knapman A, McIlwrick S, Westphal WP, Touma C and Belzung C (2016) Antidepressant treatment differentially affects the phenotype of high and low stress reactive mice. *Neuropharmacology* 110: 37–47.

Tanti A, Rainer Q, Minier F, Surget A and Belzung C (2012) Differential environmental regulation of neurogenesis along the septo-temporal axis of the hippocampus. *Neuropharmacology*, Elsevier Ltd 63(3): 374–384.

Tanti A and Belzung C (2013) Hippocampal neurogenesis: A biomarker for depression or antidepressant effects? Methodological considerations and perspectives for future research. *Cell and Tissue Research* 354(1): 203–219.

Tanti A, Westphal WP, Girault V, Brizard B, Devers S, Leguisquet AM, Surget A and Belzung C (2013) Region-dependent and stage-specific effects of stress, environmental enrichment, and antidepressant treatment on hippocampal neurogenesis. *Hippocampus* 23(9): 797–811.

Tashiro A, Sandler VM, Toni N, Zhao C and Gage FH (2006) NMDA-receptor-mediated, cell-specific integration of new neurons in adult dentate gyrus. *Nature* 442(7105): 929–33.

Tham A, Jonsson U, Andersson G, S??derlund A, Allard P and Bertilsson G (2016) Efficacy and tolerability of antidepressants in people aged 65 years or older with major depressive disorder: A systematic review and a meta-analysis. *Journal of Affective Disorders* 205:1-12.

Thierry AM, Gioanni Y, Dégénétais E and Glowinski J (2000) Hippocampo-prefrontal cortex pathway: Anatomical and electrophysiological characteristics. *Hippocampus* 10(4): 411–419.

Thomas L, Kessler D, Campbell J, Morrison J, Peters TJ, Williams C, Lewis G and Wiles N (2013) Prevalence of treatment-resistant depression in primary care: cross-sectional data. *The British Journal of General Practice* 63(617): e852-8.

Thomson PA, Parla JS, McRae AF, Kramer M, Ramakrishnan K, Yao J, Soares DC, McCarthy S, Morris SW, Cardone L, Cass S, Ghiban E, Hennah W, Evans KL, Rebolini D, Millar JK, Harris SE, … Porteous DJ (2014) 708 Common and 2010 rare DISC1 locus variants identified in 1542 subjects: analysis for association with psychiatric disorder and cognitive traits. *Molecular Psychiatry* 19(6): 668–675.

Thuret S, Toni N, Aigner S, Yeo GW and Gage FH (2009) Hippocampus-dependent learning is associated with adult neurogenesis in MRL/MpJ mice. *Hippocampus* 19(7): 658–669.

Tordera RM, Garcia-García AL, Elizalde N, Segura V, Aso E, Venzala E, Ramírez MJ and Del Rio J (2011) Chronic stress and impaired glutamate function elicit a depressive-like phenotype and common changes in gene expression in the mouse frontal cortex. *European Neuropsychopharmacology*, Elsevier B.V. and ECNP 21(1): 23–32.

Tracey KJ (2015) Approaching the next revolution? Evolutionary integration of neural and immune pathogen sensing and response. *Cold Spring Harbor Perspectives in Biology* 7(2): a016360.

Trivedi MA and Coover GD (2004) Lesions of the ventral hippocampus, but not the dorsal hippocampus, impair conditioned fear expression and inhibitory avoidance on the elevated T-maze. *Neurobiology of Learning and Memory* 81(3): 172–184.

Trivedi MH, Rush AJ, Wisniewski SR, Nierenberg AA, Warden D, Ritz L, Norquist G, Howland RH, Lebowitz B, McGrath PJ, Shores-Wilson K, Biggs MM, Balasubramani GK and Fava M (2006) Evaluation of outcomes with citalopram for depression using measurement-based care in STAR*D: Implications for clinical practice. *American Journal of Psychiatry* 163(1): 28–40.

Tusher VG, Tibshirani R and Chu G (2001) Significance analysis of microarrays applied to the ionizing radiation response. *Proceedings of the National Academy of Sciences* 98(9): 5116–5121.

Tynan RJ, Naicker S, Hinwood M, Nalivaiko E, Buller KM, Pow D V, Day TA and Walker FR (2010) Chronic stress alters the density and morphology of microglia in a subset of stress-responsive brain regions. *Brain, Behavior, and Immunity* 24(7): 1058–1068.

Uher R, Mors O, Rietschel M, Rajewska-Rager A, Petrovic A, Zobel A, Henigsberg N, Mendlewicz J, Aitchison KJ, Farmer A and McGuffin P (2011) Early and delayed onset of response to antidepressants in individual trajectories of change during treatment of major depression: A secondary analysis of data from the genome-based therapeutic drugs for

depression (GENDEP) study. *Journal of Clinical Psychiatry* 72(11): 1478–1484.

Uhr M, Tontsch A, Namendorf C, Ripke S, Lucae S, Ising M, Dose T, Ebinger M, Rosenhagen M, Kohli M, Kloiber S, Salyakina D, Bettecken T, Specht M, Pütz B, Binder EB, Müller-Myhsok B and Holsboer F (2008) Polymorphisms in the drug transporter gene ABCB1 predict antidepressant treatment response in depression. *Neuron* 57(2): 203–9.

Valentinuzzi VS, Buxton OM, Chang a M, Scarbrough K, Ferrari E a, Takahashi JS and Turek FW (2000) Locomotor response to an open field during C57BL/6J active and inactive phases: differences dependent on conditions of illumination. *Physiology & behavior* 69(3): 269–75.

Valero J, Mastrella G, Neiva I, Sánchez S and Malva JO (2014) Long-term effects of an acute and systemic administration of LPS on adult neurogenesis and spatial memory. *Frontiers in Neuroscience*, Frontiers 8(8 APR): 83.

Vallières L, Campbell IL, Gage FH and Sawchenko PE (2002) Reduced hippocampal neurogenesis in adult transgenic mice with chronic astrocytic production of interleukin-6. *The Journal of neuroscience : the official journal of the Society for Neuroscience* 22(2): 486–92.

van Praag H, Kempermann G and Gage FH (1999) Running increases cell proliferation and neurogenesis in the adult mouse dentate gyrus. *Nature Neuroscience* 2(3): 266–270.

van Tol M, Li M, Metzger CD, Hailla N, Horn DI, Li W, Heinze HJ, Bogerts B, Steiner J, He H and Walter M (2014) Local cortical thinning links to resting-state disconnectivity in major depressive disorder. *Psychological Medicine* 44(10): 2053–2065.

van Zessen R, van der Plasse G and Adan R a. H (2012) Contribution of the mesolimbic dopamine system in mediating the effects of leptin and ghrelin on feeding. *Proceedings of the Nutrition Society* 71(4): 435–445.

Vancampfort D, Mitchell AJ, De Hert M, Sienaert P, Probst M, Buys R and Stubbs B (2015) Type 2 diabetes in patients with major depressive disorder: a meta-analysis of prevalence estimates and predictors. *Depression and Anxiety* 32(10): 763–773.

Vega-Rivera NM, Ortiz-López L, Gómez-Sánchez A, Oikawa-Sala J, Estrada-Camarena EM and Ramírez-Rodríguez GB (2016) The neurogenic effects of an enriched environment and its protection against the behavioral consequences of chronic mild stress persistent after enrichment cessation in six-month-old female Balb/C mice. *Behavioural Brain Research*,

Elsevier B.V. 301: 72–83.

Vialou V, Robison AJ, LaPlant QC, Covington HE, Dietz DM, Ohnishi YN, Mouzon E, Rush AJ, Watts EL, Wallace DL, Iñiguez SD, Ohnishi YH, Steiner MA, Warren BL, Krishnan V, Bolaños CA, Neve RL, … Nestler EJ (2010) ΔFosB in brain reward circuits mediates resilience to stress and antidepressant responses. *Nature Neuroscience* 13(6): 745–752.

Vialou V, Bagot RC, Cahill ME, Ferguson D, Robison AJ, Dietz DM, Fallon B, Mazei-Robison M, Ku SM, Harrigan E, Winstanley CA, Joshi T, Feng J, Berton O and Nestler EJ (2014) Prefrontal Cortical Circuit for Depression- and Anxiety-Related Behaviors Mediated by Cholecystokinin: Role of FosB. *Journal of Neuroscience* 34(11): 3878–3887.

Vukovic J, Colditz MJ, Blackmore DG, Ruitenberg MJ and Bartlett PF (2012) Microglia Modulate Hippocampal Neural Precursor Activity in Response to Exercise and Aging. *Journal of Neuroscience* 32(19): 6435–6443.

Vyas A, Mitra R, Shankaranarayana Rao BS and Chattarji S (2002) Chronic stress induces contrasting patterns of dendritic remodeling in hippocampal and amygdaloid neurons. *The Journal of Neuroscience* 22(15): 6810–6818.

Wada N, Hirako S, Takenoya F, Kageyama H, Okabe M and Shioda S (2014) Leptin and its receptors. *Journal of Chemical Neuroanatomy*, Elsevier B.V. 61: 191–199.

Walker F, Nilsson M and Jones K (2013) Acute and Chronic Stress-Induced Disturbances of Microglial Plasticity, Phenotype and Function. *Current Drug Targets* 14(11): 1262–1276.

Wang L, Hermens DF, Hickie IB and Lagopoulos J (2012) A systematic review of resting-state functional-MRI studies in major depression. *Journal of Affective Disorders* 142(1): 6–12.

Wang N, Yu H-Y, Shen X-F, Gao Z-Q, Yang C, Yang J-J and Zhang G-F (2015) The rapid antidepressant effect of ketamine in rats is associated with down-regulation of pro-inflammatory cytokines in the hippocampus. *Upsala journal of medical sciences*, Informa HealthcareStockholm 120(4): 241–8.

Warden D, Rush AJ, Trivedi MH, Fava M and Wisniewski SR (2007) The STAR*D project results: A comprehensive review of findings. *Current Psychiatry Reports* 9(6): 449-459.

Waterhouse EG, An JJ, Orefice LL, Baydyuk M, Liao G-Y, Zheng K, Lu B and Xu B (2012) BDNF promotes differentiation and maturation of adult-born neurons through GABAergic transmission. *Journal of Neuroscience* 32(41): 14318–14330.

West AP (1990) Neurobehavioral studies of forced swimming: The role of learning and memory in the forced swim test. *Progress in Neuro-Psychopharmacology and Biological Psychiatry* 14(6): 863–IN4.

Wiborg O (2013) Chronic mild stress for modeling anhedonia. *Cell and Tissue Research*, Berlin Heidelberg: Springer-Verlag 354(1) 155-169.

Wickens R, Ver Donck L, Mackenzie A and Bailey SJ (2014) Acute And Chronic Lipopolysaccharide Induces Sickness But Fails To Produce A Depressive-Like Behaviour In Mice. *Journal of Psychopharmacology* 28(8): A107.

Willner P (1984) The validity of animal models of depression. *Psychopharmacology* 83: 1–16.

Willner P, Towell A, Sampson D, Sophokleous S and Muscat R (1987) Reduction of sucrose preference by chronic unpredictable mild stress, and its restoration by a tricyclic antidepressant. *Psychopharmacology* 93(3): 358–64

Willner P, Muscat R and Papp M (1992) Chronic mild stress-induced anhedonia: A realistic animal model of depression. *Neuroscience and Biobehavioral Reviews* 16(4): 525–534.

Willner P (1997) Validity, reliability and utility of the chronic mild stress model of depression: a 10-year review and evaluation. *Psychopharmacology* 134(4): 319–29.

Willner P (2005) Chronic mild stress (CMS) revisited: Consistency and behavioural-neurobiological concordance in the effects of CMS. *Neuropsychobiology*, Basel: Karger AG 52(2): 90-110.

Willner P, Scheel-Krüger J and Belzung C (2013) The neurobiology of depression and antidepressant action. *Neuroscience and Biobehavioral Reviews*, Elsevier Ltd 37(10): 2331-2371.

Willner P, Scheel-Krüger J and Belzung C (2014) Resistance to antidepressant drugs: the case for a more predisposition-based and less hippocampocentric research paradigm. *Behavioural Pharmacology* 25(5 and 6): 352–371.

Winslow JT (2003) Mouse social recognition and preference. In: *Current Protocols in Neuroscience*, John Wiley & Sons, Inc., p. 8.16.1–8.16.16.

Wirleitner B, Neurauter G, Schröcksnadel K, Frick B and Fuchs D (2003) Interferon-gamma-induced conversion of tryptophan: immunologic and neuropsychiatric aspects. *Current medicinal chemistry* 10(16): 1581–1591.

Wodarz N, Rupprecht R, Kornhuber J, Schmitz B, Wild K, Braner HU and Riederer P (1991) Normal lymphocyte responsiveness to lectins but impaired sensitivity to in vitro glucocorticoids in major depression. *Journal of Affective Disorders* 22(4): 241–248.

Wohleb ES, Hanke ML, Corona AW, Powell ND, Stiner LM, Bailey MT, Nelson RJ, Godbout JP and Sheridan JF (2011) Adrenergic Receptor Antagonism Prevents Anxiety-Like Behavior and Microglial Reactivity Induced by Repeated Social Defeat. *Journal of Neuroscience* 31(17): 6277–6288.

Wohleb ES, Fenn AM, Pacenta AM, Powell ND, Sheridan JF and Godbout JP (2012) Peripheral innate immune challenge exaggerated microglia activation, increased the number of inflammatory CNS macrophages, and prolonged social withdrawal in socially defeated mice. *Psychoneuroendocrinology*, Elsevier Ltd 37(9): 1491–1505.

Wohleb ES and Delpech J-CC (2016) Dynamic cross-talk between microglia and peripheral monocytes underlies stress-induced neuroinflammation and behavioral consequences. *Progress in Neuro-Psychopharmacology and Biological Psychiatry*, Elsevier Inc. in press.

Wu MD, Hein AM, Moravan MJ, Shaftel SS, Olschowka JA and O'Banion MK (2012) Adult murine hippocampal neurogenesis is inhibited by sustained IL-1β and not rescued by voluntary running. *Brain, Behavior, and Immunity* 26(2): 292–300.

Xu F, Yang J, Chen J, Wu Q, Gong W, Zhang J, Shao W, Mu J, Yang D, Yang Y, Li Z and Xie P (2015) Differential co-expression and regulation analyses reveal different mechanisms underlying major depressive disorder and subsyndromal symptomatic depression. *BMC Bioinformatics*, 16(1): 112.

Xuan NT, Wang X, Nishanth G, Waisman A, Borucki K, Isermann B, Naumann M, Deckert M and Schlüter D (2015) A20 expression in dendritic cells protects mice from LPS-induced mortality. *European Journal of Immunology* 45(3): 818–828.

Xue J, Li H, Deng X, Ma Z, Fu Q and Ma S (2015) L-Menthone confers antidepressant-like effects in an unpredictable chronic mild stress mouse model via NLRP3 inflammasome-mediated inflammatory cytokines and central neurotransmitters. *Pharmacology Biochemistry and Behavior* 134: 42–48.

Yalcin I, Belzung C and Surget A (2008) Mouse strain differences in the unpredictable chronic mild stress: a four-antidepressant survey. *Behavioural Brain Research* 193(1): 140–143.

Yancey SL and Overton JM (1993) Cardiovascular responses to voluntary and treadmill exercise

in rats. *Journal of Applied Physiology* 75(3): 1334–1340.

Yang M and Crawley JN (2010) Simple Behavioral Assessment of Mouse Olfaction. *Current Protocols in Neuroscience* July(8): 1–14.

Yang Y, Zhang Y, Luo F and Li B (2016) Chronic stress regulates NG2+ cell maturation and myelination in the prefrontal cortex through induction of death receptor 6. *Experimental Neurology*, Elsevier Inc. 277: 202–214.

Yau JLW, Noble J, Thomas S, Kerwin R, Morgan PE, Lightman S, Seckl JR and Pariante CM (2007) The Antidepressant Desipramine Requires the ABCB1 (Mdr1)-Type p-Glycoprotein to Upregulate the Glucocorticoid Receptor in Mice. *Neuropsychopharmacology* 32(12): 2520–2529.

Yirmiya R (1996) Endotoxin produces a depressive-like episode in rats. *Brain Research* 711(1–2): 163–174.

You Z, Luo C, Zhang W, Chen Y, He J, Zhao Q, Zuo R and Wu Y (2011) Pro- and anti-inflammatory cytokines expression in rat's brain and spleen exposed to chronic mild stress: Involvement in depression. *Behavioural Brain Research*, Elsevier B.V. 225(1): 135–141.

Yuen EY, Wei J, Liu W, Zhong P, Li X and Yan Z (2012) Repeated Stress Causes Cognitive Impairment by Suppressing Glutamate Receptor Expression and Function in Prefrontal Cortex. *Neuron*, Elsevier Inc. 73(5): 962–977.

Zaharia MD, Kulczycki J, Shanks N, Meaney MJ and Anisman H (1996) The effects of early postnatal stimulation on Morris water-maze acquisition in adult mice: genetic and maternal factors. *Psychopharmacology*, Springer-Verlag 128(3): 227–239.

Zhao C, Teng EM, Summers RG, Ming G-L and Gage FH (2006) Distinct morphological stages of dentate granule neuron maturation in the adult mouse hippocampus. *The Journal of Neuroscience* 26(1): 3–11.

Zhu L, Wei T, Gao J, Chang X, He H, Miao M and Yan T (2015) Salidroside attenuates lipopolysaccharide (LPS) induced serum cytokines and depressive-like behavior in mice. *Neuroscience Letters* 606: 1–6.

Zhu X, Li P, Hao X, Wei K, Min S, Luo J, Xie F and Jin J (2015) Ketamine-mediated alleviation of electroconvulsive shock-induced memory impairment is associated with the regulation of neuroinflammation and soluble amyloid-beta peptide in depressive-like rats.

Neuroscience Letters 599: 32–37.

Zhuang F, Zhou X, Gao X, Lou D, Bi X, Qin S, Sun C, Ye P, Wang Y, Ma T, Li M and Gu S (2016) Cytokines and glucocorticoid receptors are associated with the antidepressant-like effect of alarin. *Peptides* 76: 115–129.

Zitnik GA, Clark BD and Waterhouse BD (2013) The impact of hemodynamic stress on sensory signal processing in the rodent lateral geniculate nucleus. *Brain Research* 1518: 36–47.

Zuccato C (2001) Loss of Huntingtin-Mediated BDNF Gene Transcription in Huntington's Disease. *Science*, American Association for the Advancement of Science 293(5529): 493–498.

Zuccato C, Valenza M and Cattaneo E (2010) Molecular Mechanisms and Potential Therapeutical Targets in Huntington's Disease. *Physiological Reviews* 90(3): 905–981.

Zunszain PA, Anacker C, Cattaneo A, Carvalho LA and Pariante CM (2011) Glucocorticoids, cytokines and brain abnormalities in depression. *Progress in Neuro-Psychopharmacology and Biological Psychiatry*, Elsevier Inc 35(3): 722-729.

Zunszain PA, Anacker C, Cattaneo A, Choudhury S, Musaelyan K, Myint AM, Thuret S, Price J and Pariante CM (2012) Interleukin-1β: A New Regulator of the Kynurenine Pathway Affecting Human Hippocampal Neurogenesis. *Neuropsychopharmacology* 37(4): 939–949.

Zwanzger P, Domschke K and Bradwejn J (2012) Neuronal network of panic disorder: The role of the neuropeptide cholecystokinin. *Depression and Anxiety* 29(9): 762–774.

Appendix

1 Differentially expressed genes in the PFC

Table 21 Significantly differentially expressed genes in the PFC.
Fold change and q values derived from analysis conducted by Significance Analysis of Microarrays (SAM) method and R-package with FDR level set at 0

PFC UPREGULATED GENES			PFC DOWNREGULATED GENES		
Gene name	**Fold change**	**Q-value (%)**	**Gene name**	**Fold change**	**Q-value (%)**
Loc665506	2.61	0	Rgs9	0.28	0
Myl4	2.23	0	Tac1	0.29	0
Tnnc1	2.15	0	Pcp4l1	0.30	0
Nrgn	2.07	0	Calb2	0.35	0
E130012a19rik	2.06	0	Cart	0.37	0
Zfp312	2.02	0	Gng7	0.37	0
C330006p03rik	2.00	0	6330404f12rik	0.45	0
Cpne9	1.97	0	Cartpt	0.48	0
Mef2c	1.88	0	Loc100047385	0.49	0
Dkk3	1.87	0	2810011l19rik	0.49	0
Ldb2	1.86	0	Slc32a1	0.51	0
Satb1	1.82	0	Chn2	0.52	0
Stx1a	1.78	0	Cacng5	0.53	0
Pvalb	1.77	0	Lmo3	0.54	0
Nfix	1.74	0	Scg2	0.54	0
Tcrb-v8.2	1.73	0	Gad1	0.54	0
9130024f11rik	1.72	0	Hap1	0.55	0
Zfp238	1.72	0	Loc100047583	0.56	0
6330527o06rik	1.71	0	Slc17a6	0.56	0
Cck	1.67	0	Slc17a6	0.57	0
Ai850995	1.67	0	Gad1	0.57	0
Galnt9	1.65	0	Trf	0.57	0
Grit	1.63	0	Zcchc12	0.57	0
Ccl27	1.63	0	Pcp4l1	0.57	0
1700019n12rik	1.58	0	Adra2a	0.58	0
Ddit4l	1.58	0	Mobp	0.58	0
Sytl2	1.58	0	Tiam1	0.59	0
Dgkz	1.57	0	Bcl11b	0.59	0
Tshz3	1.57	0	Tpbg	0.59	0
Camk2a	1.56	0	Mag	0.59	0
Pcsk2	1.56	0	Ppp1r2	0.60	0
Osbpl1a	1.55	0	D330017j20rik	0.60	0
Nuak1	1.55	0	Meis1	0.60	0
Arpp19	1.54	0	Cacng5	0.60	0
Cckbr	1.54	0	Mbp	0.61	0

PFC UPREGULATED GENES			PFC DOWNREGULATED GENES		
Gene name	**Fold change**	**Q-value (%)**	**Gene name**	**Fold change**	**Q-value (%)**
Mapk11	1.54	0	Zic1	0.61	0
Pvrl3	1.54	0	Clic6	0.62	0
Cobl	1.53	0	H3f3b	0.63	0
Slc17a7	1.53	0	Btg1	0.63	0
Ccdc3	1.52	0	6430550h21rik	0.64	0
D10ertd610e	1.51	0	Loc100046259	0.65	0
Loc100047651	1.51	0	Cntnap2	0.65	0
Extl1	1.51	0	Sez6	0.65	0
Tmem178	1.49	0	6430550h21rik	0.65	0
Ppme1	1.48	0	Sox11	0.66	0
Gfod1	1.48	0	Spock3	0.66	0
Arhgdig	1.48	0	Doc2b	0.66	0
Syne1	1.47	0	Mog	0.66	0
Zfp238	1.47	0	Hmgn2	0.66	0
Loc100046044	1.47	0	Nrsn2	0.67	0
Olfm1	1.45	0	Fa2h	0.67	0
1110008p14rik	1.44	0	Loc100047827	0.67	0
Ldb2	1.44	0	Ednrb	0.67	0
Hapln4	1.43	0	Cldn11	0.67	0
Car10	1.43	0	Dgkb	0.67	0
Rilpl1	1.43	0	Prr18	0.68	0
Actb	1.42	0	A230065h16rik	0.68	0
Fezf2	1.42	0	Rcan3	0.69	0
Acsl5	1.42	0	A230057m07rik	0.69	0
Arhgdig	1.41	0	Tmem90a	0.69	0
Atp1a1	1.41	0	Loc268934	0.69	0
Actb	1.41	0	Krt10	0.70	0
Itpr1	1.41	0	Eg574403	0.70	0
Diras2	1.41	0	Mobp	0.70	0
Homer1	1.40	0	Actn2	0.70	0
Loc100047870	1.40	0	6430524c05rik	0.70	0
A130090k04rik	1.40	0	Fgfr2	0.71	0
Adrbk1	1.40	0	Lmo3	0.71	0
Dgkz	1.40	0	Clic4	0.71	0
Garnl3	1.40	0	Btg1	0.71	0
Garnl4	1.39	0	Mog	0.71	0
38596	1.39	0	Litaf	0.72	0
Itpka	1.39	0	Slc6a9	0.72	0
Sobp	1.39	0	Loc100042405	0.72	0
Sidt1	1.38	0	Pigp	0.72	0
Mpped1	1.38	0	Pigh	0.72	0
Fbxw7	1.38	0	Lass2	0.72	0
Camk2a	1.38	0	Nmbr	0.73	0

PFC UPREGULATED GENES			PFC DOWNREGULATED GENES		
Gene name	**Fold change**	**Q-value (%)**	**Gene name**	**Fold change**	**Q-value (%)**
Extl1	1.38	0	Dbi	0.73	0
Camk2n1	1.38	0	Fibcd1	0.73	0
Tmem132a	1.37	0	Loc100047353	0.73	0
Ly6e	1.37	0	Tubb2b	0.74	0
Loc100045359	1.37	0	Rerg	0.74	0
Tcap	1.37	0	Usp29	0.74	0
Per2	1.37	0	Dock10	0.74	0
Camta2	1.36	0	Ai851790	0.74	0
Dab2ip	1.36	0	Pptc7	0.74	0
Tspan17	1.36	0	Fhl1	0.75	0
Lasp1	1.36	0	Slc25a5	0.75	0
Mbp	1.36	0	Inpp5f	0.75	0
Loc100044468	1.35	0	Dscr1l2	0.75	0
Rab6	1.35	0	Sertad4	0.75	0
6530418l21rik	1.35	0	Mobp	0.75	0
Sema7a	1.35	0	Loc100044124	0.75	0
Rspo2	1.35	0	2210013o21rik	0.76	0
Syn1	1.34	0	Eg434280	0.76	0
Nbl1	1.34	0	Dbi	0.76	0
Diras2	1.34	0	Ndrl	0.76	0
Tuba4a	1.34	0	Abat	0.76	0
E430002g05rik	1.34	0	Pigp	0.76	0
Epb4.9	1.33	0	Nrsn2	0.76	0
Bc049806	1.33	0	Nnat	0.76	0
Faah	1.33	0	Nsep1	0.77	0
Stk16	1.33	0	Necab2	0.77	0
Galt	1.32	0	C030048h21rik	0.77	0
Rph3a	1.32	0	Sumo3	0.77	0
Nfix	1.32	0	Cited2	0.77	0
Etl4	1.32	0	Nsg2	0.78	0
Flot1	1.32	0	Kcne1l	0.78	0
Tpd52	1.31	0	Bex4	0.78	0
Cux2	1.31	0	Slc44a1	0.78	0
Mkx	1.31	0	B230369l08rik	0.79	0
Car4	1.31	0	Anln	0.79	0
Gng13	1.30	0	Psip1	0.79	0
Anxa11	1.30	0	Lrrc8d	0.79	0
D17wsu92e	1.30	0	5033414k04rik	0.79	0
Myrip	1.29	0	6330500d04rik	0.79	0
Sult4a1	1.29	0	Hnrpdl	0.79	0
Mast3	1.29	0	6330500d04rik	0.79	0
Slc2a6	1.29	0	Rbp1	0.80	0
Chrd	1.28	0	B230312l03rik	0.80	0

PFC UPREGULATED GENES			PFC DOWNREGULATED GENES		
Gene name	**Fold change**	**Q-value (%)**	**Gene name**	**Fold change**	**Q-value (%)**
Ccng1	1.28	0	Rnaset2b	0.80	0
Kcnv1	1.28	0	Gcap27	0.80	0
Pip5k1c	1.28	0	Eg433229	0.80	0
Camkk2	1.27	0	Adamts4	0.81	0
Kcnmb4	1.27	0	Dock10	0.81	0
Iqgap2	1.27	0	2310014g06rik	0.81	0
Cbln2	1.27	0	Eif2s2	0.81	0
Eg244911	1.26	0	Sox10	0.82	0
Unc13b	1.26	0	Loc100040919	0.82	0
Ccl27	1.26	0	H2-ke6	0.82	0
Mras	1.26	0	B3galt5	0.82	0
Loc100043919	1.26	0	Doc2b	0.82	0
Lingo1	1.26	0	Bc057371	0.82	0
Foxp3	1.26	0	Htr1d	0.83	0
A730017d01rik	1.25	0	Caprin1	0.83	0
Gca	1.25	0	Spint1	0.83	0
Khdrbs3	1.25	0	Ddc	0.83	0
Chrm3	1.25	0	Acvr2b	0.83	0
Cd6	1.25	0	1110018j23rik	0.83	0
Echdc2	1.25	0	Nap1l1	0.83	0
6030405a18	1.25	0	Ergic3	0.83	0
St8sia5	1.25	0	Ppap2c	0.83	0
Camk2g	1.25	0	Rab34	0.83	0
Etv5	1.24	0	Amotl1	0.83	0
E230013m07rik	1.24	0	Pbx3	0.84	0
Vasn	1.24	0	Loc100048589	0.84	0
Pop5	1.24	0	Xpa	0.84	0
Ptprk	1.24	0	Pdlim2	0.84	0
E2f1	1.24	0	Eg245190	0.84	0
Xbp1	1.24	0	Mycl1	0.84	0
Dact2	1.24	0	Gabrg1	0.84	0
Mgll	1.23	0	Plekhg3	0.84	0
Lin7b	1.23	0	C030027h14rik	0.84	0
2310045a20rik	1.23	0	Kcnip1	0.84	0
Zfpm2	1.23	0	Nts	0.85	0
Hsd11b1	1.23	0	B430201a12rik	0.85	0
Cd6	1.23	0	Kcna5	0.85	0
Ephb6	1.23	0	Samd9l	0.85	0
Atxn7l3	1.23	0	Hbp1	0.85	0
Pou6f1	1.23	0	Bc031781	0.85	0
Otx1	1.23	0	2010011i20rik	0.86	0
3110047p20rik	1.23	0	Amy2-2	0.86	0
Ppfia3	1.23	0	Lhfpl3	0.86	0

PFC UPREGULATED GENES			PFC DOWNREGULATED GENES		
Gene name	**Fold change**	**Q-value (%)**	**Gene name**	**Fold change**	**Q-value (%)**
Myadm	1.23	0	Fzd5	0.86	0
Dlk2	1.22	0	Inpp4b	0.86	0
Loc100044376	1.22	0	Vps25	0.87	0
Fbxo27	1.21	0	Gtf2ird1	0.87	0
Ly6e	1.21	0	Bc025546	0.87	0
Spcs3	1.21	0	Tmem117	0.87	0
Cacnb4	1.21	0	2700007p21rik	0.87	0
E430002g05rik	1.21	0	Sema6d	0.87	0
Arhgap25	1.20	0	Rab34	0.87	0
Slc26a4	1.20	0	Myt1	0.87	0
Sema4f	1.20	0	Scl0004175.1_57	0.87	0
Nuak1	1.20	0	Cpne2	0.88	0
Rimbp2	1.20	0	9630031f12rik	0.88	0
Iqwd1	1.20	0	Ai851790	0.88	0
Csnk2a2	1.20	0	Dhrs7	0.88	0
D4bwg0951e	1.20	0	Itgb4	0.88	0
Atmin	1.20	0	Tcf7l2	0.88	0
1700003e16rik	1.20	0	Lhfpl3	0.89	0
Apba2	1.19	0	Dlx6	0.89	0
Ubqln4	1.19	0	Ccbl1	0.89	0
Iqsec2	1.19	0	Araf	0.89	0
Efna5	1.19	0	Il13ra1	0.89	0
D330001f17rik	1.19	0	Bdh2	0.89	0
Dab2ip	1.19	0	Rps6ka5	0.89	0
9030619k07rik	1.19	0	1110059g02rik	0.90	0
Mast1	1.19	0	Efs	0.90	0
Acap3	1.19	0	Sp9	0.90	0
Dtx4	1.19	0	Ccno	0.90	0
Lgals1	1.19	0	6330505n24rik	0.90	0
A830021m18	1.19	0	Hist1h4h	0.91	0
Loc244417	1.19	0	Rasgrp2	0.91	0
Spag5	1.19	0	Arhgef6	0.91	0
Dtx4	1.18	0	Xrcc3	0.91	0
Arhgap15	1.18	0	Slc6a3	0.91	0
Apba2	1.18	0	Apoc1	0.92	0
Olfm2	1.18	0	1110012d08rik	0.93	0
Ap3m2	1.18	0	Wdr68	0.93	0
Ovol2	1.17	0			
Loc100044968	1.17	0			
Map3k10	1.17	0			
Kcnmb4	1.17	0			
Cpne9	1.17	0			
Tspan17	1.17	0			

PFC UPREGULATED GENES			PFC DOWNREGULATED GENES		
Gene name	**Fold change**	**Q-value (%)**	**Gene name**	**Fold change**	**Q-value (%)**
6330404c01rik	1.17	0			
Tmem198	1.16	0			
Tcap	1.16	0			
Loc381326	1.16	0			
D10ertd610e	1.16	0			
Acss2	1.16	0			
4632428d17rik	1.16	0			
Dkk3	1.16	0			
C77080	1.16	0			
9330175b01rik	1.16	0			
Shisa4	1.15	0			
B230339m05rik	1.15	0			
D8ertd82e	1.15	0			
Ovol2	1.15	0			
Wnt10a	1.15	0			
Glt8d2	1.14	0			
Map3k10	1.14	0			
Htatip2	1.14	0			
Loc100045780	1.14	0			
Adap1	1.14	0			
Robo3	1.14	0			
D230013b04rik	1.14	0			
Tle6	1.14	0			
Kcnk4	1.14	0			
Glt8d2	1.13	0			
Myd88	1.13	0			
Scl000490.1_983	1.13	0			
Cd6	1.13	0			
Olfm1	1.13	0			
Otud3	1.13	0			
Ccbp2	1.13	0			
Baiap2l1	1.13	0			
Megf11	1.13	0			
A830073o21rik	1.12	0			
9330102g19rik	1.12	0			
Myh3	1.12	0			
Nfix	1.11	0			
Synj2	1.11	0			
Rgs9bp	1.11	0			
Ramp3	1.11	0			
Gpr68	1.11	0			
Cbfa2t3h	1.11	0			
Ab112350	1.11	0			

PFC UPREGULATED GENES			PFC DOWNREGULATED GENES		
Gene name	**Fold change**	**Q-value (%)**	**Gene name**	**Fold change**	**Q-value (%)**
Tbc1d5	1.11	0			
H2afj	1.11	0			
Ephb2	1.11	0			
1810047k05rik	1.10	0			
D330038k10rik	1.10	0			
Dok5	1.10	0			
Chd5	1.10	0			
Ap2s1	1.09	0			
Kcnk6	1.09	0			
Clec11a	1.09	0			
Ramp3	1.09	0			
Ptprd	1.08	0			
6330540d07rik	1.08	0			
B230107j06rik	1.07	0			
Galnt9	1.06	0			
Kcng2	1.06	0			

2 Differentially expressed genes in the hippocampus and the hypothalamus

Table 22 Differential gene expression in the hippocampus and the hypothalamus analysed by SAM in R software.

THE HIPPOCAMPUS UPREGULATED GENES			THE HYPOTHALAMUS UPREGULATED GENES		
Gene name	**Fold change**	**Q-value (%)**	**Gene name**	**Fold change**	**Q-value (%)**
Mkks	1.17	0.00	C330006p03rik	1.10	4.99
Per2	1.26	0.00	Uhrf2	1.21	4.99
Mfsd2	1.22	0.00	Camk1	1.13	4.99
Zfp207	1.13	0.00	Tsc22d3	1.12	4.99
Htra1	1.21	0.00	Htra1	1.22	4.99
1110057k04rik	1.15	0.00	Mfsd2	1.22	4.99
Nrp1	1.14	0.00	Loc634015	1.15	4.99
1190003m12rik	1.07	0.00	Mrrf	1.12	4.99
Arpc2	1.30	5.83	Fam107a	1.29	4.99
Pglyrp1	1.06	6.03	Chic1	1.04	4.99
C1ql3	1.11	6.03	Agxt2l1	1.18	4.99
1190005n23rik	1.10	6.03	Copg	1.17	4.99
Fam13c	1.10	6.03	C2	1.07	4.99
Tsc22d3	1.18	9.51	Loc665506	1.07	4.99
Sh3md4	1.05	9.51	Dusp19	1.11	9.97

S3-12	1.08	9.51			
Hace1	1.13	9.51			
Smox	1.14	9.51			
THE HIPPOCAMPUS DOWNREGULATED GENES			**THE HYPOTHALAMUS DOWNREGULATED GENES**		
Gene name	**Fold change**	**Q-value(%)**	**Gene name**	**Fold change**	**Q-value(%)**
Bex4	0.90	0.00	Klhdc9	0.88	0.00
B230373p09rik	0.88	0.00	Loc385256	0.85	0.00
Hnrpdl	0.82	0.00	Nrxn2	0.88	0.00
Loc100047427	0.89	0.00	Hdgfrp2	0.83	0.00
Hint2	0.84	5.83	Gm129	0.94	9.97
Klhdc9	0.85	5.83	Pcdh19	0.92	9.97
Pllp	0.89	7.61	Vangl2	0.92	9.97
Asphd1	0.90	7.61	Cacng5	0.91	9.97
Sgcb	0.91	7.61	Dgat2	0.86	9.97
Dcx	0.95	7.61	Loc100047427	0.88	9.97
Tmem86a	0.92	7.61	Mbtps1	0.89	9.97
Mrps28	0.90	7.61	Rab34	0.88	9.97
0610007p22rik	0.81	7.61			
Slc4a3	0.88	7.61			
Hyal2	0.93	7.61			
Zfp46	0.85	7.61			
Haghl	0.85	10.29			
Krt1-12	0.89	10.29			
Blmh	0.88	10.29			
Gucy1a3	0.82	10.29			
Lmnb1	0.92	10.29			
Cyp4f13	0.95	10.29			
Wbp5	0.89	10.29			
Nr1d1	0.93	10.29			
Gdf10	0.90	10.29			
Setd5	0.89	10.29			
Ai836003	0.91	10.29			